DECIPHERING THE ROLES OF TGF-β SIGNALING IN TRIPLE NEGATIVE BREAST CANCER

By

Bojana Jovanović

Dissertation

Submitted to the Faculty of the

Graduate School of Vanderbilt University

in partial fulfillment of the requirements

for the degree of

DOCTOR OF PHILOSOPHY

In

Cancer Biology

August, 2014

Nashville, Tennessee

Approved:

Harold Moses, M.D.

Andries Zijlstra, Ph.D.

Jennifer Pietenpol, Ph.D.

Joey Barnett, Ph.D.

DEDICATION (POSVETA)

Za moju dragu mamu i tatu, za sve vase muke u zivotu kroz koje ste prosli da bi ste nas stavili na pravi put i dali nam krila da letimo ka svijetlijoj buducnosti. Rijeci ne mogu da opisu koliko sam vam zahvalna.

PUNO VAS VOLIM PICICI MOJI!

For my dear mom and dad, for all your hardship you have endured in your life in order to put us on the right path and give us wings to fly to a brighter future- words cannot describe how grateful I am to you.

I love you very much!

ACKNOWLEDGEMENTS

The grant support for the projects presented herein was provided by NIH Grants CA085492 and CA102162 (awarded to H.L. Moses), NIH Grant CA95131 (Specialized Program of Research Excellence in Breast Cancer) and a Komen for the Cure Foundation Grant SAC110030 (awarded to J.A. Pietenpol).

Vincit qui patitur- is an academic achievement award given to Berea College sophomores. It means he who endures conquers. What I want to make clear is that enduring and conquering does not happen without a strong army of support. Although I do not have an official award to give to all the people that have made an impact in my life, I would like to take this opportunity to thank everyone who has helped me reach this far.

First of all I would like to thank Dr. Hal Moses for being an amazing mentor and a wonderful human being, always kind and patient with me- a true role model. Despite of me being an alien (international) student (not eligible for training grants), he took a leap of faith by giving me freedom to design my thesis project and allowing me to bridge to Pietenpol and Zijlstra labs. Thank you Hal, for putting up with my 'crazy three-lab way' of doing things.

I would like to thank Jennifer Pietenpol, my co-mentor, for taking time out of her busy schedule to have standing meetings with me and always providing me with helpful suggestions and great discussions. Thank you for opening

doors of your lab to me and allowing me to have complete access to priceless resources without which I would not be able to come this far.

My deep thanks goes to Andries Zijlstra and his lab members. Andries was one of the faculties responsible for my recruitment into Vanderbilt IGP program. Thank you for many hours of helpful discussions, for dissecting all the data with me and for putting me on the *TGFBR3* path. Thank you for always being supportive and generous with your time and for always believing in my scientific abilities.

I would like to thank my committee member, Dr. Joey Barnett as well as my clinical mentors Dr. Ingrid Mayer, Dr. Bapsi Chak and Dr. Melinda Sanders. Joey, thank you all for all the help with my *TGFBR3* project, I had fun discussions with you and your lab members (Nora, Dan, Cindy). You have been invaluable help with data analysis and providing resources. Ingrid and Bapsi, thank you for serving as my clinical mentors for my Clinical Program in Molecular Medicine. I appreciate you allowing me to spend time at the clinic and visit with you the patients. It was indeed an eye opener, as seeing in person the limited options for some patients made me work even harder in lab. Melinda, thank you for spending hours in going over slides with me and teaching me all I know about breast tissue pathology.

I would like to thank my Moses/Pietenpol lab 'moms'. During my time in Moses lab Mary Aakre, Anna Chytil and Agnes Gorska became an amazing support all the way from training me, helping me with giant experiments for

TGFBR3 manuscript to helping me get free furniture (Mary), figuring out tax returns (Agnes) and helping me with my first plants and making me laugh (Anna). I would like to thank Kim Johnson for putting in with me about thousand hours of LCM and for keeping her hands in cold cryostat to cut probably over ten thousand slides over past five years. Thank you Kimbo (Kim Johnson) for keeping me straight and for always worrying about my state of heart and for your attempts to help me learn that 'it is what it is'. Special thanks goes to Dina Polosukhina, a quite and kind Moses lab member, who has been always supportive and respectful.

I would like to thank current and former fellow trainees in Moses, Pietenpol and Zijlstra lab. Michael (Mike) Pickup and Lauren Matise, thank you for being amazing friends, always willing to help and give your advice. Mike thank you for always cheering me up with great selections of music and for brining life to our 'half' of lab. Clayton (Clay) Marshall, thank you for being a friend since IGP, studying with me for qualifying exams and for always making me feel comfortable to talk about what we believe really matters. Christopher Pendleton (Chris P) thank you for your help during my qualifying exam preparations, your feedback made a great difference as it helped me stay focused. Thank you for always being kind, for putting up with my love for salmon during our 'cubicle' time, and sorry for stomping your foot. Jennifer Rosenbluth (JR), thanks for being kind to me when I first joined the lab and showing me the ropes for using Gene Spring and doing gene expression analysis. Katy Eby, thanks for taking time away from your schedule right before your defense to help with during my IGP rotation and

for teaching me how to do proper westerns and siRNA experiments. Chris Barton, thanks for being a good fellow Berean and for the help when I first started in lab. To the new crew - Tim Shaver, Johanna Schafer, Gabriela Santos and Scott Beeler, thanks for being hard core and for bringing new energy to the lab. It's been fun. Scott Beeler, thank you for coming right on time to help me with the last figure of the paper. Thanks for all your kindness and patience as I have asked you for millions of analyses and the explanations on how you did them. William (Will) Ashby thanks for training me how to perform MAtS assays and for always having a spare for me when I ran out. I would like to give special thanks to our adapted Moses lab member Laura Hover. Laura, thank you for being a wonderful person for checking on me during my manuscript and thesis writing crazy phases. You have been so sweet and kind. It's been a pleasure being around you. I would like to thank our research assistant professors Philip Owens, Sergey Novitskiy, Brian Lehmann and Joshua Bauer for all their technical help as well as helpful scientific discussions. Phil, thank you for all the brainstorming on *TGFBR3* and BMP and though it did not pan out it was helpful for building the story. Sergey, thanks for all the help with flow conditions and establishing proper protocols. Brian, thanks for letting me use your 587 TNBC data set before it was even published, that really triggered all the follow up experiments. Thank you also, for reviewing my manuscript at last minute notice and right before holidays! Josh, thanks for training me how to do LCM and handle teeny-tiny tissues. Peter Clark and Ty Abel, our research clinicians, thank you for all your helpful

suggestions and recommendations during Moses lab meeting- you have kept me focused on clinical relevance.

I would like to thank clinical fellows that have helped me with clinical specimens over the years. Maria Graciela Olivares, Maria Gabriela Kuba and Valeria Estrada, thank you for always being prompt with communications, for scanning and scoring thousands of slides for the trial and for being always kind and patient and willing to work hard and help things get done. I truly appreciate everything you have done. Also, special thanks to Violate Sanchez, Dr. Sanders's technical assistant, who has performed all immunohistochemistry on over seven thousands slides. Violeta, you have been an amazing help and great to work with.

I would also like to thank my former professors and college friends. I would like to thank my medical science teacher Ms. Osborn, for being an amazing teacher and friend. Thank you for making me excited about medical profession and for your help with my application to college. Dr. Ron Rosen, thank you for being an amazing mentor during my time in Berea. Thank you for your constant support and help over years. You were the one who had made a great impact and triggered my interest in pursuing research. Thank you for always believing in me, despite my poor English abilities. I would like to thank my friends Consolate, Aishe and Dikshya thank you for listening to me when I was in need of a friend. You have been encouraging and supportive all along this path, and I am truly grateful for that.

I would like to thank my adopted families over the years. My KY host family Jim and Louse Miller, for taking me into their home as an exchange student thirteen years ago and for treating me like I was their own daughter. Thank you for driving in the snow to Berea so I can submit my application on a last day. And thank you for letting the yellow house be my home away from home. I will never forget everything you have done. I would like to thank my TN host family, Bill and Paula Murray and aunt Becky Boatman. Thank you for giving a roof to a poor college student, when I first started in Nashville. Thanks for all your love and support over the years, for never quitting to call me (even though I was bad with answering), always checking in on me and making sure I was doing well. Duane, Kristen and kids Murray thanks for being a wonderful support during my time in Nashville, it has always been fun coming to your home, playing volleyball or joining you at your church. Thank you guys for always having open door policy! I would also like to thank Brucker family for all their love and support, especially Robin who has always been thoughtful with her artsy handmade cards that would light up my day.

Lastly, and most importantly, I would like to thank my family members: my mom Ruža and my dad Mladenko, my brothers Bojan and Nikola, my grandparents Nikola and Prena, my uncle Dominik and my fiancé Rob. Mom and dad thank you for teaching me how to work hard, keep pushing forward and never give up. Thank you for all your sacrifices you made so that I can be here. You have been wonderful and I will never be able to thank you for all you've done. My great brothers Bojan and Nikola, thank you for loving me, making me

laugh and for always making my heart filled with joy. I am so proud of you and what you have become and I love you very much. Grandma and grandpa, I am sorry I did not make in time for you to see this day, but I wanted to acknowledge you and thank you for giving me a great childhood memories. Thank you for loving me and for always being so proud of me. Thank you for raising me and teaching me not to be afraid of anything. I miss you dearly every day. Dajo, thank you for being supportive and for trying to help our family the best you could. I will never forget what you have done for us, as long as I live.

My sweetest Rob, thank you for being my rock. I would not have made it this far without your selfless love and support. You mean so much to me. Thank you for always being so kind, caring and understanding and for always thinking of me. Thank you for making sure I eat even if that meant bringing me food in lab. Thank you for spending so many nights in lab with me so I am not alone. You have always been a blessing in my life and I am very lucky to have you. You have helped me endure and conquer.

TABLE OF CONTENTS

LIST OF TABLES

LIST OF FIGURES

LIST OF ABBREVIATIONS

α2β1	Alpha 2 beta 1 integrin
α2-KD	Alpha 2 knockdown
AKT	V-Akt-murine thymoma viral oncogene homolog 1
ALK5	TβRI/ Type I transforming growth factor-beta receptor
AR	Androgen Receptor
ATCC	American Tissue Culture Collection
BC	Breast Cancer
BKM120	PI3K inhibitor
BL1	Basal like 1
BL2	Basal like 2
BMP	Bone morphogenetic protein
BP1	Biopsy number 1, 3-5 days post treatment
BRCA1	Breast Cancer 1, Early Onset
BRCA2	Breast Cancer 1, Early Onset
CAF	Cyclophosphamide, Adriamycin, Fluorouracil treatment combination
CAFs	Carcinoma Associated Fibroblasts
CAGA-luc	Nine tandem repeats of the motif *CAGA*-binding Smad3 and Smad4, luciferase reporter
CCL2	Chemokine (C-C Motif) Ligand 2
Cdc42	Cell Division Cycle 42
CHEK1	Checkpoint kinase 1

Co-SMADs	Common mediator Smad
DAPI	4', 6-diamidino-2-phenylindole
DAVID	Database for annotation, visualization and integrated discovery
Daxx	Death-domain associated protein
DCIS	Ductal carcinoma in situ
DMEM	Dulbecco's modified Eagle's medium
DNA	Deoxyribonucleic Acid
ΔNp63α	The p63 protein isoform
ECM	Extracellular matrix
E-Cadherin	Epithelial cadherin
EGFR	Epidermal growth factor receptor
EMT	Epithelial to mesenchymal transition
ER	Estrogen receptor
ERBB2	v-erb-b2 avian erythroblastic leukemia viral oncogene homolog 2
ERK	Extracellular-signal-regulated kinases
FGFR	Fibroblast growth factor receptor
FISH	Fluorescence in situ hybridization
FSB	Fetal bovine serum
GAPDH	Glyceraldehyde-3-phosphate dehydrogenase
GE	Gene expression
GEO	NCBI’s gene expression omnibus
GIPC	GAIP interacting protein C-terminus
GS	Glycine and serine residues rich domain

HER2	Human epidermal growth factor receptor 2
HR	Homologous recombination
IHC	Immunohistochemistry
IACUC	Institutional Animal Care and Use Committee
IDC	invasive ductal carcinomas
IGF1	Insulin-like growth factor 1
IGF1R	Insulin-like growth factor 1 receptor
IHC	Immunohistochemistry
ITGA2	Integrin alpha 2 (gene symbol)
I-Smads	Inhibitory Smads
KEGG	Kyoto Encyclopedia of Genes and Genomes
LAR	Luminal androgen receptor
LAP	Latency associated peptide
LTBP	Latent TGF-β binding protein
LCM	Laser capture microdissection
M	Mesenchymal
MAtS	Magnetic attachable stencils
MEKK1	Mitogen-activated protein kinase kinase kinase 1
MMP	Matrix Metalloproteinase
MMTV	Mouse Mammary Tumor Virus
MSL	Mesenchymal stem-like
mTOR	Mammalian repressor of rapamycin
NAFs	Normal Associated Fibroblasts

NCBI	National Center for Biotechnology Information
Near-pCR	Near pathologic complete response
NIH	National Institutes of Health
No-pCR	No pathologic complete response
PR	Progesterone receptor
PI3K	Phosphotidyl Inositide 3 Kinase
PyMT	Polyoma Middle T Virus
p53	Protein p53
p63	Protein p63
p73	Protein p73
PAM50	Prediction analysis microarray 50 genes
PAI-1	Plasminogen activator inhibitor type 1
Par6	Partitioning defective 6 homolog alpha
PARP	Poly (ADP-ribose) polymerase
pCR	Pathologic complete response
P-cadherin	Placental cadherin
PI3K	Phosphoinositide-3 kinase
POST	Post-treatment, surgical specimen
PRE	Pre-treatment biopsy
pS6	Phospho-S6 ribosomal protein
PTEN	Phosphatase and tensin homolog
PyVmT	Polyoma virus middle T antigen
qRT-PCR	Quantitative, real-time, polymerase chain reaction

Rac1	Ras-Related C3 Botulinum Toxin Substrate 1
RAD001	mTOR inhibitor (everolimus)
Ras	Rat sarcoma viral oncogene homolog
RHOA	Ras Homolog Family Member A
RNA	Ribonucleic Acid
RPA1	Replication protein A1
R-SMADs	Receptor regulated SMADs
SEM	Standard error mean
shRNA	Short hairpin RNA
siRNA	Small interfering RNA
SMAD	Mothers against decapentaplegic homolog
ssDNA	Single stranded DNA
sTβRIII	Soluable form of TβRIII
TAC	Taxane, anthracyclin, cyclophosphamide treatment combination
TAB1/TAK1	Tgf-Beta Activated Kinase 1
TAp73	The p73 protein isoform
TCGA	The cancer genome atlas
TβRI	Type I transforming growth factor-beta receptor
TβRII	Type II transforming growth factor-beta receptor
TβRIII	Type III transforming growth factor-beta receptor
TβRIII-KD	TβRIII knockdown
TGFβ	Transforming growth factor-beta
TGFβ1	Transforming growth factor-beta ligand 1

TGFβ2	Transforming growth factor-beta ligand 2
TGFβ3	Transforming growth factor-beta ligand 3
TGFBR3	Type III transforming growth factor-beta receptor
TKI	Tyrosine kinase inhibitors
TNBC	Triple negative breast cancer
3TP-lux	Three 12-O-tetradecanoylphorbol-13-acetate responsive elements, luciferase reporter
VEGFR	Vascular endothelial growth factor receptor

CHAPTER I

INTRODUCTION

Breast cancer is not a single disease (brief overview)

Breast cancer is a diverse collection of distinct neoplastic diseases that originate from luminal and adjacent myoepithelial cells lining the milk ducts. The heterogeneity of this disease was initially observed through histopathology and molecular pathology but the true extent of disease diversity became apparent through molecular stratification of breast tumors by gene expression profiling. Initially, invasive ductal carcinomas (IDC) were molecularly classified into five distinct subtypes: luminal A, luminal B, ERBB2, normal breast-like and basal-like. Furthermore, these molecular subtypes were associated with different prognostic outcomes with the basal-like subtype demonstrating the poorest overall outcome (Sorlie*, et al*, 2003) (Figure 1). In the clinical setting, based on immunohistochemical classification, these subtypes fall into two categories: estrogen receptor (ER)-positive (luminal A and B) and two derived from ER-negative tumors (basal-like and ERBB2) (Sorlie*, et al*, 2001; Sorlie*, et al*, 2003). The overall frequency of these two categories of breast cancer subtypes in the population is 65-70% ER-positive and 30-35% ER-negative (Polyak & Metzger Filho, 2012).

Even though it has been over a decade since Sorlie and colleagues initially demonstrated the molecular complexity of breast cancer, achieving

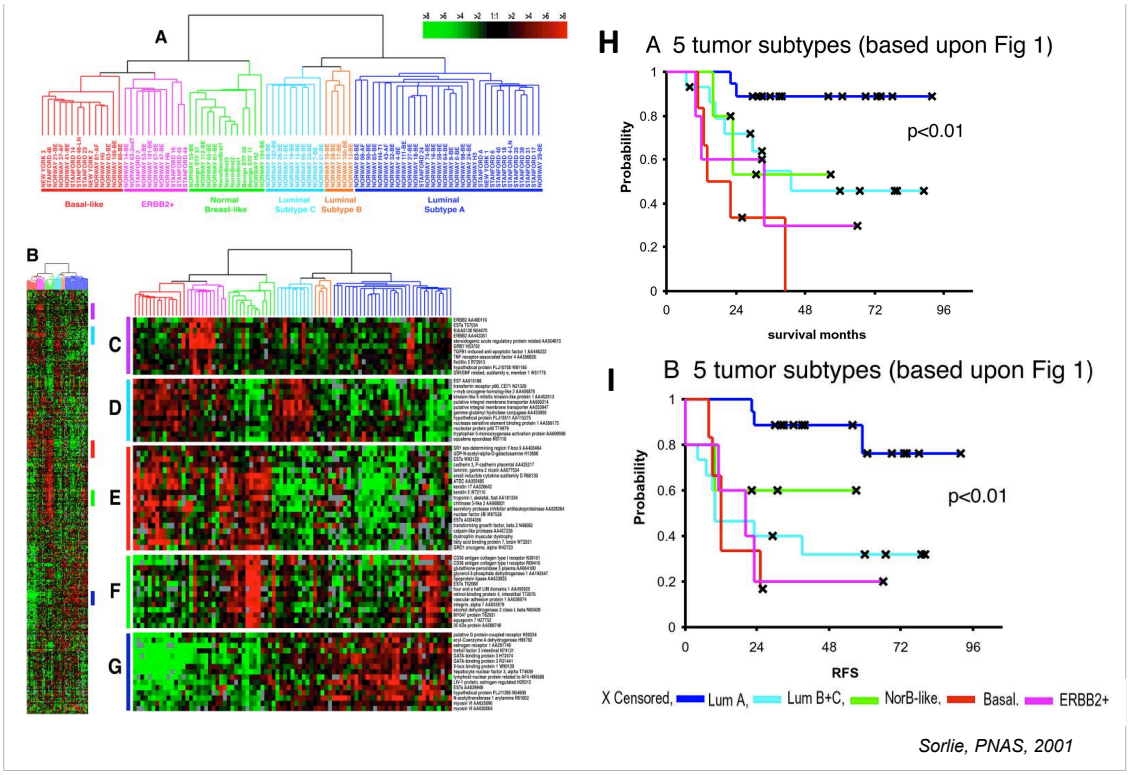

Figure 1. Breast cancer molecular classification and clinical implications.

Figure 1. Breast cancer molecular classification and clinical implications. Gene expression patterns of 85 experimental samples representing 78 carcinomas, three benign tumors, and four normal tissues, analyzed by hierarchical clustering using the 476 cDNA intrinsic clone set. (A) The tumor specimens were divided into five (or six) subtypes based on differences in gene expression. The cluster dendrogram showing the five (six) subtypes of tumors are colored as: luminal subtype A, dark blue; luminal subtype B, yellow; luminal subtype C, light blue; normal breast-like, green; basal-like, red; and ERBB21, pink. (B) The full cluster diagram scaled down (the complete 456-clone cluster diagram is available as Figure 4). The colored bars on the right represent the inserts presented in C–G. (C) ERBB2 amplicon cluster. (D) Novel unknown cluster. (E) Basal epithelial cell-enriched cluster. (F) Normal breast-like cluster. (G) Luminal epithelial gene cluster containing ER. (H-I) Overall and relapse-free survival analysis of the 49 breast cancer patients, uniformly treated in a prospective study, based on different gene expression classification. (H) Overall survival and (I) relapse-free survival for the five expression-based tumor subtypes based on the classification presented in (A) (luminals B and C were considered one group). ***(Figure 1 and 3, Sorlie, PNAS, 2001)***

appropriately aligned treatment to the disease subtype is still in progress. This is evident by the estimated 40,000 breast cancer deaths this year, ranking it as a second cause of cancer death in women (Society, 2014). This calls for further assessment of the treatment approaches currently used in clinical settings.

The present standard-of-care treatment has been broken down based on the expression of the protein markers ER, progesterone (PR) and human epidermal growth factor receptor 2 (HER2). The ER-positive patients (Luminal A/B) undergo anti-estrogen therapy (ex. tamoxifen) (Group, 2011). The therapies for HER2-positive patients are based on combination of targeted drugs (ex. trastuzumab/Herceptin) and cytotoxic chemotherapy (Piccart-Gebhart*, et al*, 2005). It is important to point out that since the introduction of the targeted therapy in HER2-positive patients there has been a dramatic improvement in long-term outcome. Unfortunately, unlike the three subtypes mentioned above, there are no targeted therapies for the basal-like breast cancers.

The best definition for basal-like breast cancer is still a 'black hole' as there still is no consensus about how best to define a basal-like breast cancer (Bertucci*, et al*, 2008; Carey*, et al*, 2010; Kreike*, et al*, 2007; Lehmann & Pietenpol, 2014). Different immunohistochemical markers are used to identify this phenotype, but there is no universally acceptable criteria or set of markers in use to define this subtype of breast cancer (Abd El-Rehim*, et al*, 2004; Nielsen*, et al*, 2004; van de Rijn*, et al*, 2002). It has been suggested that, until these criteria are developed, staining for ER, PR, and HER2 would correctly classify the majority of basal-like breast cancers. In fact, the basal-like category significantly, but not

completely, overlaps with triple-negative breast cancers (TNBC), that is, tumors that are negative for ER, PR and HER2. Using ER, PR, and HER2 status, analysis of large series of triple-negative breast cancers with long-term follow-up found that patients with the disease have an increased likelihood of distant metastasis and death compared to women with other types of breast cancer (Dent*, et al*, 2007). Despite differences in taxonomy, there is a consistent trend across all studies confirming the relatively poor prognosis of the triple negative or basal-like breast cancer subgroup (Abd El-Rehim*, et al*, 2005; Abd El-Rehim*, et al*, 2004; Jones*, et al*, 2004; Nielsen*, et al*, 2004; van de Rijn*, et al*, 2002). The lack of association between tumor size and lymph node positivity, the high rates of distal metastasis, and the relative rarity of local recurrence all suggest that patients with triple negative breast cancer have a tendency to develop visceral metastases early in the course of their disease. Chemotherapy is the main therapy for these women (Huober*, et al*, 2010; Liedtke*, et al*, 2008; Rouzier*, et al*, 2005). There is a major need to better understand the molecular basis of triple negative breast cancer and to develop effective therapeutic options to target this aggressive type of breast cancer. Both are goals of the studies reported in this thesis.

Triple Negative Breast Cancer

TNBC characteristics: pathologic, clinical and molecular features

In addition to molecular-profiling diversity, variation in histopathology types marks TNBC as a heterogeneous entity. The majority of TNBC fall under ductal histologic type (~88.7%), however other histologic types have been observed in

TNBC tumors thus highlighting further the heterogeneity of this disease. Among non-ductal histologic TNBC type, apocrine (~3.7%), lobular (~2.3%), adenoid cystic (~1.3%), metaplastic (~1.3%) (Montagna*, et al*, 2013) have been identified and these types of TNBC appear to have better prognosis (Montagna*, et al*, 2013; Rakha*, et al*, 2007; Reis-Filho & Tutt, 2008; Weigelt*, et al*, 2008). Specifically, the absence of lymph node involvement has been demonstrated in all adenoid cystic, 60% of metaplastic, 55% of apocrine and 44% of lobular carcinoma (Montagna*, et al*, 2013).

A main feature of TNBC is high frequency of p53 mutations (~54% of TNBC) (Polyak & Metzger Filho, 2012). Among others, pathologic features include elevated mitotic count, high apoptotic rate, lymphocyte infiltration and metaplasia (Rakha*, et al*, 2007). Furthermore, TNBC frequently express EGFR (HER1) and basal cytokeratins (predominantly, 5, 14 and 17) (Reis-Filho & Tutt, 2008; Viale*, et al*, 2009). Compared to other tumor types, TNBC are less likely to express epithelial markers (e.g., E-cadherin) (Rakha*, et al*, 2007) while being more likely to express myoepithelial markers (e.g., p63, P-cadherin) (Matos*, et al*, 2005). They also have high expression of cyclin E while low levels of cyclin D1 (Bostrom*, et al*, 2009; Voduc*, et al*, 2008). It is important to note that a majority of these features are associate with poor prognosis in breast cancer (Bostrom*, et al*, 2009; Shin*, et al*, 2008; Tsutsui*, et al*, 2002; van de Rijn*, et al*, 2002; Viale*, et al*, 2009).

Epidemiologically, TNBC occurs more frequently in younger patients (<50 years old) and generally have more aggressive characteristics (Bauer*, et al*,

2007). Dent and colleagues have shown that in a cohort of 1061 breast cancer (BC) patients, the TNBC group separated from rest of breast cancer with an increased risk of distant recurrence following diagnosis (Dent*, et al*, 2007). Furthermore, analysis of distant recurrence pattern indicated a highest recurrence for TNBC with 1-3 years after the initial diagnosis. In addition, the overall survival among TNBC patients was shorter in comparison to other BC subtypes (Dent*, et al*, 2007). Similar observations were presented in cohort of 1100 BC patients, where three year overall survival was significantly lower in TNBC patients (Liedtke*, et al*, 2008).

An interesting population-based study indicated that in premenopausal African American women developing breast cancer, TNBC is more prevalent (39%) then in premenopausal women from other racial groups (Carey*, et al*, 2006; Lund*, et al*, 2009). Studies further indicate that after adjusting for age and stage frequency of TNBC is 2-3 times greater in African American women (47% of their breast tumors) compared to European American (22% of their tumors) (Carey*, et al*, 2006; Lund*, et al*, 2009). African American women more likely to have higher grade tumors, generally larger in size, presented with higher mitotic activity. In addition some of the characteristics in these tumors include expression of genes related to cell cycle and apoptosis (ex. p53, p16, cyclin E, cyclin D, Bcl-2 etc.) (Lund*, et al*, 2009). Additionally, Bauer and colleagues have emphasized in their population-based study that in addition to race/ethnicity, younger age was found to be an important risk factor in TNBC (Bauer*, et al*, 2007). Other risk factors that have been correlated with predisposition to

developing TNBC, independent of race status, include young age at first birth, usage of oral contraceptive (especially in women ≤45 years of age) (Dolle*, et al*, 2009), and obesity (if premenopausal) (Kwan*, et al*, 2009; Millikan*, et al*, 2008). Although multiple studies link the African American women to higher predisposition to TNBC, we need to keep in mind that besides genetic/molecular differences, other factors such as socioeconomic status of the patient, could be contributing to these observations.

Molecular subtypes of TNBC and their clinical relevance

The severity of TNBC disease has raised the need for further understanding and alternative drug treatment approach. Since TNBC lacks well-defined molecular targets, integrative and comprehensive genomics and molecular analyses of TNBC were required to understand the complexity of the disease as well as to allow identification of uniform subsets and driver pathways that can then be therapeutically targeted.

Lehmann and colleagues compiled an extensive number of TNBC gene expression (GE) profiles and initiated molecular subtyping of the disease (Lehmann*, et al*, 2011). This led to novel discovery of six distinct TNBC subtypes, shedding light on complexity and heterogeneity of this disease and unique biology within each subtype (Figure 2). The identified subtypes consisted of two basal-like TNBC subtypes (BL1 and BL2); two mesenchymal subtypes (M and MSL); an immunomodulatory (IM) type; and a luminal subtype driven by androgen signaling (LAR). BL1 subtype was enriched for cell division and DNA

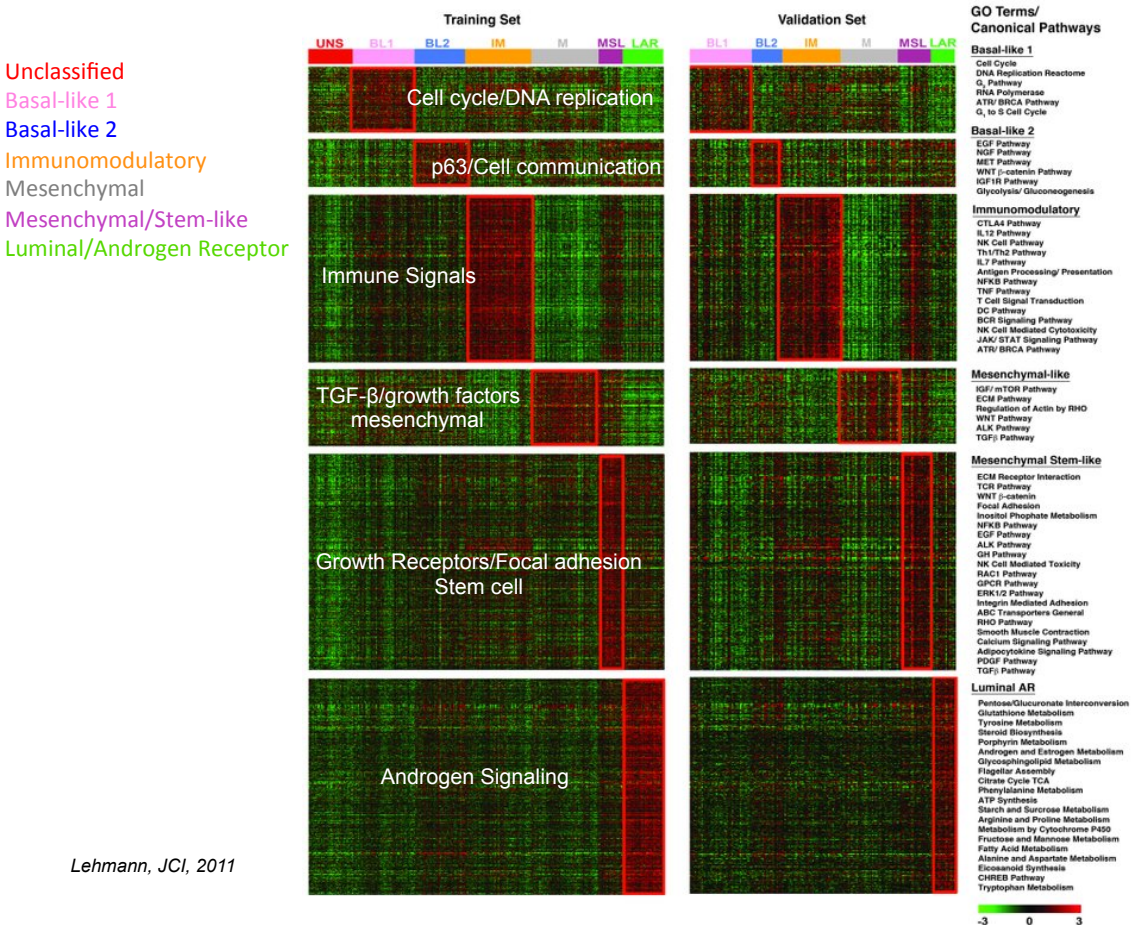

Lehmann, JCI, 2011

Figure 2. Triple negative breast cancer subtypes

Figure 2. Triple negative breast cancer subtypes

GE patterns within TNBC subtypes are reproducible. Heat maps showing the relative GE (log2, –3 to 3) of the top differentially expressed genes ($P < 0.05$) in each subtype in the training set (left) and the same differentially expressed genes used to predict the best-fit TNBC subtype of the validation set (right). Overlapping gene ontology (GO) terms for top canonical pathways in both the training and validation sets as determined by GSE-A are shown to the right of the heat maps. ***(Figure 3, Lehmann, JCI, 2011)***

damage response pathway components while BL2 was had high expression of growth factor signaling (EGF, IGF1R, WNT/β-catenin) and TP63. M/MSL subtypes were represented with genes involved in epithelial to mesenchymal transition (EMT), motility, extracellular matrix (ECM) and cell differentiation pathways. Unlike M, MSL subtype was enriched for genes associated with cell 'stemness' while decreased expression of proliferation genes (Lehmann*, et al*, 2011).

Furthermore, the differential GE was used to define 25 TNBC cell line models representative of these subtypes (Lehmann*, et al*, 2011). Predicted driver signaling pathways were pharmacologically targeted in these preclinical models as proof of concept that analysis of distinct GE signatures can inform therapy selection. In this case it was demonstrated that representative BL1 and BL2 subtype cell lines significantly respond to cisplatin. The mesenchymal subtype cell lines had the greatest sensitivity to phosphatidylinositol 3-kinase (PI3K) inhibitor while luminal AR were more responsive to anti-androgen therapy (bicalutamide) (Figure 3).

TNBC were classically considered as synonymous of the basal-like breast cancer molecular subtype portrayed by Perou and colleagues (Perou*, et al*, 2000). However, only 80% of TNBC present with basal-like molecular characteristics according to gene-expression profiling (Bertucci*, et al*, 2008), so TNBC and the basal-like breast cancer should be considered as distinct categories with incomplete overlap (Bastien*, et al*, 2012; Rakha & Ellis, 2009;

Tan*, et al*, 2008). The main overlap includes high frequency of p53 mutation, lack of ER/PR and HER2 expression as well as being more likely to be high-grade tumors. The part that makes them distinct has been recently demonstrated using a GE comparison between prediction analysis microarray 50 genes (PAM50) and TNBC subtype signature applied to 374 TNBC patients identified from 14 independent datasets (n=2441 samples) (Lehmann & Pietenpol, 2014). The result indicated that based on PAM50 the majority of the TNBC samples, when normalized within 2441 cohort of all breast cancers, were classified as basal-like (81%), as expected based on the previous studies, while the remaining subtypes were HER2 (10%), normal-like (5%), luminal B (3%), and luminal A (1%) (Figure 4) (Lehmann & Pietenpol, 2014). However, when 374 TNBC samples were removed from the 2441 cohort and normalized independently, then analyzed using PAM50 the results shift across the subtypes with basal-like still being the dominant one (52%), HER2 (8%), and increase in normal-like (9%), luminal B (19%) and luminal A (12%). These results indicate that it is easy to misclassify TNBC samples, as it is highly dependent on the normalization approach driven by the sample size. This study has further analyzed TNBC subtypes (BL1, BL2, IM, M, MSL and LAR) using PAM50. Basal like subtypes (BL1, BL2), immunomodulatory (IM) and mesenchymal (M) were primarily represented as basal-like ranging from 85% to 99%. In contrast, MSL and LAR were represented with ~50% and ~2% basal-like, respectively. The LAR subtype was heavily enriched with HER2 subtype (74%) based on PAM50, which is counterintuitive, as these are TNBC patients. Ongoing emerging preclinical and clinical data

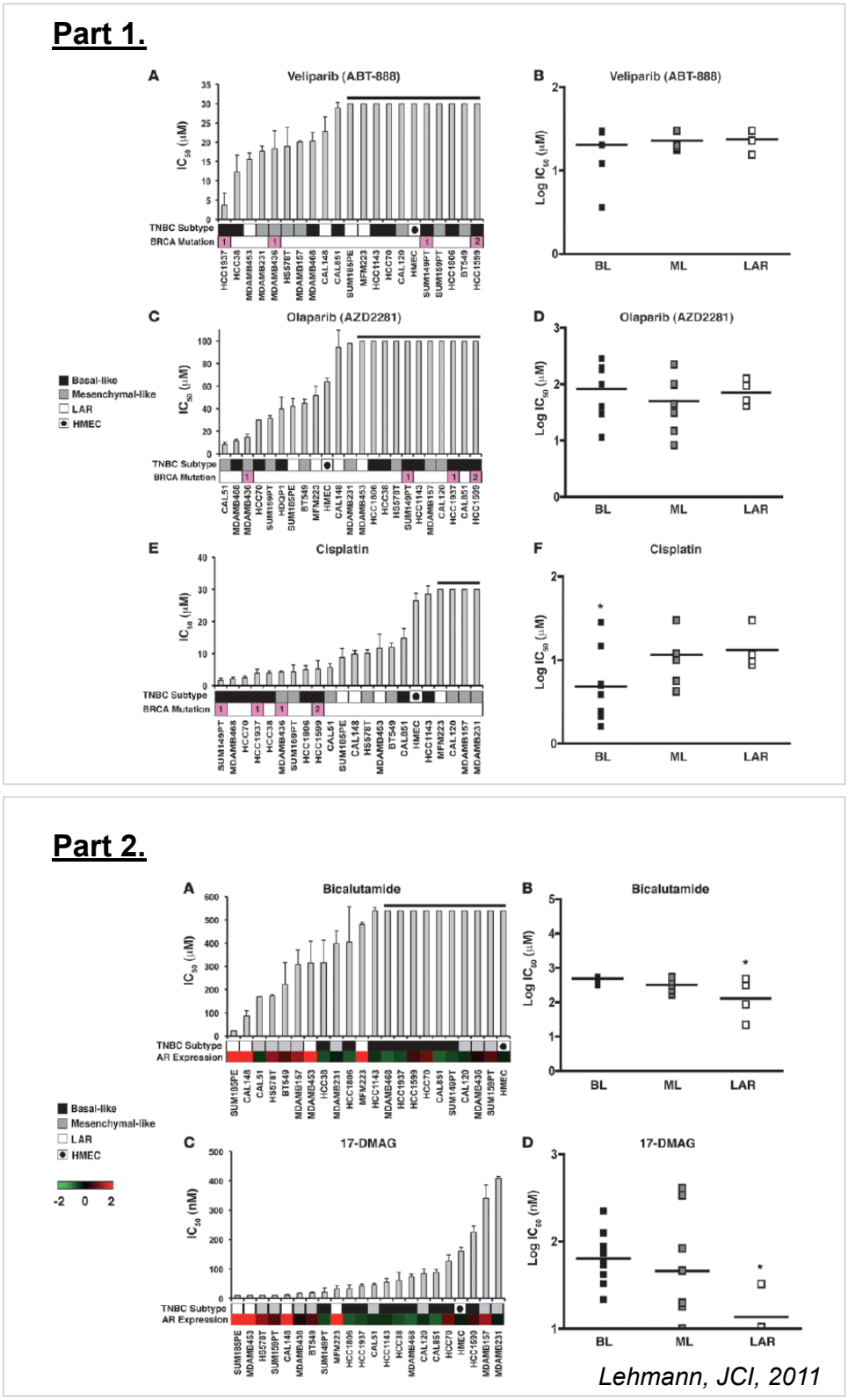

Figure 3. Drug treatments of TNBC subtypes.

Figure 3. Drug treatments of TNBC subtypes.
Part 1. Basal-like TNBC subtypes have differential sensitivity to DNA-damaging agents. IC50 values for TNBC cell lines treated with PARP inhibitors (A) veliparib, (C) olaparib, or (E) cisplatin for 72 hours. Error bars reflect SEM for 3 independent experiments. Black horizontal lines above various bars in the plots indicate cell lines that failed to achieve an IC50 at the highest dose of veliparib (30 μM), olaparib (100 μM), or cisplatin (30 μM). Cell lines that carry BRCA1 or BRCA2 mutations (pink) are displayed below the graph. Dot plot shows the log distribution of drug sensitivity to PARP inhibitors (B) veliparib, (D) olaparib, or (F) cisplatin in the basal-like subtypes (BL = BL1 + BL2), the mesenchymal-like subtypes (ML = M + MSL), and the LAR subtype. Black horizontal bars in the dot plot indicate the mean IC50 for each of the subtypes. *Statistically significant differences in IC50 values of BL compared with ML (P = 0.017) and LAR (P = 0.032), as determined by Mann-Whitney U test. Part 2. Differential sensitivity of the LAR TNBC subtype to AR and Hsp90 inhibitors. IC50 values for each TNBC cell line after treatment with (A) bicalutamide or (C) the Hsp90 inhibitor 17-DMAG for 72 hours. Black bar above bicalutamide indicates cell lines that failed to achieve an IC50. Heat map displays relative AR expression (log2) across TNBC cell lines. Dot plot shows log distribution of drug sensitivity to (B) bicalutamide or (D) 17-DMAG in the basal-like (BL = BL1 + BL2), mesenchymal-like (ML = M + MSL), and LAR subtypes. Black horizontal bars in the dot plot indicate the mean IC50 for each of the subtypes. *Statistically significant differences in IC50 values of LAR versus BL (P = 0.007) or ML (P = 0.038) after bicalutamide and LAR versus BL and ML (P = 0.05) after 17-DMAG treatments, as determined by Mann-Whitney U test. ***(Figures 4, 5, Lehmann, JCI, 2011)***

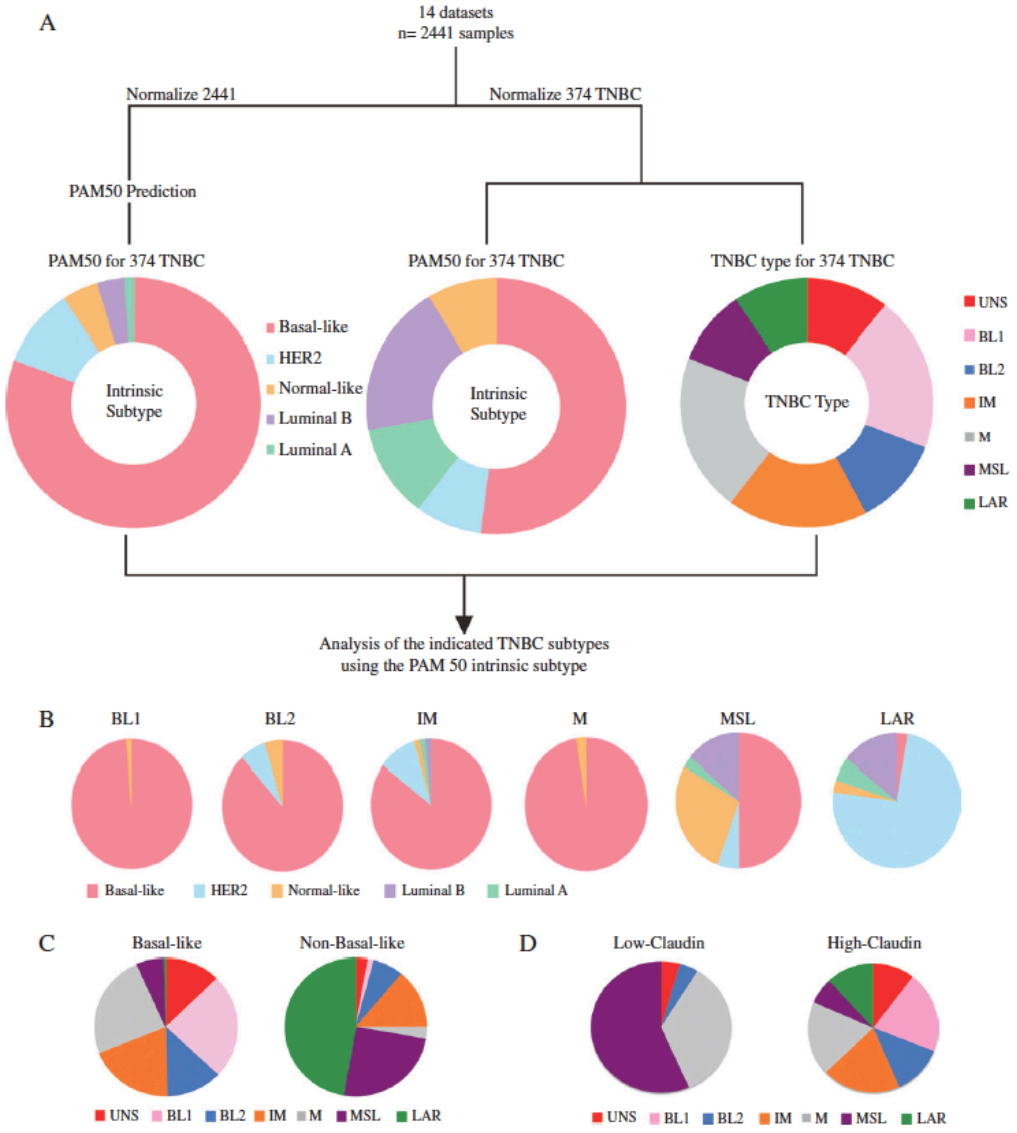

Lehmann, J Pathol,, 2014

Figure 4. TNBC subtype comparison with intrinsic PAM50 subtyping.

Figure 4. TNBC subtype comparison with intrinsic PAM50 subtyping.
Relationship between molecular TNBC subtypes and the intrinsic breast cancer subtypes. (A) Using a bimodal filter on ER, PR and HER2 expression, 374 TNBC samples were extracted from 2441 breast cancer gene expression microarray profiles originating from 14 datasets (GSE1456, GSE1561, GSE2034, GSE2109, GSE2990, GSE2603, GSE5327, GSE5460, GSE5847, GSE7390, GSE11121, GSE12276, GSE18864 and GSE20194). The TNBC samples were either normalized with all samples (left dendrogram branch), followed by PAM50 prediction for intrinsic breast subtypes, or normalized alone (right dendrogram branch), followed by prediction with PAM50 (left) or TNBCtype (right). Doughnut pie charts display the relative distribution of the same 374 TNBC samples analysed using the indicated subtype tools. (B) Pie charts represent analysis of the indicated TNBC subytpes using the PAM50 intrinsic subtype tool. Pie charts display the TNBCtype composition of either (C) basal-like or non basal-like TNBC or (D) low-claudin versus high-claudin TNBC. BL1, basal-like 1; BL2, basal-like 2; IM, immunomodulatory; M, mesenchymal; MSL, mesenchymal stem-like; LAR, luminal AR. ***(Figure 1, Lehmann, 2014, J Pathol)***

suggest that the androgen receptor may serve as a therapeutic target in LAR TNBC subtype (Lehmann*, et al*, 2011). Although this is currently an active areas of investigation it does beg the question regarding current aligning of treatments with the breast diseases and why we might not have success in treating TNBC compared to rest of breast cancers types.

Although Lehmann and colleagues have demonstrated that TNBC is heterogeneous and as such can be classified into 6 groups with distinct molecular signatures, the clinical application of this finding was still needed. The first steps were performed by Chen and colleagues in which they developed a web-based subtyping tool (TNBCtype) that determines TNBC molecular subtype using Lehmann's gene expression meta data thus independent of platform (Chen*, et al*, 2012). The TNBCtype tool displays for each candidate TNBC sample a prediction of a subtype, which is based on correlation coefficient, and the permutation *p*-value. The overall purpose of TNBCtype tool was to subtypes for new TNBC samples and as such used as a potential way to facilitate diagnostics thus help tailor treatments for TNBC (Chen*, et al*, 2012). This idea of distinguishing TNBC types and aligning it with an appropriate targeted therapy based on gene expression signature was recently translated to a clinical relevancy by Masuda and colleagues (Masuda*, et al*, 2013). They have revalidated Lehmann and colleagues results by performing analysis of an independent cohort of TNBC consisted of 130 cases treated with neoadjuvant Adriamycin/Cytoxan/Taxol–containing chemotherapy (Masuda*, et al*, 2013). Although the overall pathologic complete remission (pCR) rate was 28%,

subtype-specific responses differed substantially with the BL1 subtype having highest pCR rate (52%) while the BL2, LAR, and MSL subtypes had the lowest response (0%, 10%, and 23%, respectively). Additionally, TNBC subtype was shown to be an independent predictor of pCR status (p= 0.022) by a likelihood ratio test.

Masuda's findings were further confirmed using 163 primary cases in The Cancer Genome Atlas (TCGA) that were defined as TNBC (Mayer*, et al*, 2014). These TCGA TNBC tumors were subtyped using the TNBCtype tool described above. The conclusions of this follow up study were that there was a very similar distribution of subtypes and subtype-specific differences in survival as reported by Masuda and colleagues.

It is becoming evident that TNBC cannot be treated in similar fashion as the rest of breast cancers. A specific alignment of TNBC patient subtype to the treatment appears to be warranted, based on the recent findings of heterogeneity (Shah*, et al*, 2012) and classification of TNBC (Lehmann*, et al*, 2011; Lehmann & Pietenpol, 2014) as well as its clinical relevance (Masuda*, et al*, 2013). Recently TNBC subtype specific therapies were proposed (Davis*, et al*, 2014) based on Lehmann's cell culture data and knowledge of key pathways 'drivers' in each subtype (Table 1). Overall the field is becoming more aware of the complexity of TNBC. Even though treatment according to the molecular TNBC subtypes has not been evaluated in a clinical setting, the emerging findings suggest a potential for translation to clinical setting.

Table 1. Proposed TNBC subtype specific therapies

TNBC subtypes	Molecular characteristics	Potential therapies
Basal-like 1	Cell cycle function Proliferation DNA damage response	Chemotherapy PARP inhibitor
Basal-like 2	Cell cycle function Proliferation Growth factor signaling	Chemotherapy PARP inhibitor
Mesenchymal	EMT Cell motility Differentiation Proliferation	Src inhibitor PI3K pathway inhibitor Wnt pathway inhibitor
Mesenchymal stem-like	EMT Cell motility Differentiation Growth factor signaling Angiogenesis	Src inhibitor PI3K pathway inhibitor Wnt pathway inhibitor
Luminal androgen receptor	AR signaling Luminal cytokeratine	AR antagonist Hsp90 inhibitor PI3K pathway inhibitor
Immunomodulatory	Immune cell processes	Immune targeted agents

AR, androgen receptor; EMT, epithelial mesenchymal transition; PARP, poly ADP ribose polymerase; TNBC, triple-negative breast cancer.

Table 1 Davis, Ther Adv Med Oncol 2014, Vol. 6(3) 88–100

Current standard of care for TNBC and new therapeutic strategies

Treatment of patients with TNBC has been challenging due to the heterogeneity of the disease and the absence of well-defined molecular targets agreeable to therapeutic intervention (Carey*, et al*, 2007; Pegram*, et al*, 1998; Wiggans*, et al*, 1979). The current standard of care treatment is based mainly on chemotherapy, however ongoing trials are exploring alternative avenues including variety of combination therapies targeting specific receptors/pathways some of which are described below.

Chemotherapy

Currently, the cytotoxic chemotherapy is the standard of care treatment for TNBC patients, despite the promise of targeted therapies as demonstrated by Lehmann and colleague (Lehmann*, et al*, 2011). Current best chemotherapy regimen for early breast cancer based on anthracyclines and taxanes. Studies have shown that anthracycline-based chemotherapy of TNBC patients results in 23% increase in disease-free survival (DSF) (Di Leo*, et al*, 2010). Furthermore, in a separate neoadjuvant study, basal-like patients treated with paclitaxel-CAF [cyclophosphamide, doxorubicin (adriamycin), fluorouracil] chemotherapy were associated with increased likelihood of pathologic complete response (pCR) (Rouzier*, et al*, 2005). Similarly, in a neoadjuvant setting consisting of a large cohort of 1118 patients (MD Anderson Cancer Center) treated with chemotherapy (anthracyclines-based regimen) achieved a pCR of 22% (or 28% with addition of taxane) in TNBC patients in comparison to 11% pCR in non-TNBC patients (Liedtke*, et al*, 2008). In a GeparTrio study consisting of taxane-

anthracyclin (TAC: docetaxel, doxorubicin, cyclophosphamide) chemotherapy, the higher pCR rates were in TNBC (38.9%) compared to non-TNBC (15.2%) (Huober*, et al*, 2010). In general, based on the results of clinical trials, non-metastatic TNBC treated with neoadjuvant chemotherapy appear to have better response compared to non-TNBC. This is paradoxical as the overall prognosis for TNBC patients is poorer compared to non-TNBC patients. This was demonstrated in the 1118 cohort where TNBC patients despite having higher pCR (22%, 28%) compared to non-TNBC (11%); only had 74% survival (3 years) compared to 89% survival in non-TNBC patients (Liedtke*, et al*, 2008). Thus even though a fraction of TNBC patients do respond favorably to chemotherapy the side effects toxicities are significant, but most importantly ultimately even the pCR patients eventually relapse. Overall, the standard of care revolving around anthracycline/taxane-based regimen might not be the most appropriate option for TNBC as it benefits a small percentage and it does not guarantee an absence of relapse.

Chemotherapies are likely to preferentially benefit a fraction of TNBC patients because of rapid proliferation rates as well as the intrinsic genomic instability of TNBC cells dictated by deficiency in DNA repair (Graeser*, et al*, 2010). However, the observed high frequency of BRCA1 mutation in TNBC (Gonzalez-Angulo*, et al*, 2011; Turner*, et al*, 2010) has stimulated the idea to use platinum-based chemotherapy (cisplatin, carboplatin) more routinely in TNBC patients. Considering that BRCA1 and BRCA2 are crucial in regulating DNA double-strand break repair by mediating homologous recombination (HR) and

thus maintaining DNA stability (McCabe*, et al*, 2006), it has been hypothesized that mutations in these genes would lead to higher sensitivity to platinum agents as these cause to DNA cross-link strand breaks. The idea that TNBC would be sensitive to platinum salts was suggested by a cisplatin-based TNBC study (Garber trial) where overall efficacy in neoadjuvant setting was 22% and pCR was associated with both mutation of and low expression of BRCA (Silver*, et al*, 2010). Further studies demonstrated an 83% pCR rates in women with BRCA1-positive breast cancers after neoadjuvant chemotherapy with single-agent cisplatin (Byrski*, et al*, 2010). Additional evidence for efficacy of platinum agents, this time addition of carboplatin to TNBC patients (N= 315) from GeparSixto trial (GBG 66) resulted in an increase of the pCR rate from 37.9% to 58.7% (Von Minckwitz*, et al*, 2013). By contrast, the addition of carboplatin did not improve pCR in the GEICAM 2006-03 phase II randomized trial (Alba*, et al*, 2012). This raises a couple of points, first that carboplatin might not be as effective as cisplatin but also that platinum-based regimen is affected by the rich molecular diversity of TNBC (similar to what we see in anthracyclin/taxane treatments). Considering that the heterogeneity of TNBC poses problems to current treatments, it is critical to identify predictive biomarkers to inform a better selection of more precise therapies for patients. Investigation of new therapeutic approaches based on the genetic and biological underpinnings of TNBC subtypes is of a great need (Mayer*, et al*, 2014).

Targeted therapy

Targeting genomic instability (DNA repair mechanisms and PARP inhibitors)

As mentioned above, BRCA mutations are frequent in TNBC patients (Foulkes*, et al*, 2003) while the TNBC patients without BRCA mutation still exhibit defects that are associated with BRCA related functions (Turner*, et al*, 2004). Through homologous recombination, BRCA genes are involved in repair of double-stranded breaks. Thus, in tumors with BRCA mutation, inhibiting additional pathways of DNA repair could lead to cell death. Considering that BRCA-deficient tumors rely on poly-AD-ribose polymerase (PARP) to mediate DNA repair it was a logical step to pursue PARP inhibitors as a new target in TNBC. Since PARP enzymes are critical for appropriate processing and repair of DNA breaks (Johnson*, et al*, 2011), PARP inhibition resulted in high antitumor activity (Farmer*, et al*, 2005; Fong*, et al*, 2009; Lord*, et al*, 2006; Tutt & Ashworth, 2008; Tutt*, et al*, 2010) due to unrepaired single-strand breaks that degenerate to double-strand breaks. Similar to platinum compounds, PARP inhibition (iniparib) has shown an impressive clinical response (Telli ML*, et al*, 2011) especially in patients with BRCA1-mutations where disease-free and overall survival significantly improved (from 32% to 52%) when combined with carboplatin and gemcitabine (O'Shaughnessy*, et al*, 2011a). However, other TNBC patients that appeared to have a BRCA-deficient phenotype have not responded as expected to PARP inhibition (olaparib) (Gelmon*, et al*, 2011). Further more, a large multicenter phase III trial evaluating addition of iniparib to carboplatin and gemcitabine failed to meet its specified endpoints goals for progression-fee and overall survival. Although the trial failed its specified statistical criteria did not

show a signal of efficacy to determine its mechanism of action, thus there may be TNBC patients that could be sensitive (O'Shaughnessy*, et al*, 2011b). In addition to iniparib and olaparib, other studies have evaluated valiparib and have demonstrated promising results in metastatic breast cancers of any type with BRCA-mutation (Fong*, et al*, 2009) (Somlo*, et al*, 2013). Overall, these mixed results speak again to the biological, genetic and biochemical diversity of TNBC, which has not been addressed in trials to date.

Targeting the adaptive cellular state (PI3K/AKT/mTOR pathways)

The phosphatidylinositol 3 kinase (PI3K), V-Akt-murine thymoma viral oncogene homolg 1 (AKT) and mammalian repressor of rapamycin (mTOR) pathway is a known oncogenic driver in human cancer and it can regulate cell proliferation, apoptosis and migration among others (Bader*, et al*, 2005). Activation of PI3K can be triggered via growth factor receptor pathways or integrin-mediate pathways, and once PI3K is active it leads to downstream signaling which result in AKT activation, and ultimately activation of mTOR (Vivanco & Sawyers, 2002). Mutations in PI3K pathway are commonly found in both ER/PR/HER2 positive as well as TNBC cancers (PIK3CA 10.2%) (Baselga, 2011; Lopez-Knowles*, et al*, 2010; Marty*, et al*, 2008). PIK3CA mutations have also been observed in metaplastic breast carcinomas (47%), which as described above, is an infrequent and very aggressive TNBC subtype (Hennessy*, et al*, 2009). It is also interesting to note that studies have demonstrated an association between upregulation of PI3K/AKT pathway and PTEN (a tumour suppressor and negative regulator of the PI3K pathway) loss, which occurs in ~30% of TNBC and

is associated with poorer overall survival (Adamo*, et al*, 2011; Korse*, et al*, 2012).

The PI3K/AKT/mTOR pathway is becoming a promising therapeutic target in TNBC, as indicated by emerging preclinical finding and ongoing clinical trials. Preclinical *in vitro* and *in vivo* studies suggested combining PI3K inhibitors with PARP. For example, in an *in vitro* study, administration of PARP inhibitor and PI3K combination was more efficacious, as they significantly decreased cell growth, then when applied individually to breast cancer cells (Kimbung*, et al*, 2012). Furthermore, in BRCA1 deficient breast cancer mouse model, treatment with a combination of PI3K (BKM120) and PARP inhibitors (olaparib) resulted in a significant decrease in tumor growth, suggesting a synergistic effect is more favorable then mono-therapy approach.

Overall, data suggest that targeting the PI3K pathway could be clinically relevant in TNBC. In addition, although there are no published results to date, the ongoing mTOR clinical trials will further elucidate the role of everolimus and other mTOR inhibitors (ex. temsirolimus) in neoadjuvant setting.

Targeting growth factor receptors

EGFR: Based on multiple reports, the expression of epidermal growth factor receptor (EGFR) in the TNBC is not uncommon as it can found in 45%-70% of TNBC (Nielsen*, et al*, 2004). This finding has made EGFR an attractive target for therapy. Multiple trials have attempted various drug combination approaches, to test the efficacy of EGFR inhibitors. It is not a surprise that once again we will be witnessing mixed results as far as the current progress in

treating TNBC patients with EGFR drugs.

In the Translational Breast Cancer Consortium (TBCRC 001) randomized phase II study, when cetuximab, anti-EGFR monoclonal antibody, was used alone it was less effective (6% response rate); however it did improve efficacy, although still low, when used in combination with carboplatin (17% response rate) (Carey*, et al*, 2012). Furthermore, in US Oncology 225200 Trial, adding cetuximab to carboplatin and irinotecan increased the response rate from 30% to 49%, however it did not improve progression-free survival (O'Shaughnessy*, et al*, 2007). Modest benefits of addition of cetuximab to cisplatin was observed in the largest EGFR trial, BALI-1, which evaluated 173 TNBC patients. The results of the trial indicated improvement in progression–free survival, however no change in response rate or overall survival was achieved (Baselga*, et al*, 2013). Besides cetuximab, tyrosine kinase inhibitors (TKIs) targeting EGFR were tested, such as erlotinib, lapatinib and gefitinib in addition to the standard chemotherapy regimens (Bernsdorf*, et al*, 2011; Finn*, et al*, 2009a; Finn*, et al*, 2009b; Sharma*, et al*, 2010) and these once again yielded modest results.

Overall it would appear, based on the results of multiple trials across multiple EGFR inhibitors, that only small subset of TNBC patients do respond to EGFR therapy. The inconsistency in the results would indicate that there should be a better selection process of TNBC patients that should receive the EGFR inhibitors.

FGFR: Fibroblast growth factor receptor (FGFR) plays role in regulation of

cell survival, proliferation, differentiation, and migration (Haugsten*, et al*, 2010). In approximately 10-13% of breast cancers (9% TNBC) FGFR1 amplification has been observed while in only 1-2% of breast cancer (2-4% TNBC) FGFR2 is found amplified; and both are associated to poor outcome (Courjal*, et al*, 1997; Gelsi-Boyer*, et al*, 2005). Currently, FGFRs are being exploited therapeutically with specific FGFR inhibitors that show activity in preclinical models and patients with breast cancer (Andre*, et al*, 2013; Gozgit*, et al*, 2012; Shiang*, et al*, 2010). *In vitro* testing of Pan-FGFR TKIs was shown to reduce cell growth in breast cancer cells that had activated FGFR signaling, but the same drugs had little to no effect on cells without the activated pathway (Gozgit*, et al*, 2012; Shiang*, et al*, 2010). Clinical trials with FGFR inhibitors are currently ongoing, however Andre and colleagues have reported their finding for the phase II trial of dovitinib, a first generation multi-tyrosine kinase inhibitor that targets FGFR1, FGFR2 and FGFR3 in patients with metastatic breast cancer (n= 81) prescreened for FGFR1 amplification (Andre*, et al*, 2013). Their results indicated that the ER+ patients who did not have FGFR1 amplification did not respond compared to the ER+ patients with the FGFR1 amplification (Andre*, et al*, 2013). Thus, dovitinib is showing better activity in breast cancers with FGFRs amplified. Targeting FGFRs is still an under explored area however initial results look promising and could potentially be applicable targeting approach for TNBC patients as they too present with FGFR amplification (9-13%).

VEGFR: Vascular endothelial growth factor receptor (VEGFR) plays an important role in angiogenesis and as such it has been an attractive therapeutic

target in cancers. Similarly to EGFR trials, targeting VEGFR alone has shown a limited activity as demonstrated in Phase II sunitinib trial of pre-treated metastatic patients where overall response was 11% however it is interesting to note that TNBCs had higher response in this cohort (15%) (Burstein*, et al*, 2008). Furthermore, additional studies have shown increase in overall outcome when treated with sorafenib in combination with chemotherapy (Gomez*, et al*, 2010; Hudis*, et al*, 2011). The SOLTI-0701 trial focused on an analysis of TNBC patients (N = 53) and have shown an improvement in median progression-free survival when sorafenib added to capecitabine (Baselga*, et al*, 2009). Contrary to these findings, a phase III adjuvant therapy in triple negative breast cancer (BEATRICE) trial in which bevacizumab was added to the standard adjuvant chemotherapy demonstrated no significant improvement in progression-free survival (Cameron*, et al*, 2013).

The TGF-β superfamily and signaling in cancer

Transforming growth factor beta (TGF-β) related cytokines have effects on numerous cellular processes (during normal development and carcinogenesis) among which are cell proliferation, differentiation, morphogenesis, tissue homeostasis and regeneration, apoptosis, cytoskeletal organization, migration, and adhesion. The signal transduction process for TGF-β is fairly complex and highly dependent on the cellular context (e.g. cell type, microenvironment, epigenetic landscape). The signaling process has been studied for over two decades and, for the most part, it is firmly in hand. However, the promiscuity of the TGF-β pathway dictated by the cellular context is not very well understood.

The paradoxical idea that TGF-β can act as both suppressor and promoter is very intriguing and is of current interest in the TGF-β field, driven by the need to further understand its capabilities and behavior.

Signaling by TGF-β superfamily members

TGF-β superfamily includes close to 40 ligands in mammals (among which there are three TGF-β isoforms, 10 bone morphogenetic proteins/BMPs, four activin β-chains, one nodal and 11 growth/differentiation factors/GDFs); similar orthologs are found in other species (e.g. Drosophila, Xenopus, C. elegans) (Figure 5) (Schmierer & Hill, 2007). The receptors for TGF-β superfamily can be broken down into two groups; type I and type II receptors, which are encoded by seven and five genes in the human genome, respectively (Schmierer & Hill, 2007). Furthermore these receptors, for the most part, are comprised of diverse cysteine-rich extracellular domain, a single-pass transmembrane domain, and serine/threonine kinase domain (a feature unique to this family) (Shi & Massague, 2003).

The mechanism of signaling for TGF-β ligands is similar among all the ligands, as they all require two types of serine/threonine kinase receptors (type II and type I) to signal downstream. Some ligands have lower affinity thus require assistance from co-receptors in order to bind at optimal level (Schmierer & Hill, 2007). Among this large family of ligands are three TGF-β isoforms: TGF-β1, TGF-β2 and TGF-β3.

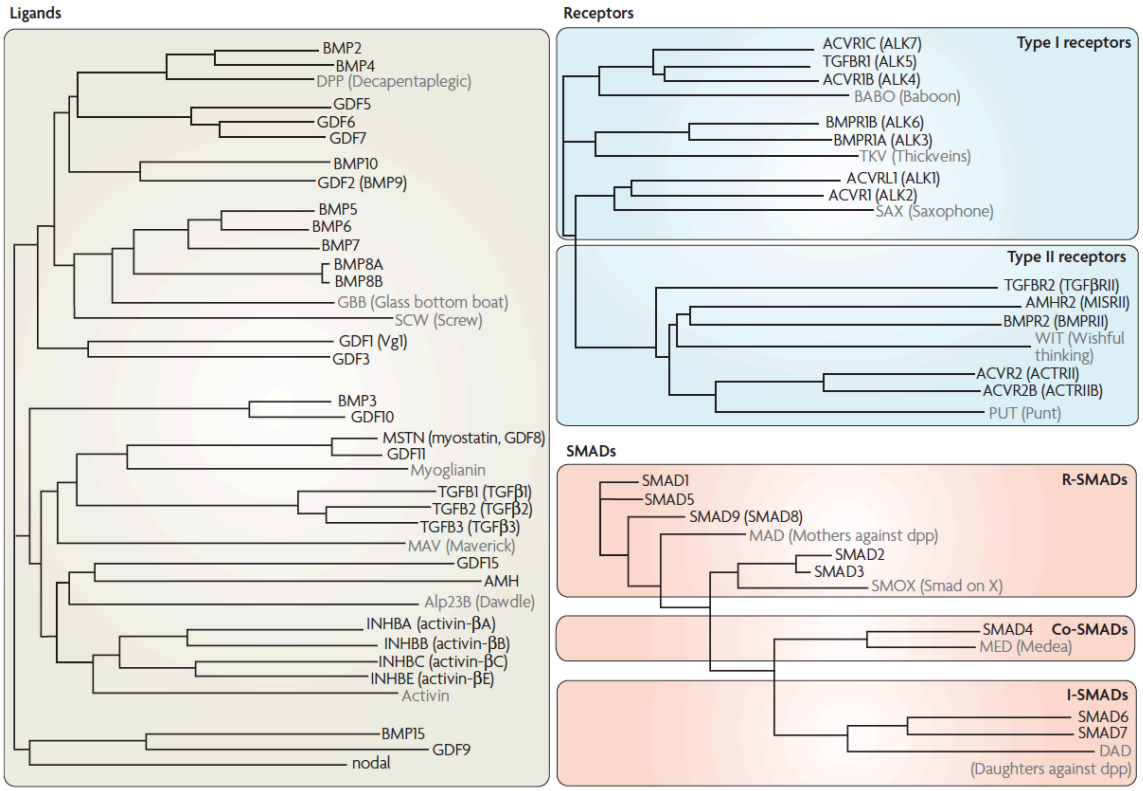

Schmierer, Nature, 2007

Figure 5. TGF-β superfamily: ligands, receptors and smads.
Phylogenetic trees141 derived from protein alignments of the core components of TGFβ signalling pathways in humans and Drosophila melanogaster. Human proteins are shown in black and D. melanogaster proteins are in grey. Protein symbols are given with alternative names in parentheses. For the ligands, the putative, mature, fully processed forms were used to construct the tree. ACVR, activin receptor; ALK, activin receptor-like kinase; AMH, anti-Muellerian hormone; AMHR2, AMH receptor-2; BMP, bone morphogenetic protein; BMPR, BMP receptor; GDF, growth and differentiation factor; I-SMAD, inhibitory SMAD; R-SMAD, receptor-regulated SMAD; TGF, transforming growth factor; TGFBR, TGFβ receptor. ***(Figure 1, Schmierer, Nature 2007)***

Each one of these ligands is encoded by separate gene (Derynck*, et al*, 1988; ten Dijke*, et al*, 1988) synthesized as precursor polypeptide, which is processed into an inactive (latent) form composed of latency associated peptide (LAP) bound through disulfide bonds to latent TGF-β binding protein (LTBP) (Munger*, et al*, 1997). Latent TGF-β is then secreted and accumulates within the extracellular matrix, and until activated (LAP dissociates from mature TGF-β) they are unable to bind to receptors (Stover*, et al*, 2007). Once activated, the TGF-β ligands TGF-β1, TGF-β2 and TGF-β3 can interact with the transforming growth factor receptors - type II (*TGFBR2*/TβRII), type I (TGFBR1/TβRI or ALK5), and type III (betaglycan/*TGFBR3*/TβRIII) (Bierie & Moses, 2006b; Derynck & Zhang, 2003; Siegel*, et al*, 2003). The TGF-β1 and TGF-β3 ligands can interact with TβRII directly due to their high affinity for this receptor while TGF-β2 binding requires the presence of TβRIII in order for high affinity binding to TβRII to occur (López-Casillas*, et al*, 1994; Lopez-Casillas*, et al*, 1993). TβRII is a serine/threonine kinase receptor that is constitutively active through autophosphorylation. Once bound to TGF-β ligands, TβRII is able to recruit and transphosphorylate TβRI at several serine/threonine residues in juxtamembrane domain rich in glycine and serine residues (GS domain; conserved in type I receptors) (Feng & Derynck, 2005).

The transactivation of GS domain of TβRI enables recruitment of the receptor regulated SMADs (R-SMADs: SMAD2, SMAD3) promoting downstream Smad-dependent (canonical pathway) and Smad-independent signaling (non-canonical pathway) (Brown*, et al*, 2007; Siegel*, et al*, 2003). In the classic

canonical smad-dependent signaling cascade, TβRI phosphorylates Smad2 and Smad3 on two serine residues leading to their activation which results in their release and subsequent heteromeric complex formation with the common mediator Smad (Co-Smad), Smad4 (Shi & Massague, 2003).

The active heteromeric R-Smad/Smad4 complex is able to bind DNA in the nucleus along with other transcription factors, co-activators and co-repressors where they are directly involved in regulating transcription of target genes (among which are genes associated with TGF-β mediated cell cycle arrest), both positively and negatively (Brown*, et al*, 2007; Siegel*, et al*, 2003). In addition to signaling through activated Smad complexes, TGF-β is able to regulate cell behavior though Smad-independent signaling cascades. The major Smad-independent networks that have been directly associated with TGF-β signaling are known to include genes involved in regulation of migration and invasion (ex. RhoA, Cdc42, Rac1), polarity protein which leads to disassembly of tight junctions (Par6) thus important in TGF-β-mediated epithelial to mesenchymal transition (EMT) (Ozdamar*, et al*, 2005), and many other genes (e.g. Ras, PI3K, PP2A, MEKK1, TAB1/TAK1, Daxx) (Bierie & Moses, 2006b; Derynck & Zhang, 2003; Siegel*, et al*, 2003) (Figure 6). Finally, it is important to note that TGF-β response of each of these pathways, both Smad dependent and independent, is determined by level of receptor expression and net activation for each pathway present at the time of stimulation (Moses & Barcellos-Hoff, 2011).

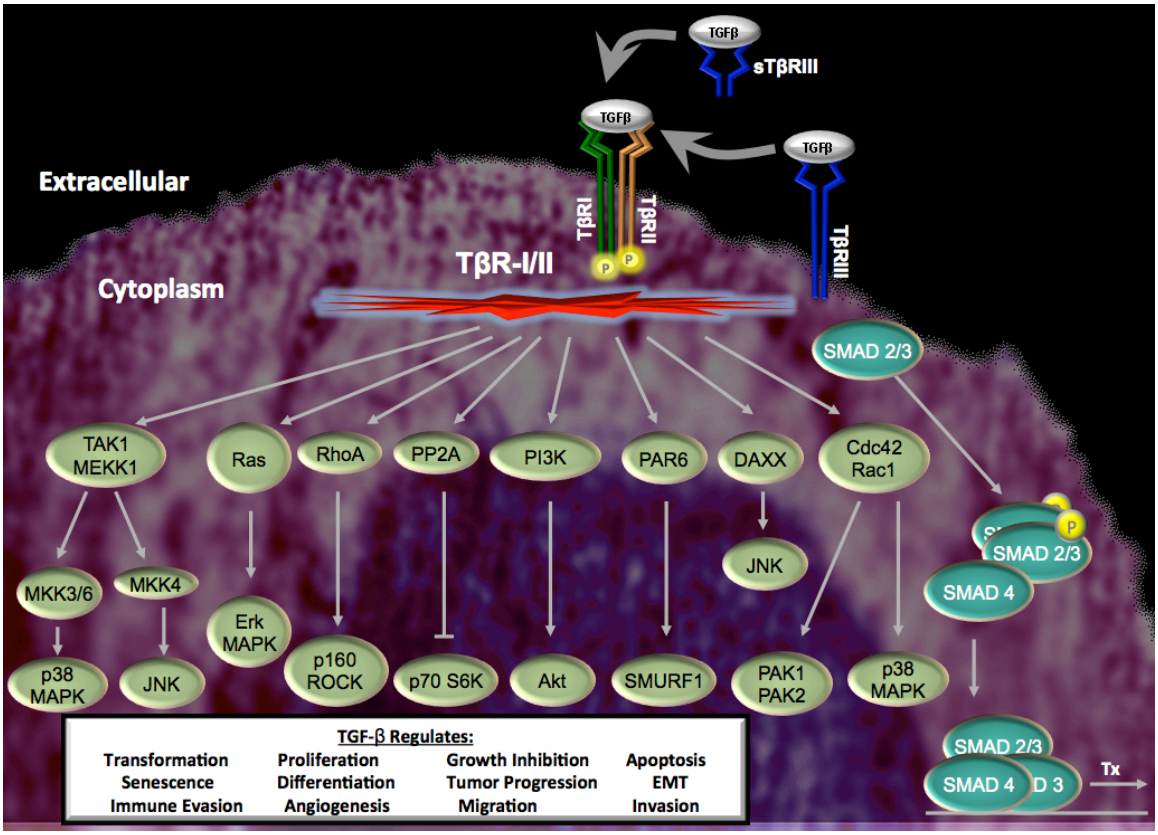

Figure 6. Simplified overview of TGF-β signaling pathway

Eventually, the termination of TGF-β signaling is thought to be mediated by another group of Smads known as inhibitory Smads (I-Smads: Smad 6 and Smad 7) (Itoh & ten Dijke, 2007).

TGF-β signaling pathways are powerful regulators of cancer initiation and progression through tumor cell autonomous and non-autonomous signaling (Bierie & Moses, 2006a; Bierie & Moses, 2006b; Bierie*, et al*, 2008; Roberts & Wakefield, 2003). Initially thought of as a tumor suppressor and then as a mediator of tumor progression, TGF-β signaling demonstrates important functions in regulating cancer.

The regulation of normal and carcinoma associated epithelial cell behavior was first described almost three decades ago (Shipley*, et al*, 1986; Tucker*, et al*, 1984). Subsequently, a large number of studies have been able to demonstrate a diverse range of tumor cell autonomous and tumor cell independent mechanisms for the regulation of carcinoma initiation and progression by TGF-β both *in vitro* and *in vivo*. Within normal epithelium TGF-β is known to induce arrest of the cell cycle, and during early tumor progression it is thought that this regulation is a major contribution to carcinoma cell autonomous TGF-β mediated tumor suppression (Bierie & Moses, 2006a; Siegel*, et al*, 2003). While In later stages of tumor progression, TGF-β signaling is thought to increase tumor progression (Akhurst & Derynck, 2001; Bierie & Moses, 2006b; Cui*, et al*, 1996). TGF-β stimulation in some normal and carcinoma associated epithelial cell populations is also known to induce EMT, which may promote enhanced carcinoma cell migration and invasion (Brown*, et al*, 2004; Cui*, et al*, 1996; Miettinen*, et al*,

1994). Combined, these observations suggested that TGF-β has a dual function both as an epithelial cell autonomous tumor suppressor or tumor promoter depending on the cell type and context of stimulation.

Genetically engineered mouse models of breast cancer provide support that epithelial TGF-β signaling has a tumor suppressive role during early stage of tumorigenesis (Massague, 2008) while enhancing late tumor progression through increasing of carcinoma cell invasion and metastasis (Oft*, et al*, 1998; Oft*, et al*, 1996). Conditional deletion of TβRII in epithelial cells *in vivo* resulted in increased lobular-alveolar cell proliferation/hyperplasia (Chytil*, et al*, 2002; Forrester*, et al*, 2005). When the floxed *Tgfbr2* mouse was crossed with MMTV-Cre, it was shown that TGF-β signaling suppressed hyperplastic growth of mammary lobular-alveolar units and had a role in promoting mammary epithelial cell survival. Notably, when TβRII was deleted in the MMTV-PyVmT mouse model, a decrease in the tumor latency as well as a dramatic increase in lung metastases was observed (Forrester*, et al*, 2005). Furthermore, the decreased expression of TβRII in human breast cancers has been shown to be associated with increased breast cancer progression (Gobbi*, et al*, 1999). Even though it has been established that TGF-β signaling is context dependent, it is surprising that to date we know little about the role of TGF-β in progression across different molecular subtypes of breast cancer. A recent study by Lehmann and colleagues has demonstrated that among the top differentially expressed pathways that define mesenchymal and mesenchymal-stem like subtype of triple negative breast cancer are pathways is TGF-β pathway along with pathways/processed that are

TGF-β-mediated such as ECM receptor interaction, focal adhesion, cell motility, cell differentiation, and integrin pathways (Lehmann*, et al*, 2011).

TβRIII - the 'orphan' of the TGF-β superfamily

There has been significant focus on TβRI and TβRII due to their receptor-kinase activity; however, research on TβRIII has lagged due to its lack of intrinsic enzymatic activity. *TGFBR3*/TβRIII (also known as betaglycan) is a transmembrane proteoglycan with a large extracellular domain (766AA) and very short cytoplasmic domain (42AA). The core of TβRIII protein has a predicted molecular weight of around 100kDa, but can also range in sizes between 180-400kDa due to glycosaminoglycan post-translational modifications (López-Casillas*, et al*, 1994; Wang*, et al*, 1991).

TβRIII can be found as membrane bound and soluable protein. The extracellular domain is the source of the soluable form of TβRIII (sTβRIII). It is secreted into extracellular environment due to presence of proteolytic cleavage site in the extracellular domain (adjacent to transmembrane domain), thus TβRIII can be detected in the serum and extracellular matrix (Andres*, et al*, 1991; Andres*, et al*, 1989; Lopez-Casillas*, et al*, 1991). The short cytoplasmic domain lacks enzymatic activity and it is not essential for arbitrating ligand presentation. However studies have shown that TβRIII's cytoplasmic domain can play a role in regulating TGF-β signaling (Blobe*, et al*, 2001a; Blobe*, et al*, 2001b; Lee*, et al*, 2010; López-Casillas*, et al*, 1994; You*, et al*, 2007) since it can bind to cytoplasmic domain of TβRII leading to formation of an active TβRII-TβRI

signaling complex. The cytoplasmic domain of TβRIII interacts with β-arrestin2 and GAIP interacting protein C-terminus (GIPC) (Blobe*, et al*, 2001a; Chen*, et al*, 2003). The interaction of TβRIII with β-arrestin2 has been shown to down-regulate TGF-β signaling (Chen*, et al*, 2003), while interaction with GIPC leads to stabilization of TβRIII at the cell surface and enhancement of TGF-β signaling (Blobe*, et al*, 2001a).

TβRIII is the most abundantly expressed TGF-β superfamily receptor with twenty-times more receptors per cell membrane then TβRI or TβRII (Cheifetz*, et al*, 1986; Massague, 1985; Massague & Like, 1985; Wang*, et al*, 1991). This protein is best characterized as a TGF-β superfamily co-receptor due to its ability to present TGF-β ligand to TβRII. Recent studies implicate TβRII as playing an essential role in heart and whole organism development (Blobe*, et al*, 2001b; Chen*, et al*, 2003). Deletion of exon 2 of *Tgfbr3* resulted in embryonic lethality in murine system. TβRIII null mouse embryos demonstrated increased apoptosis in the liver and defects in development of heart ventricles leading ultimately to the lethality of the embryo (Stenvers*, et al*, 2003). Embryonic lethality due to defects in heart development was also observed in TβRIII mouse model with exon 3 deletion (Compton*, et al*, 2007). The phenotype in this model demonstrates defects in coronary vasculogenesis as well as shape irregularities and size reduction of coronary vessels. Embryos also exhibited abnormal epicardium (Compton*, et al*, 2007)**.** Both of these TβRIII knockout mouse models demonstrate that TβRIII is required for the normal somatic development, especially in the case of cardiac development and is thus it is essential for

viability.

As previously mentioned TGF-β is a critical regulator of growth and development of normal mammary gland but also is involved in human breast cancer. Recently studies have demonstrated a frequent loss of TβRIII in human breast cancers (Dong*, et al*, 2007). The loss of TβRIII expression was correlated to progression from pre-invasive to invasive state of breast cancer. In addition, restoring expression of TβRIII in breast cancer cell line led to decrease of tumor invasiveness *in vitro* and tumor invasion and metastasis *in vivo* (Dong*, et al*, 2007).

To this date the functional context of TβRIII remains controversial in breast cancer. Some reports demonstrate a tumor suppressive function of TβRIII (Dong*, et al*, 2007), while other reports indicate a tumor-promoting role (Criswell*, et al*, 2008). This project will challenge the current paradigms not only in the field of TβRIII but also in the TGF-β and the TGF-β superfamily.

Targeting TGF-β signaling

Currently there are three strategic approaches to therapeutic targeting of TGF-β signaling. The first approach revolves around targeting ligands using small molecules to prevent TGF-β synthesis on mRNA level. Second approach entails inhibition of receptor-ligand interaction using a 'ligand trap' (e.g. monoclonal antibodies, soluble receptors). The third approach is involves usage of small molecule receptor kinase inhibitors to prevent TGF-β signal transduction (Padua & Massague, 2009).

Each one of these therapeutic approaches has representative drugs, which are currently either in pre-clinical or early stages of clinical testing for different types of cancers (e.g., glioblastoma, pancreatic, lung, breast etc.) (Lampropoulos*, et al*, 2012; Muraoka*, et al*, 2002; Nam*, et al*, 2008; Oettle*, et al*, 2012; Rowland-Goldsmith*, et al*, 2002; Yang*, et al*, 2002). An antisense RNA molecule, AP12009 (Trabedersen, Pharma), has shown promising results in Phase I/II study in patients with high-grade glioma overexpressing TGF-β2 (Hau*, et al*, 2007; Schlingensiepen*, et al*, 2011). Other pre-clinical studies are being done in prostate, non-small lung cancer and melanoma using AP11014 and AP15012 antisense molecules (Lampropoulos*, et al*, 2012).

'Ligand traps' is another approach for controlling excess of TGF-β production and these include monoclonal neutralizing antibodies such as 1D11 (binds TGF-β1, 2 and 3) (Nam*, et al*, 2008); soluable TGF-β receptors such as TβRII and TβRIII (Meulmeester & Ten Dijke, 2011) and TGF-β receptors antibodies such as anti-TβRI monoclonal antibody (Goff*, et al*, 2012). A third approach, the signal transduction blockage, can be broken down into two strategies. The first strategy involves usage of receptor kinase inhibitors, while the second revolves around targeting TGF-β signaling components (e.g., Smads) using aptamers (peptides that specifically binding to a targeted molecule) (Connolly*, et al*, 2012). Although, there are currently three major therapeutic designs targeting TGF-β, there is still more evaluations to be done. Overall, the complexity of TGF-β dictated by the dual role in cancer creates roadblocks to successful therapeutics, thus further studies of contextual-dependence of TGF-β

are necessary.

Role of tumor microenvironment in breast cancer

Importance of stroma in normal mammary gland development and tumor progression

The focus of studies of breast development and cancer has been on the epithelial cell component of the mammary gland. Recently, rather than being considered simply as structural support, stromal components have been recognized as an important regulator of epithelial cell behavior (Mueller & Fusenig, 2004; Wiseman & Werb, 2002). The composition of the stroma associated with the normal mammary gland is greatly different than the tumor stroma. In the case of the normal gland, there is little connective tissue, which is mainly concentrated around the ducts. In addition, the stromal compartment of the normal mammary gland is mainly composed of adipose tissue. The microenvironment of the normal gland sends out positional cues to the mammary epithelial cells, which allow for the orientation of epithelial cells into regular structures. In the cancerous gland, this process is interrupted (Bissell*, et al*, 2002). Mammary stroma is a structurally complex and heterogeneous tissue with numerous components: fibroblasts, adipocytes, extracellular matrix, basement membrane, blood vessels and inflammatory cells. These components are essential for normal mammary gland development (Djonov*, et al*, 2001; Gouon-Evans*, et al*, 2000; Kuperwasser*, et al*, 2004) and during tumor formation and progression each of these components can be exploited allowing the epithelial

cell invasion into the surrounding stroma (Iyengar*, et al*, 2003; Pollard, 2004; Shekhar*, et al*, 2001).

Unlike scarce connective tissue in the normal breast stroma, the tumor stroma contains abundant connective tissue. The high levels of connective tissue are associated with increased secretion of growth factors that can affect the behavior of epithelial cells both mechanically due to stromal stiffness (Paszek*, et al*, 2005) and biochemically due to altered signaling (Wiseman & Werb, 2002). Among previously mentioned stromal components, lying embedded within the matrix are spindle shaped cells known as fibroblasts. These cells are responsible for connective tissue production, due to their ability to secrete extracellular matrix components and growth factors. They can also regulate wound healing, differentiation and morphogenesis of epithelial cells. It has been shown that fibroblasts play an important role in tumor progression such as their ability to form a dense microenvironment due to collagen secretion (Weaver & Werb, 2007). Fibroblasts are important in maintaining the composition of the extracellular matrix by secreting collagen types I, III and V, fibronectin and matrix metalloproteinases (Lu*, et al*, 2012). In addition, these cells are also involved in basement membrane formation due to their ability to secrete laminin and type IV collagen (Kalluri & Zeisberg, 2006). The presence of a dense collagenous stroma containing fibroblasts is observed in breast carcinomas and is thought to contribute to tumor progression. This phenomenon of secretion of large amounts of collagen and other extracellular matrix proteins is known as a desmoplastic response (Shao*, et al*, 2000).

Desmoplasmic response-derived changes in the extracellular matrix promote alterations in breast density, which have been recognized as a high risk factor for developing breast cancer (Walker, 2001).

In addition to their role in the maintenance of the extracellular matrix, fibroblasts are vital for the differentiation and homeostasis of many epithelial tissues (Kalluri & Zeisberg, 2006; Shannon & Hyatt, 2004). Recent studies demonstrate the importance of fibroblasts in normal mammary gland development but also in tumorigenesis. Stromal-epithelial interactions in the mouse mammary gland have been studied using a widely applied technique called the mammary fat pad clearing transplantation system. With this technique the undeveloped gland is removed from the fat pad prior to puberty. Removal of the epithelial glandular component leaves a fat pad "cleared" after which mammary epithelial cells can be grafted in and grown to form a functional mammary gland (Deome*, et al*, 1959). This system has been exploited by developing a mouse model in which both the stromal and epithelial components of the reconstructed mammary gland are of human origin (Kuperwasser*, et al*, 2004). Kupperwasser and colleagues have demonstrated that by co-injecting immortalized human breast fibroblasts with mixture of primary human mammary epithelial cells, stroma can be humanized and as a result the cells grew to form functional ductal and lobuloalveolar structures. This suggests the importance of fibroblasts for mammary epithelial growth and invasion in both development and tumorigenesis (Kuperwasser*, et al*, 2004). Stroma can modify the tumor cells' ability to recognize or respond to autocrine and paracrine signals. Thus, the

surrounding microenvironment can have an effect on tumor progression.

Alteration in stromal composition as a risk factor in breast cancer

Stromal cells have a substantial influence on the behavior of epithelial cells in the mammary gland. It has been shown that alterations in stromal characteristics can physically affect the nearby epithelial cells. Weaver and collegues have demonstrated that if mammary epithelial acini are cultured under different collagen concentrations they exhibit alterations in acini morphology as well as localization of signaling molecules (Paszek*, et al*, 2005). Their results illustrate that an increase in the stiffness induces an increase in cell growth, disrupts lumen formation by altering adhesion proteins and cellular polarity. This illustrates that tumor stroma stiffness can have mechanical influence on tumor cell behavior.

This is not the only example of negative influence of stiff stroma, based on the American Cancer Society Surveillance Research, breast density is found among top relative risk factors for developing breast cancer (Society, 2009). An interesting study performed by Boyd and colleagues has illustrated different categories of breast density in cancer free patients ranging from a low (0%) to high (50% to 75%) percentage (Boyd*, et al*, 2005). The study associated these breast density percentages with collagen levels and showed that increased breast density correlates with an increase of collagen. They further demonstrated that with an increase of breast density there is a decrease of fat levels and an increase of collagen levels in the breast (Figure 7). In addition, females with higher levels of breast density were at higher risk for developing breast cancer

Part 1

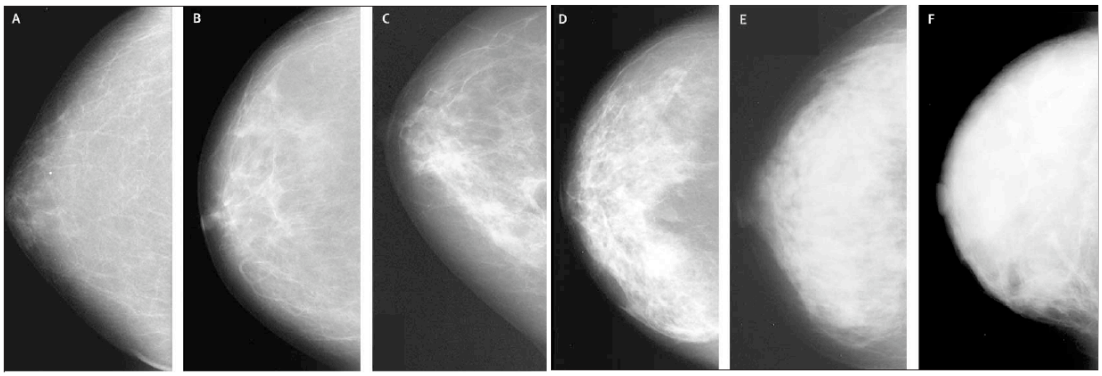

Part 2

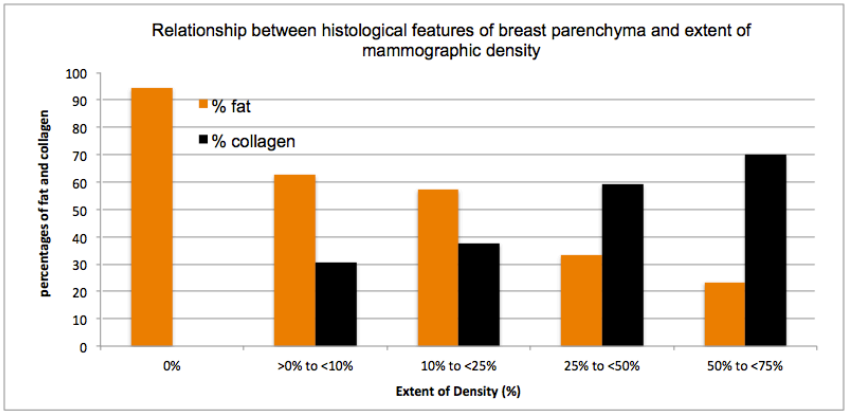

Boyd, The Lancet, 2005

Figure 7. Relationship between mammographic density and histological features of breast parenchyma.

Part1. Categories of percentage mammographic density estimated by radiologists A=0. B=10%. C=25%. D=50%. E=75%. F=75%. Reproduced with permission from ref 8. (*Figure 2: Boyd et al. N Engl J Med 2002; 347: 886–94*)

Part 2. Column bar graph representing relationship between mammographic density and histological features of breast parenchyma was graphed based on the *Table 6, Boyd et al, J Nat Can Inst; Vol. 84, No. 15, August 5, 1992.*

(Boyd*, et al*, 1992).

Another study has looked at ratios of previously mentioned stromal components to tumor in breast cancer patients. The focus of their study was to determine how the stromal characteristics affect patient outcome. Their goal was to evaluate the prognostic value of stroma to tumor ratio in breast cancer patients. The experimental approach consisted of analyzing a cohort of about 600 patients using visual estimation performed by a trained pathologist (Kruijf*, et al*, 2010). Based on their analysis they grouped patients into two groups: (i) stroma rich and (ii) stroma poor (Figure 8). Stroma rich patient samples consisted of more than 50% of intra-tumor stroma while patients with less than 50% of intra-tumor stroma were quantified as stroma poor patients. This study demonstrated that the tumor to stroma ratio in the primary tumor is a prognostic factor in early breast cancer patients due to the fact that stroma rich tumor patients had a shorter overall survival and worse relapse free period in comparison to stroma poor breast cancer patients (Figure 8C) (Kruijf*, et al*, 2010).

Stromal gene expression profiles can predict outcome

Molecularly based classification of breast cancer performed by Perou and colleagues of whole tumor tissues, demonstrating the heterogeneity within breast cancer has been demonstrated over a decade ago (Perou*, et al*, 2000). Furthermore Sorlie and colleagues have aligned these breast cancer subtypes to the clinical outcomes, demonstrating that some of the subtypes performed bett

Part 1. Stromal stiffness and tumor progression

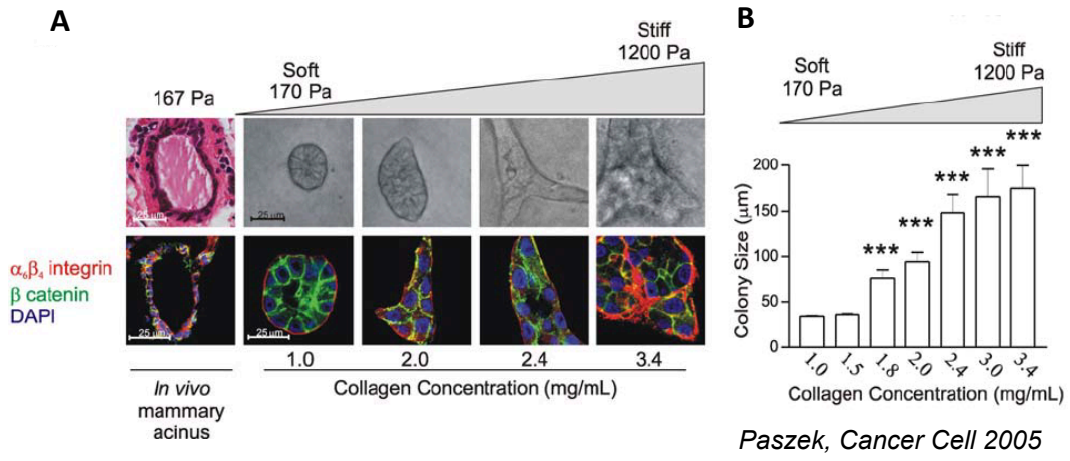

Paszek, Cancer Cell 2005

Part 2. Poorer prognosis for stroma-rich breast cancer patients

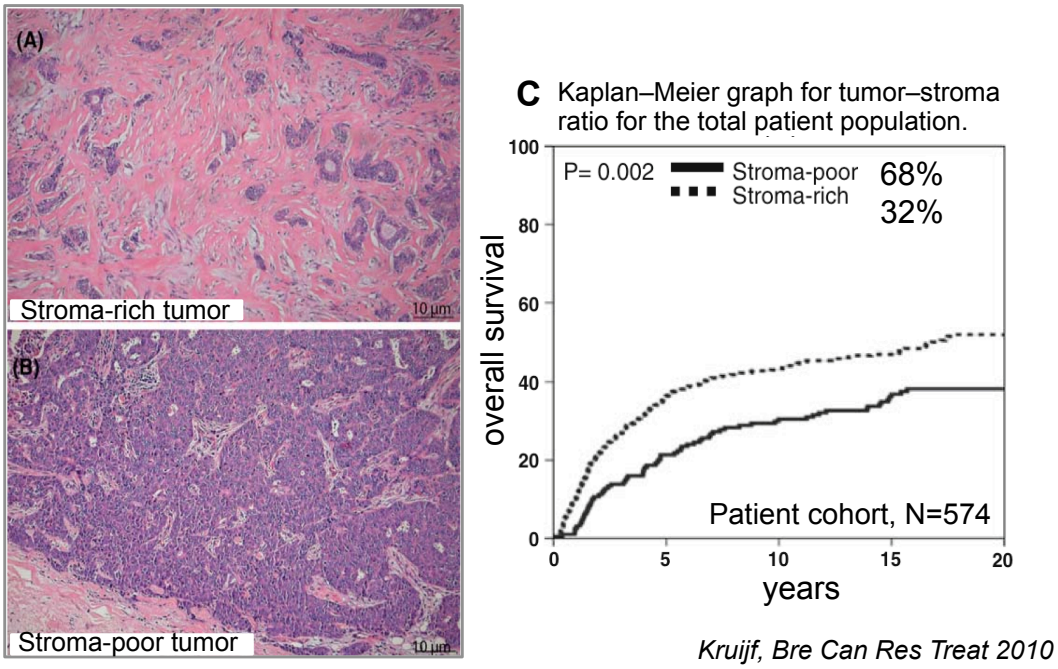

Kruijf, Bre Can Res Treat 2010

Figure 8. Stromal stiffness and poorer patients prognosis.

Figure 8. Stromal stiffness and poorer patients prognosis.
Part 1. Stromal stiffness and tumor progression A: Top right: phase images and H&E-stained tissue showing typical morphology of a mammary gland duct in a compliant gland (167 Pa), compared with MEC colonies grown in BM/COL I gels of increasing stiffness (170–1200 Pa). Bottom: confocal immunofluorescence (IF) images of tissue section of a mammary duct and cryosections of MEC colonies grown as above, stained for β-catenin (green), α6 or β4 integrin (red), and nuclei (blue). B: Colony size of MECs grown as described in A. ***p % 0.001. ***(Figure 1, Paszek, Weaver Cancer Cell 2005)*** Part 2. Poorer prognosis for stroma-rich breast cancer patients (A, B) Haematoxylin and eosin (H and E)-stained 4-lm paraffin sections of primary breast tumors; 1009 magnification (109 objective). A: Tumor–stroma ratio estimated as 80%: stroma-rich. B: Tumor– stroma ratio estimated as 20%: stroma-poor. C: Kaplan–Meier graphs for tumor–stroma ratio for the total patient population. Patients with stroma-rich tumors show a significant worse relapse-free period (a) and overall survival (b) compared to patients with stroma-poor tumors ***(Figures 1, 2, Kruijf, Bre Can Res Treat 2010)***

than others (Sorlie*, et al*, 2001). About a decade later, Finak and colleagues have taken a further step and performed laser capture microdissection allowing them to specifically isolate tumor-adjacent stroma. The findings were exciting as this was a first demonstration that the molecular profiling of tumor stroma alone can be aligned to the patient outcomes (Figure 9) (Finak*, et al*, 2008). As this is still a fairly new discovery the efforts in this field are still under development and require major depth. The main point is that this study contributes to the current awareness that tumor stroma does have affect on disease outcome.

This insight is essential for the development of new therapeutic strategies, or improvement of the current ones. Furthermore, stroma might be able to be used as a diagnostic tool for predicting the aggressiveness of breast cancer. As previously stated changes in the stroma are predictive of patient survival, as demonstrated by Boyd and colleagues who linked the stromal biology to the tumor progression. Furthermore, pathways associated with remodeling of matrix within the stroma (e.g., MMPs, extracellular matrix) lead to worse prognosis and could be possibly used to explain reduced survival (Finak*, et al*, 2008; Kruijf*, et al*, 2010).

Together, stromal studies are on the rise with experimental and clinical evidence that points to the role of the stroma in tumor progression, underscoring the need for further studies in order to develop even more robust biomarkers. The challenge for moving forward is to assay these biomarkers and to find ways to utilize these biomarkers to assist clinical side.

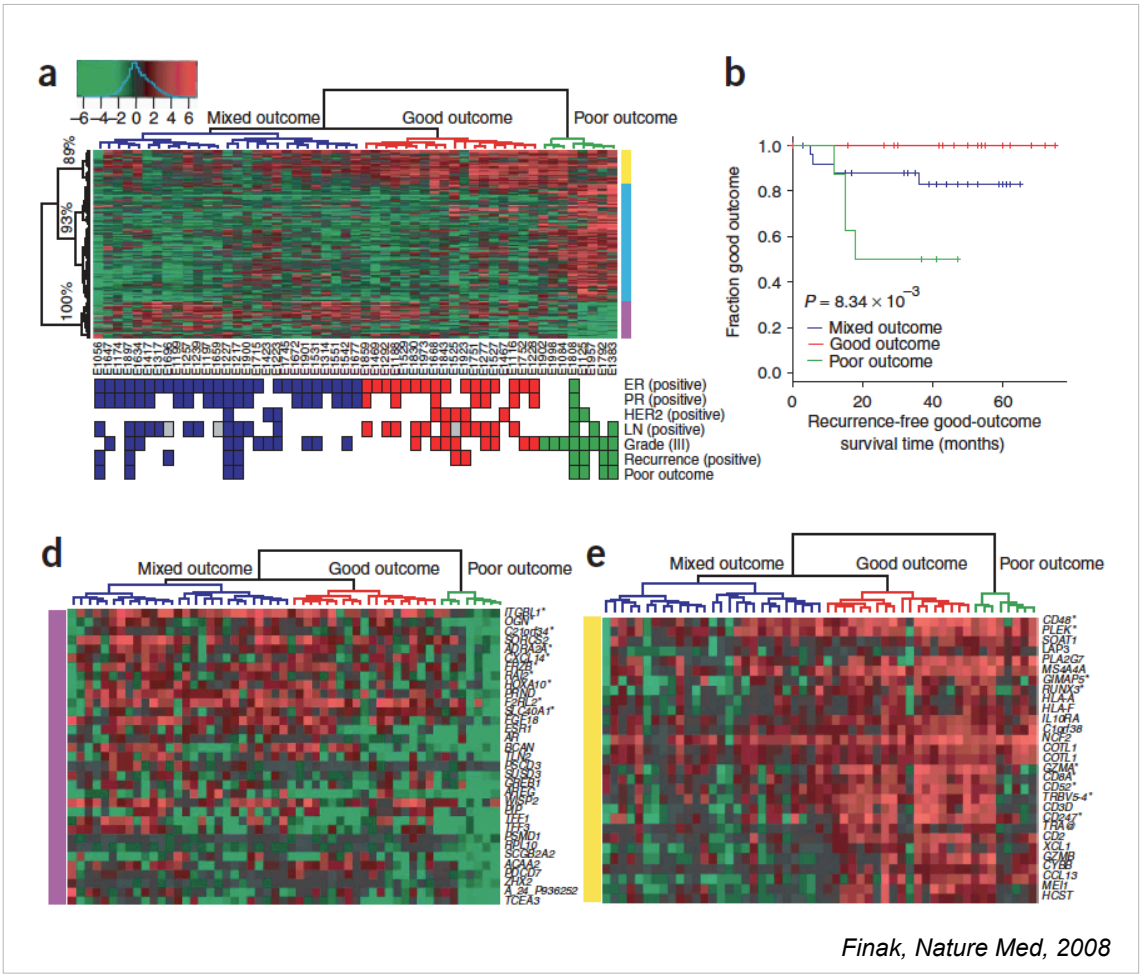

Finak, Nature Med, 2008

Figure 9. Stromal molecular profiling predicts outcomes.

Figure 9. Stromal molecular profiling predicts outcomes.

Class distinction of tumor stroma. (a) Hierarchical clustering of tumor stroma samples with the 163 genes differentially expressed between clusters 1, 2 and 3 of Figure 1b. Gene clusters are labeled with significance from bootstrap analysis, and color bars represent the three gene clusters described in the text. Heat map colors represent meancentered fold change expression in log-space. (b) Kaplan-Meier curves for each of the three clusters. (c) Expanded view of the genes expressed predominantly in samples of the pooroutcome cluster. (d) Genes expressed predominantly in samples of the mixed-outcome cluster. (e) Genes expressed predominantly in samples of the good-outcome cluster. *, member of the SDPP gene set. ***(Figure 2, Finak et al, Nature 2008)***

Summary

Treatment of patients with TNBC has been challenging due to the heterogeneity of the disease and the absence of well-defined molecular targets agreeable to therapeutic intervention (Carey*, et al*, 2007; Pegram*, et al*, 1998; Wiggans*, et al*, 1979). As previously mentioned, TNBCs frequently affected younger patient population (Dent*, et al*, 2007) and clinically these tumors are generally larger in size, higher in grade, with lymph node involvement at diagnosis biologically more aggressive (Haffty*, et al*, 2006). Overall women with metastatic TNBC survive three to five years (~30%) and despite aggressive chemotherapy the majority die of their disease (Haffty*, et al*, 2006). This presents an opportunity to further understand TNBC so that we can improve and/or discover better treatment methods, especially because there are currently no effective targeted therapies. As the field is becoming more aware of the complexity of TNBC, demonstrated by the molecular profiling identifying subtypes with unique biological drivers within TNBC, it became evident that better understanding of these drivers and how to effectively target them was needed.

In order to contribute to the efforts of TNBC field this thesis is comprised of three approaches dedicated to deciphering this highly heterogeneous disease. The first approach was to further investigate the role of one of these newly defined TNBC's biological drivers – the TGF-β pathway. This pathway was demonstrated to be one of the upregulated drivers in mesenchymal (M) and mesenchymal-stem like (MSL) TNBC subtypes. Considering that TGF-β pathway can promote tumorigenesis and metastasis it was natural to pursue this pathway

and evaluate its role in TNBC. The second approach in this thesis was to determine if we can predict response to drug treatment based on genomic signatures of TNBC tumors. In this case we have utilized the TNBC clinical trial whose focus was to explore the pathologic complete response rate for each individual treatment arm (cisplatin ± everolimus/mTOR inhibitor). Finally, using the laser capture microdissection approach I was successful in not only collecting tumor but also its adjacent stroma. The goal was to look into the role of tumor microenvironment in TNBC in regard to the clinical response and decipher whether stroma aligns to the TNBC tumor subtypes and has unique driver pathways that might be contributing to the stroma state, thus feeding into the aggressiveness of the tumor.

The cumulative results of this thesis provide insight into the TGF-β signaling axis within the TNBC MSL subtype implicating its prognostic and therapeutic utility in TNBC. It also indicates that within the clinical trial TNBC patients with MSL/M genomic signatures fall into the non-responder categories thus reinforcing the need for better-targeted therapy for this subtype, making TGF-β signaling axis more attractive candidate for targeted therapy. In addition, we have shown that expression profiling of tumor stroma can also predict the response of TNBC patients to chemotherapy. The combination of these intriguing results helps identify new pieces for the TNBC puzzle, thus helping us make one step forward to better managing this disease.

CHAPTER II

MATERIALS AND METHODS

Cell culture and treatments

SUM159 cells (Asterand) were maintained in Dulbecco's Modified Eagle Medium: Nutrient Mixture F12 (DMEM-F12, GIBCO) supplemented with 5% FBS (GIBCO) and 0.5μg/ml hydrocortisone. MDA-MB-231 and MDA-MB-157 (ATCC) were maintained in Dulbecco's Modified Eagle Medium (DMEM, GIBCO) supplemented with 10% FBS. Stable TβRIII-KD SUM159 cell lines were generated by lentiviral infection with virus carrying four independent shRNA clones (sequence-verified shRNA, pLKO.1-puro), [Sigma-Aldrich, Mission shRNA library #SHCLNG-NM_003243: clone#TRCN0000033433 (TβRIII-KD), clone#TRCN0000359000 (TβRIII-KD2), clone#TRCN0000359001 (TβRIII-KD3), and clone# TRCN0000359081 (TβRIII-KD4)](Jovanovic B & HL.) followed by puromycin selection (Invitrogen-Life Technology, Inc). MDA-MB-231 and MDA-MB-157 were stably infected with clone# TRCN0000033433. Integrin-α2 was stably knocked down in TβRIII-KD MSL cells using lentiviral particles carrying shRNA to integrin-α2 (α2-KD) *(*Sigma-Aldrich, Mission shRNA validated library, #SHCLNG-NM_002203, clone#TRCN0000308081).

Cisplatin (APP Biopharmaceuticals, Schaumburg, IL) was used at 25 mM, paclitaxel (Sigma) was used at 100 nM, and RAD001 (everolimus, Novartis, Basel, Switzerland) was used at 20 nM. For cell death experiment doxorubicin

was used at 1 and 3 μM while Taxol was used at 1, 5 and 10nM. For these experiments cells were plate at 50% confluence, than at 70-80% confluency they treated for 48hrs.

Cell proliferation assays

Cell counts: Cells were plated into 6-well plates at density of 1.25 x 10^5 cells/well. The following day cells were treated with 1 ng/ml TGF-β1 (R&D Systems, #102-B1) and TGF-β2 (R&D Systems, #102-B2). After 72 h treatment with TGF-β, viable cells were counted.

^{3}H-Thymidine incorporation assay: 2.5 × 10^4 cells were plated in a 24-well dish and allowed to grow overnight. The next day the medium was aspirated and replaced with complete medium containing +/- TGF-β1 or TGF-β2 (1ng/ml). The cells were then subjected to [^{3}H] thymidine incorporation assay as previously described (Bierie*, et al*, 2009).

Overview of clinical trial design (VICC BRE0904).

In 2009 we activated a randomized two-arm neoadjuvant phase II trial of cisplatin (25 mg/m^2 IV week) + paclitaxel (80 mg/m^2 IV week) ± RAD001 (5mg PO daily) in patients with stage II and III triple negative with triple negative locally advanced breast cancer (Figure 25 in Chapter IV). The primary objective of the trial was to determine the pathologic complete response (pCR). Additional aims were to determine the efficacy and safety of the drug combinations in each treatment group, evaluate therapy-mediated changes in correlative molecular markers (i.e. examine changes in proliferation, the p53/p63/p73 signaling axis

and mTOR signaling pathways) and determine the ability of GE signatures to predict patient response. The trial was randomized 2:1 with Arm 1 patients treated with RAD001+ cisplatin for one week followed by addition of paclitaxel to the combination for additional 11 weeks. Arm 2 was set up in same manner with exception of RAD001 being replaced with a placebo. In addition, ultrasound guided core biopsies for molecular markers and correlative studies were collected. First at the time of diagnosis (baseline/pre-treatment biopsy) and two additional collections, biopsy 1 (BP1) prior to addition of paclitaxel to the cisplatin ± RAD001 treatment combinations, and at time of surgery (Post) (Figure 25 in Chapter IV).

Three-dimensional culture assay

The wells in 48 well plates were coated with 50 µl of growth factor reduced BD Matrigel (BD Biosciences #356231) and allowed to polymerize at 37°C for 15 min. 5 x 10^5 cells were resuspended in 200 µl of growth factor reduced BD Matrigel and plated onto the Matigel-coated wells. Plates were incubated for 30 min after which 1 ml of media was added to the top of the matrigel. Media was replenished every 48 h. Images were taken at day six. Quantification of the images was performed using Fiji Software.

Flow cytometry

Cells were detached using Accutase (Life Technologies), pelleted, washed and counted. One million cells were incubated with TβRIII antibody (Cell Signaling, #5544) for 30min, washed, and then incubated at 4^{o}C with Alexa Fluor 488 conjugated secondary antibody (Life Techologies, #A11034) for 30min. One

million cells were labeled with fluorescence-conjugated integrin-α2 antibody (BioLegend, #314308) for 30 min at 4^{o}C. Cells were washed three times then analyzed on a FACSCalibur flow cytometer (Beston Dickinson) using CellQuest Pro software. Data were analyzed with FlowJo software (Tree Star).

Immunoblotting

Standard protein preparation and electrophoresis procedures were used as described (Bierie*, et al*, 2008). Western membranes were blocked in 5% milk and incubated with primary antibody overnight. The antibody list with concentrations and the catalog numbers are available in supplemental methods (Table 2).

Immunohistochemistry

Formalin fixed paraffin embedded tissues from BRE0904 trial have been sectioned and processed for immunohistochemistry by Violeta Sanchez from Dr. Melinda Sanders' group. Antibodies used for results in Chapter IV are outlined with their known conditions (Table 2). Dr. Sanders and her fellows Maria Gabriela Kuba and Valeria Estrada have performed all the IHC scorings.

Laser capture microdissection and expression analysis

Laser Capture Microdissection (LCM) was performed on 5 μm frozen breast core tumor biopsies sections on an Arcturus PixCell IIe microscope at the Vanderbilt Translational Pathology Shared Resource. LCM-captured RNA was isolated using an RNAqueous-Micro kit (Ambion) and validated for array quality (Vanderbilt Genome Sciences Resource). Subsequent cDNA synthesis and

Table 2. Immunoblotting and immunohistochemistry conditions

ANTIBODY	COMPANY	CATALOG #	SPECIES	ASSAY	SPECIES TESTED	Dilution	Temp	Duration	Diluent
AKT	Cell Signaling	9272S	rabbit	Western	human	1:1000	4°C	over night	5% BSA. 1xTBS, 0.1% Tween
AKT, phospho	Cell Signaling	4060L	rabbit	Western	human	1:2000	4°C	over night	5% BSA. 1xTBS, 0.1% Tween
cleaved Caspase-3	Cell Signaling	9661	rabbit	Western	human	1:1000	4°C	2X overnight	5% milk
ERK	Cell Signaling	9107	mouse	Western	human	1:2000	4°C	over night	5% milk
ERK, phospho	Cell Signaling	4370	rabbit	Western	human	1:2000	4°C	over night	5% BSA. 1xTBS, 0.1% Tween
FAK	Cell Signaling	3285S	rabbit	Western	human	1:1000	4°C	over night	5% BSA. 1xTBS, 0.1% Tween
FAK, phospho	Cell Signaling	3283S	rabbit	Western	human	1:1000	4°C	over night	5% BSA. 1xTBS, 0.1% Tween
ITGA2	Santa Cruz	SC74466	mouse	Western	human	1:500	4°C	over night	5% milk
p38	Cell Signaling	8690P	rabbit	Western	human	1:1000	4°C	over night	5% BSA. 1xTBS, 0.1% Tween
p38, phospho	Cell Signaling	4511P	rabbit	Western	human	1:1000	4°C	over night	5% BSA. 1xTBS, 0.1% Tween
PARP	Cell Signaling	9542	rabbit	Western	human	1:1000	4°C	2X overnight	5% milk
Smad2	Cell Signaling	5339	rabbit	Western	human	1:1000	4°C	over night	5% milk
Smad2, phospho	Cell Signaling	3101s	rabbit	Western	human	1:1000	4°C	over night	5% milk
Smad3, phospho	Cell Signaling	8769	rabbit	Western	human	1:1000	4°C	over night	5% milk
TβRII	Santa Cruz	SC400	rabbit	Western	human	1:4000	4°C	over night	5% milk
TβRIII	SDIX	2703.00.02	rabbit	Western	human	1:10000	RT	over night	5% milk
AR	Dako	M3562	mouse	IHC	human	1:200	4°C	over night	Violeta Sanchez?
ki67	Dako	M7240	mouse	IHC	human	1:100	4°C	over night	Violeta Sanchez?
p53	Epitomics	1005-1	rabbit	IHC	human	1:200	4°C	over night	Violeta Sanchez?
p63	Sigma	P3737	mouse	IHC	human	1:500	4°C	over night	Violeta Sanchez?
p73	Epitomics	1636-1	rabbit	IHC	human	1:200	RT	1hr	Violeta Sanchez?
pS6	Cell Signaling	4857	rabbit	IHC	human	1:80	4°C	over night	Violeta Sanchez?

amplification was completed by VANTAGE. Reactions were run in 96 well format with 10ng of Total RNA used per reaction in the NUGEN FFPE Kit (Cat#3400-60, Lot#1009255-C). The reactions were run through First Strand and Second Strand synthesis, followed by 2 rounds of SPIA amplification to generate cDNA. The cDNA was frozen overnight at -20C and cleaned up the next day. The ss cDNA targets were quantitated on the Nanodrop. Overall the yields were robust, with an average yield of 10.2ug providing enough amplified product for hybridization to the Hu Gene 1.0ST array.

Luciferase reporter assay

Cells were seeded at a density of 2 X 10^4 cells/well in 12-well tissue culture plates. The following day, cells were transiently transfected using Transfectin lipid reagent following the manufacturer's protocol (Bio-Rad #170-3351). Cells were transfected with 1.5 μg 3TP-Lux (Wrana*, et al*, 1992) or CAGA(9)-Luc (Kusanagi*, et al*, 2000) pRL-CMV-renilla (Promega #E2261) was co-transfected and used as an internal control to correct for transfection efficiency. Eighteen hours after transfection, cells were treated with 1 ng/ml TGF-β1 or TGFβ-2 (R&D Systems, #102-B1 and #102-B2, respectively). Twenty-four hours after TGF-β treatment, cells were harvested and assayed for promoter specific luciferase activity using a Dual-Luciferase Reported Assay System (Promega #E1910) according to the manufacturer's protocol. Luciferase activity was measured using a BD/Pharmigen Monolight 3010 luminometer.

Microarray Gene Expression Analysis

Public database analysis*:* Human tissue and cell line microarray datasets were analyzed using GeneSpring GX 12.0 microarray analysis software (Agilent). Previously published TNBC gene expression profiles (n=587 patients) (Lehmann*, et al*, 2011) consisting of publically available microarray data sets (the GEO registration numbers are referenced in Additional File 1) were obtained and processed as previously described and were in compliance with ethical requirements (Lehmann*, et al*, 2011). Comparisons between expression of *TGFBR3* and *ITGA2* for different TNBC subtypes were performed in R 3.0.1 (R Core Team, 2013) using the *t test* function for paired two-tail Student *t*-tests and graphically represented using ggplot2 (Wickham, 2009).

In vitro 3D culture analysis: RNA was extracted from SUM159 3D culture samples was hybridized to the human gene 1.0ST array, scanned with Affymetrix using AGCC v. 3.2.4 and then analyzed in R 3.0.1 using the oligo package. Samples were normalized with the RMA algorithm, genes were annotated with the pd.hugene.1.0.st.v1 package, and differential gene expression analysis was conducted using the limma package. The 3D culture microarray data discussed in this publication have been deposited in NCBI's Gene Expression Omnibus (Edgar*, et al*, 2002) and are accessible through GEO Series accession number GSE54756 (Jovanovic B & HL.).

Microarray Gene Expression GEO registration numbers

Breast Cancer GE data sets used to derive TNBC training and validation sets: GSE-3494, GSE-7904, GSE-2109, GSE-7390, E-TABM-158, GSE-2034,

GSE-2990, GSE-1456, GSE-22513, GSE-28821, GSE-28796, GSE-11121, GSE-2603, MDA133, GSE-5364, GSE-1561, GSE-5327, GSE-5847, GSE-12276, GSE-16446, GSE-18864, GSE-19615, GSE-20194. (*Lehmann BD, Bauer JA, Chen X, Sanders ME, Chakravarthy AB, Shyr Y, Pietenpol JA: Identification of human triple-negative breast cancer subtypes and preclinical models for selection of targeted therapies. The Journal of clinical investigation 2011,* ***121****(7):2750-2767.)*

Migration and Invasion Assays

Magnetic attachable stencils (MAtS) migration assays: This migration method serves as a more reproducible alternative to the scratch assay. The use of magnetic force to attach stencil to the multi-well plates is a new strategy that creates defined and reproducible cell-free voids for quantitation of cell migration and has been well characterized and described by Ashby et. al. (Ashby*, et al*, 2012). MAtS were attached to the surfaces of each well of 12-well plate by placing a platform with magnets underneath and in direct contact with the 12-well plate. Cells were then plated in triplicate at 7.5 x 10^5 cells per well around the MAtS in serum-free media. The next day the MAtS were removed and cells were treated with 1 ng/ml TGF-β1 (R&D Systems, #102-B1) and 1 ng/ml TGF-β2 (R&D Systems, #102-B2). Gap closure was quantified (Tscratch software) at both 0 and 24 h and percent of closure determined with the following equation; (percent of closure) = average of ([gap area: 0hr] – [gap area: 24h])/[gap area: 0hr] using images from 12 different microscopic fields per well (4X magnification).

Transwell assays*:* Migrations (Costar, #3422) were conducted by plating 2.5 x 10^4 cells in the top of the transwell and media with 10% FBS in the bottom of the well to act as a chemoattractant. Cells were fixed in 4% paraformaldehyde and stained with 4', 6-diamidino-2-phenylindole (DAPI). Quantification was performed by taking pictures of multiple regions of the membrane after which cells' nuclei were counted using Metamorph software. The same migration assay was used to measure blocked integrin-α2 function. The TβRIII-KD cells were incubated for 30 minutes with integrin-α2 blocking antibody (Abcam, #ab24697) washed two times with PBS and plated in the top of the transwell. Invasion assays were conducted by plating 5 x 10^5 cells in serum-free media in the upper chamber, pre-coated with growth factor reduced Matrigel. In the bottom chamber DMEM with 10% FBS was used as a chemoattractant (Bioscience, #354483). Cells that had invaded through the Matrigel were fixed in 4% paraformaldehyde and stained using DAPI. Quantification of cells that invaded into the Matrigel was performed using the same protocol as described for the transwell assays.

Xenograft tumor studies

One milllion cells embeded in collagen were implanted into the number four gland of six to eight week female athymic nude- Foxn1$^{nu/nu}$ mice (purchased from Harlan Sprague- Dawley, Inc., Indianapolis, IN). Mice were monitored weekly for tumor growth. Tumor measurements were performed once a week for five weeks after palpable tumors formed. Tumor volume was measured at the indicated times with calipers, and tumor volumes were calculated as width^2 x

length/2. All mouse experiments have been approved by the Vanderbilt University Institutional Animal Care and Use Committee (IACUC).

RNA preparation and quantitative PCR

RNA was isolated and purified using an RNeasy Mini Kit and an RNase-Free DNase Set (Qiagen). A total of 750 µg of RNA was used to synthesize cDNA using Superscript III reverse transcriptase as described by the manufacturer (Invitrogen). Bio-Rad iCycler and CFX96 machines were used for qPCR employing *Power* SYBR Green (Applied Biosystems) or SsoAdvanced SYBR Green Supermix (Bio-Rad), respectively. C_t values were normalized to GAPDH for statistical analyses. Primer sequences are available in supplemental methods (Table 3).

Statistical Analysis

All data were analyzed using unpaired two-tailed Student *t* test (GraphPad Prism 5). Error bars show mean ± SEM. A two-sided P value less than 0.05 were considered significantly different.

Table 3. Primer sequences.

The following primer sequences (5' to 3') were used:	
Gene	**Sequence**
h*TGFBR3* forward	TGGGGTCTCCAGACTGTTTTT
h*TGFBR3* reverse	CTGCTCCATACTCTTTTCGGG
h*PAI-1* forward	GACATCCTGGAACTGCCCTA
h*PAI-1* reverse	GGTCATGTTGCCTTTCCAAGT
h*SMAD7* forward	CCAACTGCAGACTGTCCAGA
h*SMAD7* reverse	CAGGCTCCAGAAGAAGTTGG
h*ITGA2* forward	CCTACAATGTTGGTCTCCCAGA
h*ITGA2* reverse	AGTAACCAGTTGCCTTTTGGATT

CHAPTER III

TGF-β RECEPTOR TYPE III IS A TUMOR PROMOTER IN MESENCHYMAL-STEM LIKE TRIPLE NEGATIVE BREAST CANCER

Abstract

There is a major need to better understand the molecular bases of triple negative breast cancer (TNBC) in order to develop more effective therapeutic strategies. Using gene expression data from 587 TNBC patients we previously identified six subtypes of the disease, among which a Mesenchymal-Stem Like (MSL) subtype. The MSL subtype has significantly higher expression of the transforming growth factor beta (TGF-β) pathway-associated genes relative to other subtypes, including the TGF-β receptor type III (TβRIII). We hypothesize that TβRIII is tumor promoter in mesenchymal-stem like TNBC cells.

Representative MSL cell lines SUM159, MDA-MB-231 and MDA-MB-157 were used to study the roles of TβRIII in the MSL subtype. We stably expressed short hairpin RNAs specific to TβRIII (TβRIII-KD). These cells were then used for xenograft tumor studies *in vivo*; and migration, invasion, proliferation and three dimensional culture studies *in vitro.* Furthermore, we utilized human gene expression datasets to examine TβRIII expression patterns across all TNBC subtypes.

TβRIII was the most differentially expressed TGF-β signaling gene in the MSL subtype. Silencing TβRIII expression in MSL cell lines significantly

decreased cell motility and invasion. In addition, when TβRIII-KD cells were grown in a three dimensional (3D) culture system or nude mice, there was a loss of invasive protrusions and a significant decrease in xenograft tumor growth, respectively. In pursuit of the mechanistic underpinnings for the observed TβRIII-dependent phenotypes, we discovered that integrin-α2 was expressed at higher levels in MSL cells after TβRIII-KD. Stable knockdown of integrin-α2 in TβRIII-KD MSL cells rescued the ability of the MSL cells to migrate and invade at the same level as MSL control cells.

We have found that TβRIII is required for migration and invasion *in vitro* and xenograft growth *in vivo.* We also show that TβRIII-KD elevates expression of integrin-α2, which is required for the reduced migration and invasion, as determined by siRNA knockdown studies of both TβRIII and integrin-α2. Overall, our results indicate a potential mechanism by which TβRIII modulates integrin-α2 expression to effect MSL cell migration, invasion, and tumorigenicity.

Introduction

The term “triple negative breast cancer” (TNBC) is used to classify the 10%-20% of all breast cancers that lack estrogen receptor (ER) and progesterone receptor (PR) expression as well as amplification of the human epidermal growth factor receptor 2 (HER2) (Lehmann & Pietenpol, 2014) . Disease heterogeneity and the absence of well-defined molecular targets have made treatment of TNBC challenging. There is a major need to better understand the molecular basis of this type of breast cancer in order to develop effective therapeutic strategies (Lehmann & Pietenpol, 2014). In a previous study, we performed gene expression (GE) analyses and identified six distinct molecular TNBC subtypes with unique biological drivers (Lehmann*, et al*, 2011) including one that was enriched for mesenchymal-associated genes termed mesenchymal-stem like (MSL). The MSL subtype is characterized by increased expression of genes related to TGF-β signaling as well as pathways that play roles in extracellular matrix (ECM), focal adhesion, cell motility and cell differentiation (Lehmann*, et al*, 2011). Of note, TβRIII (gene symbol: *TGFBR3*) was among the differentially expressed TGF-β signaling components in the MSL subtype.

TGF-β signaling pathway has been implicated in cancer initiation and progression through tumor cell autonomous and non-autonomous signaling (Bierie*, et al*, 2008; Roberts & Wakefield, 2003). Initially identified as a tumor suppressor and then as a mediator of tumor progression, TGF-β signaling demonstrates diverse capabilities in cancer. The TGF-β pathway suppresses tumor growth through regulation of epithelial and stromal cell signaling (Bierie &

Moses, 2006b). Dysfunction of the pathway leads to carcinoma progression and metastasis (Roberts & Wakefield, 2003). While there has been significant focus on TGF-β receptor type I (TβRI) and TGF-β receptor type II (TβRII), research on TGF-β receptor type III (TβRIII) has lagged. Prior studies have demonstrated that TβRIII can regulate TGF-β signaling either via delivering TGF-β2 ligand to TβRII (Blobe*, et al*, 2001a; Blobe*, et al*, 2001b; Lee*, et al*, 2010; López-Casillas*, et al*, 1994) or by binding to cytoplasmic domain of TβRII, forming an active TβRI-TβRII signaling complex (Cheifetz*, et al*, 1986; Massague, 1985; Massague & Like, 1985; Wang*, et al*, 1991). Currently, analysis of gene expression data sets generated from multiple cancer types indicates that TβRIII expression is decreased in higher-grade cancers (Copland*, et al*, 2003; Gordon*, et al*, 2008; Hempel*, et al*, 2007; Turley*, et al*, 2007). However, the role of TβRIII is controversial in breast cancer, since it has been reported that TβRIII can act as either a tumor suppressor or promoter in this cancer (Criswell*, et al*, 2008; Dong*, et al*, 2007).

In the current study, we focused our investigations on the functional role of TβRIII in the mesenchymal-like (MSL) subtype of TNBC. We used a loss-of-function approach in representative MSL cell lines to demonstrate that TβRIII is required for maintenance of tumorigenicity in MSL TNBC cell lines and that regulation of integrin-α2 (gene symbol: *ITGA2*) expression is mechanistically involved in the observed phenotypes. This study demonstrates that TβRIII promotes the *in vivo* growth of a subset of TNBC and provides pre-clinical

rationale for consideration of TβRIII as a potential target for further discovery efforts.

Results

Human mesenchymal-stem like triple negative breast tumors and representative cell lines have increased TβRIII expression.

Using a gene expression data set generated from 587 TNBC tumors, we examined the relative mRNA levels of TGF-β receptors and ligands across subtypes of TNBC. We observed elevated expression of *TGFBR3* in basal-like1 (BL1), mesenchymal (M) and mesenchymal-stem like (MSL) tumors (Figure 10A). The highest relative level of *TGFBR3* expression was in the MSL subtype (Figure 10B). Average probe intensities for the TGF- β receptors I and II as well as TGF- β ligands 1 and 3 were also elevated in MSL subtype in comparison to the rest of the TNBC subtypes (Figure 11). Analysis of The Cancer Genome Atlas (TCGA) TNBC data demonstrates a similar pattern of *TGFBR3* expression across TNBC subtypes with the highest levels observed in the MSL subtype (Figure 12). Similarly, analysis of *TGFBR3* gene expression across a panel of TNBC cell lines, representative of the various subtypes, demonstrates that the M and MSL subtypes have relatively higher levels of *TGFBR3* mRNA (Figure 10C-D). These findings were validated by qPCR (Figure 10E) and immunoblot analyses for TβRIII protein levels (Figure 10F). Although the TNBC mesenchymal (M) subtype cell lines also showed increased levels of TβRIII expression, we focused our studies of this receptor on the MSL subtype as expression is more consistent with human datasets (Figure 10A-B).

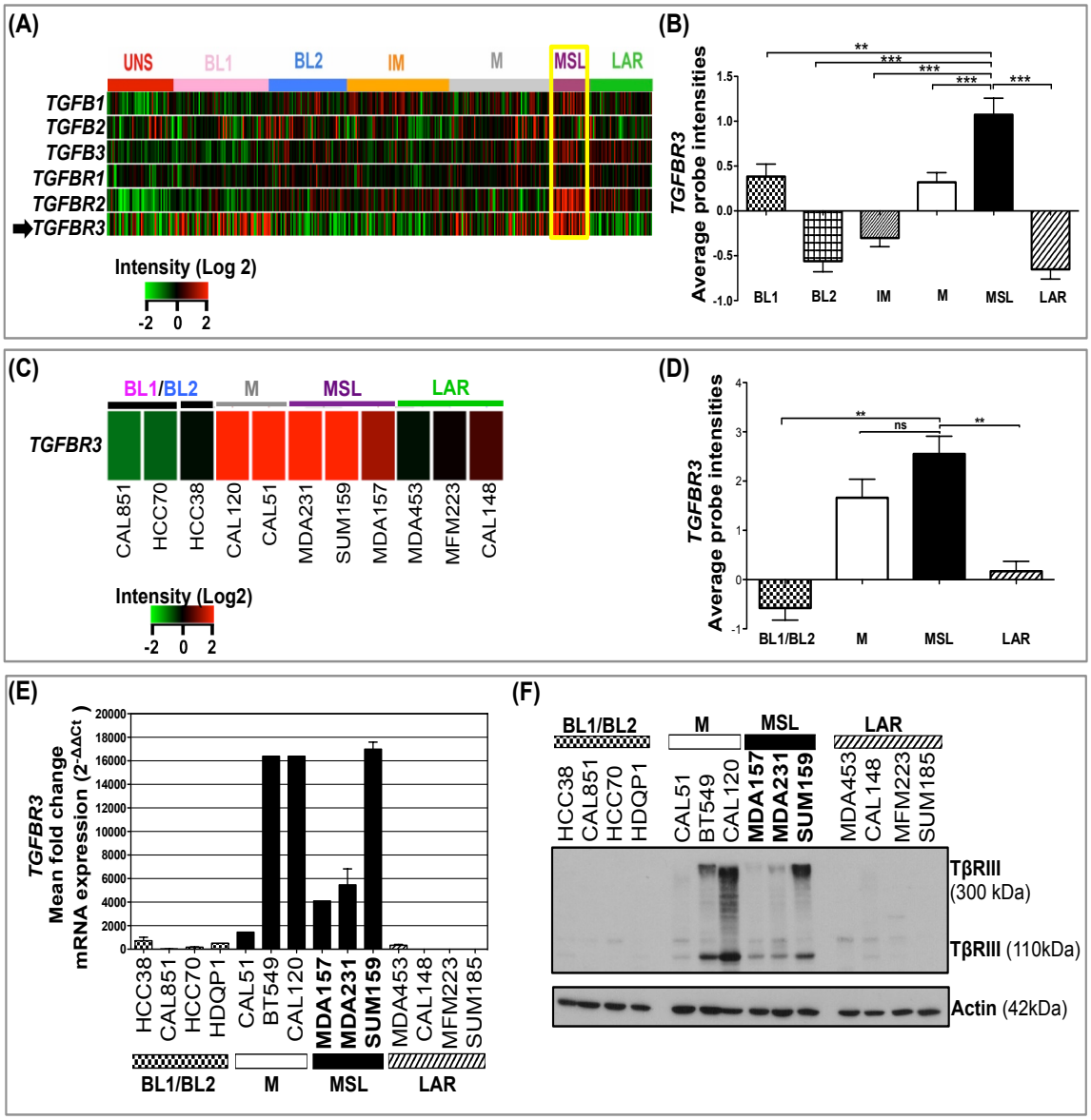

Figure 10. *TGFBR3 gene* expression levels are elevated in mesenchymal-stem like (MSL) subtype of TNBC.

Figure 10. TGFBR3 gene expression levels are elevated in mesenchymal-stem like (MSL) subtype of TNBC.

A, Heat map representation of gene expression for 587 TNBC tumors for each TGF-β ligand and receptor. **B,** quantification of average *TGFBR3* gene expression across TNBC tumor subtypes, average based on individual TNBC tumor probe intensity values (**P = 0.004; ***P < 0.0003 for a two-tail Student *t*-test). **C,** heat map of *TGFBR3* mRNA expression in TNBC representative cell lines. **D,** quantification of *TGFBR3* gene expression across representative TNBC cell lines (** P = 0.004; for a two-tail Student *t*-test, ns = not significant). **E,** qRT-PCR analysis of *TGFBR3* average mRNA expression ($2^{-\Delta\Delta Ct}$) (Livak & Schmittgen, 2001) from representative TNBC cell lines; graph bars represent the mean of 3 replicates with SEM error bars. **F,** immunoblot analysis of TβRIII protein expression in TNBC representative cell lines, results representative of two independent experiments.

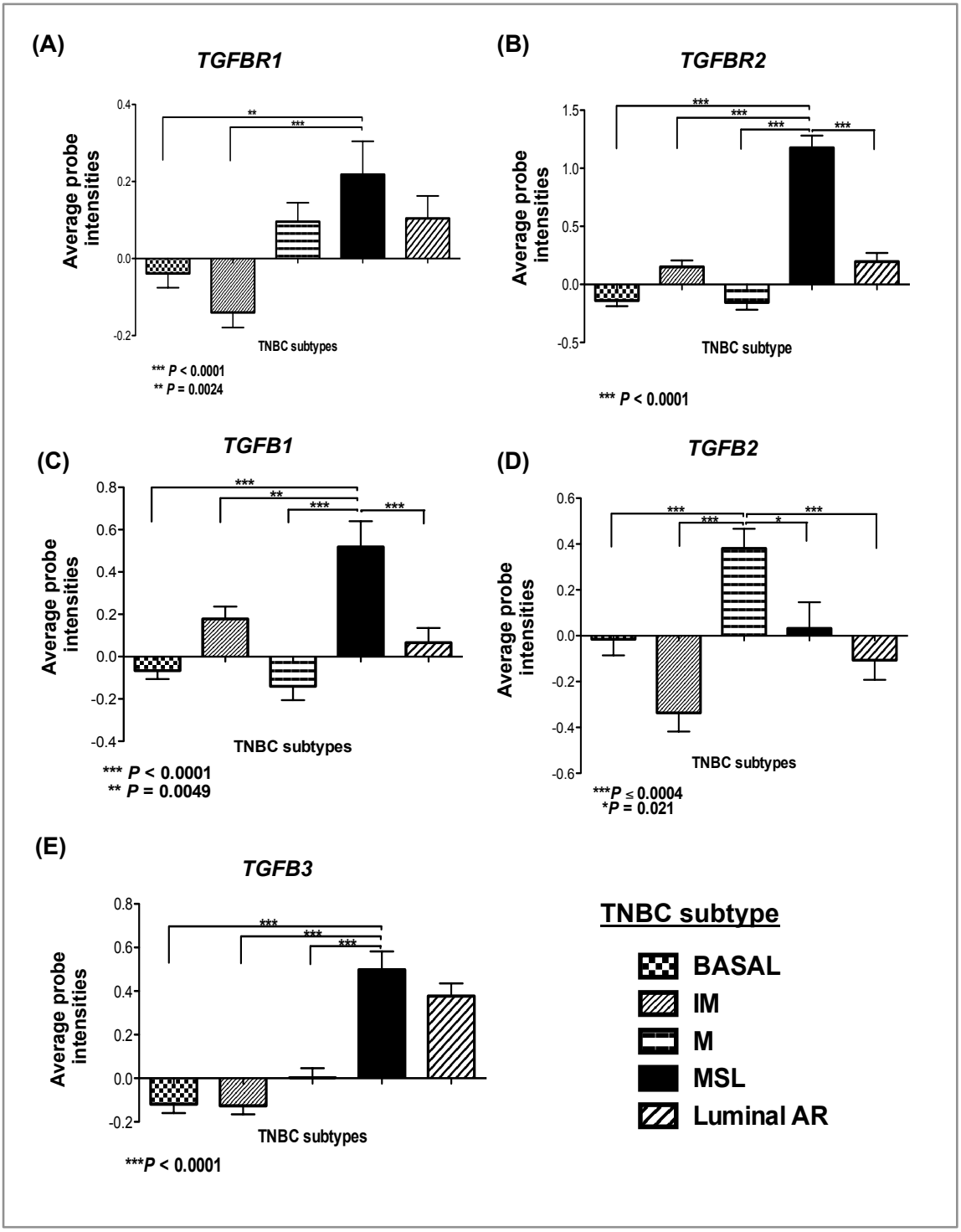

Figure 11. Average probe intensities for TGF-β receptors and ligands across 587 TNBC patients.

Figure 11. Average probe intensities for TGF-β receptors and ligands across 587 TNBC patients.

A-B, quantification of average *TGFBR1 and TGFBR2* mRNA expression across TNBC tumor subtypes. **C-E**, quantification of average *TGFB1, TGFB2 and TGFB3* mRNA expression across TNBC tumor subtypes. Bar graph represents averages based on individual TNBC tumor probe intensity values. P values are outlined in the graph and were generated using a two-tail Student *t*-test.

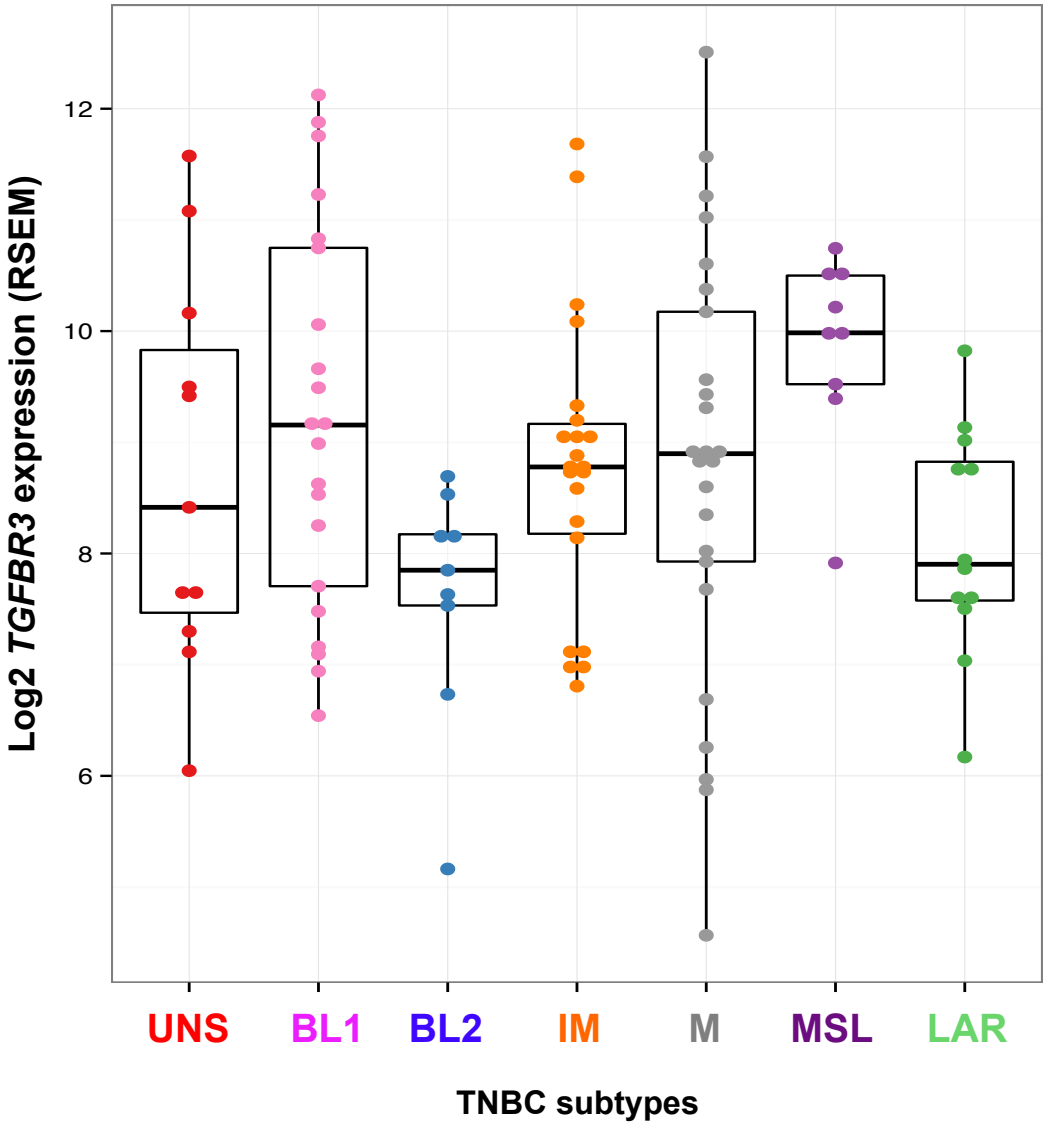

Figure 12. *TGFBR3* expression across TNBC subtypes in the Cancer Genome Atlas (TCGA).

TGFBR3 transcript quantification from RNA-seq TCGA data demonstrating log2 *TGFBR3* levels (RSEM) across each TNBC subtype.

Knockdown of TβRIII in MSL TNBC cells leads to decreased tumorigenicity in vivo.

In order to determine the significance of the TβRIII expression in MSL TNBC cell behavior, we knocked down TβRIII in MSL cells and performed orthotopic xenograft tumor studies. We used a panel of four shRNA expression vectors to optimize TβRIII knockdown, as validated by immunoblot and flow cytometry analyses (Figure 13A-C). We utilized immunocompromised nude mice to establish orthotopic xenograft tumors from cell lines representing MSL subtype of TNBC with and without TβRIII knockdown. Initially we tested SUM159 cells with two shRNA expression vectors (TβRIII-KD and TβRIII-KD4) to eliminate off target effects of the shRNA (Figure 14). After establishing that both expression vectors resulted in a similar phenotype, we used a single shRNA (TβRIII-KD) in all subsequent experiments across three MSL cell lines. Knockdown of TβRIII in the SUM159 and MDA-MB-231 MSL cell lines significantly decreased xenograft tumor growth (Figure 13D-E). MDA-MB-157 showed inconsistent results (Figure 15A) and after further investigation we discovered that the TβRIII-KD tumors expressed TβRIII (Figure 15B). Thus, either there was a selection against the knockdown *in vivo* and thus the tumor cells expressed TβRIII or there was a small subpopulation of MDA-MB-157 cells at the start of the experiment that retained expression and seeded the tumor growth. Regardless, both explanations provide further evidence for the tumor-promoting effect of TβRIII.

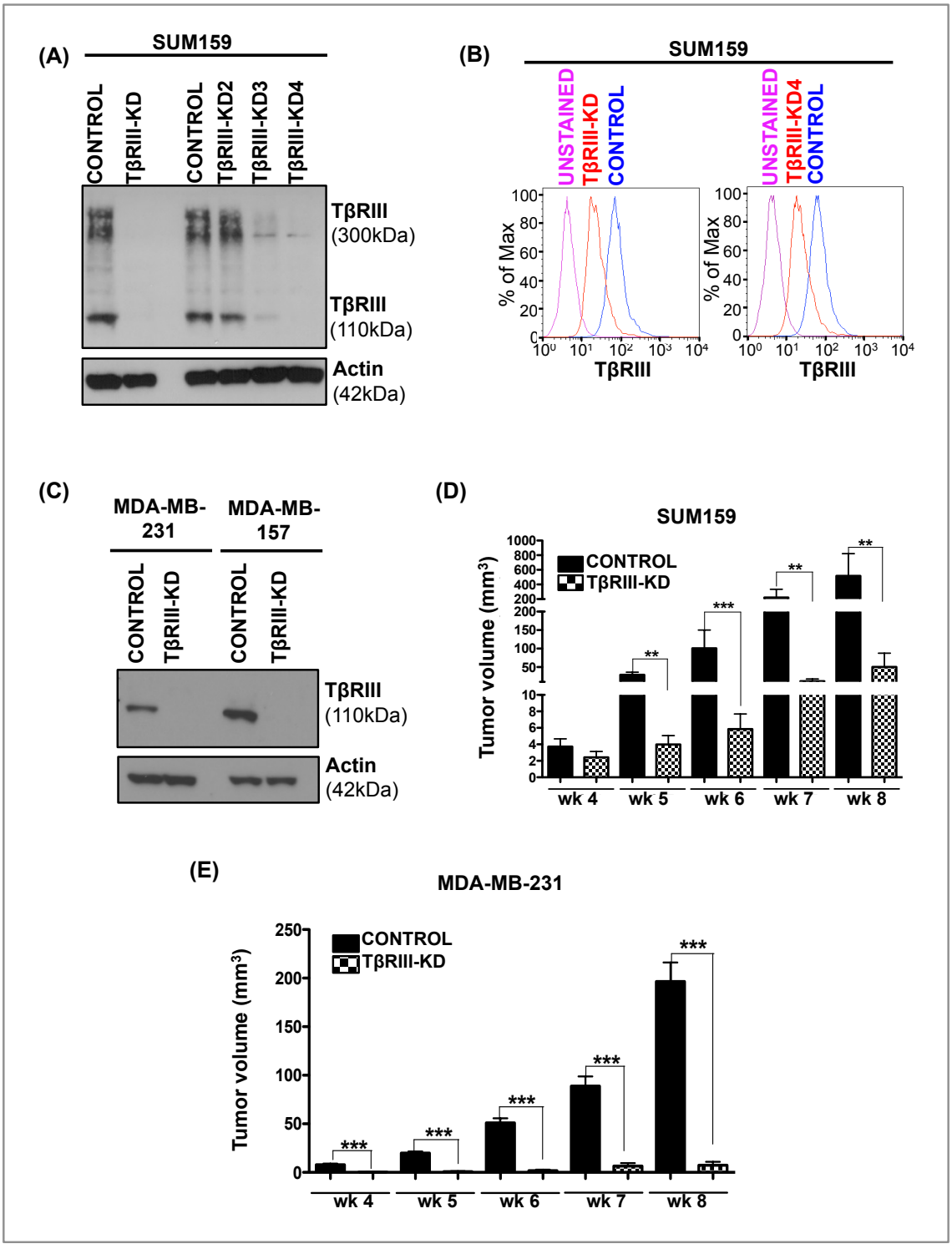

Figure 13. Stable knockdown of TβRIII in MSL TNBC cells reduces xenograft tumor growth.

Figure 13. Stable knockdown of TβRIII in MSL TNBC cells reduces xenograft tumor growth.

A, immunoblot analysis of TβRIII protein expression in lysates harvested from SUM159 cells stably expressing control and four different TβRIII shRNA vectors (TβRIII-KD, KD2-4). **B,** flow cytometry analysis of TβRIII protein levels in SUM159 controls, TβRIII-KD and TβRIII-KD4. **C**, immunoblot analysis of TβRIII protein expression in lysates harvested from MDA-MB-231 and MDA-MB-157 cells stably expressing control and TβRIII-KD. **D-E,** tumors in nude mice were palpable 3 weeks post implantation of MSL cell line (D, SUM159 and E, MDA-MB-231). Serial tumor volumes (mm^3) were measured weekly for 5 weeks post palpation for both controls and TβRIII-KD. Each data bar represents the mean tumor volume of 10 tumors; error bar represents SEM (**P ≤ 0.005, ***P < 0.0001 for a two-tail Student *t*-test).

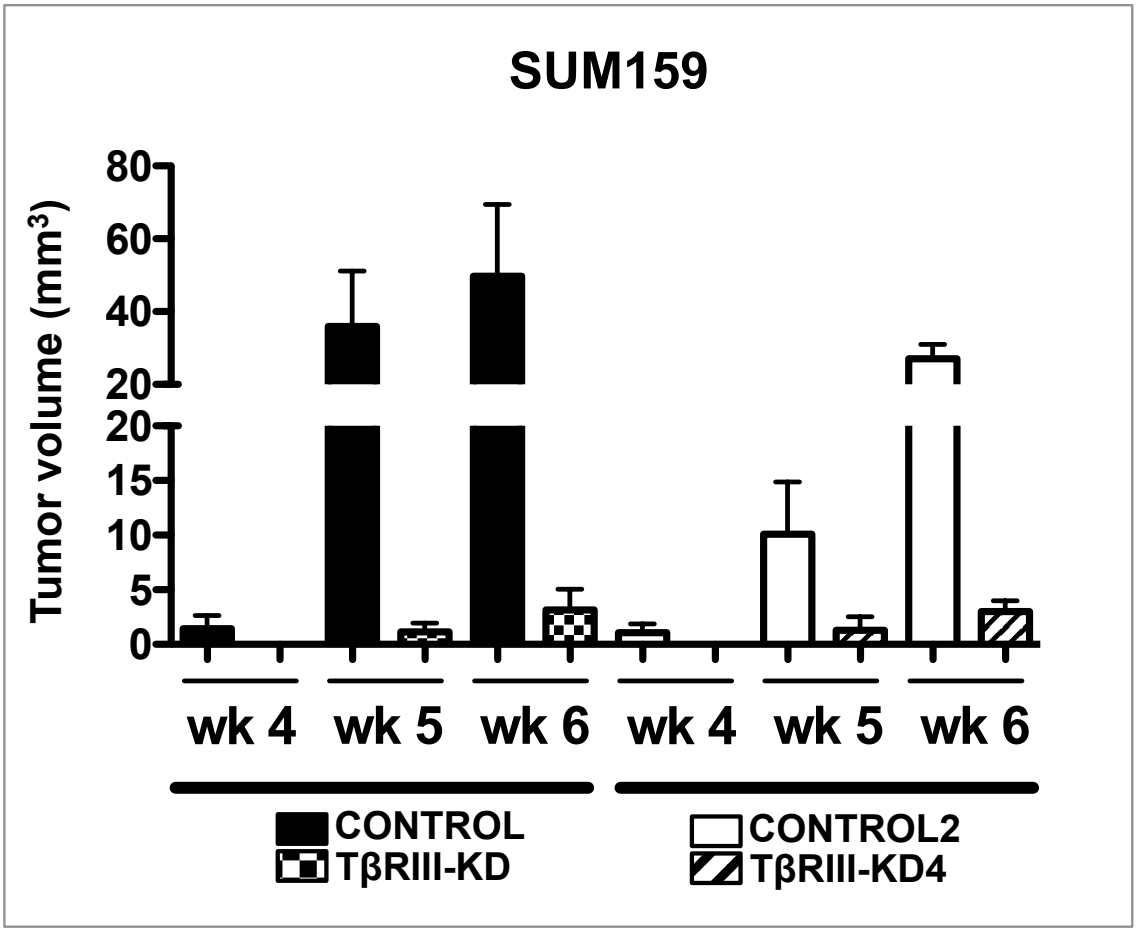

Figure 14. Knockdown of TβRIII with two independent shRNA vectors decreases tumor volume of SUM159 xenografts.

TβRIII-KD and TβRIII-KD4 vectors were used to stably knockdown TβRIII in SUM159 cells. Cells were then implanted orthotopically into nude mice. Tumors were palpable 3 weeks post implantation of SUM159 cell line with two independent TβRIII knockdown vectors. Serial tumor volumes (mm^3) were measured weekly for 5 weeks post palpation for both controls and TβRIII-KDs. Each data bar represents the mean tumor volume of 8 tumors; error bar represents SEM.

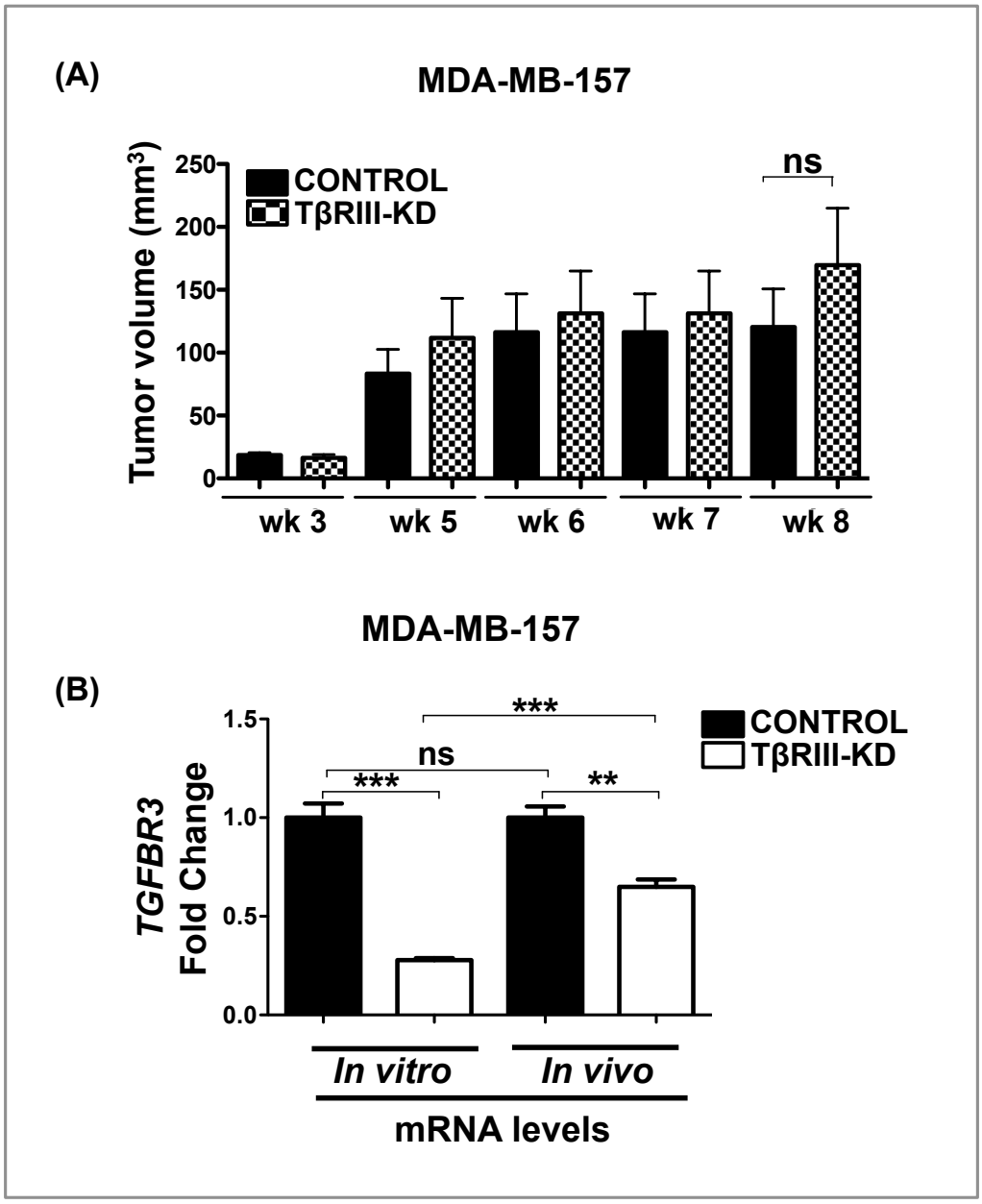

Figure 15. MDA-MB-157 expresses TβRIII after implanted *in vivo* thus does not exhibit significant change in tumor growth.

Figure 15. MDA-MB-157 expresses TβRIII after implanted *in vivo* thus does not exhibit significant change in tumor growth.

A, Tumors in nude mice were palpable 2 weeks post implantation of MDA-MB-157 MSL cell line. Serial tumor volumes (mm^3) were measured weekly for 5 weeks post palpation for both controls and TβRIII-KD. Each data bar represents the mean tumor volume of 10 tumors; error bar represents SEM (P = ns, not significant). **B**, qRT-PCR comparison of *TGFBR3* expression of RNA isolated from MDA-MB-157 cells before implantation (*in vitro* mRNA) and RNA isolated from tumors generated by MDA-MB-157 implantation (*in vivo* mRNA) (ns= not significant, **P =0.002 and ***P <0.0001 for a two-tail Student *t*-test).

Knockdown of TβRIII in MSL cell lines does not affect cell proliferation or viability.

Since TβRIII-KD markedly decreased the tumorigenic potential of mesenchymal TNBC cells, we further explored whether this was due to a proliferation defect. TβRIII can bind to all TGF-β ligands but with highest affinity for TGF-β2 (Andres*, et al*, 1991; Andres*, et al*, 1989), therefore cells were treated with TGF-β2 in addition to TGF-β1. Both controls and TβRIII-KD MSL cell lines responded similarly to the ligands (Figure 16A-B). TβRIII-KD did not alter the proliferation rates of MSL cell lines (SUM159, MDA-MB-231, and MDA-MB-157) by live cell counts (Figure 16A) or ^{3}H-thymidine incorporation assay (Figure 16B). Consistent with an intact TGF-beta signaling pathway (22,23) we have observed an increase in phospho-SMAD2 following ligand treatment (Figure 17). In order to examine cell viability and determine whether knockdown of TβRIII influenced apoptosis, we analyzed cleaved-caspase 3 and cleaved-PARP and we did not detect any difference between control and TβRIII-KD MSL cells (Figure 16C).

Knockdown of TβRIII in MSL cells impairs motility, invasion and the ability to form invasive protrusions in 3D cultures.

Using a validated method (please see methods section for details) for measurement of cell migration (Ashby*, et al*, 2012), we found that TβRIII-KD

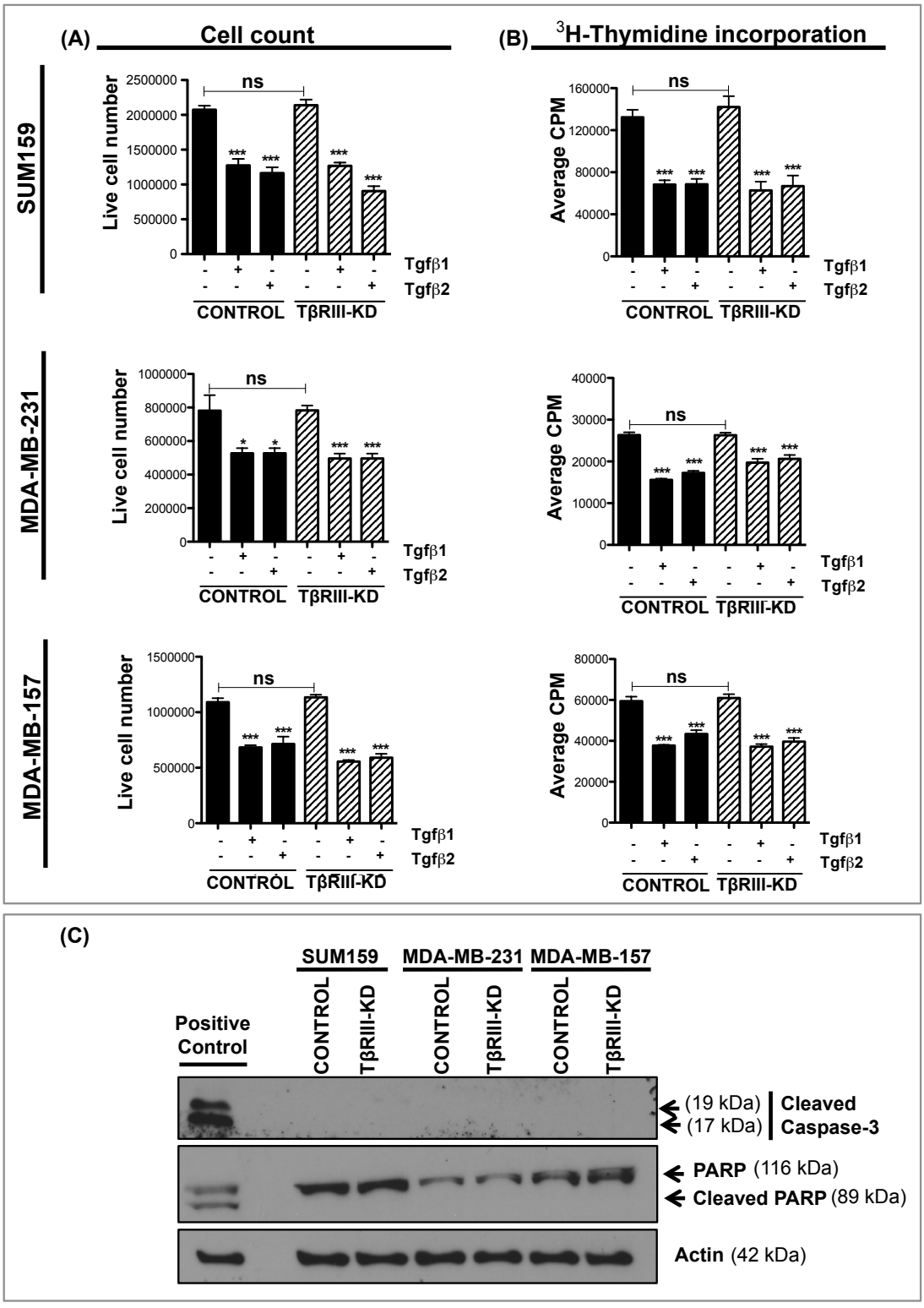

Figure 16. TβRIII-KD in MSL cell lines does not affect cell proliferation.

Figure 16. TβRIII-KD in MSL cell lines does not affect cell proliferation.
A, Live cell count proliferation assay for SUM159, MDA-MB-231 and MDA-MB-157 controls versus TβRIII-KD 72hrs post treatment with TGF-β1 and TGF-β2 ligands; graph bars represent the mean of 6 replicates with SEM error bars (ns = not significant; *P < 0.01, ***P ≤ 0.0005 for a two-tail Student *t*-test). **B,** thymidine incorporation proliferation assay for SUM159, MDA-MB-231 and MDA-MB-157 controls versus TβRIII-KD in presence or absence of TGF-β1 and TGF-β2 ligands; graph bars represent the mean of 6 replicates with SEM error bars (***P ≤ 0.0004 for a two-tail Student *t*-test). **C,** immunoblot analysis of cleaved-caspase 3 and PARP protein expression using lysates harvested from SUM159, MDA-MB-231 and MDA-MB-157 stably expressing control and TβRIII-KD. Results are representative of three independent experiments.

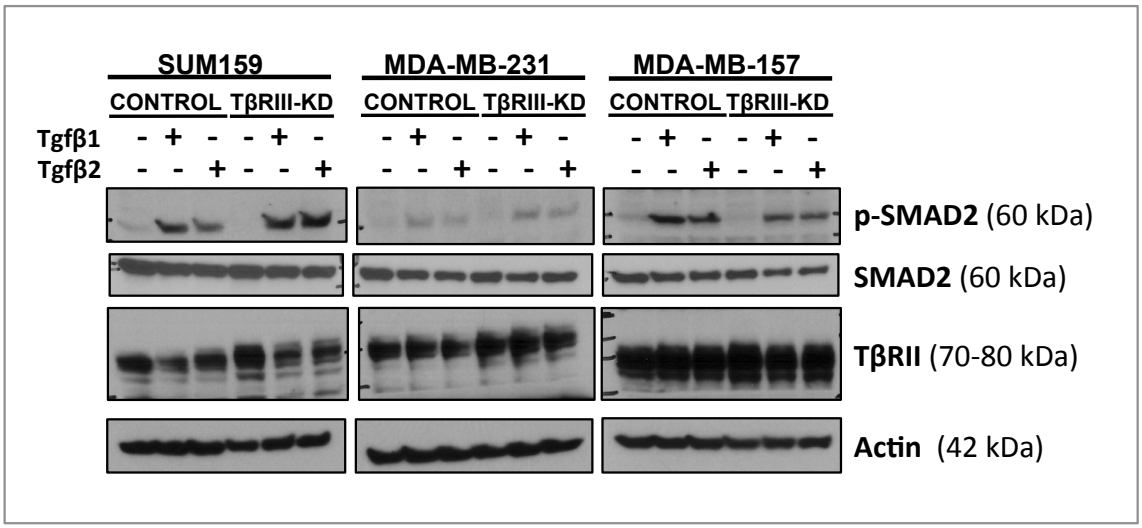

Figure 17. p-SMAD2 and TβRII levels indicate that TGF-β signaling is intact in TβRIII controls and TβRIII-KD MSL lines.

Immunoblot analysis for phospho-SMAD2, SMAD2 and TβRII using protein harvested from SUM159, MDA-MB-231 and MDA-MB-157 cells with TβRIII-KD in presence or absence of TGF-β1 and TGF-β2 ligands.

significantly decreased the migration of SUM159, MDA-MB-231 and MDA-MB-157 cells (Figure 18A-C). Treatment with TGF-β ligands had no effect on migration. In order to determine the invasive properties of MSL lines we analyzed their ability to migrate through a barrier using an invasion transwell assay. TβRIII-KD impaired the ability of the MSL cell lines to invade through Matrigel pre-coated transwells and the addition of TGF-β ligands had little effect on invasion in either controls or knockdowns (Figure 18D-F). Next, we examined the effect of TβRIII-KD on the ability of MSL cells to form colonies in 3D Matrigel culture. After five days in culture, SUM159 cells with TβRIII-KD had smooth edges around cell spheres while control cells had multiple protrusions invading into the surrounding matrix (Figure 18G). These results were quantified by calculations of the perimeter, which show a, significant difference between controls and TβRIII-KD (Figure 18H). Overall, the data above indicate that TβRIII modulates migration and invasion, independent of TGF-β stimulation, in MSL cells. To further investigate TGF-β pathway signaling in the MSL lines we examined both canonical (SMAD-dependent) and non-canonical (SMAD-independent) signaling pathways (Derynck & Zhang, 2003). We used standard CAGA-luc (Figure 19A) and 3TP-lux (Figure 19C) reporter assays for measurement of TGF-β activity (Kusanagi*, et al*, 2000; Wrana*, et al*, 1992). Assays were performed either in presence of TGF-β1 or TGF-β2 ligands and compared to untreated controls (Andres*, et al*, 1989; Lopez-Casillas*, et al*, 1991). In addition, we performed qPCR analysis for SMAD7 (Figure 19B) and PAI-1 (Figure 19D) gene expression as readout for downstream targets for canonical and non-canonical TGF-β

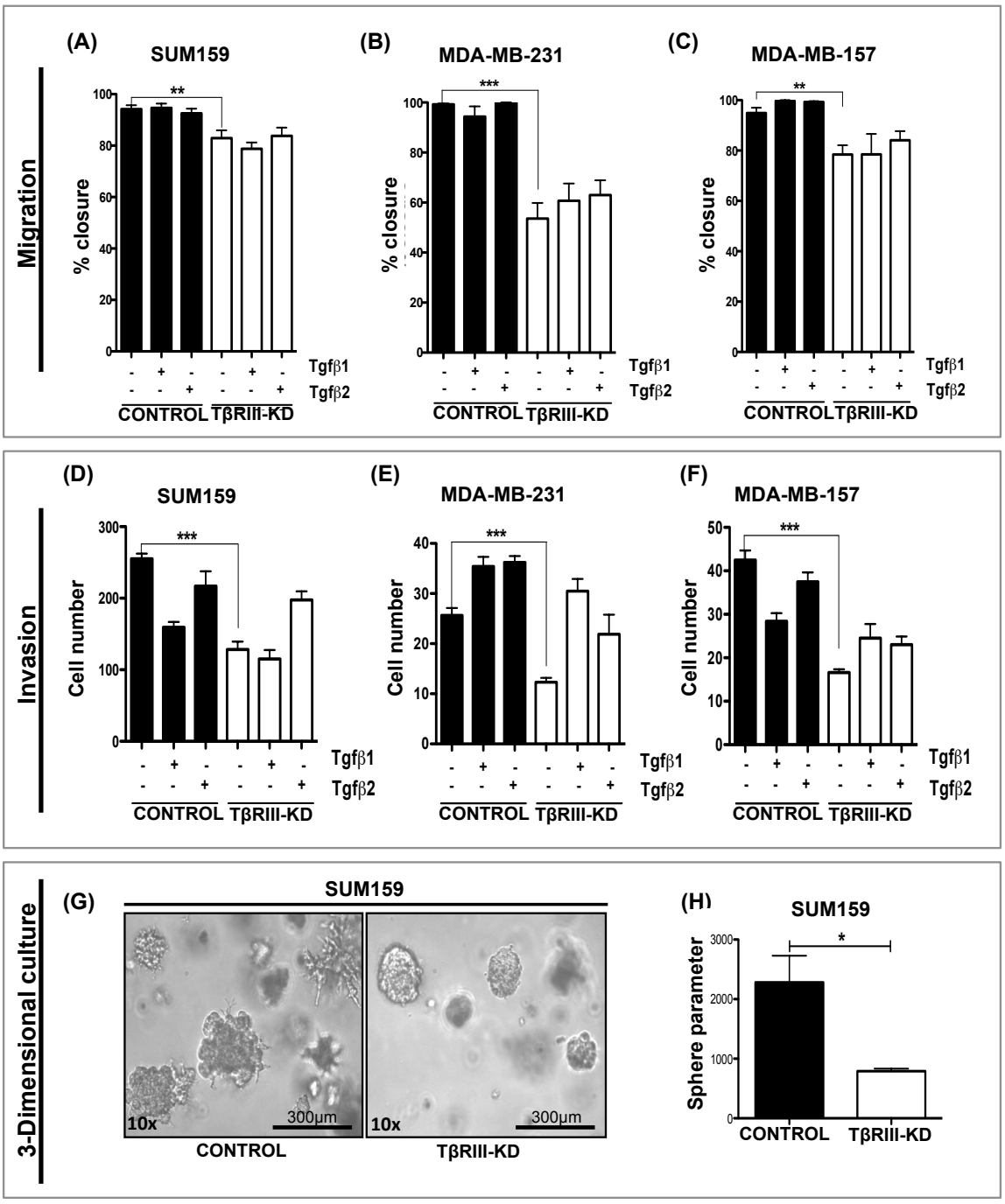

Figure 18. Phenotypic effect of TβRIII knockdown in MSL cells.

Figure 18. Phenotypic effect of TβRIII knockdown in MSL cells.
A-C, Cells were plated around magnetic stencils. After cells had adhered the magnetic stencils were removed and migration assay was monitored for 24hrs. Bar graphs represent percentages of closure for each MSL cell line with TβRIII-KD in comparison to control with or without TGF-β1 and TGF-β2 treatment; graph bars represent the mean of 3 replicates with SEM error bars (***P* = 0.001, ****P* < 0.0001 for a two-tail Student *t*-test). **D-F,** number of MSL cells that invaded through Matrigel pre-coated transwells with or without 24hr pre-treatment of cells with TGF-β1 and TGF-β2 ligands (****P* < 0.0001 for a two-tail Student *t*-test). **G,** Representative 10x images of SUM159 controls versus TβRIII-KD cells embedded in 3D matrigel culture. Scale bar: 300μm. **H,** quantification of SUM159 3D Matrigel culture; bar graph represent tumor-sphere perimeter derived from mean of 3 replicates with SEM error bars (**P* = 0.029 for a two-tail Student *t*-test).

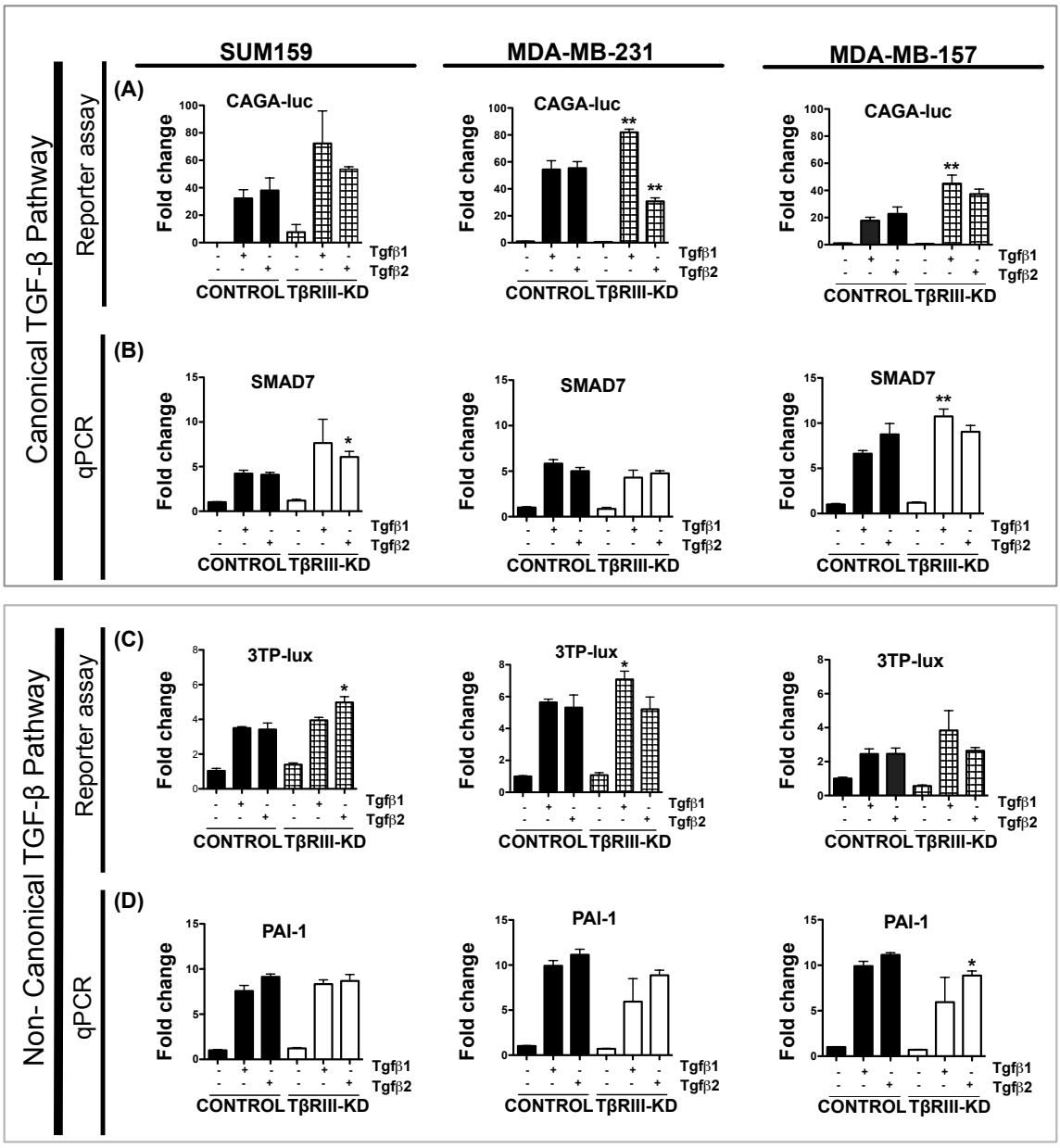

Figure 19. TGF-β signaling appears to remain functional in TβRIII-KD MSL cell lines.

Figure 19. TGF-β signaling appears to remain functional in TβRIII-KD MSL cell lines.

A, Controls and TβRIII-KD MSL cells were co-transfected with CAGA-Luc and pRL-CMV renilla (used as internal control to correct for transfection efficiency). Eighteen hours post transfection cells were treated for 24hrs with 1ng/ml of TGF-β1 and TGF-β2. Cells were then collected and tested for promoter specific luciferase activity using a dual-luciferase reporter assay system was. Bar graph data represents mean of 4 replicates with SEM error bars (**P≤ 0.009 for a two-tail Student *t*-test). **B,** qRT-PCR analysis for *SMAD7* mRNA expression from TβRIII-KD MSL cells; graph bars represent the mean of 3 replicates with SEM error bars (*P ≤ 0.03, **P≤ 0.009) for a two-tail Student *t*-test) **C,** controls and TβRIII-KD MSL cells were co-transfected with 3TP-lux and pRL-CMV renilla (used as internal control to correct for transfection efficiency). 18hrs post transfection cells were treated for 24hrs with 1ng/ml of TGF-β1 and TGF-β2. Cells were then collected and tested for promoter specific luciferase activity using a dual-luciferase reporter assay system was. Bar graph data represents mean of 4 replicates with SEM error bars (*P ≤ 0.03 for a two-tail Student *t*-test). **D,** qRT-PCR analysis for *PAI-1* mRNA expression from TβRIII-KD MSL cells; graph bars represent the mean of 3 replicates with SEM error bars (*P ≤ 0.03 for a two-tail Student *t*-test).

activity, respectively (Keeton*, et al*, 1991; Shimanuki*, et al*, 2007). The results of both assays indicate that knockdown of TβRIII does not modulate either arm of TGF-β signaling pathway. Thus, MSL lines with TβRIII knockdown have resulting phenotypic changes without concomitant changes in the TGF-β signaling pathways measured. Considering these results and knowing that TβRIII can also bind to BMPs (bone morphogenetic proteins) (Kirkbride*, et al*, 2008), we treated the engineered MSL cell lines with BMP4. We did not observe significant changes in Smad1/5/8 phosphorylation in TβRIII-KD versus control MSL cells (data not shown). The results suggest that TβRIII modulates the tumorigenic potential of MSL TNBC cells through other signaling pathways.

Knockdown of TβRIII is associated with increased expression of integrin-α2 in MSL TNBC cells.

To determine which genes and/or signaling pathways are significantly altered in MSL cells after TβRIII knockdown; we performed gene expression microarray analyses on SUM159 cells grown in 3D cultures. The integrin signaling pathway, along with other cell adhesion pathways, were among the most significant pathways differentially expressed in TβRIII-KD MSL cells relative to control cultures (Table 4). Analysis of individual genes of the integrin pathway revealed that integrin-α2 (*ITGA2*) was a top gene that was significantly increased upon TβRIII knockdown (Table 5). *In vitro* qRT-PCR analysis indicate a statistically significant (above 2-fold) upregulation of integrin-α2 in the TβRIII-KD MSL cells

Table 4. Integrin pathway is among significantly changed signaling pathways in SUM159 TβRIII-KD 3D culture system.

Genes were considered differentially expressed and included for pathway analysis if they met a cutoff of |log2FC|>0.5 and FDR adjusted P value<0.05. Pathway analysis was performed by querying against the C2 Canonical Pathways in the Molecular Signature Database (MSigDB).

Gene Set Name	# Genes in Gene Set (K)	# Genes in Overlap (k)	p-value
REACTOME_CELL_JUNCTION_ORGANIZATION	78	8	7.67E-07
REACTOME_CELL_CELL_COMMUNICATION	120	9	2.24E-06
PID_INTEGRIN1_PATHWAY	66	7	3.03E-06
KEGG_CELL_ADHESION_MOLECULES_CAMS	134	8	4.31E-05
PID_INTEGRIN3_PATHWAY	43	5	5.20E-05
KEGG_FOCAL_ADHESION	201	9	1.35E-04
REACTOME_CELL_CELL_JUNCTION_ORGANIZATION	56	5	1.87E-04
PID_AVB3_INTEGRIN_PATHWAY	75	5	7.29E-04
REACTOME_INTEGRIN_CELL_SURFACE_INTERACTIONS	79	5	9.23E-04
KEGG_ECM_RECEPTOR_INTERACTION	84	5	1.22E-03
REACTOME_EXTRACELLULAR_MATRIX_ORGANIZATION	87	5	1.42E-03
REACTOME_ADHERENS_JUNCTIONS_INTERACTIONS	27	3	2.05E-03

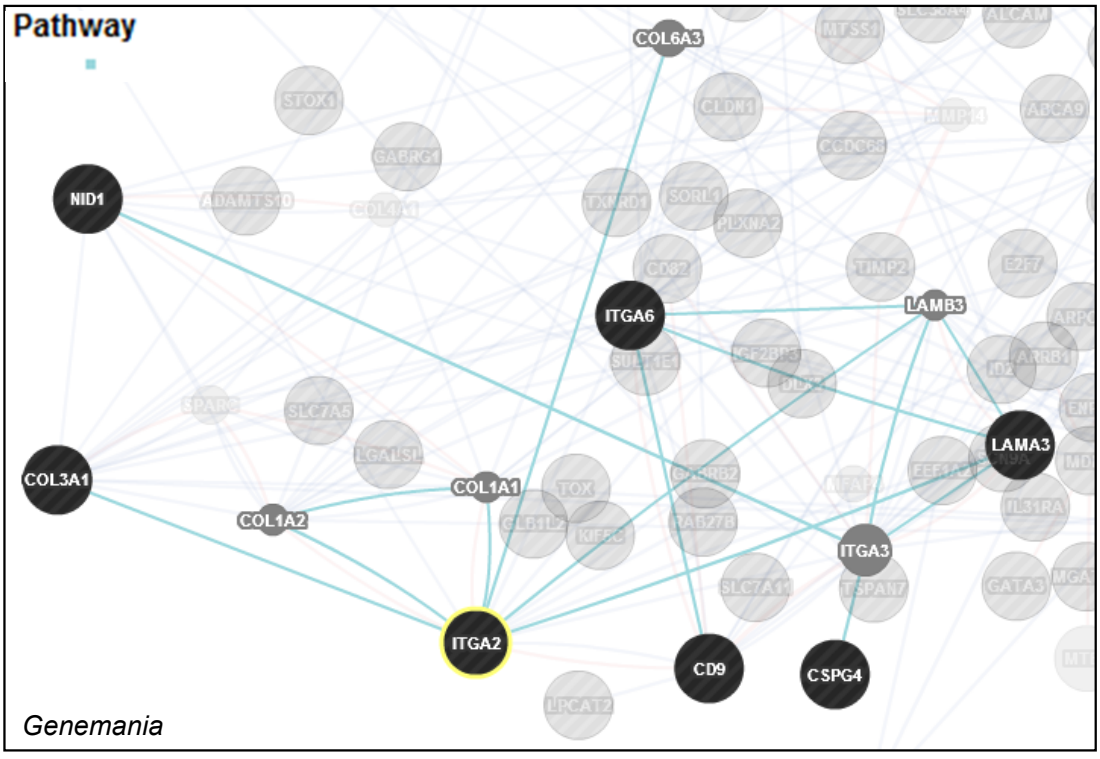

Table 5. Integrin family members in SUM159 cells with TβRIII-KD grown in three-dimensional cultures.

Table represents list of integrin family genes from microarray analysis. Genes are ordered based on adjusted *P values* (low to high). *ITGA2* was the top integrin gene with lowest *p value* (*P= 0.00310994*)

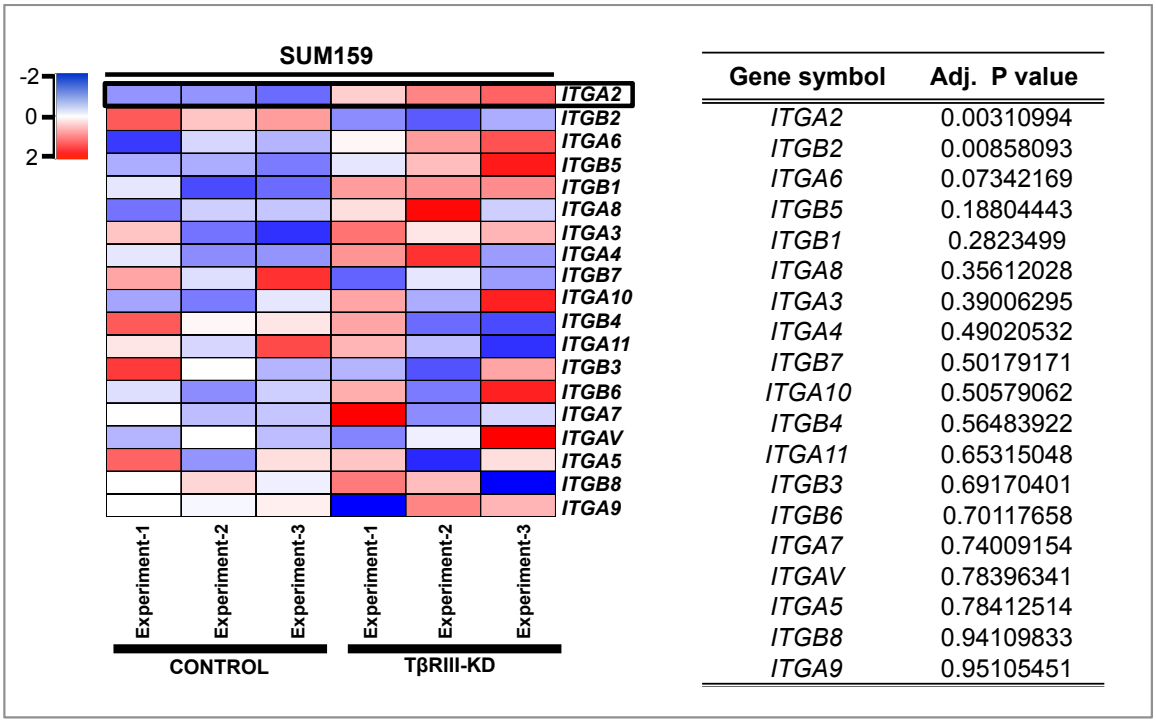

Gene symbol	Adj. P value
ITGA2	0.00310994
ITGB2	0.00858093
ITGA6	0.07342169
ITGB5	0.18804443
ITGB1	0.2823499
ITGA8	0.35612028
ITGA3	0.39006295
ITGA4	0.49020532
ITGB7	0.50179171
ITGA10	0.50579062
ITGB4	0.56483922
ITGA11	0.65315048
ITGB3	0.69170401
ITGB6	0.70117658
ITGA7	0.74009154
ITGAV	0.78396341
ITGA5	0.78412514
ITGB8	0.94109833
ITGA9	0.95105451

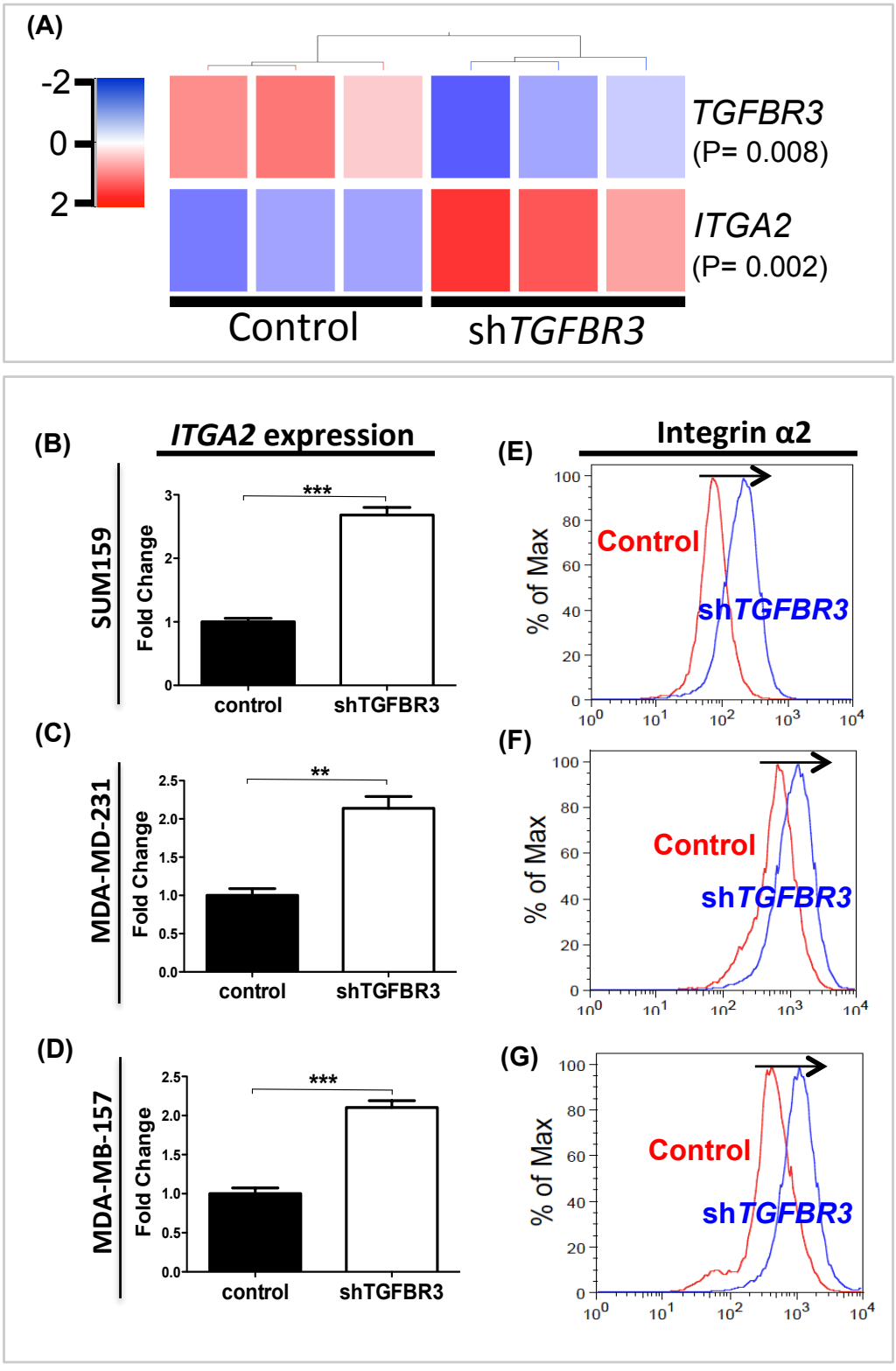

Figure 20. TβRIII-KD modulates expression of integrin-α2 (*ITGA2*) in MSL cells.

Figure 20. TβRIII-KD modulates expression of integrin-α2 (ITGA2) in MSL cells.

A, heatmap representing levels of *ITGA2* between control and sh*TGFBR3*. **B-D,** qRT-PCR analysis for *ITGA2* mRNA expression from MSL TNBC cell lines with TβRIII-KD; graph bars represent the mean of 3 replicates with SEM error bars (**P = 0.003, ***P ≤ 0.0007 for a two-tail Student *t*-test). **E-G,** flow cytometry analysis for integrin-α2 in controls and TβRIII-KD MSL; arrow pointing to the right shows a shift towards an increase in protein levels of integrin-α2 in TβRIII-KD MSL cell lines.

(Figure 20B-D). The upregulation of integrin-α2 was further validated by flow analysis across all MSL cell lines studied (Figure 20E-G).

TβRIII modulation of integrin-α2 expression is required for the migratory and invasive MSL cell line phenotypes.

Using a clinically relevant, spontaneous mouse model of breast cancer progression and metastasis, Ramirez et al. demonstrated that integrin-α2β1 acts as a tumor suppressor; and α2-null cells were more motile and invasive (Ramirez*, et al*, 2011). The *in vivo* and *in vitro* findings were further correlated with analysis of microarray gene expression datasets of human breast and prostate cancers, which showed a correlation between decreased expression of *ITGA2* and poor prognosis (Ramirez*, et al*, 2011). Considering this role of integrin-α2 in breast cancer, we hypothesized that the decrease in migration and invasion upon TβRIII-KD in MSL cells could be rescued by concomitant knockdown of integrin-α2. To test our hypothesis, we stably knocked down integrin-α2 (α2-KD) in the MSL TβRIII-KD cells and performed migration and invasion assays (Figure 21A-B, Figure 22A-B). Knockdown of integrin-α2 was sufficient to reverse the migration (Figure 21C, Figure 22C) and invasion (Figure 21E, Figure 22D) phenotype of MSL cells with TβRIII-KD to those of control cells. In addition, using an integrin-α2 neutralizing antibody we rescued the migratory phenotype (Figure 21D) in a manner similar to that observed after α2-KD in TβRIII-KD cells. Knelson and colleagues showed that knockdown of TβRIII leads to diminished FGF2-mediated ERK phosphorylation (Knelson*, et al*, 2013).

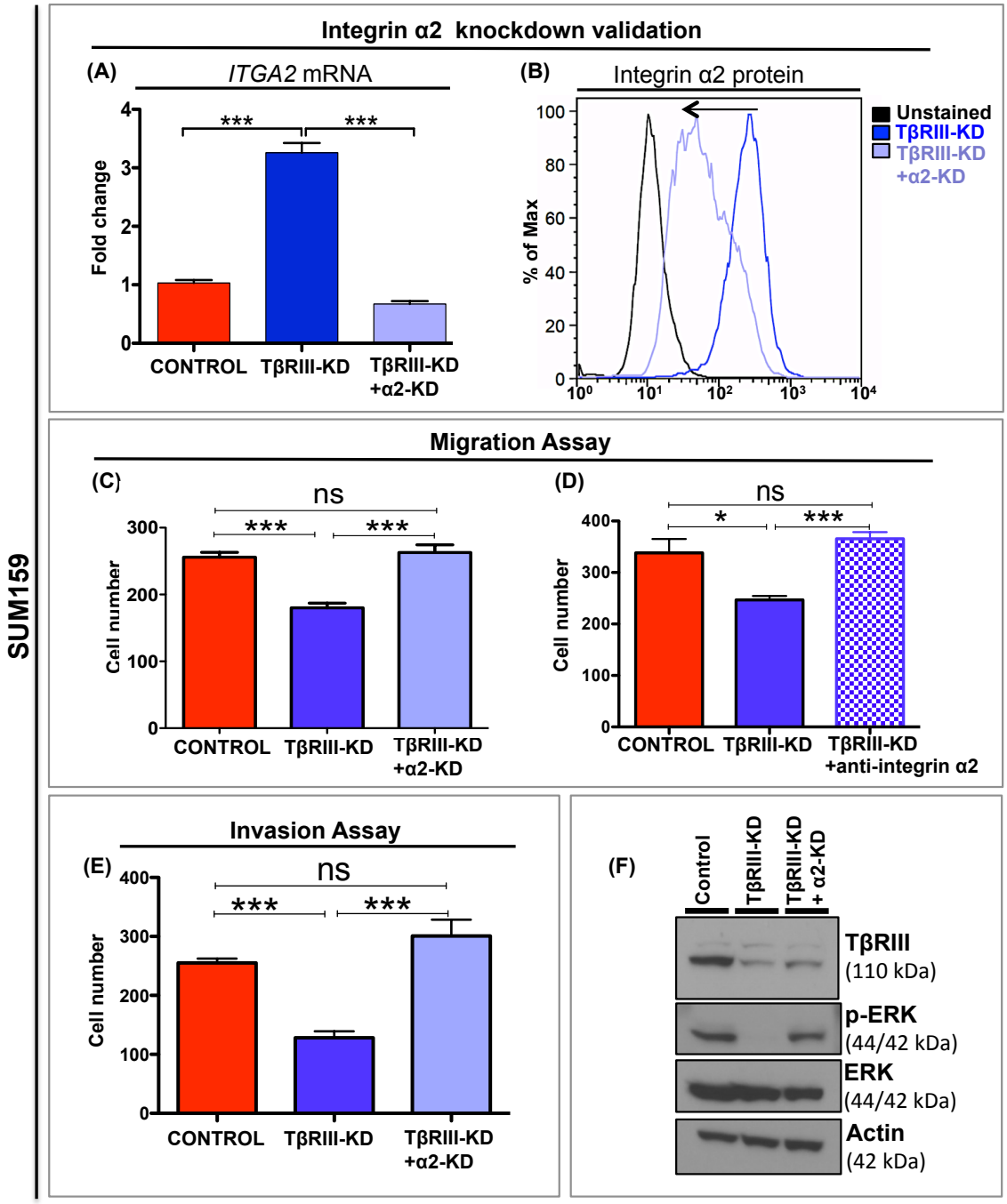

Figure 21. Knockdown of integrin- α2 in TβRIII-KD MSL cells reverses migratory and invasive TβRIII-KD phenotypes.

Figure 21. Knockdown of integrin- α2 in TβRIII-KD MSL cells reverses migratory and invasive TβRIII-KD phenotypes.

A, qRT-PCR analysis for *ITGA2* mRNA expression before and after stable knockdown of integrin-α2 (α2-KD) in SUM159 cells with TβRIII-KD; graph bars represent the mean of 3 replicates with SEM error bars (***P < 0.0001 for a two-tail Student *t*-test)**. B,** Flow cytometry analysis of α2-KD; arrow pointing to the left shows a shift towards a decrease in protein amount of integrin-α2 in TβRIII-KD SUM159 cell lines after α2-KD. **C,** transwell migration assay representing number of cells migrated through transwell upon α2-KD in TβRIII-KD SUM159 cell line (ns= not significant, ***P < 0.0001 for a two-tail Student *t*-test); bar graph represents a mean of 3 replicates with SEM error bars. **D,** transwell migration assay representing number of cells migrated upon treatment of TβRIII-KD SUM159 cell line with anti-α2 blocking antibody (ns= not significant, *P = 0.011, ***P < 0.0001 for a two-tail Student *t*-test). **E,** transwell invasion assays with inserts pre-coated with Matrigel allowing for testing the number of cells that can invade upon α2-KD in TβRIII-KD SUM159 cells (ns= not significant, ***P < 0.0001 for a two-tail Student *t*-test). **F,** immunoblot analysis for phospho-ERK using protein harvested from SUM159 cells with TβRIII-KD and TβRIII-KD /α2-KD.

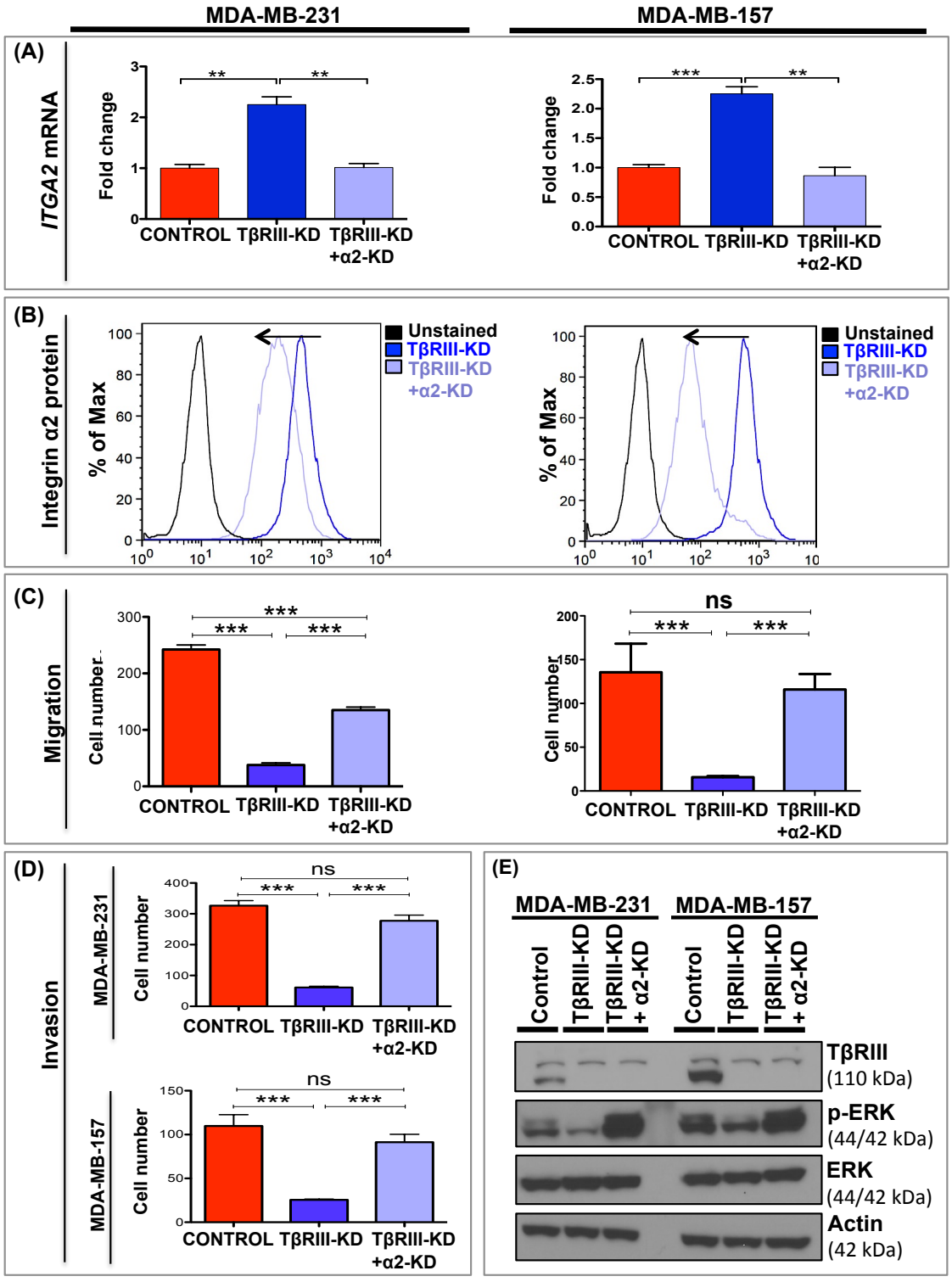

Figure 22. Knockdown of integrin-α2 in TβRIII-KD MSL cells reverses migratory and invasive TβRIII-KD phenotypes

Figure 22. Knockdown of integrin- α2 in TβRIII-KD MSL cells reverses migratory and invasive TβRIII-KD phenotypes.

A, qRT-PCR analysis for *ITGA2* mRNA expression before and after stable knockdown of integrin-α2 (α2-KD) in MDA-MB-231 and MDA-MB-157 cells with TβRIII-KD; graph bars represent the mean of 3 replicates with SEM error bars (**$P \leq 0.002$, *** $P \leq 0.0007$ for a two-tail Student *t*-test)**. B,** Flow cytometry analysis of α2-KD; arrow pointing to the left shows a shift towards a decrease in protein amount of integrin-α2 in MDA-MB-231 and MDA-MB-157 cells with TβRIII-KD after α2-KD. **C,** transwell migration assay representing number of cells migrated through transwell upon α2-KD in TβRIII-KD MDA-MB-231 and MDA-MB-157 cell lines (ns= not significant, *** $P < 0.0007$ for a two-tail Student *t*-test); bar graph represents a mean of 3 replicates with SEM error bars. **D,** transwell invasion assays with inserts pre-coated with Matrigel allowing for testing the number of cells that can invade upon α2-KD in TβRIII-KD MDA-MB-231 and MDA-MB-157 cells (ns= not significant, *** $P < 0.0007$ for a two-tail Student *t*-test). **F,** immunoblot analysis for phospho-ERK using protein harvested from MDA-MB-231 and MDA-MB-157 with TβRIII-KD and TβRIII-KD /α2-KD.

Consistent with this previous study, after knockdown of TβRIII in the MSL cells, the phospho-ERK levels decreased and were restored in the cells after simultaneous integrin-α2 and TβRIII knockdown (Figure 21F and, Figure 22E).

Relationship between gene expression of TβRIII and integrin-α2 in TNBC patient dataset.

To further investigate the association between TβRIII (*TGFBR3)* and integrin-α2 (*ITGA2*) in TNBC, we used the TNBC patient dataset described in Figure 1A (Lehmann*, et al*, 2011) to analyze the relationship between *TGFBR3* and *ITGA2* gene expression. Our results indicate an inverse correlation between *ITGA2* and *TGFBR3* expression across TNBC subtypes. In particular, we see the strongest inverse correlation in TNBC subtypes with either high *TGFBR3* expression (MSL; *P= 5.274e-06*); or low *TGFBR3* expression (Basal-like 2; with *P= 5.16e-07* and Luminal AR (LAR); with *P= 1.759e-07)* (Figure 23A-B). The clinical association between *ITGA2* and *TGFBR3* expression is relevant as it further links the impact of the interplay between TGF-β and integrin pathways in TNBC.

Discussion

Currently, the functional role of TβRIII is controversial in breast cancer. Some reports suggest a tumor suppressive function of TβRIII (Dong*, et al*, 2007),

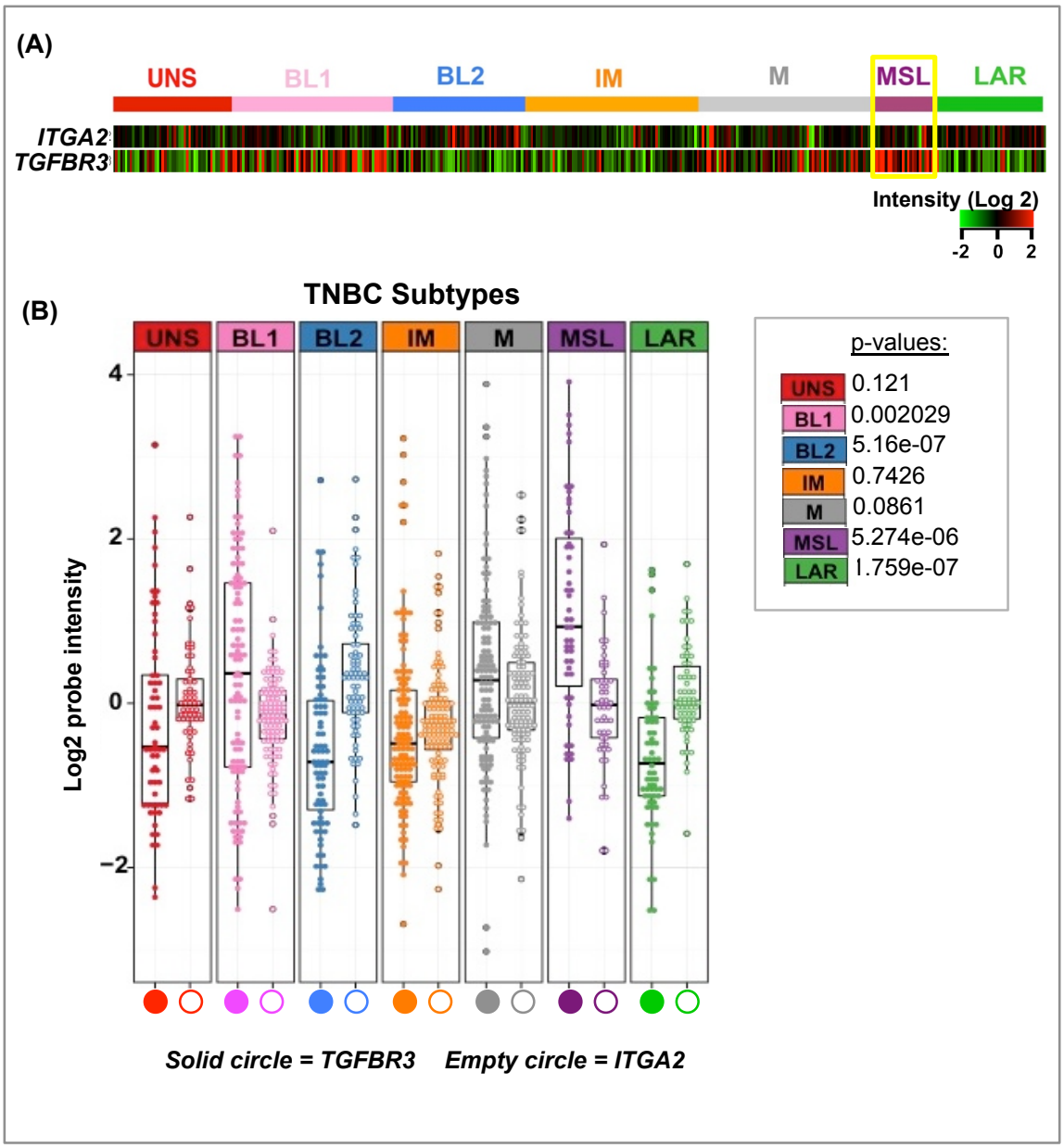

Figure 23. TNBC patient dataset shows that expression of *TGFBR3* is inversely correlated with expression of *ITGA2*.

A, Heat map representation of ***TGFBR3* and *ITGA2*** gene expression for 587 TNBC tumors for each *TGFBR3* and *ITGA2*. **B,** quantification of gene expression for *TGFBR3* (solid circles) and *ITGA2* (empty circles) across TNBC tumor subtypes using log2 probe intensity values. The whiskers of the boxplot extend to the highest value that is within 1.5 interquartile range. P values were generated by performing a paired two-tail Student *t*-test.

while other reports indicate a tumor-promoting role (Criswell*, et al*, 2008; Jelinek*, et al*, 2003; Liu*, et al*, 2003; Woszczyk*, et al*, 2004). Through genomic expression (GE) analysis of 587 TNBC patients, we demonstrated that the *TGFBR3* is expressed at higher level and most consistently in MSL subtype of TNBC. Furthermore, we have identified MSL cell line models that express high levels *TGFBR3*. To better understand the molecular basis of *TGFBR3* GE we used representative MSL cell lines and a TβRIII loss-of-function approach. The data presented herein supports our hypothesis of an oncogenic role for TβRIII in MSL subtype of TNBC. Biologically, knockdown of TβRIII in TNBC MSL cell lines resulted in decreased motility and invasion, a lack of invasive protrusion in 3D culture *in vitro,* and a significant decrease in tumor growth in xenograft mouse model. The observed migratory and invasive cell line phenotypes were further associated with modulation of the integrin- α2 pathway.

Previously, the loss of TβRIII expression was correlated to progression from a pre-invasive to an invasive state of breast cancer (Dong*, et al*, 2007). In addition, restoring expression of TβRIII in a breast cancer cell line led to a decrease of tumor invasiveness *in vitro* and tumor invasion and metastasis *in vivo* (Dong*, et al*, 2007). Other studies have demonstrated a frequent loss of TβRIII in human cancers (Copland*, et al*, 2003; Gordon*, et al*, 2008; Hempel*, et al*, 2008; Hempel*, et al*, 2007; Turley*, et al*, 2007). However, these studies lacked genomic analysis of tumors, thus their difference in conclusion can be due to the difference in their study models. Taking into account the dependency of TGFβ signaling on the context (Massagué, 2012) as well as the heterogeneity of breast

cancers, especially TNBC (Lehmann*, et al*, 2011; Lehmann & Pietenpol, 2014), we took a more focused approach to study the role of TβRIII in breast cancer progression. Since it has been previously established that TβRIII can modulate TGF-β signaling (Andres*, et al*, 1992; Bernabeu*, et al*, 2009; Esparza-Lopez*, et al*, 2001; López-Casillas*, et al*, 1994; Lopez-Casillas*, et al*, 1993), it is not surprising that TβRIII has been shown to have both pro- and anti-tumorigenic effects in breast cancer. Our study shows that knockdown of TβRIII in MSL cells appears not to alter the cells' ability to respond to TGF-β either through the canonical and non-canonical arms of the pathway, or the BMP pathway. Rather, we observed that loss of TβRIII results in a decrease in cell motility and invasion. To further investigate potential mechanisms by which TβRIII regulates these cell functions, we performed gene expression analysis on cells after TβRIII knockdown. We found that the expression of genes involved in integrin signaling and cell-ECM interactions were significantly differentially regulated after TβRIII knockdown.

Previous work has shown that inhibition of integrins can reverse the transformed state of breast cancer cells and that α2β1 integrin can play a role in cancer progression (Zutter*, et al*, 1990). A more recent study demonstrated that α2β1 integrin acts as a metastasis suppressor in breast cancer, where migratory and invasive abilities of tumor cells are enhanced after loss of α2β1 integrin expression (Ramirez*, et al*, 2011). This supports our finding wherein a decrease in the migratory and invasive phenotype, upon TβRIII knockdown, was linked to increased integrin- α2 expression levels. The precise mechanistic link between

TβRIII and integrin- α2 expression levels is unknown. The only other association between integrins and TβRIII was reported in MCF10A breast epithelial cells where TβRIII was shown to regulate integrin- α5 localization (Mythreye*, et al*, 2013).

Knockdown of integrin- α2 in TβRIII-KD MSL TNBC cells reverses the loss of motility and invasion that occurs upon TβRIII knockdown alone. One explanation for the observed rescue of migratory and invasive phenotype is through the regulation of ERK phosphorylation possibly mediated by integrin- α2. As shown in Figures 12 and 13, upon knockdown of TβRIII we observed a decrease of phospho-ERK simultaneous with an increase in integrin- α2. Furthermore, upon knockdown of integrin- α2 in TβRIII-KD cells we see and increase in phopho-ERK suggesting that integrin- α2 is suppressing ERK activity. This is in agreement with other studies that have shown that integrins can regulate ERK activity (Chen*, et al*, 1996; Miyamoto*, et al*, 1996; Renshaw*, et al*, 1999). In addition, studies have demonstrated that continuous ERK activity can regulate invasion and migration by regulating transcription of genes or directly regulating enzymes necessary for cell movement (Glading*, et al*, 2001; Huang*, et al*, 2004).

Therefore the increase in phospho-ERK seen upon integrin- α2 knockdown could be an explanation for increase in mobility of our TβRIII-KD cells. Our data show a correlation between TβRIII's modulation of migration and invasion and the reduction of phospho-ERK levels possibly mediated by integrin-

α2. Further studies will be required to elucidate the precise mechanistic relationship between TβRIII and integrin- α2.

Conclusions

In summary, our studies using MSL TNBC models demonstrate that TβRIII is an oncogenic driver of migration and invasion *in vitro* as well as tumor growth *in vivo*. Further mechanistic characterization of MSL TNBC would provide insights on how to use of this protein and/or signaling pathway as a biomarker or to provide insights to new targets for therapy. Considering the limitations of *in vitro* studies it is necessary to develop a mouse TβRIII breast cancer model to further elucidate the role of this molecule. Such a model would provide more accurate observations for studying the role of TβRIII in the tumor microenvironment. The results of this study provide mechanistic insight into the role of TβRIII in TNBC and highlight an association between TβRIII and integrin-α2 expression and regulation of cell motility, invasion, and tumorigenicity. In addition, this study provides pre-clinical rationale for consideration of TβRIII as a potential target for further discovery efforts.

CHAPTER IV

GENE EXPRESSION PROFILES OF TRIPLE NEGATIVE BREAST CANCER EPITHELIAL AND STROMAL CELLS ARE PREDICTIVE OF TREATMENT RESPONSE

Abstract

In this study we compared responses of triple negative breast cancer (TNBC) patients to addition of mTOR inhibitor RAD001 (everolimus) to cisplatin and cisplatin+paclitaxel. The purposes of this study were to evaluate if the combined use of drugs (RAD001, cisplatin, and paclitaxel) would have synergistic effects and promote apoptosis, enhanced upon inhibition of mTOR with RAD001; and to identify biomarkers of drug sensitivity that will provide insight to novel combination therapies for the different subtypes of TNBC.

145 TNBC patients with clinical stage II/III were randomized 2:1 into two arms. Arm 1 consisted of RAD001 (5 mg daily for 12 weeks)+ cisplatin (25 mg/m^2 q week for 12 weeks) + paclitaxel (80 mg/m^2 q week for 11 weeks) while Arm 2 consisted of placebo (5 mg daily for 12 weeks)+ cisplatin (25 mg/m^2 q week for 12 weeks) + paclitaxel (80 mg/m^2 q week for 11 weeks) until definitive surgery. Biopsy specimens were obtained at baseline (pre), at day 5 of cycle 1 (bp1) and at surgery (post). Primary endpoint was pathological complete response (pCR). The study design provided 90% power to detect a difference in pCR rate of 35% vs. 20% with a two-sided significance level equal to 0.1 (type I error) for each arm.

The overall pathologic clinical response data indicate that out of 145 patients, 52 patients (36%) had pathologic complete response (pCR); 26 patients (18%) had partial-pCR (Near-pCR); 53 patients (36%) did not respond to treatment and 14 patients (10%) were not evaluable (due to disease progression, toxicity or withdrawal). Furthermore, Arms 1 and 2 demonstrated no statistically significant difference in pathologic clinical responses. However, based on clinical patient evaluation addition of RAD001 to the combination of cisplatin and paclitaxel was associated with higher toxicities demonstrated by elevation of transaminase, neutropenia, thrombocytopenia, mucositis and rash. Analysis of Ki67 indicates that an increase of ki67 positive cells was associated with increased pCR rate. Furthermore, tumors with androgen receptor expression were highly associated with NO-pCR patients. Our preliminary genomic results indicate that there is differential gene expression (GE) in both tumor epithelial as well as stromal cells in pretreatment biopsies of pCR versus NO-pCR patients. Patients with higher expression of proliferation genes such as MKI67, KIFCI, AURKB, E2F3, and DNA damage response genes TP53BP2, CHEK1, RPA1, BLM were more responsive to treatment compared to non-responders. Furthermore, responders were more likely to have basal-like subtype while non-responders mesenchymal and luminal-AR (LAR) subtypes.

To our knowledge, this is the largest randomized neoadjuvant study in TNBC with an mTOR pathway inhibitor. Results suggest the combination of paclitaxel and cisplatin is well tolerated and active in TNBC. The addition of RAD001 did not improve pCR or clinical response rates and was associate with

more adverse events. A molecular signature of baseline (pre) biopsies predicts clinical response and TNBC subtypes seem to correlate with the response as well.

Introduction

The clinical term, triple negative breast cancer (TNBC), is a diagnosis of exclusion as it is based on lack of protein expression of estrogen receptor (ER), progesterone receptor, and amplification of the human epidermal growth factor receptor 2 (HER2) (Dent*, et al*, 2007; Society, 2014). TNBC comprise 10%-20% of all breast cancers and is biologically more aggressive than ER+ disease, with higher rates of relapse in the early stage and decreased overall survival in the metastatic setting (Haffty*, et al*, 2006; Morris*, et al*, 2007). TNBC heterogeneity, that likely contributes to variable clinical outcomes, and the absence of well-defined molecular targets makes current state of treatment for TNBC limited to poorly efficient cytotoxic chemotherapy and short disease-free survival (Di Leo*, et al*, 2010). Thus, there is a need to decipher the molecular basis of TNBC as well as develop effective targeted therapy.

The p53 family of transcription factors, p53, p63, and p73, are key regulators of tumor suppressor signaling pathways in breast cancer (Kaufmann*, et al*, 2003). The p53 tumor suppressor is mutated in ~30% of breast cancers (Borresen-Dale, 2003; Fisher*, et al*, 1997), but incidence of p53 mutation is higher in aggressive (ER)-negative breast cancers (Bear*, et al*, 2003) and is strongly associated with the 'basal-like' group (Bear*, et al*, 2003; Smith*, et al*, 2002; Sorlie*, et al*, 2001). Furthermore, the p53 mutation status as well as

expression of the p63 and p73 might modulate gene expression patterns in TNBC.

The p63 and p73 proteins are important regulators of development and tumorigenesis. Studies have shown that the p63 isoform expressed in breast tumors (ΔNp63α) can suppress transcriptional activity (Barbieri*, et al*, 2005; Barbieri & Pietenpol, 2006; Barbieri*, et al*, 2006; Westfall*, et al*, 2003). Further, in a fraction of basal-like tumors, p63 is coordinately expressed with p73 and may antagonize p73-mediated apoptosis (Yang*, et al*, 1999). Together, these studies suggest that the p63/p73 signaling axis could potentially be molecular target for the treatment of triple negative tumors.

Targetable properties of p63/p73 has been previously reported. The study has shown that a p63-dependent tumor survivor pathway directly mediated cisplatin sensitivity in triple-negative tumors (Leong*, et al*, 2007). Specifically, breast tumor cells co-expressing ΔNp63 and TAp73 were more sensitive to cisplatin, however this behavior was not observed when cells were treated with common chemotherapeutic agents used for breast cancer treatment (Leong*, et al*, 2007; Silver*, et al*, 2010). These results suggest a novel mechanism for cisplatin sensitivity in triple-negative cancers (Leong*, et al*, 2007). To further corroborate these findings, a separate group (Rocca*, et al*, 2007) conducted a retrospective analysis of core biopsies of breast cancer patients treated with neoadjuvant chemotherapy, and showed that regimens including cisplatin yielded a significantly higher rate of pCR in p63-positive tumors.

Mammalian repressor of rapamycin (mTOR) pathway is a known oncogenic driver in human cancer and it can regulate multiple cell processes including cell proliferation and apoptosis (Bader*, et al*, 2005). Using a gene expression–based chemical genomics approach, Rosenbluth and collegues have identified a class of drugs (mTOR inhibitors) that modulated p73 activity (Rosenbluth*, et al*, 2008). The *in vitro* TNBC cell line data (Pietenpol lab, Figure 24 unpublished) have further confirmed that mTOR inhibitor (RAD001) and additional drugs (cisplatin, paclitaxel) could elevate p73 and decrease p63.

In summary, based on previous findings that mTOR inhibitors can activate p73 (Rosenbluth*, et al*, 2008); mTOR inhibitors can enhance chemosensitivity of cancer cells to carboplatin (Mondesire*, et al*, 2004), cisplatin (Mabuchi*, et al*, 2007), and paclitaxel (Mondesire*, et al*, 2004), three agents that have been shown to activate p73 (Gong*, et al*, 1999; Lin*, et al*, 2004); and based on studies showing that paclitaxel can inhibit p63 expression (Westfall*, et al*, 2005), we hypothesized that combined use of an mTOR inhibitor, an alkylating agent, and paclitaxel would have synergistic effects in triple negative breast cancer. Considering all the preclinical data on mTOR inhibitors, knowing the efficacy of paclitaxel and cisplatin as neoadjuvant treatments for triple negative breast cancers, and discovering that these three agents in combination can synergistically regulate the p63/p73 signaling axis and apoptosis in breast epithelial cells, we proposed a randomized Phase II clinical trial to study the activity of cisplatin and paclitaxel ± RAD001 (everolimus) in patients with triple negative breast cancer. Furthermore, our overall purpose is to identify

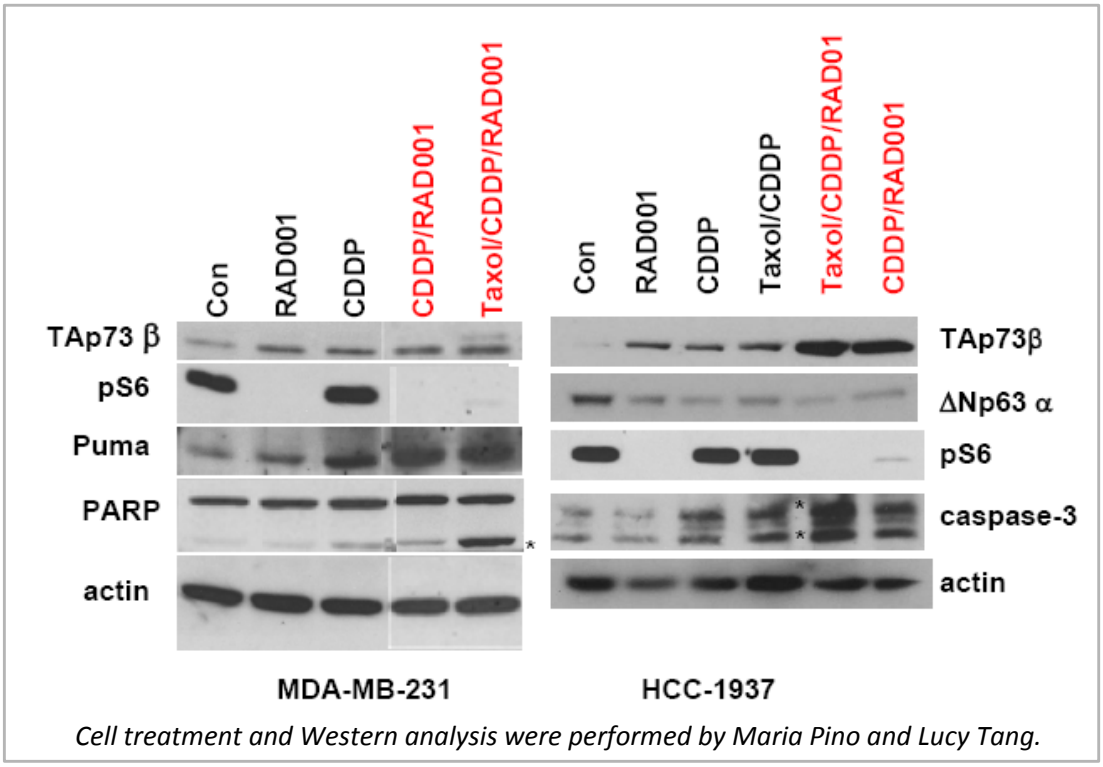

Cell treatment and Western analysis were performed by Maria Pino and Lucy Tang.

Figure 24. Drug modulation of mTOR activity and p63/p73 signaling TNBC cells.

MDA-MB-231 and HCC-1937 cell lines were treated with RAD001 (20nM), cisplatin (CDDP, 25μM), or paclitaxel (Tax, 100nM) alone or with the indicated combinations. Protein lysates were harvested at 24hr and western analysis performed for p63, p73, pS6, Puma, PARP, caspase-3, and actin. Maria Pino and Lucy Tang performed cell treatment and western analysis. This unpublished figure was adapted from Jennifer Rosenbluth.

biomarkers of drug sensitivity that will provide insight to novel combination therapies for the different subtypes of TNBC.

Results

Overview of clinical trial design (VICC BRE0904).

In 2009 we activated a randomized two-arm neoadjuvant phase II trial of cisplatin (25 mg/m^2 IV week) + paclitaxel (80 mg/m^2 IV week) ± RAD001 (5mg PO daily) in patients with stage II and III triple negative with triple negative locally advanced breast cancer (Figure 25). The primary objective of the trial was to determine the pathologic complete response (pCR). Additional aims were to determine the efficacy and safety of the drug combinations in each treatment group, evaluate therapy-mediated changes in correlative molecular markers (i.e. examine changes in proliferation, the p53/p63/p73 signaling axis and mTOR signaling pathways) and determine the ability of GE signatures to predict patient response. The trial was randomized 2:1 with Arm 1 patients treated with RAD001+ cisplatin for one week followed by addition of paclitaxel to the combination for additional 11 weeks. Arm 2 was set up in same manner with exception of RAD001 being replaced with a placebo. In addition, ultrasound guided core biopsies for molecular markers and correlative studies were collected. First at the time of diagnosis (baseline/pre-treatment biopsy) and two additional collections, biopsy 1 (BP1) prior to addition of paclitaxel to the cisplatin ± RAD001 treatment combinations, and at time of surgery (Post) (Figure 25).

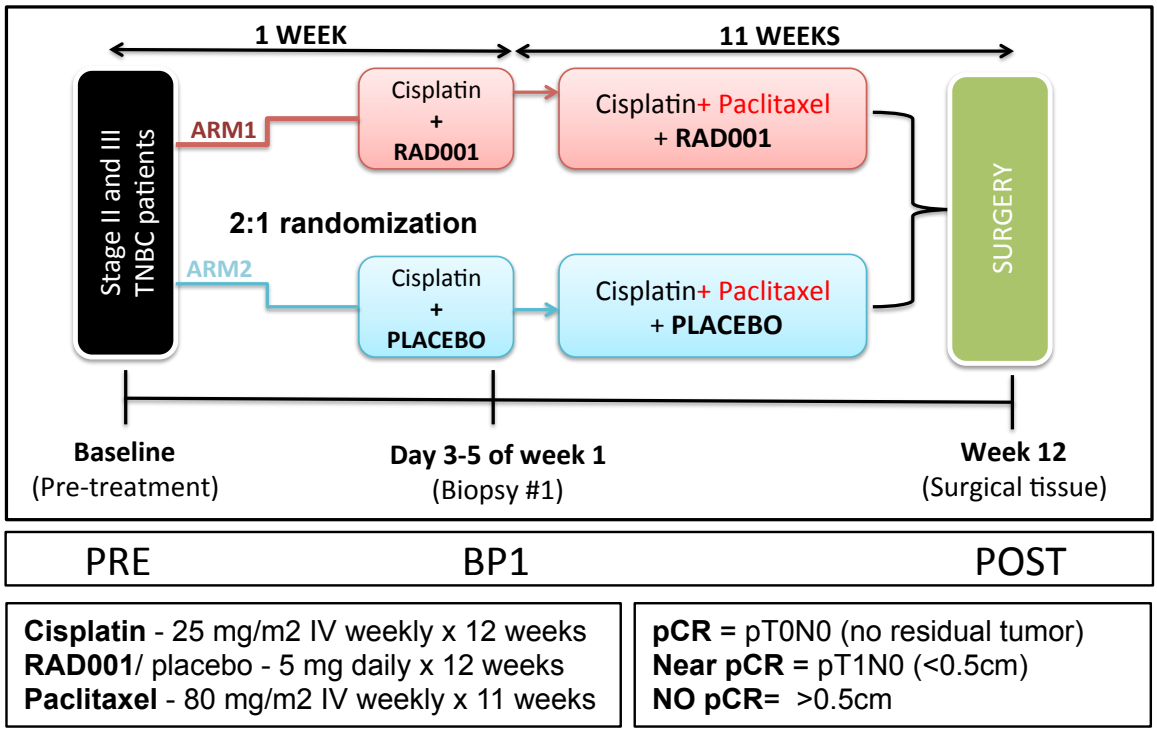

Figure 25. Schematic of randomized neoadjuvant phase II trial of cisplatin + paclitaxel ± RAD001 in patients with stage II and III triple negative breast cancers.

Figure 25. Schematic of randomized neoadjuvant phase II trial of cisplatin + paclitaxel ± RAD001 in patients with stage II and III triple negative breast cancers.

This is a randomized phase II neoadjuvant study of cisplatin (platinol), paclitaxel (taxol) with or without RAD001 (everolimus, an mTOR inhibitor). Patients that fit the eligibility criteria were randomly assigned to each arm of the trial in a 2:1 ratio. Arm 1 has a sample size of 96 and Arm 2 has a sample size of 49. A baseline (pre-treatment) and two research biopsies (biopsy 1 and post-treatment) were be collected from each patient accrued. Drug treatment consisted of cisplatin (25 mg/m2 IV weekly for 12 weeks)± RAD001 (5 mg PO daily for 12 weeks) + paclitaxel (80 mg/m2 IV weekly for 11 weeks). The diagram outlines each arm of treatment. Patients that had near-pCR (tumor size criteria<0.5cm) or no-pCR (tumor size criteria>0.5cm) had undergone surgery at the end of the trial at which point post-treatment tissue was collected. Patients with no residual tumor (tumor size= 0cm) and no lymph node involvement were considered pathologic complete responders (pCR).

RAD001 did not improve clinical response rate but caused slightly higher adverse events.

The baseline of patients' and their tumor characteristics between arms were similar with median age 52 (ranging between 28 – 81yrs), median breast tumor size of 2 cm (ranging between 0.1 – 7.6 cm). Overall, 72% of tumors were histologic grade III, and 70% of patients had clinical stage III disease (data not shown). The trial has accrued 145 patients, with 131 patients having completed the trial; 52 patients have had pCR (36%) and 26 had near-pCR (<0.5 cm residual disease). 53 patients (36%) had no response (>0.5 cm residual disease) and 14 patients (10%) did not complete treatment due to progression of disease, withdrawal or toxicity (Figure 26A). The clinical response data suggest that neoadjuvant cisplatin and/or cisplatin ± RAD001 followed by paclitaxel is effective in TNBC. Similar rates of pCR and clinical response were observed in both arms indicating that addition of RAD001 did not improve the clinical response rate (Figure 26B). The lack of change in response rate between the arms was also evident by ultrasound evaluation (Figure 26C).

Evaluation of side effects indicated that addition of RAD001 to the combination of paclitaxel and cisplatin was associated with slight increase in adverse events, while the paclitaxel and cisplatin combination was better tolerated, with lower incidence of mild to moderate (grade 1 and 2) thrombocytopenia, rash, mucositis, transaminase elevation and low incidence of severe (grade 3 and 4) neutropenia (Table 6).

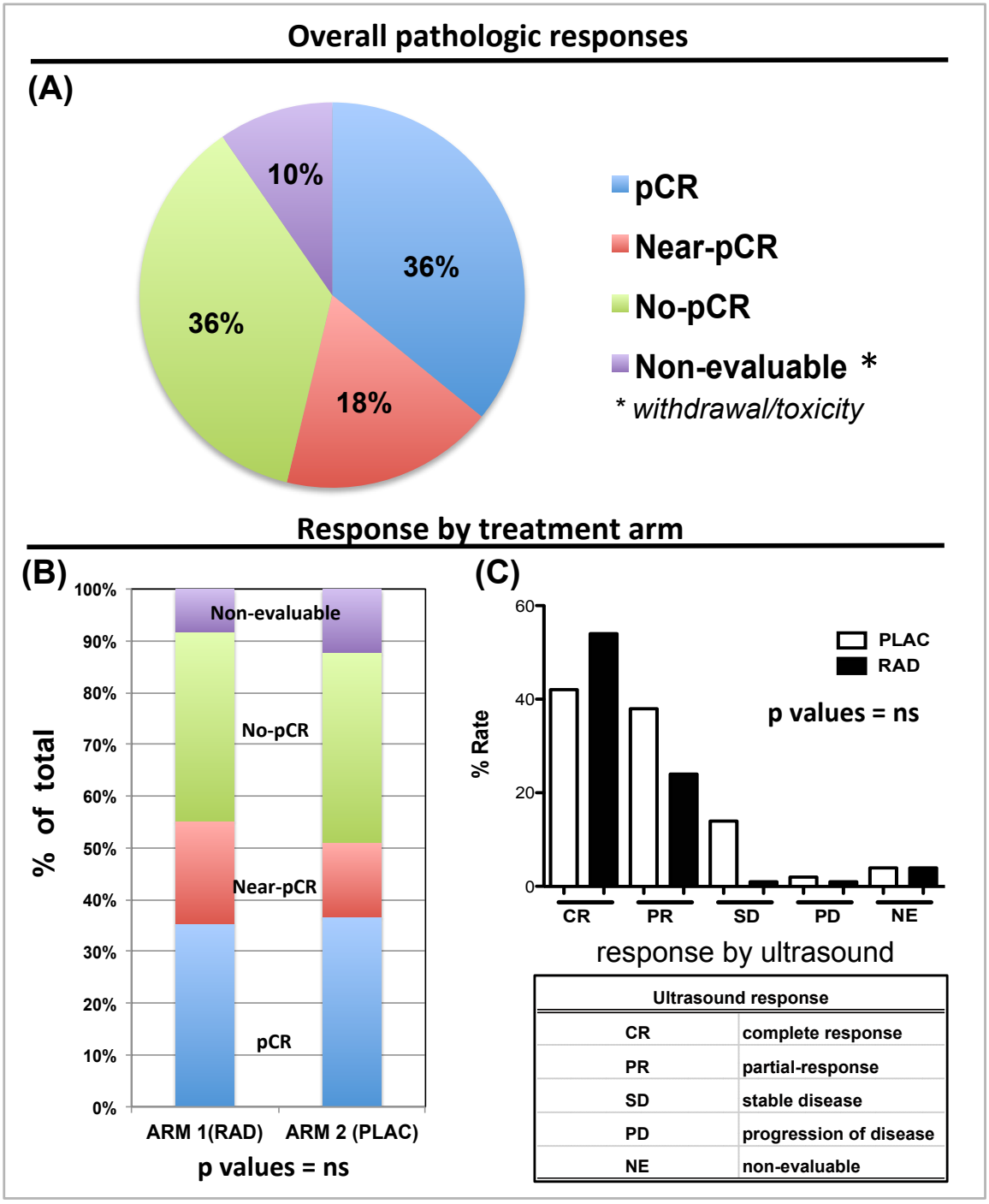

Figure 26. Pathologic clinical response analysis for the TNBC patients accrued to BRE0904 trial.

Figure 26. Pathologic clinical response analysis for the TNBC patients accrued to BRE0904 trial.

The degree of tumor response to neoadjuvant cisplatin, paclitaxel, and the mTOR inhibitor everolimus (RAD001) versus cisplatin and paclitaxel therapy was determined in evaluable patients with triple negative breast tumors. **A,** pie diagram representing the percentages of response with 36% pCR; 18% near-pCR; 36% no-pCR and 10% non-evaluable patients (patients off-study, due to toxicities, withdrawal or death). **B,** stacked column bar graph (for pCR, near-pCR, no-pCR and non-evaluable patients) represents evaluation of clinical response within individual arm of treatment. Arm 1 consists of patients treated with RAD001, cisplatin and paclitaxel while Arm 2 represents patients treated with placebo, cisplatin and paclitaxel. No statistical significant differences were found. **C,** column bar graph for evaluation of tumor response to treatment (plac versus rad) as measured by ultrasound prior to definitive surgery. Ultrasound responses are broken down into five categories complete response (CR), partial-response (PR), stable disease (SD), progression of disease (PD) and non-evaluable (NE). No statistical significant differences were observed.

Table 6. Clinical patient evaluation of side effects

Most common adverse events (%)		
	EVEROLIMUS	**PLACIBO**
Anemia	65	77
* **Neutropenia**	**52**	**38**
Thrombocytopenia	**40**	**9**
Fatigue	64	75
Rash	**49**	**29**
Mucositis	**39**	**20**
Nausea	60	66
Diarrhea	32	29
Dyspepsia	30	35
Hypercholesterolemia	9	7
Hyperglycemia	51	42
Transaminase elevation	**63**	**18**
Pneumonitis	1	-

* *Grade 3 and 4*

Based on clinical patient evaluation:

- addition of everolimus to the combination of paclitaxel and cisplatin was associated with slightly higher adverse events (* grade 3 and 4)
- paclitaxel and cisplatin combination was well tolerated overall, with low incidence of neuropathy or neutropenic fever

Molecular analysis of biopsies for markers of clinical response.

Molecular analysis of biopsy material was performed to assess therapy-mediated changes in proliferation, mitosis, phospho-S6 ribosomal protein (pS6) levels, as well as levels and phosphorylation status of p53, p63, and p73. Based on preclinical data (data not shown), we anticipated a decrease in cell proliferation, an increase in mitotic index, a decrease in pS6 and p63 levels and an elevation in p73 activity, after cisplatin, RAD001, and paclitaxel treatment.

Ki67 indicates higher cell proliferation in responders versus non-responders.

Proliferation rates were estimated by measuring Ki67 expression levels. The levels of expression were based on the percentage of tumor cell nuclei positively stained for Ki67 using immunohistochemistry (IHC). Although Ki67 staining is not currently standardized as a prognostic marker for routine clinical use partially due to mixed results for the ability of Ki67 to differentiate between a good or poor outcome (Stuart-Harris*, et al*, 2008), recent study suggests that higher ki67 expression levels prior to neoadjuvant chemotherapy was significantly correlated with higher path CR (Kwan*, et al*, 2014; Nishimura*, et al*, 2010). BRE0904 Ki67 analysis of both arms of patients with available cores, demonstrate statistically significant difference in pre-treatment Ki67 between pCR and no-pCR patients, with pCR patients having higher percent of Ki67 expression (Figure 27A). Interestingly, near-pCR patients also show statistically higher Ki67 when compared to no-pCR patients (Figure 27B). The preclinical tumor studies in which cisplatin, paclitaxel, and RAD001 were used as single

(A)

ki67 Summary

Treatment Arm	Response (#)	Average % Ki67 positive cells		
	pCR	PRE	BP1	POST
ARM 1: cis+plac	14	81%	80%	0%
ARM 2: cis+rad	27	78%	79%	0%
ARMs 1+2	41	**80%**	**80%**	**0%**
	Near-pCR	PRE	BP1	POST
ARM 1: cis+plac	5	83%	76%	60%
ARM 2: cis+rad	11	82%	63%	55%
ARMs 1+2	16	**82%**	**68%**	**54%**
	NO-pCR	PRE	BP1	POST
ARM 1: cis+plac	13	61%	65%	50%
ARM 2: cis+rad	24	71%	62%	57%
ARMs 1+2	37	**65%**	**63%**	**52%**

(B)

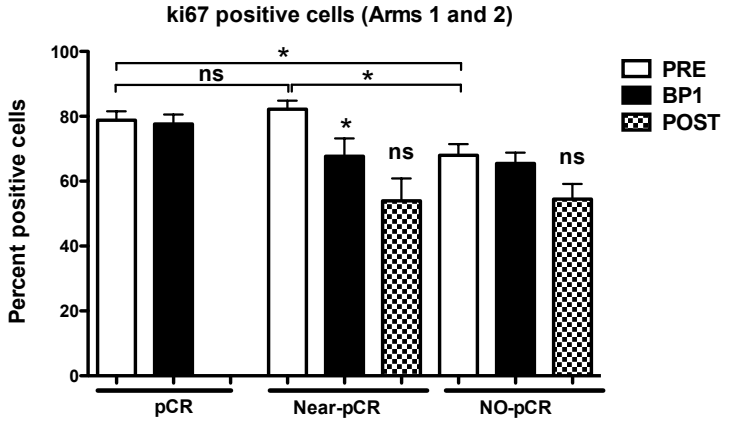

(C)

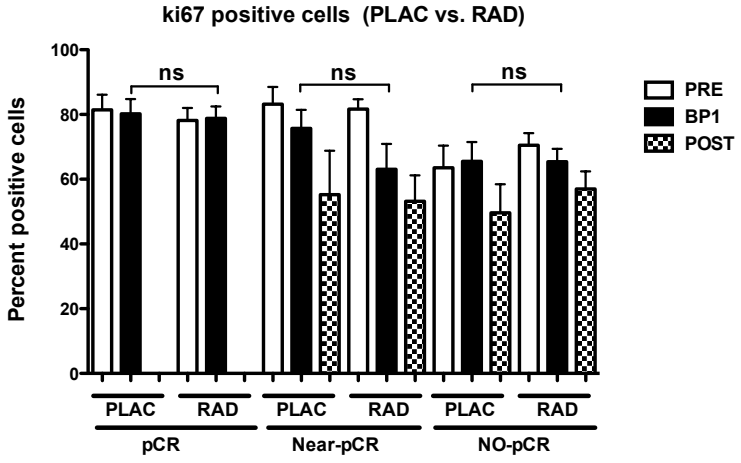

Figure 27. IHC protein expression analysis of Ki67 across evaluable BRE0904 TNBC patients.

Figure 27. IHC protein expression analysis of Ki67 across evaluable BRE0904 TNBC patients.

A, summary of average percent of ki67 positive cells for 94 patient with evaluable biopsies, across arm 1 (cisplatin+placebo; N=14 pCR, N=5 near-pCR and N=13 no-pCR patients), arm 2 (cisplatin+ rad001; N=27 pCR, N=11 near-pCR and N=24 no-pCR patients) and both arms (arms 1+2; N= 41 pCR, N=16 near-pCR and N=37 no-pCR patients). **B,** bar graph for percent of Ki67 positive cells in pre-treatment, biopsy 1 and post-treatment biopsies in pCR, near-pCR and no-pCR patients (trial arms combined). Each data bar represents the mean percent of Ki67 positive cells of 41 pre-treatment and biopsy 1 pCR patients, 16 pre-treatment, biopsy 1 and post-treatment near-pCR patients and 37 pre-treatment, biopsy 1 and post-treatment no-pCR patients; error bar represents SEM (ns = not significant, *P < 0.01 for a two-tail Student **t**-test). **C,** bar graph for percent of Ki67 positive cells in pre-treatment, biopsy 1 and post-treatment biopsies in pCR, near-pCR and no-pCR patients; Arm 1 (RAD) versus Arm 2 (placebo). Each data bar represents the mean percent of ki67 positive cells of pCR patients' pre-treatment and biopsy 1 (N=14 plac and N=27 RAD), near-pCR patients' pre-treatment, biopsy 1 and post-treatment (N= 5 plac and N=11 RAD) no-pCR pre-treatment, biopsy 1 and post-treatment (N= 13 plac and N=24 RAD); error bar represents SEM (ns = not significant for a two-tail Student t-test).

agents, demonstrated significant reduction in Ki67, and although we do not have statistical difference upon treatment there still a consistent decrease in Ki67 in both arms of treatment (cisplatin, paclitaxel ± RAD001) (Figure 27C).

Evaluation of mTOR activity by pS6 expression levels indicates robust expression of pS6 but no change in RAD001 arm.

Considering that we were evaluating efficacy of RAD001 inhibition of mTOR, we performed IHC analysis of phospho-S6, a marker of drug activity, on all available biopsy material (pre, bp1 and post-treatment). Previously, it has been shown that detection of the phospho-S6 (Ser-235/236) in human tumor tissue is robust and that drug-induced decreases are readily detectable in human tumor specimens (Choe*, et al*, 2003; Wang*, et al*, 2006). Thus, it would be anticipated that decreases in phospho-S6 would be detected in sensitive tumors in ARM1 patients (RAD001) of the trial. Based on the trial design, the most robust change in phospho-S6 would be expected in bp1 biopsy material (3-5 days of cisplatin + RAD001 versus cisplatin+placibo arm) from RAD001 sensitive patients. Phospho-S6 analysis revealed, as anticipated, robust baseline expression of pS6 across all TNBC patients (Figure 28A and B). When comparing baseline and bp1 biopsies in Arm 1 (RAD001) no statistically different changes were observed although there was a slightly less pS6 in pCR and near-pCR patients while no change in no-pCR patients. Interestingly, there was significant difference in pS6 in post-treatment biopsies (paclitaxel added) in both Arms 1 and 2 in near and no-pCR patients. Although a significant decrease was not observed across every post-treatment biopsy, the decrease in pS6 trend was consistent across all post-treatments. Overall, these results suggest that addition

(A) pS6 Summary

Treatment Arm	Response (#)	Average pS6 H-scores		
	pCR	PRE	BP1	POST
ARM 1: cis+plac	14	205	215	0
ARM 2: cis+rad	26	211	191	0
ARMs 1+2	40	**209**	**200**	**0**
	Near-pCR	PRE	BP1	POST
ARM 1: cis+plac	7	174	191	106
ARM 2: cis+rad	12	178	165	153
ARMs 1+2	19	**177**	**175**	**138**
	NO-pCR	PRE	BP1	POST
ARM 1: cis+plac	7	147	108	94
ARM 2: cis+rad	35	220	223	180
ARMs 1+2	42	**208**	**204**	**166**

(B)

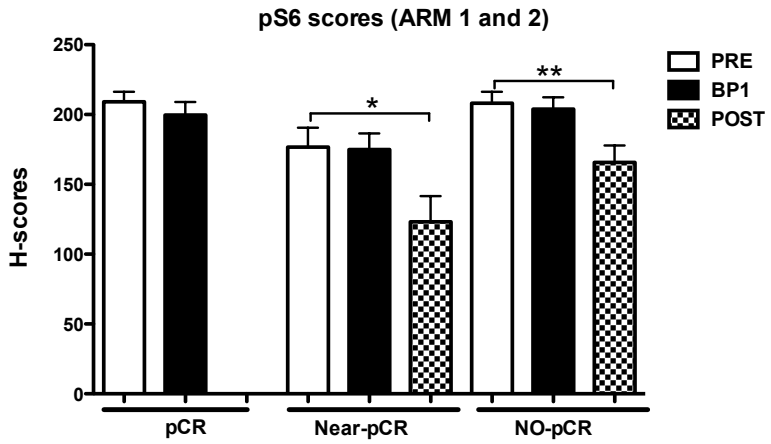

(C)

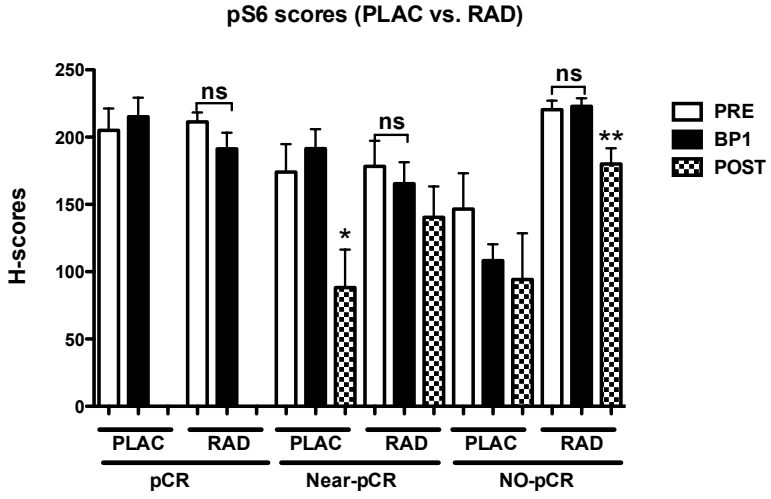

Figure 28. IHC protein expression analysis of pS6 across evaluable BRE0904 TNBC patients

Figure 28. IHC protein expression analysis of pS6 across evaluable BRE0904 TNBC patients.

A, summary of H-scores for pS6 positive cells for 101 patient with evaluable biopsies, across arm 1 (cisplatin+placebo; N=14 pCR, N=7 near-pCR and N=7 no-pCR patients), arm 2 (cisplatin+ rad001; N= 26 pCR, N=12 near-pCR and N=7 no-pCR patients) and both arms (arms 1+2; N= 40 pCR, N=19 near-pCR and N=42 no-pCR patients). **B,** bar graph for average pS6 H-scores in pre-treatment, biopsy 1 and post-treatment biopsies in pCR, near-pCR and no-pCR patients (trial arms combined). Each data bar represents the mean pS6 H-score of 40 pre-treatment and biopsy 1 pCR patients, 19 pre-treatment, biopsy 1 and post-treatment near-pCR patients and 42 pre-treatment, biopsy 1 and post-treatment no-pCR patients; error bar represents SEM (*P < 0.01, **P < 0.001 for a two-tail Student t-test). **C,** bar graph for average pS6 H-scores in pre-treatment, biopsy 1 and post-treatment biopsies in pCR, near-pCR and no-pCR patients; Arm 1 (RAD) versus Arm 2 (placebo). Each data bar represents the mean pS6 H-score of pCR patients' pre-treatment and biopsy 1 (N=14 plac and N=26 RAD), near-pCR patients' pre-treatment, biopsy 1 and post-treatment (N= 7 plac and N=12 RAD) no-pCR pre-treatment, biopsy 1 and post-treatment (N= 7 plac and N=35 RAD); error bar represents SEM (ns = not significant, *P < 0.01, **P < 0.001 for a two-tail Student t-test).

of paclitaxel might have an effect on pS6 levels (Figure 28C). Further assessments would be required to evaluate this observation, especially as the result contradict the *in vitro* results in human cell lines.

Assessment of the expression of p53 expression reveals no difference between responders and non-responders.

The percent of p53 positive cells was evaluated across the trial and analyses were performed to determine how p53 expression correlated with the overall clinical response as well as individual treatment arm (Figure 29). The data suggested that there was no statistically significant difference between pCR and near-pCR or no-pCR patients. However, as it would be expected, there was robust expression of p53 across the trial (Figure 29A and B). The presence of a strong IHC signal for p53 has been previously correlated with the presence of mutant p53, and considering high p53 mutation rate in breast cancer as well as its strong association with TNBC (Borresen-Dale, 2003; Sorlie*, et al*, 2001) our data indicating the higher number of patients (60-100% range of p53 positive cells) (Figure 29 B and C) goes along with previous findings. Although, at this point we do not have data that would verify mutation status in the patients with high p53, our prediction would be that a significant percentage of these patients would have p53 mutant tumors. As far as correlation of p53 IHC signal between the two arms of the trial there is no significant difference (Figure 29C). Although, the p53 results only confirmed what was already known and thus did not reveal anything novel it was important to establish the status of p53 so that it can be correlated to p63 and p73 expression status in the tumors.

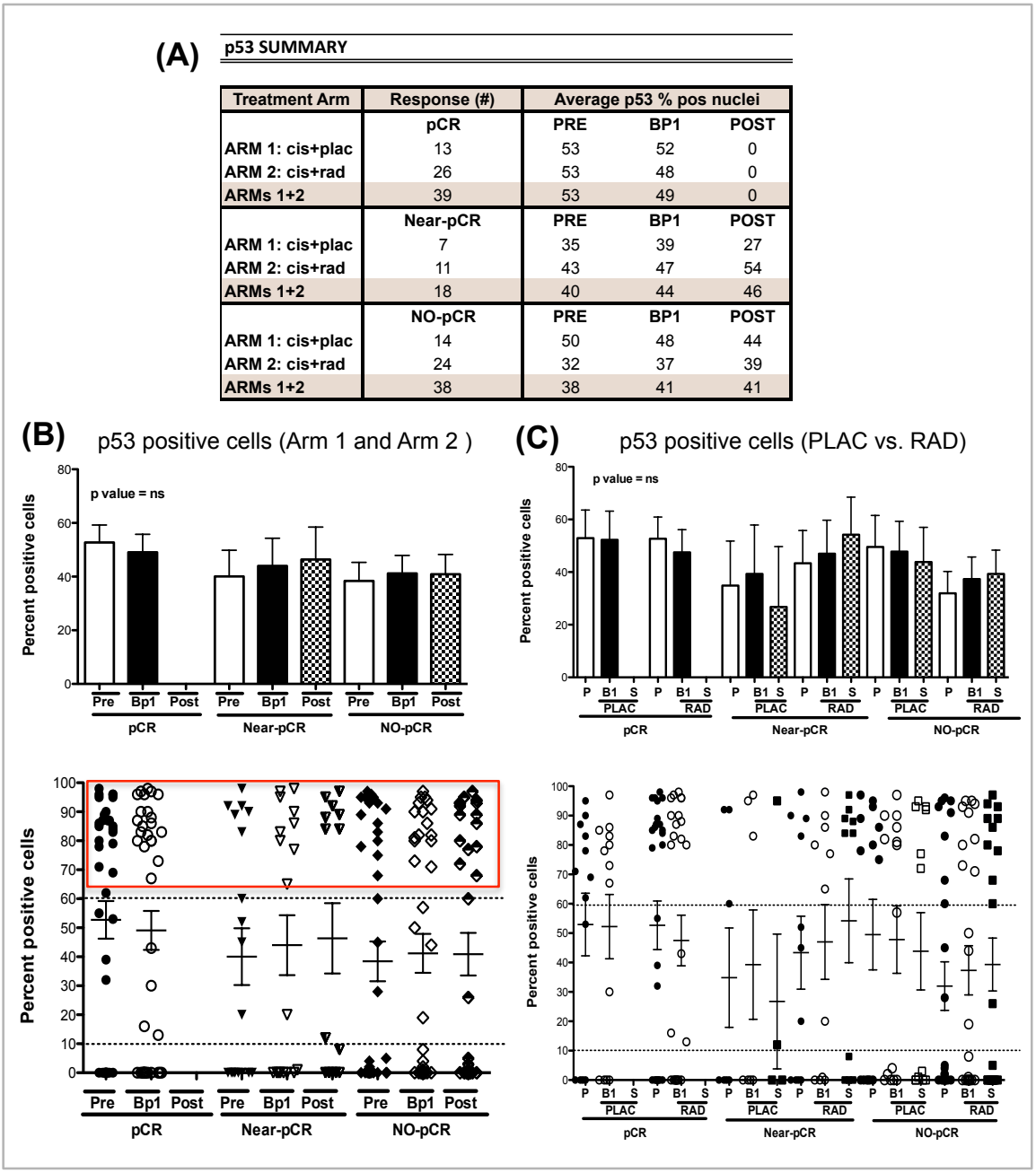

Treatment Arm	Response (#)	Average p53 % pos nuclei		
	pCR	PRE	BP1	POST
ARM 1: cis+plac	13	53	52	0
ARM 2: cis+rad	26	53	48	0
ARMs 1+2	39	53	49	0
	Near-pCR	PRE	BP1	POST
ARM 1: cis+plac	7	35	39	27
ARM 2: cis+rad	11	43	47	54
ARMs 1+2	18	40	44	46
	NO-pCR	PRE	BP1	POST
ARM 1: cis+plac	14	50	48	44
ARM 2: cis+rad	24	32	37	39
ARMs 1+2	38	38	41	41

Figure 29. IHC protein expression analysis of p53 across evaluable BRE0904 TNBC patients.

Figure 29. IHC protein expression analysis of p53 across evaluable BRE0904 TNBC patients.

A, summary of average percent of p53 positive nuclei for 95 patient with evaluable biopsies, across arm 1 (cisplatin+placebo; N=13 pCR, N=7 near-pCR and N=14 no-pCR patients), arm 2 (cisplatin+ rad001; N=26 pCR, N=11 near-pCR and N=24 no-pCR patients) and both arms (arms 1+2; N= 39 pCR, N=18 near-pCR and N=38 no-pCR patients). **B,** bar graph and vertical scatter plot for percent of p53 positive nuclei in pre-treatment, biopsy 1 and post-treatment biopsies in pCR, near-pCR and no-pCR patients (trial arms combined). Each data bar represents the mean percent of p53 positive cells of 39 pre-treatment and biopsy 1 pCR patients, 18 pre-treatment, biopsy 1 and post-treatment near-pCR patients and 38 pre-treatment, biopsy 1 and post-treatment no-pCR patients; error bar represents SEM (ns = not significant, for a two-tail Student t-test). **C,** column bar graph and vertical scatter plot for percent of p53 positive nuclei in pre-treatment, biopsy 1 and post-treatment biopsies in pCR, near-pCR and no-pCR patients; Arm 1 (RAD) versus Arm 2 (placebo). Each data bar represents the mean percent of p53 positive nuclei of pCR patients' pre-treatment and biopsy 1 (N=13 plac and N=26 RAD), near-pCR patients' pre-treatment, biopsy 1 and post-treatment (N= 7 plac and N=11 RAD) no-pCR pre-treatment, biopsy 1 and post-treatment (N= 14 plac and N=24 RAD); error bar represents SEM (ns = not significant for a two-tail Student t-test).

p63 and p73 expression levels are highest in patients with pathologic complete response

In our preclinical data we demonstrated that p63 levels are decreased in cells (HCC-1937) that expressed the protein upon single treatment with RAD001 and cisplatin or with RAD001/cisplatin combination (Figure 24). In this study, for p63 and p73 we assessed levels of the prominent isoforms, ΔNp63α and TAp73 that have been observed in triple negative breast cancer cells (Leong*, et al*, 2007). The IHC results summary for p63 indicates low robust differences in staining across both arms of trial (Figure 30A). Based on what was detected by IHC, the data indicated that baseline tissues (pre-treatment) of pCR patients have higher levels of p63, although not statistically significant when compared to near and no-pCR pre-treatment tissues (Figure 30B). Interestingly, there was a significant decrease of p63 in pCR patients upon treatment with RAD001/cisplatin (Figure 30C), which is what we expected based on our pre-clinical data (Figure 24).

Although we would also expect to see decrease of p63 upon treatment with cisplatin alone (Figure 24), this was not the case. Previously it has been shown that mTOR is a regulator of p73 (Rosenbluth*, et al*, 2008). We found that RAD001 and cisplatin could elevate p73 levels when used as single agents or in combination, but the combination yielded more apoptosis (Figure 24). The p73 IHC summary (Figure 31A) indicates overall higher levels of expression than what we have seen for p63 (Figure 30A).

(A)

p63 Summary

Treatment Arm	Response (#)	Average p63 positive cells		
	pCR	PRE	BP1	POST
ARM 1: cis+plac	14	2	2	0
ARM 2: cis+rad	27	10	2	0
ARMs 1+2	41	7	2	0
	Near-pCR	PRE	BP1	POST
ARM 1: cis+plac	7	0	0	0
ARM 2: cis+rad	12	2	2	1
ARMs 1+2	19	1	1	1
	NO-pCR	PRE	BP1	POST
ARM 1: cis+plac	16	1	3	1
ARM 2: cis+rad	25	5	2	2
ARMs 1+2	41	3	3	2

(B)

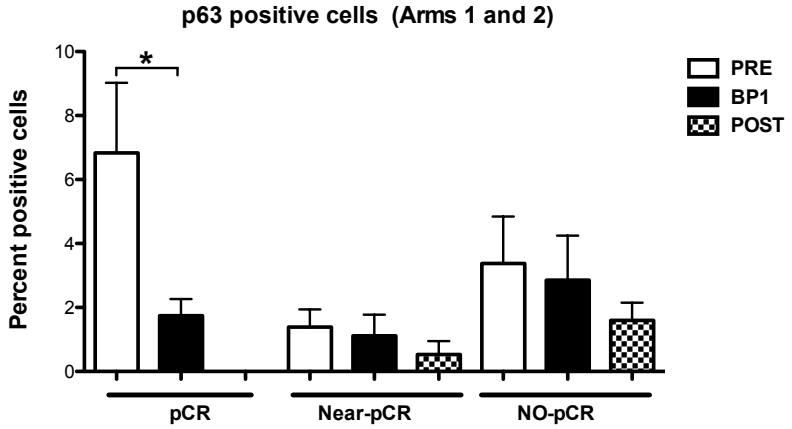

(C)

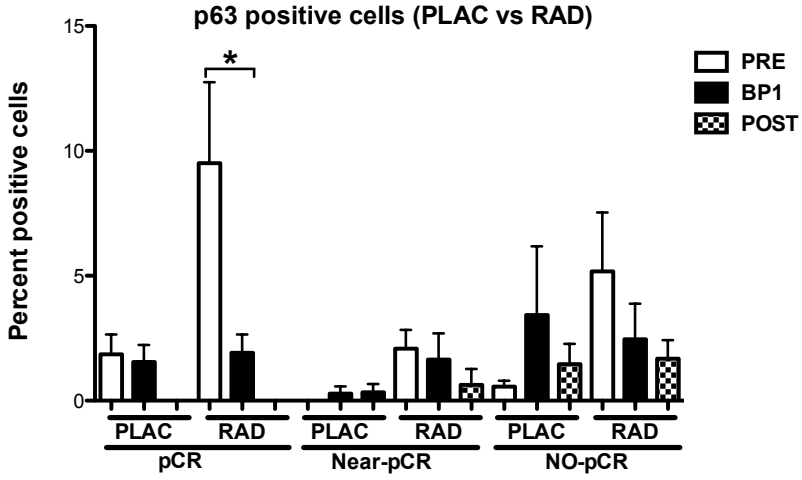

Figure 30. IHC protein expression analysis of p63 across evaluable BRE0904 TNBC patients.

Figure 30. IHC protein expression analysis of p63 across evaluable BRE0904 TNBC patients.

A, summary of average percent of p63 positive cells for 101 patient with evaluable biopsies, across arm 1 (cisplatin+placebo; N=14 pCR, N=7 near-pCR and N=15 no-pCR patients), arm 2 (cisplatin+ rad001; N=27 pCR, N=12 near-pCR and N=25 no-pCR patients) and both arms (arms 1+2; N= 41 pCR, N=19 near-pCR and N=41 no-pCR patients). **B,** bar graph for percent of p63 positive cells in pre-treatment, biopsy 1 and post-treatment biopsies in pCR, near-pCR and no-pCR patients (trial arms combined). Each data bar represents the mean percent of p63 positive cells of 41 pre-treatment and biopsy 1 pCR patients, 19 pre-treatment, biopsy 1 and post-treatment near-pCR patients and 41 pre-treatment, biopsy 1 and post-treatment no-pCR patients; error bar represents SEM (unless indicated p value is not significant, *P < 0.01 for a two-tail Student t-test). **C,** bar graph for percent of p63 positive cells in pre-treatment, biopsy 1 and post-treatment biopsies in pCR, near-pCR and no-pCR patients; Arm 1 (RAD) versus Arm 2 (placebo). Each data bar represents the mean percent of p63 positive cells of pCR patients' pre-treatment and biopsy 1 (N=14 plac and N=27 RAD), near-pCR patients' pre-treatment, biopsy 1 and post-treatment (N= 7 plac and N=12 RAD) no-pCR pre-treatment, biopsy 1 and post-treatment (N= 16 plac and N=25 RAD); error bar represents SEM (unless indicated p value is not significant, *P < 0.01 for a two-tail Student t-test).

An important observation was that baseline p73 expression was significantly higher in pCR compared to the no-pCR patients (Figure 31B). Although we would expect to see further increase in p73 upon treatment with RAD001, cisplatin, or the combination, based on our preclinical data, no statistically significant difference was observed (Figure 31C). However, we are seeing a trend of higher expression of p73 in bp1 tissues (cisplatin±RAD001 treatment) (Figure 31C). We would also expect to see similar trend of increased p73 expression upon addition of paclitaxel to cisplatin±RAD001 but that was not consistent across the evaluable post-treatment tissues (Figure 31C).

Androgen receptor analysis reveals significantly higher expression of AR in non-responders and no change to any treatments used.

GE analyses of 587 TNBC patients had led our group to identify six distinct molecular TNBC subtypes with unique drivers, one of which was androgen receptor (AR) within luminal AR TNBC subtype (LAR) comprising 9-10% of TNBC (Lehmann*, et al*, 2011). Considering that LAR subtype was correlated with poorer response in patients and LAR cell lines were not as responsive to cisplatin (as basal-like TNBC subtype) we decided to perform AR analysis in our trial. The results indicated that out of 119 patients with available AR score in pre-treatment tissues 13 patients (~14%) had high expression of AR ranging from 45%-99% AR positive nuclei (data not shown). The AR summary of IHC result indicates low expression in both trial arms in patients with pCR and near-pCR, while higher expression in no-pCR patients. (Figure 32A).

(A) **p73 Summary**

Treatment Arm	Response (#)	Average p73 positive cells		
	pCR	**PRE**	**BP1**	**POST**
ARM 1: cis+plac	13	31	35	0
ARM 2: cis+rad	29	29	34	0
ARMs 1+2	42	30	35	0
	Near-pCR	**PRE**	**BP1**	**POST**
ARM 1: cis+plac	6	11	27	24
ARM 2: cis+rad	14	28	44	12
ARMs 1+2	20	23	37	16
	NO-pCR	**PRE**	**BP1**	**POST**
ARM 1: cis+plac	12	9	16	27
ARM 2: cis+rad	22	20	28	24
ARMs 1+2	34	16	23	25

(B)

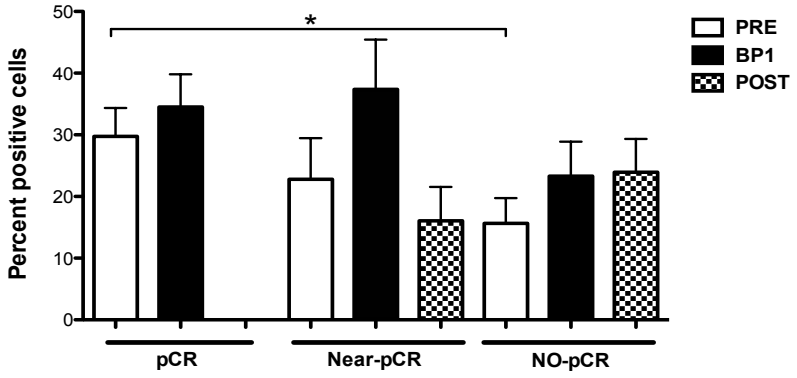

(C)

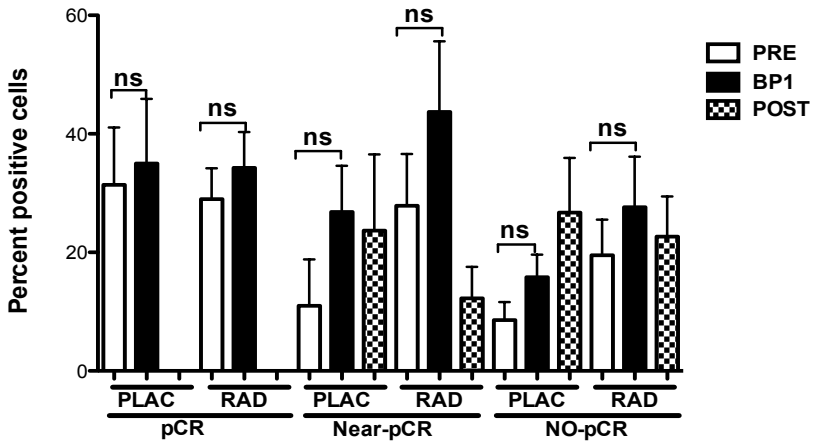

Figure 31. IHC protein expression analysis of p73 across evaluable BRE0904 TNBC patients.

Figure 31. IHC protein expression analysis of p73 across evaluable BRE0904 TNBC patients.

A, summary of average percent of p73 positive cells for 96 patient with evaluable biopsies, across arm 1 (cisplatin+placebo; N=13 pCR, N=6 near-pCR and N=12 no-pCR patients), arm 2 (cisplatin+ rad001; N=29 pCR, N=14 near-pCR and N=22 no-pCR patients) and both arms (arms 1+2; N= 42 pCR, N=20 near-pCR and N=34 no-pCR patients). **B,** bar graph for percent of p73 positive cells in pre-treatment, biopsy 1 and post-treatment biopsies in pCR, near-pCR and no-pCR patients (trial arms combined). Each data bar represents the mean percent of p73 positive cells of 42 pre-treatment and biopsy 1 pCR patients, 20 pre-treatment, biopsy 1 and post-treatment near-pCR patients and 34 pre-treatment, biopsy 1 and post-treatment no-pCR patients; error bar represents SEM (unless indicated p value is not significant, *P < 0.01 for a two-tail Student t-test). **C,** bar graph for percent of p73 positive cells in pre-treatment, biopsy 1 and post-treatment biopsies in pCR, near-pCR and no-pCR patients; Arm 1 (RAD) versus Arm 2 (placebo). Each data bar represents the mean percent of p73 positive cells of pCR patients' pre-treatment and biopsy 1 (N=13 plac and N=29 RAD), near-pCR patients' pre-treatment, biopsy 1 and post-treatment (N= 6 plac and N=14 RAD) no-pCR pre-treatment, biopsy 1 and post-treatment (N= 12 plac and N=22 RAD); error bar represents SEM (unless indicated p value is not significant, for a two-tail Student t-test).

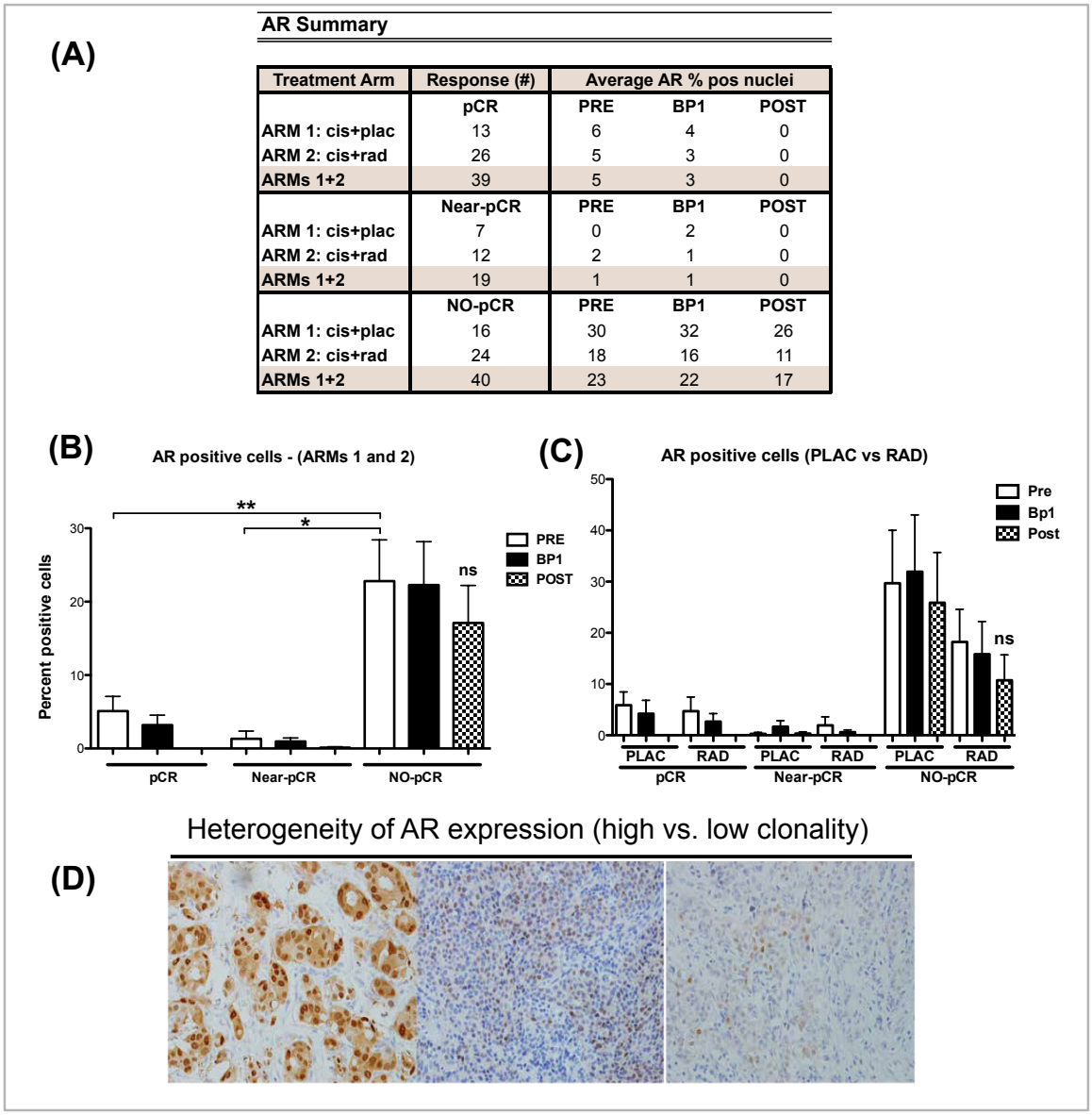

Figure 32. IHC protein expression analysis of AR across evaluable BRE0904 TNBC patients.

Figure 32. IHC protein expression analysis of AR across evaluable BRE0904 TNBC patients.

A, summary of average percent of AR positive cells for 98 patient with evaluable biopsies, across arm 1 (cisplatin+placebo; N=13 pCR, N=7 near-pCR and N=16 no-pCR patients), arm 2 (cisplatin+ rad001; N=26 pCR, N=12 near-pCR and N=24 no-pCR patients) and both arms (arms 1+2; N= 39 pCR, N=19 near-pCR and N=40 no-pCR patients). **B,** bar graph for percent of AR positive cells in pre-treatment, biopsy 1 and post-treatment biopsies in pCR, near-pCR and no-pCR patients (trial arms combined). Each data bar represents the mean percent of AR positive cells of 39 pre-treatment and biopsy 1 pCR patients, 19 pre-treatment, biopsy 1 and post-treatment near-pCR patients and 40 pre-treatment, biopsy 1 and post-treatment no-pCR patients; error bar represents SEM (unless indicated p value is not significant (ns), *$P < 0.01$, **$P < 0.001$ for a two-tail Student t-test). **C,** bar graph for percent of AR positive cells in pre-treatment, biopsy 1 and post-treatment biopsies in pCR, near-pCR and no-pCR patients; Arm 1 (RAD) versus Arm 2 (placebo). Each data bar represents the mean percent of AR positive cells of pCR patients' pre-treatment and biopsy 1 (N=13 plac and N=26 RAD), near-pCR patients' pre-treatment, biopsy 1 and post-treatment (N= 7 plac and N= 12 RAD) no-pCR pre-treatment, biopsy 1 and post-treatment (N= 16 plac and N= 24 RAD); error bar represents SEM (unless indicated p value is not significant, for a two-tail Student t-test). **D,** representative IHC images of heterogeneous AR expression.

The addition of the drug in either arm makes no difference and does not alter AR expression (Figure 32C). Another interesting observation we made was the presence of heterogeneous expression of AR (Figure 32D). This observation is interesting as the molecular heterogeneity of TNBC at the time of diagnosis may have implications for approaches to the biology of primary tumors by considering low versus high clonality.

Gene expression profiling of pre-treatment tumor biopsies can predict response to treatment.

The power of gene signatures has already been extensively proven in breast cancer (Lehmann*, et al*, 2011; Perou*, et al*, 2000; Sorlie*, et al*, 2001; Sorlie*, et al*, 2003; van 't Veer*, et al*, 2003; van 't Veer*, et al*, 2002; van de Vijver*, et al*, 2002). The molecular markers described above provide insight and correlative information that can be linked to tumor response. Considering that the result of the trial are negative as the addition of RAD001 did not the improve the overall responsiveness, we performed a microarray-based GE analysis as this approach was more likely to provide better insight to the status of signaling pathways that could serve as predictors of drug sensitivity or tumor response.

In order to determine whether differential GE would correlate and predict clinical response we performed microarray analysis on laser-capture microdissected (LCM) tumor cells from the baseline (pre-treatment) biopsies (N=12 patients). In addition to performing differential GE analysis we also performed *in sillico* prediction of TNBC subtypes for these patients to determine if

their TNBC subtype would correlate with clinical response. The preliminary results indicated that LCM tumors from responders had significantly different GE patterns when compared to non-responders (Figure 33). Specifically, there were 370 differentially expressed genes, with 208 genes significantly down-regulated and 162 genes significantly up-regulated in non-responders. Gene set enrichment analysis showed no overlap for genes up-regulated in non-responders; while genes down-regulated in non-responders were involved in cell cycle, chromosome maintenance and transcription (Figure 33).

In addition, the responding tumors had elevated expression of proliferation markers (e.g., KIFCI, MKI67, AURKB) and DDR signaling genes (e.g., CHEK1, TP53BP2, RPA1) (Table 7), and were consistent with their basal-like TNBC subtype. The non-responders were more likely to be mesenchymal or LAR TNBC subtype, which was consistent with what we were expecting based on our previous findings (Lehmann*, et al*, 2011) (Figure 33). Since we already had evaluated ki67 expression by IHC (Figure 26), we aligned the Ki67 IHC values with the Ki67 mRNA values from patients on which we had performed microarray analysis and prediction of TNBC subtype. The results indicated significantly decreased Ki67 IHC levels in mesenchymal-like TNBC and LAR (non-responder patients), however due to low number of LAR patients Ki67 decrease was not statistically significant (Figure 34).

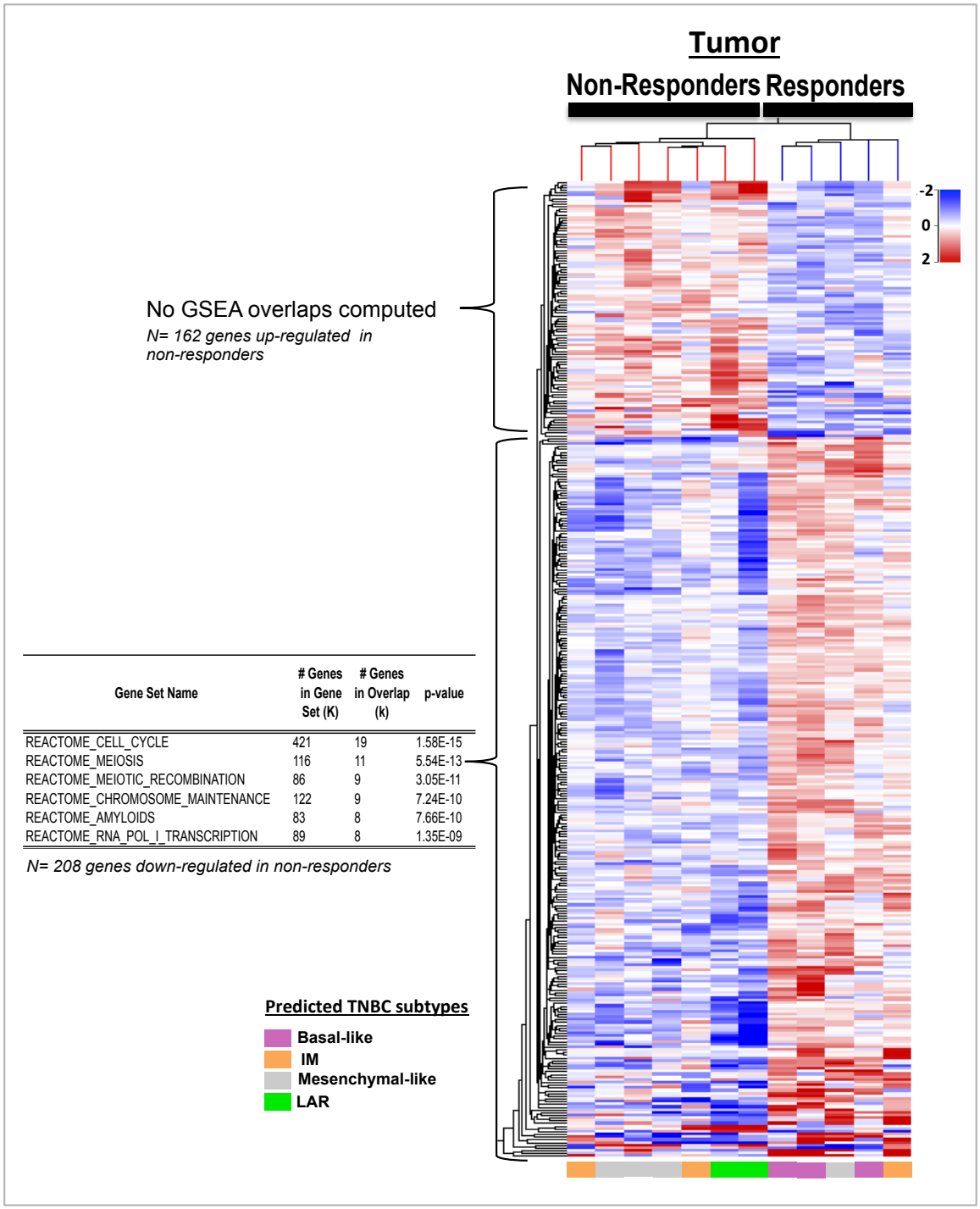

Figure 33. Microarray based gene expression analysis of pre-treatment LCM tumors.

Figure 33. Microarray based gene expression analysis of pre-treatment LCM tumors.

A, heatmap of hierarchical combined clustering of LCM pre-treatment tumor tissues (N=12 patients) representing responders (pCR+ near-pCR) and non-responders (no-pCR). Heatmap represents N=370 differentially expressed genes, with fold change>1.5 and p value <0.05. Blue color indicates genes with decreased expression and red color indicated genes with increased expression. A web-based prediction tool was used for making TNBC calls for patients with microarray data. The predicted TNBC subtypes (based on correlation coefficients, and the permutation p-value) are displayed for basal-like, immunomodulatory (IM), mesenchymal-like and luminal androgen receptor (LAR) below the heatmap. There were 208 down-regulated and 162 up-regulated genes in non-responders. GSEA analysis shows no overlap for up-regulated genes. Overlaps were present in down-regulated genes as outlined.

Table 7. Anticipated proliferative (KIFC1, MKI67 and AURKB) and DNA damage genes (TP53BP2, CHEK1, RPA1) were significantly decreased on mRNA level in non-responders (proof-of-concept).

Gene symbol	Transcript ID	p value	Regulation
KIFC1	8179564	0.0046	down
* MKI67	7937020	0.0283	down
AURKB	8012403	0.0043	down
CHEK1	7945014	0.0453	down
TP53BP2	7924526	0.0400	down
RPA1	8003679	0.0003	down

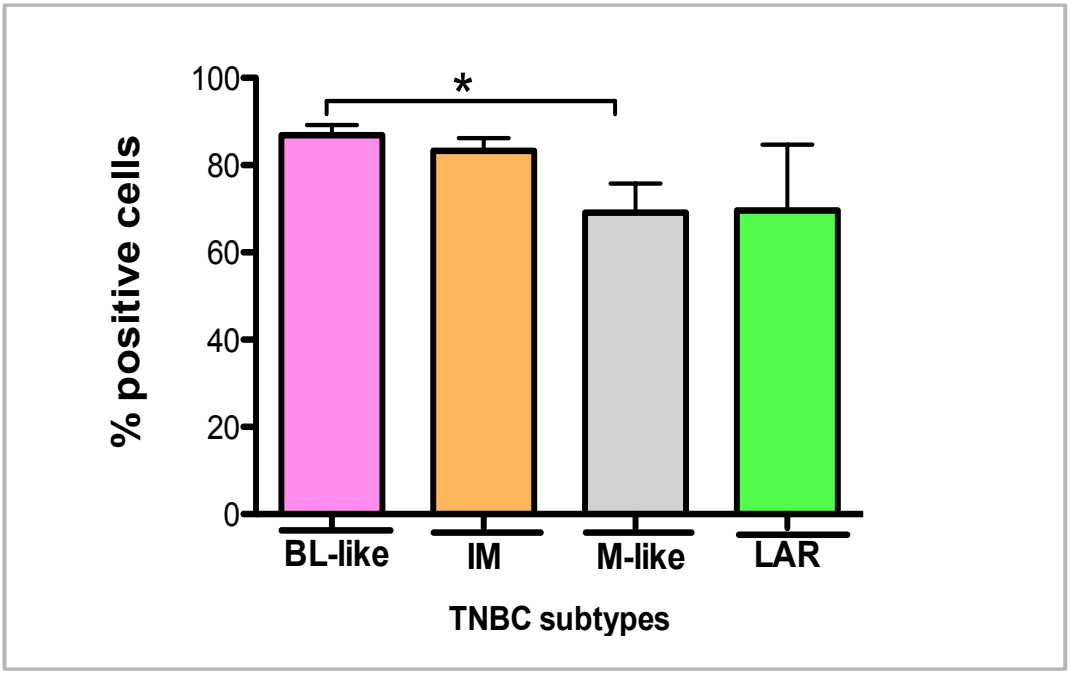

Figure 34. Ki67 IHC based expression levels in pre-treatment biopsies across TNBC patients with predicted subtypes.

Basal-like (BL); immunomodulatory (IM), mesenchymal-like (M) and luminal androgen receptor (LAR)); error bar represents SEM (unless indicated p value is not significant (ns), *P < 0.01 for a two-tail Student t-test.

In addition to Ki67, we also compared how our LAR predicted TNBC subtypes matched to AR IHC analysis. As expected we see that all the LAR subtyped TNBC patients have high levels of AR by IHC (Figure 35A), and that LAR patient are significantly associated with poor clinical response (Figure 35B).

As this study is still in progress, further analyses and a larger cohort will be required to make further conclusions. We plan on continuing and completing GE analyses using RNA-seq for analysis of gene expression changes but also determining mutation status in responders versus non-responders (including residual disease of non-responders). We anticipate identifying biomarkers of drug sensitivity.

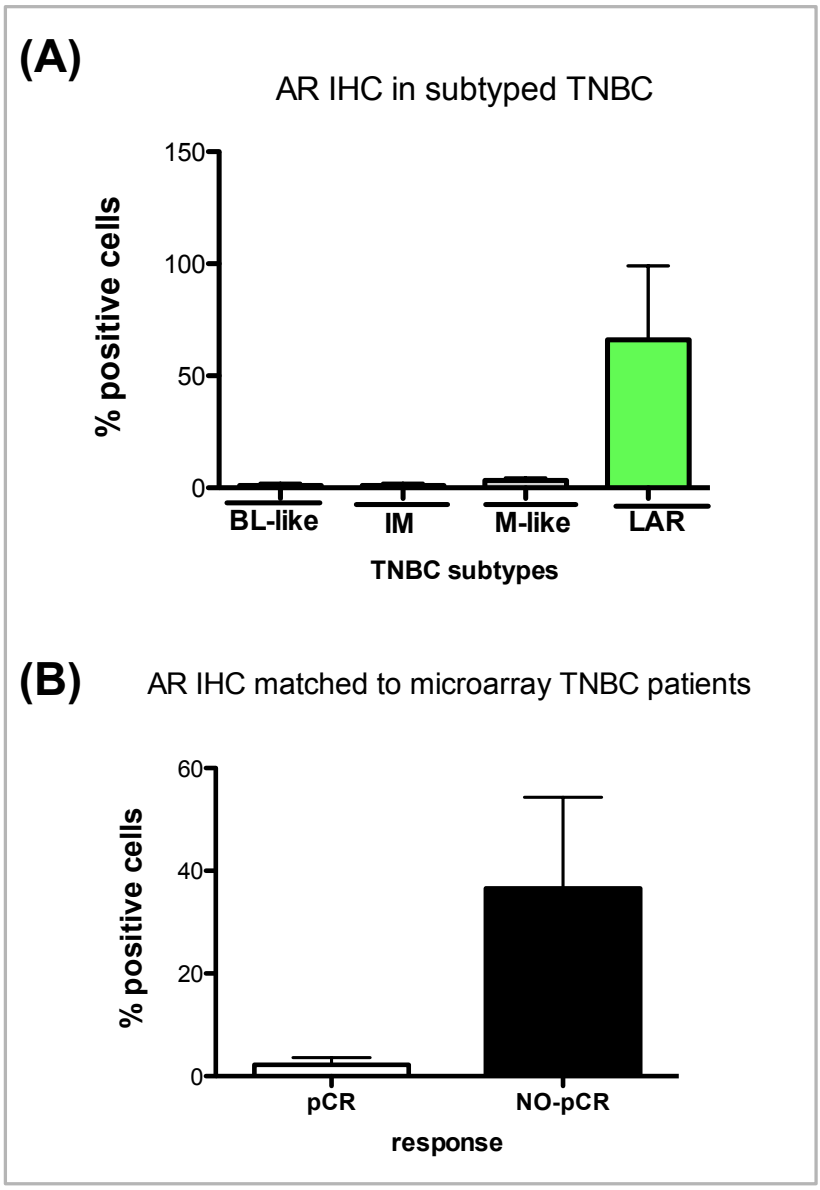

Figure 35. Protein expression of AR in TNBC predicted subtype and correlation to response.

A, column bar graph representing percent of AR IHC based expression levels in pre-treatment biopsies across TNBC patients with predicted subtypes; error bar represents SEM (unless indicated p value is not significant (ns) for a two-tail Student t-test). **B,** column bar graph for percent of AR positive cells in pre-treatment biopsies from pCR and no-pCR TNBC patients with predicted subtypes; error bar represents SEM (unless indicated p value is not significant (ns) for a two-tail Student t-test).

Differential gene expression analysis of tumor stroma is predictive of clinical response.

To further decipher the contribution of tumor adjacent stroma to the biology of TNBC and clinical response to treatments, we performed GE analysis in the same manner as described above this time on matched pre-treatment LCM tumor stroma. Our goal was to evaluate whether GE analysis of stromal cellscould be predictive of clinical response. Prior to differential gene expression analysis we performed unsupervised principal component analysis (PCA) to demonstrate that we indeed had a clean separation of the tumor and adjacent stroma by LCM (Figure 36). After we established that tumor-stroma separation was adequate we performed statistical analysis for differentially expressed genes then applied these gene to determine if we would observe separation between responding and non-responding patients. Results of our analysis indicated that stroma had larger set of statistically significant differentially expressed genes (N=679). The distribution of number of genes that were significantly down-regulated or up-regulated was similar with 335 down-regulated and 344 up-regulated genes in the non-responders compared to responders (Figure 37). Similarly to the tumor we noticed changes in cell proliferation and DNA-damage genes. Patients with higher expression of proliferation genes such as MKI67, KIFC1, AURKB, E2F3, and DNA damage response genes TP53BP2, CHEK1, RPA1, BLM were more responsive to treatment compared to non-responders (data not shown). Unlike tumor GSEA, stromal gene set enrichment analysis has further demonstrated changes in genes related to regulation of metabolic

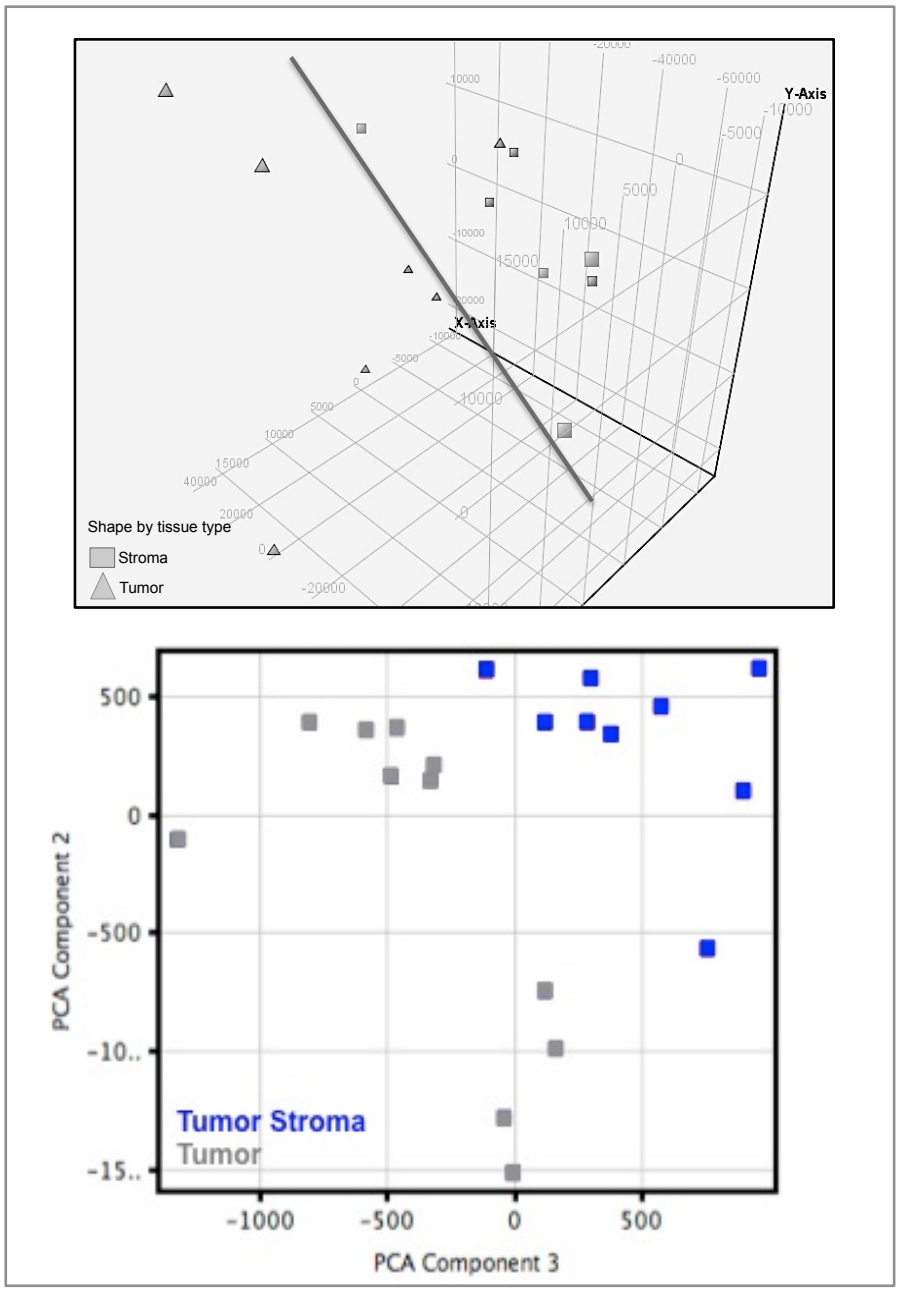

Figure 36. Principal component analysis on LCM tumors and matched stroma.

Shapes by tissue type are as follows: gray triangles represent LCM tumors and gray squares represent adjacent LCM stroma from individual TNBC patients

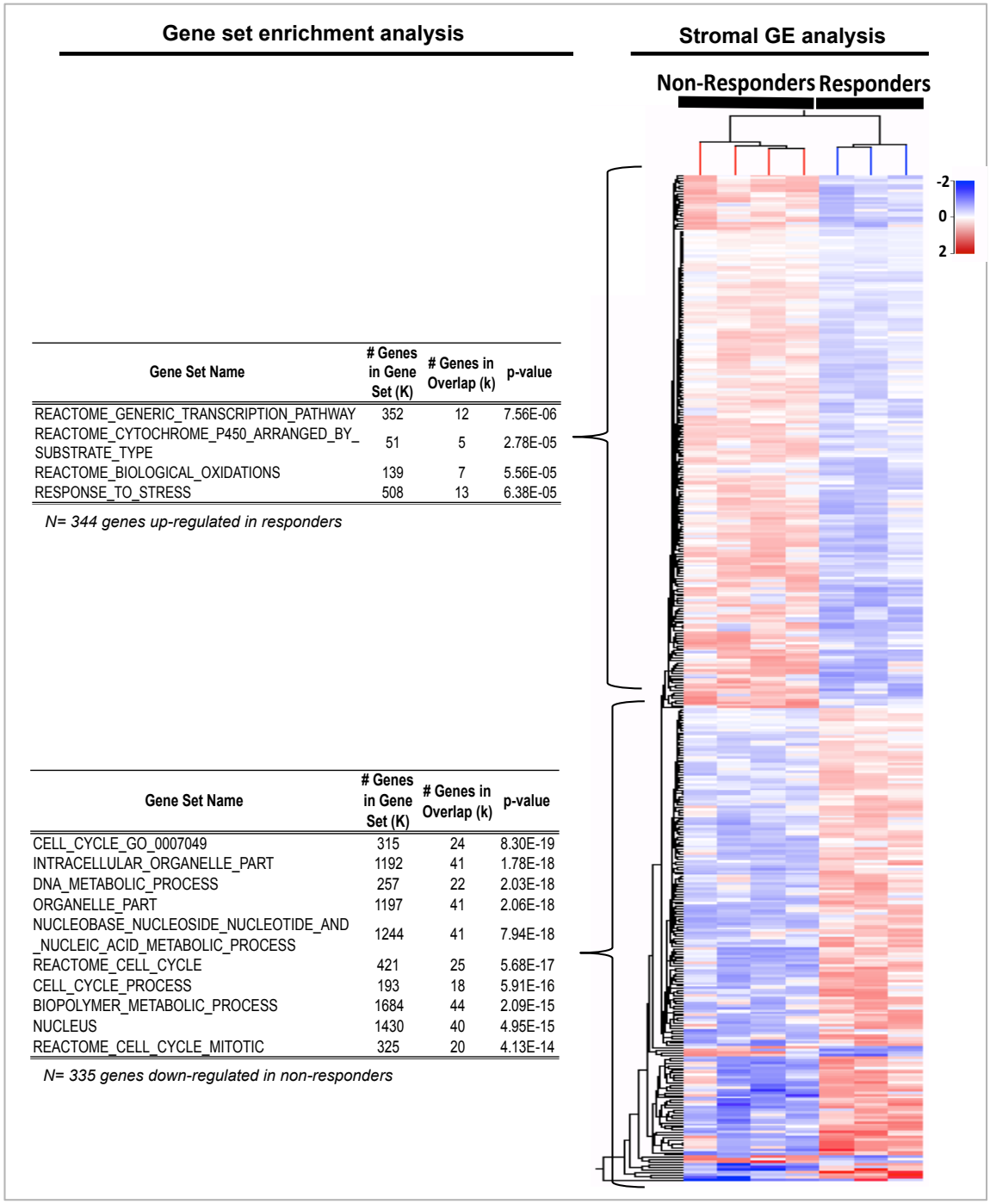

Gene Set Name	# Genes in Gene Set (K)	# Genes in Overlap (k)	p-value
REACTOME_GENERIC_TRANSCRIPTION_PATHWAY	352	12	7.56E-06
REACTOME_CYTOCHROME_P450_ARRANGED_BY_SUBSTRATE_TYPE	51	5	2.78E-05
REACTOME_BIOLOGICAL_OXIDATIONS	139	7	5.56E-05
RESPONSE_TO_STRESS	508	13	6.38E-05

N= 344 genes up-regulated in responders

Gene Set Name	# Genes in Gene Set (K)	# Genes in Overlap (k)	p-value
CELL_CYCLE_GO_0007049	315	24	8.30E-19
INTRACELLULAR_ORGANELLE_PART	1192	41	1.78E-18
DNA_METABOLIC_PROCESS	257	22	2.03E-18
ORGANELLE_PART	1197	41	2.06E-18
NUCLEOBASE_NUCLEOSIDE_NUCLEOTIDE_AND_NUCLEIC_ACID_METABOLIC_PROCESS	1244	41	7.94E-18
REACTOME_CELL_CYCLE	421	25	5.68E-17
CELL_CYCLE_PROCESS	193	18	5.91E-16
BIOPOLYMER_METABOLIC_PROCESS	1684	44	2.09E-15
NUCLEUS	1430	40	4.95E-15
REACTOME_CELL_CYCLE_MITOTIC	325	20	4.13E-14

N= 335 genes down-regulated in non-responders

Figure 37. Microarray based gene expression analysis of pre-treatment LCM stroma.

Figure 37. Microarray based gene expression analysis of pre-treatment LCM stroma.

Heatmap of hierarchical combined clustering of LCM pre-treatment stroma tissues (N= 7 patients) representing responders (pCR+ near-pCR) and non-responders (no-pCR). Heatmap represents N=679 differentially expressed genes, with fold change>1.5 and p value <0.05. Blue color indicates genes with decreased expression and red color indicated genes with increased expression. Gene set enrichment analysis for genes significantly up-regulated (N=344) or down-regulated (N=335) in non-responders are outlined in the figure.

processes, oxidation and response to stress (e.g. change of cell activity in terms of movement, secretion, enzyme production) (Figure 37).

To further evaluate the ability of stromal signature to predict patient response additional analyses have been performed between the tumor and stroma. To determine possible relation between tumor gene set and stromal gene set of differential genes, we used the list differential genes from tumor-specific (N= 329) and from stroma-specific (N= 660) analysis to create a Venn diagram (Figure 38). The results indicate that there was a very small overlap between tumor-specific and stromal-specific differential genes (N=64), thus the number of unique genes was large within both tumor (N= 265) and stroma (N= 596). Furthermore, when each subset of the Venn diagram was analyzed using gene set enrichment analysis (Table 8) we see that stromal unique differential genes were linked once again to metabolic process and proliferation, while in tumor gene set enrichment analysis indicated changes in regulation of transcription, meiosis. The genes that were common between tumor and stroma were linked to cell cycle (Table 8).

Since the gene enrichment analysis for the genes upregulated in the tumors from the non-responders did not yield an overlap (Figure 33), we performed further analysis in an attempt to evaluate the connectivity between these genes. Using an online software (genemania), we queried all the genes and found a small subset of genes that had been previously shown to physically interact (Figure 39).

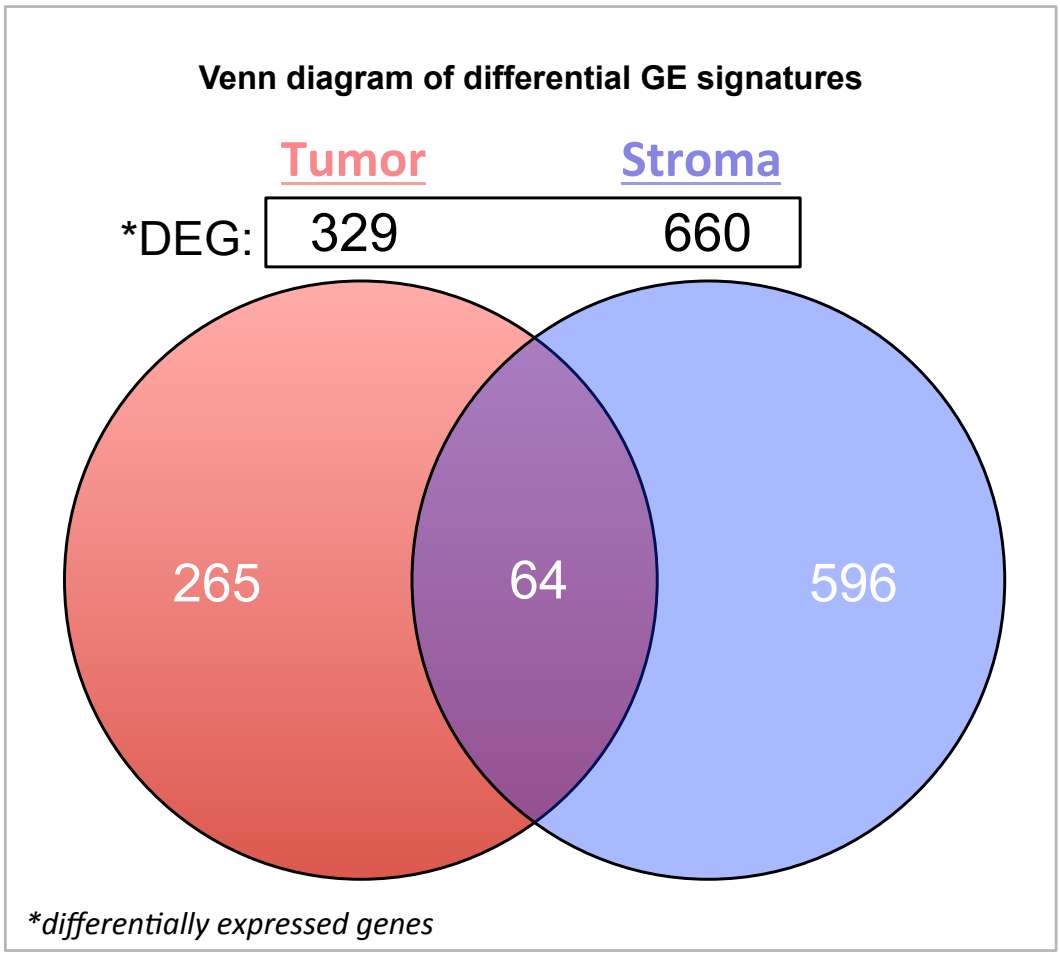

Figure 38. Clinical response GE prediction signatures from tumor and stroma.
Venn diagram represents overlap of differentially expressed genes (DEG) from tumors (N=329) and stroma (N=660). Green area of venn diagram represents genes unique to tumor (N=265), red area of venn diagram represent genes unique to stroma (N= 660) and the yellow area represents common genes between tumor and stroma (N=64).

Table 8. Gene set enrichment analysis for genes unique to tumor, stroma, and genes common to both.

Genes unique to stroma (N=596)

Gene Set Name	# Genes in Gene Set (K)	# Genes in Overlap (k)	p-value
NUCLEOBASENUCLEOSIDENUCLEOTIDE_AND_NUCLEIC_ACID_METABOLIC_PROCESS	1244	48	2.31E-13
DNA_METABOLIC_PROCESS	257	22	3.09E-13
CYTOPLASM	2131	64	1.62E-12
BIOPOLYMER_METABOLIC_PROCESS	1684	54	9.25E-12
INTRACELLULAR_ORGANELLE_PART	1192	44	1.03E-11
ORGANELLE_PART	1197	44	1.19E-11
CELL_CYCLE_GO	315	21	1.20E-10
CELL_PROLIFERATION_GO_	513	25	1.53E-09
REACTOME_IMMUNE_SYSTEM	933	33	1.21E-08
INTRACELLULAR_NON_MEMBRANE_BOUND_ORGANELLE	631	26	2.25E-08

Common genes between tumor and stroma (N=64)

Gene Set Name	# Genes in Gene Set (K)	# Genes in Overlap (k)	p-value
REACTOME_CELL_CYCLE	421	9	2.99E-09
INTRACELLULAR_NON_MEMBRANE_BOUND_ORGANELLE	631	10	6.40E-09
NON_MEMBRANE_BOUND_ORGANELLE	631	10	6.40E-09
INTRACELLULAR_ORGANELLE_PART	1192	12	2.61E-08
ORGANELLE_PART	1197	12	2.73E-08
CELL_CYCLE_PROCESS	193	6	1.71E-07
CYTOSKELETON	367	7	4.15E-07
CYTOSKELETAL_PART	235	6	5.44E-07
MITOTIC_CELL_CYCLE	153	5	1.52E-06
REACTOME_MITOTIC_M_M_G1_PHASES	172	5	2.70E-06

Genes unique to Tumor (N=265)

Gene Set Name	# Genes in Gene Set (K)	# Genes in Overlap (k)	p-value
CYTOPLASM	2131	35	4.15E-10
NUCLEUS	1430	28	6.28E-10
REACTOME_CELL_CYCLE	421	13	2.08E-07
REACTOME_RNA_POL_I_TRANSCRIPTION	89	7	3.10E-07
REACTOME_MEIOSIS	116	7	1.88E-06
REACTOME_RNA_POL_I_RNA_POL_III_AND_MITOCHONDRIAL_TRANSCRIPTION	122	7	2.63E-06
REACTOME_AMYLOIDS	83	6	3.64E-06
NEGATIVE_REGULATION_OF_CELLULAR_PROCESS	646	14	4.62E-06
NEGATIVE_REGULATION_OF_BIOLOGICAL_PROCESS	677	14	7.83E-06

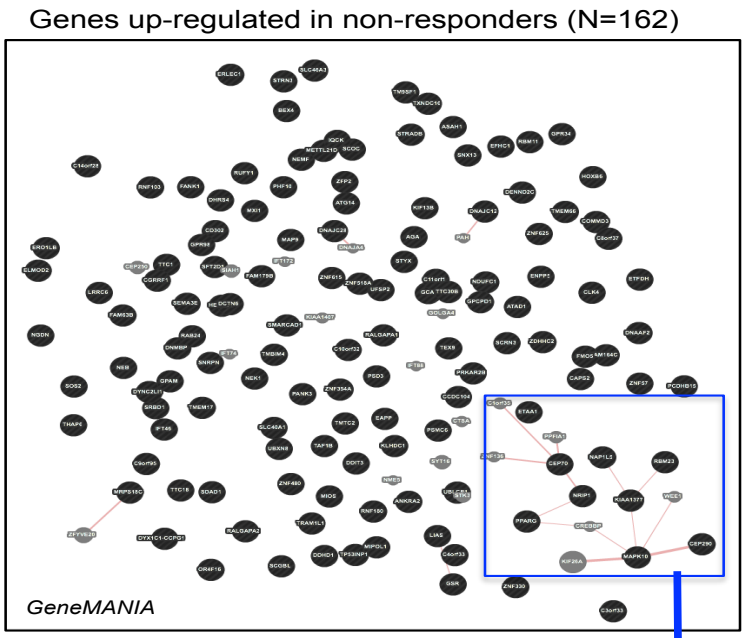

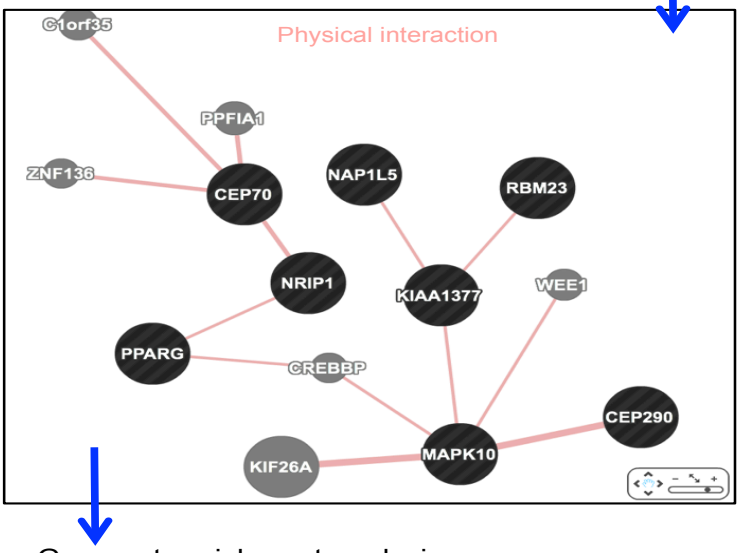

Gene set enrichment analysis

Gene Set Name	# Genes in Gene Set (K)	# Genes in Overlap (k)	p-value
PID_WNT_NONCANONICAL_PATHWAY	**32**	**2**	**7.03E-06**
REACTOME_LOSS_OF_NLP_FROM_MITOTIC_CENTROSOMES	59	2	2.42E-05
REACTOME_RECRUITMENT_OF_MITOTIC_CENTROSOME_PROTEINS_AND_COMPLEXES	66	2	3.04E-05
REACTOME_MITOTIC_G2_G2_M_PHASES	81	2	4.58E-05

Figure 39. Evaluation of the genes up-regulated in the LCM tumors of non-responders.

Figure 39. Evaluation of the genes up-regulated in the LCM tumors of non-responders.

162 upregulated genes in non-responders were queried using online software GeneMANIA. Red lines connecting queried genes represent known physical interaction. Round black circles represent genes queried (N=162) while gray circles represent software-based predicted interaction genes. Gene set enrichment analysis has been performed for genes with physical interaction. Results are outlined in the figure.

Using this subset of genes we performed gene set enrichment analysis, which demonstrated that these genes were involved in WNT non-canonical pathway (Figure 39), which is an interesting finding since Lehmann and colleagues have shown that WNT upregulation was present in TNBC subtypes correlated to poorer prognosis (Lehmann*, et al*, 2011).

In addition to performing analysis on dissected tumor and adjacent stroma, we have also done analysis for whole tissue (tumor and stroma not separated). Using a smaller sample size of responders (N=3) and non-responders (N=3) we performed RNA-seq analysis of pre-treatment whole tissues. The results yielded a list of significantly differentially expressed genes (N=228) between responders and non-responders. Similar to our tumor and stroma analysis steps, we did gene set enrichment analysis on RNA-seq derived genes. As anticipate, these results revealed some overlap with GSEA analysis from tumor and stroma. Interestingly, the ranking favors some of the stromal specific GSEA (Table 9).

Discussion

In this study, we evaluated the therapeutic efficacy of each individual treatment arm of the neoadjuvant cisplatin + paclitaxel±RAD001 combination in patients with triple-negative locally advanced breast cancer. Additionally, we assessed the safety profile of neoadjuvant cisplatin + paclitaxel ± RAD001 combination, tumor response to treatment as measured by ultrasound (US) prior to definitive surgery. We also analyzed therapy-mediated changes of proliferation (ki67), mTOR inhibition evaluated by pS6, and status of p53, p63 and p73.

Table 9. GSEA analysis for significant differentially expressed genes between responders vs. non-responders (RNA-seq on whole tissues)

Rank	Gene Set Name	# Genes in Gene Set (K)	# Genes in Overlap (k)	p-value
1	SIGNAL_TRANSDUCTION	1634	27	1.54E-08
2	**OXIDOREDUCTASE_ACTIVITY**	289	11	1.42E-07
3	RESPONSE_TO_EXTERNAL_STIMULUS	312	11	3.04E-07
4	**OXIDOREDUCTASE_ACTIVITY_GO_0016616**	58	6	3.23E-07
5	CELL_SURFACE_RECEPTOR_LINKED_SIGNAL_TRANSDUCTION_GO_0007166	641	15	4.34E-07
6	**OXIDOREDUCTASE_ACTIVITY_ACTING_ON_CH_OH_GROUP_OF_DONORS**	64	6	5.85E-07
7	SKELETAL_DEVELOPMENT	103	7	6.02E-07
8	**KEGG_METABOLISM_OF_XENOBIOTICS_BY_CYTOCHROME_P450**	70	6	9.99E-07
9	**ICOSANOID_METABOLIC_PROCESS**	17	4	1.06E-06
10	EXTRACELLULAR_REGION	447	12	1.56E-06
11	ANATOMICAL_STRUCTURE_DEVELOPMENT	1013	18	1.62E-06
12	RECEPTOR_BINDING	377	11	1.93E-06
13	MEMBRANE	1994	26	2.61E-06
14	MULTICELLULAR_ORGANISMAL_DEVELOPMENT	1049	18	2.63E-06
15	RESPONSE_TO_CHEMICAL_STIMULUS	314	10	2.63E-06
16	MEMBRANE_PART	1670	23	4.25E-06
17	REGULATION_OF_APOPTOSIS	341	10	5.45E-06
18	REGULATION_OF_PROGRAMMED_CELL_DEATH	342	10	5.59E-06
19	**RESPONSE_TO_STRESS**	508	12	5.76E-06
20	KEGG_STEROID_HORMONE_BIOSYNTHESIS	55	5	6.15E-06
21	APOPTOSIS_GO	431	11	6.90E-06
22	PROGRAMMED_CELL_DEATH	432	11	7.05E-06
23	NEGATIVE_REGULATION_OF_APOPTOSIS	150	7	7.43E-06
24	NEGATIVE_REGULATION_OF_PROGRAMMED_CELL_DEATH	151	7	7.76E-06
25	REGULATION_OF_DEVELOPMENTAL_PROCESS	440	11	8.37E-06
26	NEGATIVE_REGULATION_OF_CELLULAR_PROCESS	646	13	1.30E-05
27	SYSTEM_DEVELOPMENT	861	15	1.54E-05
28	ANTI_APOPTOSIS	118	6	2.08E-05
29	NEGATIVE_REGULATION_OF_BIOLOGICAL_PROCESS	677	13	2.12E-05
30	CARBOXYLIC_ACID_METABOLIC_PROCESS	178	7	2.25E-05
31	**KEGG_DRUG_METABOLISM_CYTOCHROME_P450**	72	5	2.32E-05
32	CELL_FRACTION	493	11	2.39E-05
33	ORGANIC_ACID_METABOLIC_PROCESS	180	7	2.42E-05
34	LIPID_METABOLIC_PROCESS	325	9	2.53E-05
35	REACTOME_GPCR_LIGAND_BINDING	408	10	2.56E-05
36	REACTOME_PEPTIDE_LIGAND_BINDING_RECEPTORS	188	7	3.20E-05
37	RESPONSE_TO_WOUNDING	190	7	3.42E-05
38	**CELL_PROLIFERATION_GO_0008283**	513	11	3.43E-05
39	EXTRACELLULAR_REGION_PART	338	9	3.44E-05
40	NEGATIVE_REGULATION_OF_DEVELOPMENTAL_PROCESS	197	7	4.31E-05
41	CHEMOKINE_ACTIVITY	42	4	4.54E-05
42	KEGG_TYROSINE_METABOLISM	42	4	4.54E-05
43	CHEMOKINE_RECEPTOR_BINDING	43	4	4.98E-05
44	MONOCARBOXYLIC_ACID_METABOLIC_PROCESS	88	5	6.11E-05
45	**WNT_SIGNALING**	89	5	6.45E-05
46	INTRINSIC_TO_MEMBRANE	1348	18	7.28E-05
47	BEHAVIOR	153	6	8.91E-05
48	ORGAN_DEVELOPMENT	571	11	8.91E-05
49	CELL_DEVELOPMENT	577	11	9.77E-05
50	REACTOME_CLASS_A1_RHODOPSIN_LIKE_RECEPTORS	305	8	1.04E-04

Furthermore, we analyzed the genomics data sets generated from pre-treatment biopsies, for prediction of response gene signatures. Overall, the study has met the primary endpoint with a pCR rate of 36%. However, based on the evaluation of clinical and correlative molecular results the addition of RAD001 to the combination of cisplatin and paclitaxel did not improve pCR clinical response rates. Furthermore, RAD001 was associated with slightly more adverse events while cisplatin and paclitaxel combination was well tolerated.

Although ki67 is not currently a marker for routine clinical diagnostic use, studies do show it to have a potential for distinguishing good and poor outcome in breast cancer (Inwald*, et al*, 2013; Urruticoechea*, et al*, 2005). In our study the correlation of molecular markers Ki67 to response demonstrated significant decreased in non-responders compared to responders, evident by both IHC as well as microarray analyses. This suggests that Ki67 might be a useful as a predictor of response in TNBC. In addition, Ki67 was higher in the basal like while lower in mesenchymal and luminal-AR TNBC subtypes, which is what we would expect knowing that basal-like TNBC subtypes are usually associated with better response (Lehmann*, et al*, 2011).

Our initial hypotheses for the trial (based of the preclinical evidence described in introduction above) was that the combined use of drugs that can target the p63/p73 signaling axis at multiple points with RAD001 (mTOR inhibitor), cisplatin, and paclitaxel would have synergistic effects and promote apoptosis. Since our clinical response data between the two arms of trial demonstrated no significant difference, meaning that addition of RAD001 did

improve response, we evaluated levels of phospho-S6 (the downstream target of RAD001). If the RAD001 did target mTOR efficiently we would expect to see a decrease in phospho-S6, which was not the case in our data. This would indicate that dosage of RAD001 was not high enough to achieve adequate mTOR inhibition. The ability to identify and determine the critical pathways that impact responsiveness to RAD001 may be crucial for future development of this agent as a therapy with efficacy in a population of breast cancer patients with poor outcome. However, we do need to consider that the higher percent of adverse events was associated with RAD001, making it difficult to make dosage adjustments in treatment regimen.

Triple negative tumors will have differential gene expression patterns depending on p53 mutational status and expression of the two other p53 family members, p63 and p73. In a fraction of basal-like tumors, p63 is coordinately expressed with p73 and may antagonize p73-mediated apoptosis (Leong*, et al*, 2007). Additionally, the combined use of drugs that can target the p63/p73 signaling axis at multiple points may have synergistic activity. In the remaining fraction of triple negative tumors that lack p63 expression, but express p73, other pathways are selected that modulate p73 apoptotic activity and promote tumor cell survival. Thus we proposed that in tumors with intact p63/p73 signaling axis the treatment with cisplatin, paclitaxel±RAD001 would promote a higher pCR. Our IHC results indicate that on average the p53, p63 and p73 were expressed in TNBC patients, with p63 having the least robustness. Neither p53 nor p63 showed significant aptitude to predict the clinical response while p73 was

significantly higher in pCR patient. Even though we would expect an induction of p73 post mTOR inhibition (Rosenbluth*, et al*, 2008) we do not see significant change post treatment, which is not surprising considering that mTOR might not have been inhibited adequately in our trial.

We have shown that TNBC can be molecularly subtyped into six subtypes among which LAR TNBC is associated with poorer outcome. This would indicate that the treatment used might not have been appropriate for these patients, which we were able to demonstrate *in vitro* (Lehmann*, et al*, 2011). Interestingly, based on the AR expression by IHC we do see a significant associate of AR high levels with poorer outcome indicating that once again we are using a wrong type of therapy for this TNBC subtype.

In addition to identification of subtypes of TNBC we took further step in deciphering the contribution of the tumor and its adjacent stroma to the response to drug treatments. Our specific question was if we can we identify a pre-treatment gene signature that would predict response. Our goal was to determine if we could predict patients clinical response based on analysis of both tumor and stroma prior to treatment. Although not extensive (as it is still work in progress) our results indicate that both tumors and stroma in responders have significantly different gene expression patterns in comparison to non-responders. Interestingly, patients with basal-like subtype TNBC were more likely to achieve a pCR from the paclitaxel/ cisplatin combination; whereas the ones with mesenchymal or LAR subtypes were not.

Based on the impact of our subtyping and identification of molecular drivers of TNBC subtypes as well as taking into a context the impact of tumor microenvironment, there is a possibility that we will uncover novel combination therapies for the various subtypes of TNBC disease. Moreover, a better understanding of pathway alterations that lead to drug resistance as well as the development of new biomarkers will aid in more precise alignment of patients for current and future therapies. Discovering the molecular pathways that mediate intrinsic resistance to targeted therapy will provide predictive biomarkers that allow for better patient selection for first line therapy. Equally significant, the identification of mechanisms of acquired resistance after first line therapy will enable discovery of novel agents that overcome these resistance mechanisms. Improving the efficacy of targeted therapies in the future will require expanding our understanding of resistance mechanisms as well as the ability to take into consideration the cross-talk between tumor and adjacent stroma.

CHAPTER V

GENE EXPRESSION PROFILING OF LASER CAPTURE MICRODISSECTED TUMOR AND STROMA

Abstract

The TGF- β pathway plays a major role in tumor suppression through regulation of epithelial and stromal cell signaling. Dysfunction of the pathway can lead to carcinoma progression and metastasis. To gain insight into the role of the TGF-β pathway signaling in breast cancer, we have performed laser capture microdissection (LCM) on tissues from 45 breast cancer patients and control reduction mammoplasty samples from 10 patients. We microdissected tumor cells and tumor stroma and isolated high quality RNA. A large microarray screen was performed on both tumor and adjacent stroma from all 45 patients and 10 controls. Our data demonstrated that we are able to get a clean separation of tumor and its adjacent stroma. A major finding was that the expression of the TGF-β receptor type III (TβRIII) is greatly decreased in both peri-tumoral stroma compared to control breast tissue. Among all the TGF-β pathway related genes TβRIII demonstrated the most consistent change. In order to verify these results, we have performed quantitative real-time PCR analysis on LCM samples for TβRIII. These results supported our microarray data by demonstrating a 44-fold decrease in TβRIII in tumor stroma in comparison to control tissue. After further investigation using publicly available microarray datasets, we have confirmed that TβRIII levels did indeed decrease in the tumor stroma in the reported human

patients. In addition, immune-histochemistry performed on 37 patients' tissues demonstrated that there is again significant decrease of protein expression levels of TβRIII. Finally, after linking this data to clinical outcome in publicly available microarray datasets, we have determined that lower TβRIII expression level is correlated to poorer clinical outcome. Based on these findings, we are interested in validating the prognostic and functional contribution of TβRIII to breast cancer.

Introduction

It is currently accepted that tumor progression depends not only on the intrinsic malignancy of the tumor cell but also on the surrounding microenvironment composed of stromal cells. Using a cohort of 600 patients, Kruijf and colleagues have evaluated the prognostic values of carcinoma stroma in breast cancer. They have demonstrated that tumor-stroma ratio in the primary tumor is a prognostic factor in early breast cancer patients (Kruijf*, et al*, 2010). The stroma-rich tumor patients had a shorter overall survival in comparison to stroma-poor breast cancer patients (Kruijf*, et al*, 2010).

Although there have been many advances in early detection, diagnosis and treatment of breast cancer, metastatic breast cancer remains a problem. Human breast cancer is a diverse group of diseases. Previous molecular profiling of whole tumor tissues has identified five major breast cancer phenotypes: luminal A, luminal B, Her2-like, Normal breast-like and Basal-like (Perou*, et al*, 2000). Furthermore these breast cancer phenotypes correlate to the patient survival with the luminal B subtype demonstrating the poorest overall outcome (Sorlie*, et al*, 2001) however stromal molecular differences within these have not

been addressed.

Progress on the stromal molecular profiling is ongoing, but its depth is lagging behind the molecular profiling of the tumor epithelium. Almost a decade after tumor molecular profiling Finak and colleagues have demonstrated that stromal signatures are important to pursue. Their molecular profiling of tumor stroma has revealed three subtypes of tumor stroma classified as: mixed outcome, good outcome and poor outcome (Finak*, et al*, 2008). This was based on a correlation between the overall patient outcome and stromal gene expression. Overall, this study contributes to the current awareness that tumor stroma does have effect on disease outcome and that a better understanding of the stromal gene expression changes could potentially offer new targets for therapy to prevent and suppress breast cancer progression.

Over the course of the past several years, it has become apparent that stromal cells adjacent to normal or transformed epithelium can significantly regulate the initiation and progression of cancer *in vivo*. Our attention has been focused on understanding tumor microenvironment in the context of TGF-β signaling. Using primarily mouse models we have shown that loss of TGF-β signaling in stromal fibroblasts can lead to tumorigenesis of the adjacent epithelial cells (Bhowmick*, et al*, 2004a) as well as promote carcinoma growth and invasion due to increased secretion of chemokines (Cheng*, et al*, 2005; Cheng*, et al*, 2007). As far as the human disease progression it has been previously shown that during the advanced stages of human cancer progression *TGFBR2* is lost in the epithelial carcinoma cells (Gobbi*, et al*, 2000).

Considering that it has not been established what effect stromal gene expression changes have on the tumor progression it is necessary to further our understanding of stroma. Stromal-epithelial interactions offer new targets for adjuvant therapy to prevent and suppress human breast cancer progression. Current strategies to treat human breast cancer are predominantly focused on targeting the carcinoma cell population specifically, however there are a significant number of patients that will develop distant metastases even though standard therapies are applied.

Results

Laser capture microdissection (LCM) of human mammary periductal and peritumoral stromal cells.

Considering that the TGF-β signaling has not been intensively studied in human stroma we have decided to collect tumor and tumor stroma using frozen tumor cores from breast cancer patients (Figure 40). In addition, as our control we performed LCM on human breast reduction mammoplasty, collecting epithelial cells and peri-ductal fibroblasts (Figure 40A-D). Our goal for LCM was to enrich fibroblast collection by avoiding obvious immune cells and blood vessels. Pictures were taken before and after LCM to document the tissue captured and the cell type (Figure 40D and H). RNA was obtained from the captured stromal and tumor cells, and has proved to be of high quality (Figure 40I). Currently we have collected forty-five breast tissues and eleven controls (Figure 40J) and performed analysis on twenty-two breast cancer patients and eight controls.

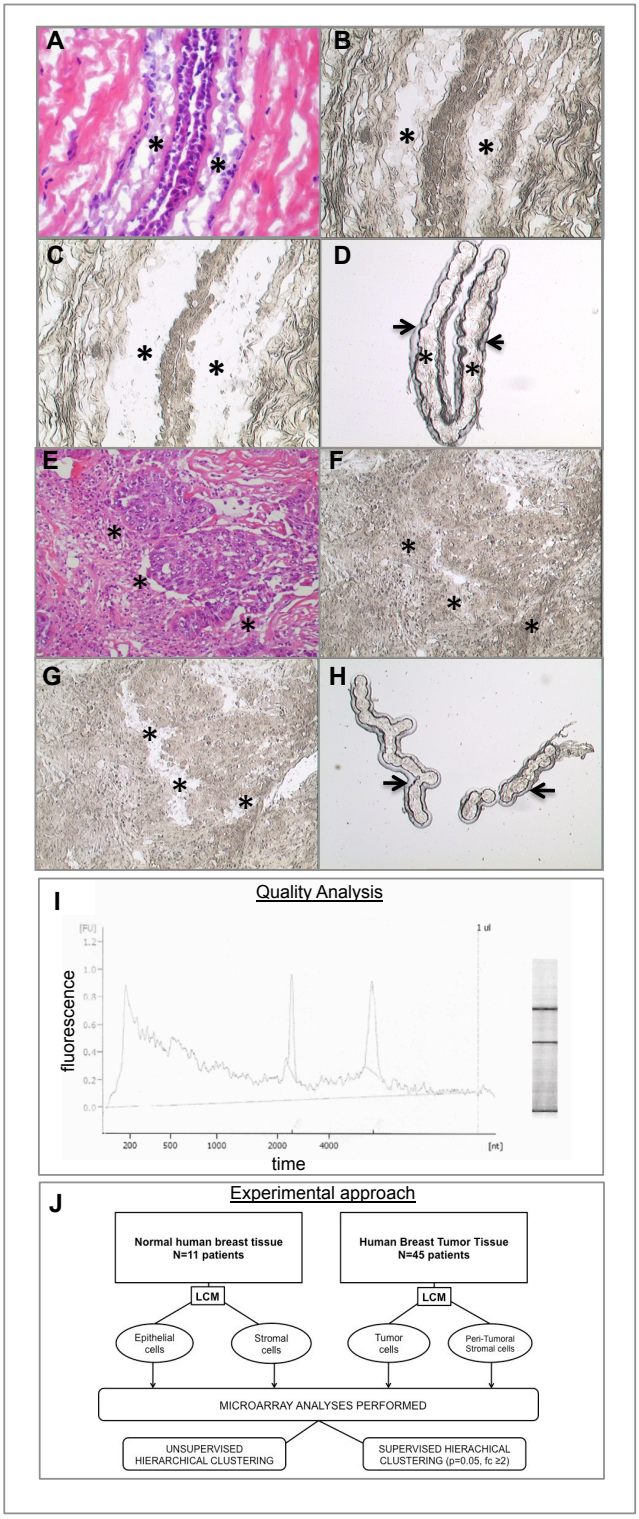

Figure 40. Laser capture microdissection (LCM) of human mammary periductal and peritumoral stromal cells and experimental approach.

Figure 40. Laser capture microdissection (LCM) of human mammary periductal and peritumoral stromal cells and experimental approach.
(A) H&E stained frozen section of reduction mammoplasty specimen. Note stromal cells (*) flanking ductal epithelial cells. (B) Unstained frozen section as seen in the LCM microscope before capture. Stromal cells (*) are easily distinguished from the ductal epithelial cells. (C) Frozen section after capture showing absence of stromal cells (*). (D) Captured tissue on LCM cap. Note grey areas outside the black line (arrows) are light refraction artifact. (*) captured stromal tissue. (E-H) Human invasive ductal adenocarcinoma fibroblasts were microdissected and the images shown are similar to that described for the control tissue in A-D. (I) 100 ng of RNA was obtained from the captured stromal cells, which proved to be of high quality with a 28s/18s rRNA ratio of 1.6 and lack of significant degradation. Subsequent amplification of 10 ng using NuGen protocols was successful providing ample material for DNA microarray analysis. (J) experimental approach.

Hierarchical clustering demonstrates distinct separation between controls tumor stroma and tumor.

Based on gene expression controls segregate into completely different group (with exception of one outlier) (Figure 41). A distinct separation was also evident from analysis of a larger cohort of patients in which comparisons were made between tumor stroma and controls as well as tumor and control epithelial cells (Figure 42). Furthermore, we narrowed down our analysis by performing supervised hierarchical clustering to determine genes that are statistically different between tumor stroma and tumor. The results show a statistically significant change in 177 transcripts (with multiple testing corrected p-value< 0.05 and fold change > 2) (Figure 43).

In silico analysis of TGF-β pathway related genes reveals TGFBR3 to be significantly changed in tumor stroma.

Since our primary focus is TGF-β signaling, we have narrowed down the genes and looked at the ones directly related to TGF-β signaling pathway. Decrease of *TGFBR3* expression in tumor stroma was the most consistent change among all the TGF-β pathway related genes. The *TGFBR3* levels were decreased in tumor stroma in 75% patients while expression was intact across all the controls (Figure 44). To verify our microarray results we used publically available stromal datasets as represented in Table 10. Note there are only limited stromal gene expression datasets available.

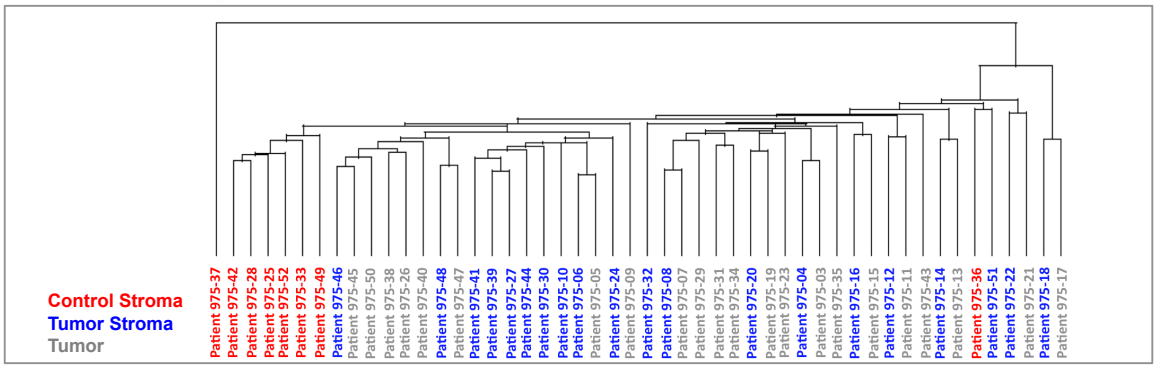

Figure 41. Unsupervised hierarchical clustering: control versus tumor stroma versus tumor.

Unsupervised hierarchical clustering was performed on 29,000 genes without any filters. LCM based microarray data demonstrate that control stroma separates well from the tumor stroma (with exception of one outlier).

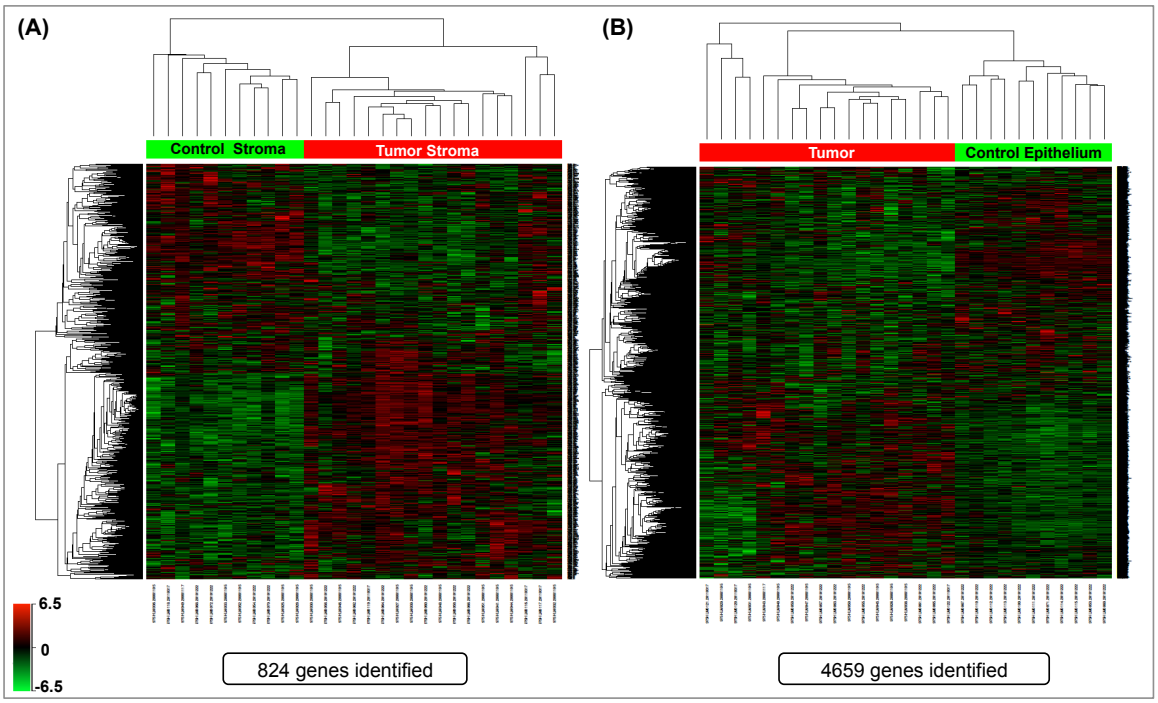

Figure 42. Supervised hierarchical clustering- comparisons to control tissues.

Control stroma versus tumor stroma demonstrated 824 differentially expressed genes while control epithelium versus tumor demonstrated 4659 differentially expressed genes with multiple testing corrected p-value< 0.05; fold change > 2.

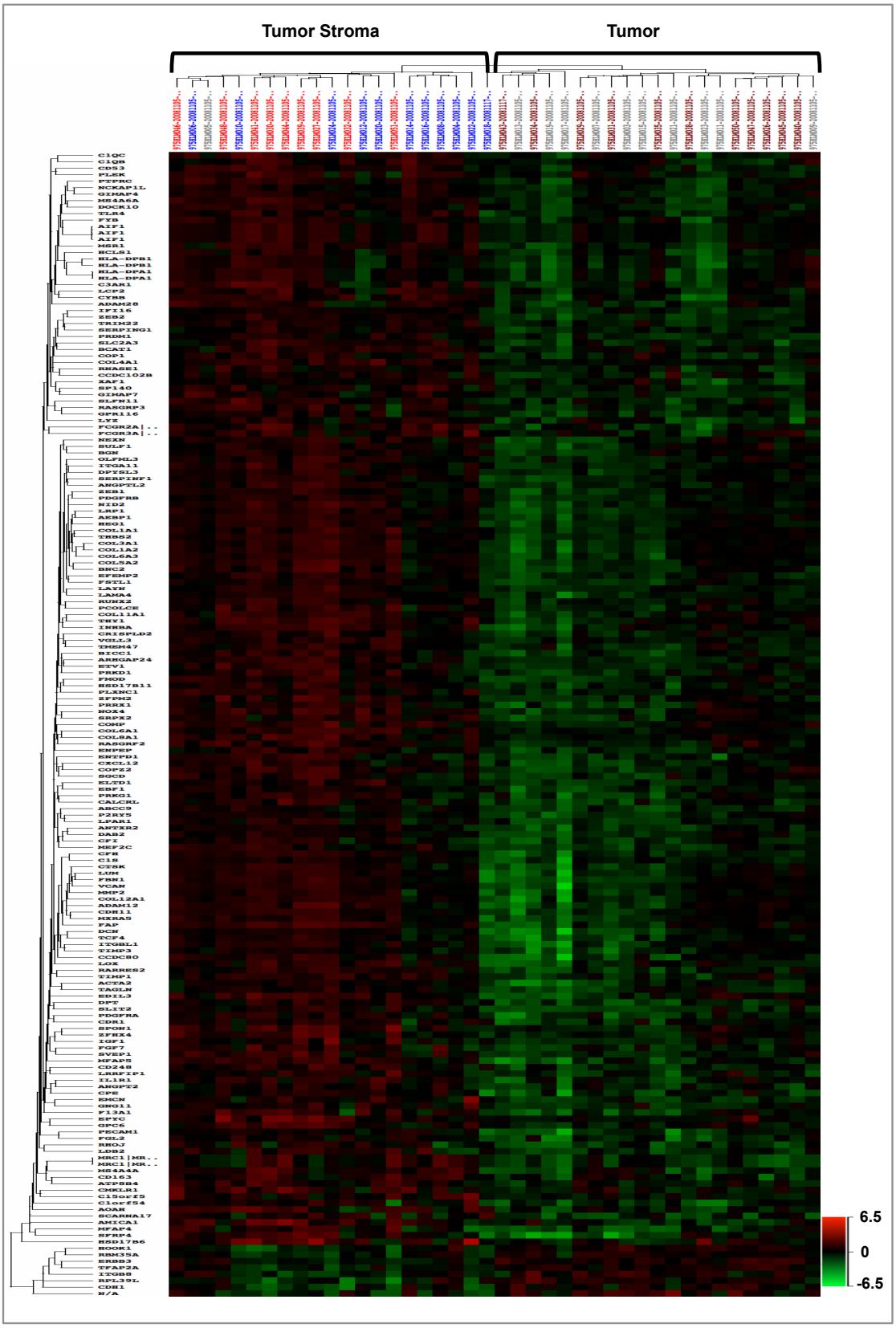

Figure 43. Supervised hierarchical clustering- tumor stroma to tumor.

Figure 43. Supervised hierarchical clustering- tumor stroma to tumor.
Supervised hierarchical clustering was used for determining genes that are statistically different between tumor stroma and tumor. 177 transcripts with multiple testing corrected p-value< 0.05; fold change > 2.

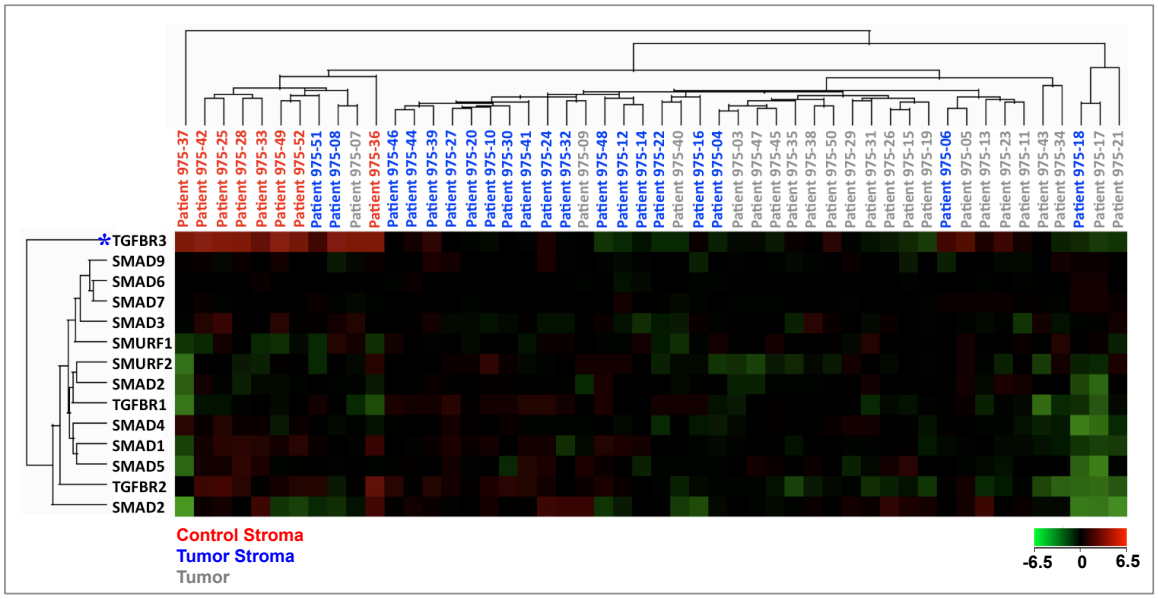

Figure 44. TGF-β pathway related genes.
Microarray analyses indicate loss of *TGFBR3* (*) in the tumor stroma in comparison to the control stroma. The *TGFBR3* gene expression levels in patients' tissues were increased in all control stroma and decreased in 78% of tumor stroma.

Table 10. *TGFBR3* levels based on published studies involving stromal microarray analyses.

Study	Description	Result	GSE	Source
Ma et. al. *Breast Cancer Res 2009*	Stroma from 14 normal vs 9 invasive breast carcinoma	-8.72 fold (p=0.003)	GSE14548	NextBio
Casey et. al. *Breast Cancer Res Treat 2009*	Stroma from 5 normal vs. 28 invasive breast carcinoma	-2.69 fold (p=0.003)	GSE10797	NextBio
Finak et. al. *Nature Medicine 2008*	Stroma from 6 normal vs. 53 invasive breast carcinoma	-3.23 fold (p=0.0001)	GSE9014	Oncomine
Karnoub et. al. *Nature 2007*	Stroma from 15 normal vs. 7 invasive breast carcinoma	-4.34 fold (p=0.0001)	GSE8977	NextBio

Analyses of these stromal datasets suggest once again a significant decrease in *TGFBR3* levels in the human breast stroma, thus confirming our microarray findings. It is important to note that these studies have not specifically looked at *TGFBR3* expression changes. Figure 45 is a visual representation demonstrating a significant loss of *TGFBR3* in the invasive breast carcinoma stroma compared to the control stroma (Finak*, et al*, 2008; Karnoub*, et al*, 2007). Interestingly, based on analysis of the Ma et. al. dataset it appears that this decrease in *TGFBR3* occurs gradually during breast cancer progression as demonstrated by the control stroma, ductal carcinoma in situ (DCIS) and invasive ductal carcinoma (IDC) (Figure 45B) (Ma*, et al*, 2009).

Validations of the microarray findings in the stromal tissues and cell lines confirm a significant decrease of TGFBR3 both at mRNA and protein levels.

Furthermore, quantitative real-time PCR validated our *TGFBR3* microarray findings by demonstrating a significant 44-fold decrease of *TGFBR3* in tumor stroma (Figure 46A). Immunohistochemistry (IHC) for TβRIII performed on tissues from thirty-seven breast cancer patients show similar expression patterns to our microarray data expression. IHC staining intensity scores (assigned by pathologist) indicate a lower expression level of TβRIII in the human breast tumor stroma (Figure 46B). Interestingly, the *in vitro* cell line data consisted of cancer-associated fibroblasts (CAFs) and normal-associated fibroblasts (NAFs) demonstrate a decrease of *TGFBR3* in CAFs at both mRNA (Figure 47A) and protein levels (Figure 47B).

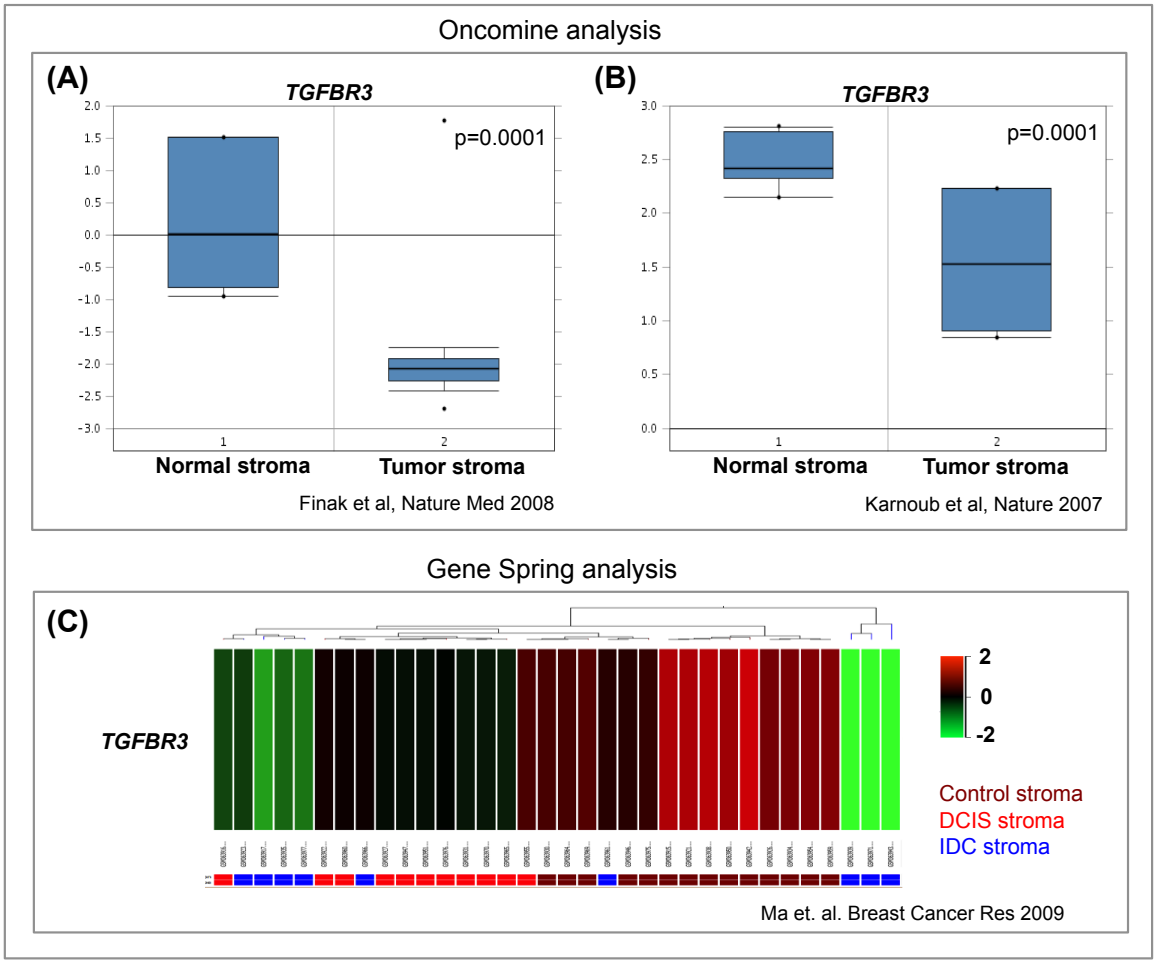

Figure 45. *TGFBR3* levels of expression in publicly available microarray datasets.

(A) Oncomine transcriptome profiles, yield results demonstrating a significant decrease in *TGFBR3* levels in the human breast tumor stroma. (C) Furthermore, Ma et al data set consisting of stroma derived from normal, ductal carcinoma in situ (DCIS) and invasive ductal carcinoma (IDC) shows gradual decrease of *TGFBR3* from normal to IDC state. Note that these studies have not looked at *TGFBR3*.

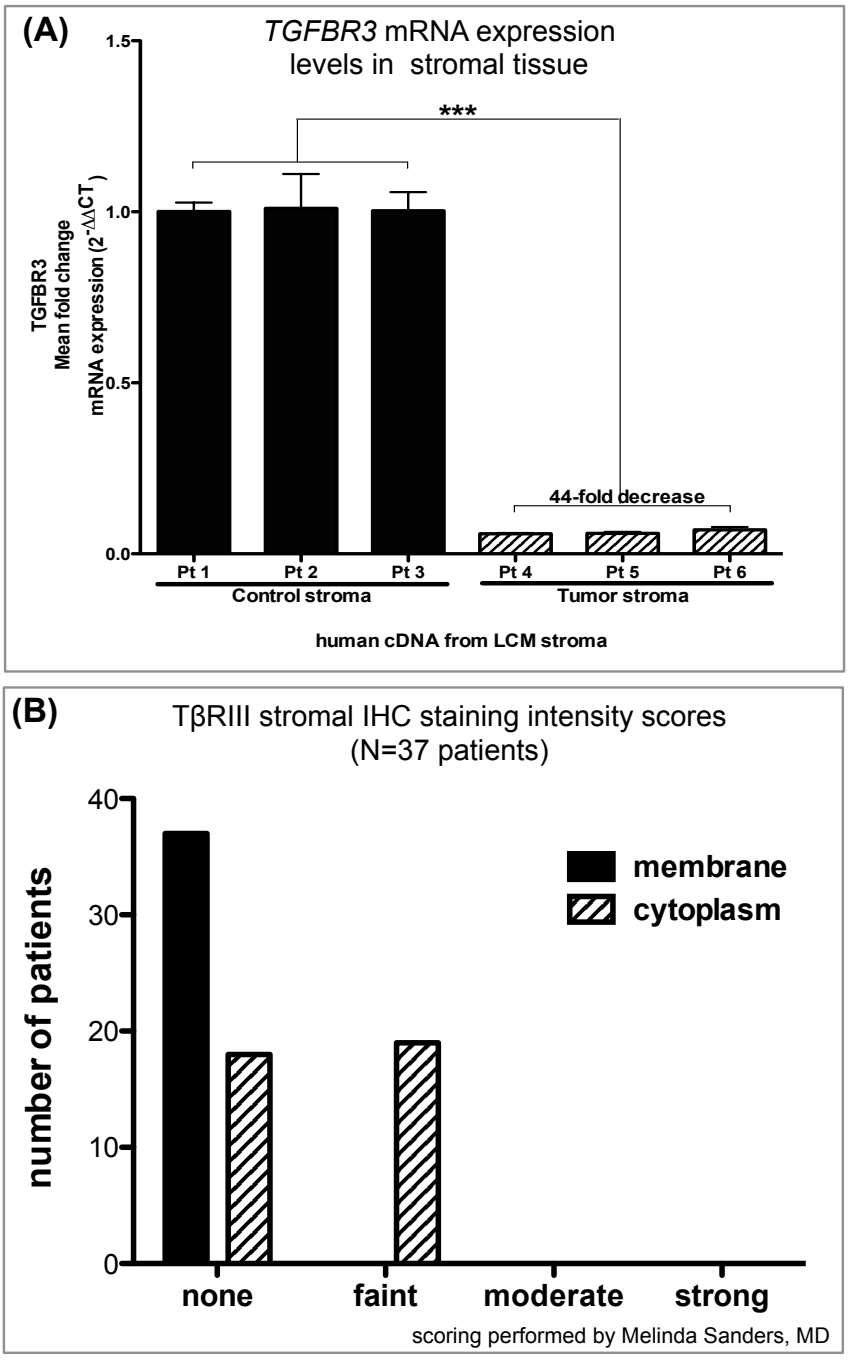

Figure 46. Validations by qRT-PCR and IHC.

A, qRT-PCR analysis of *TGFBR3* average mRNA expression ($2^{-\Delta\Delta CT}$) from human cDNA acquired by LCM; graph bars represent the mean of 3 replicates with SEM error bars. On average there is 44-fold decrease of *TGFBR3* in tumor stroma in comparison to control stroma (***P<0.0001; for a one-way ANOVA). **B,** IHC results for TβRIII protein levels across 37 breast cancer patients.

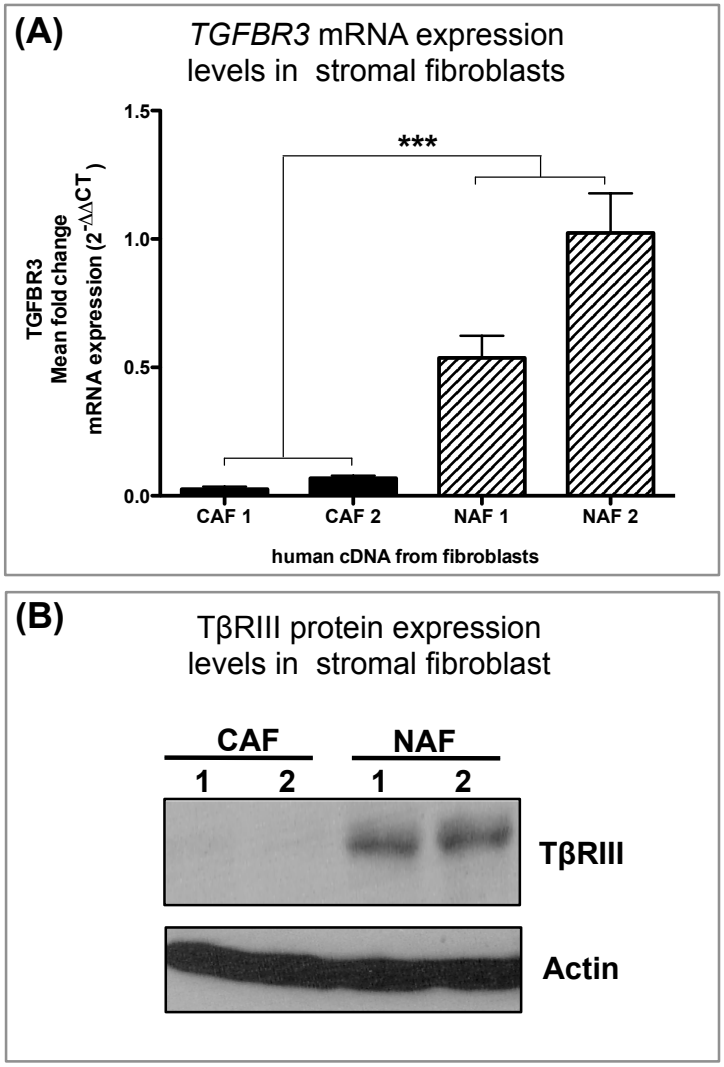

Figure 47. *In vitro* validation of TβRIII protein/RNA levels in human breast cancer fibroblast.

A, qRT-PCR analysis of *TGFBR3* average mRNA expression ($2^{-\Delta\Delta CT}$) from human cDNA from cancer associated fibroblasts (CAFs) and normal associate fibroblasts (NAFs); graph bars represent the mean of 3 replicates with SEM error bars (***P<0.0001; for a one-way ANOVA). **B,** immunoblot analysis of TβRIII protein expression in CAFs and NAFs.

Validations of the microarray findings in tumor stroma.

Survival as a function of TGFBR3 in whole tissues.

Kaplan-Mayer analysis for patient clinical outcome indicates a correlation of survival with *TGFBR3* loss. This analysis suggests that patients with low mRNA expression levels of *TGFBR3* are linked to poorer survival (Figure 48).

Differences in expression of genes encoding proteins important in TGF-β regulated chemokines.

In addition to analyzing pivotal genes within TGF-β pathway, we also looked at the chemokine genes, which we have previously linked to TGF-β using mouse model. We have shown that TGF-β can regulate fibroblast-derived chemokines that can act directly upon the adjacent tumor/epithelium to contribute to carcinoma progression and metastasis (Cheng*, et al*, 2005; Cheng*, et al*, 2007). Interestingly, in Table 11 we demonstrate that the expression of many, including CCL2 (MCP-1) from our previous findings, chemokines are increased in the carcinoma stroma. However, this is the result of only one comparison and many other patient samples must be examined before firm conclusions can be properly derived.

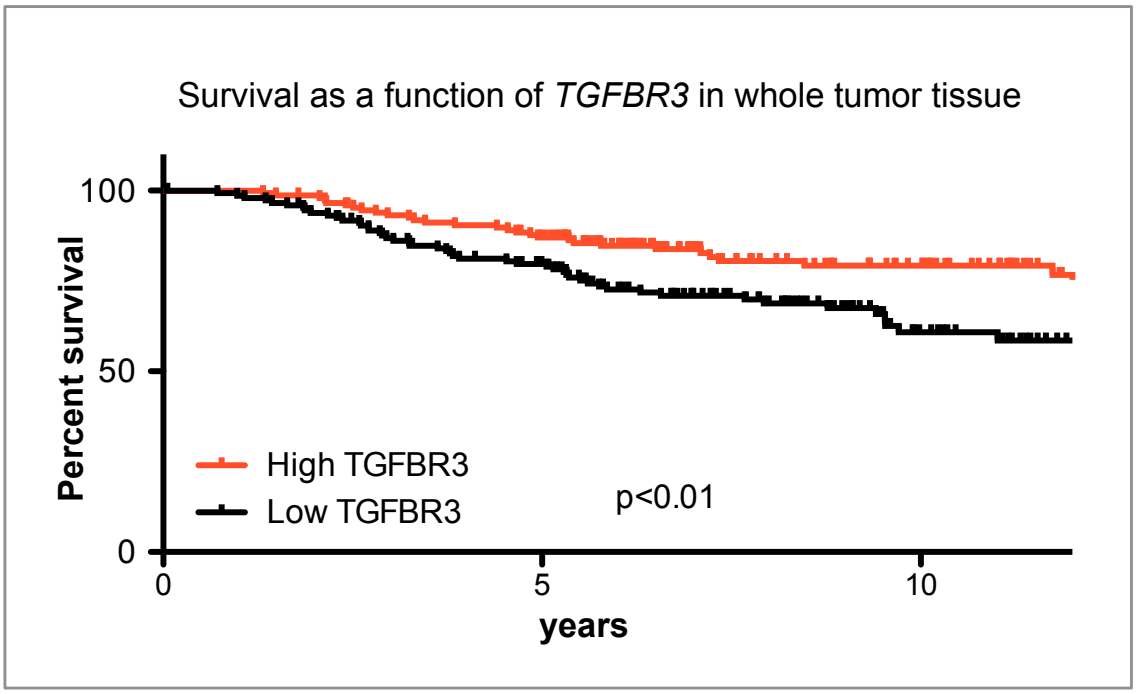

Figure 48. Percent survival as a function of *TGFBR3* in whole tumor tissue. Based on Kaplan Mayer analysis of whole tumor patients with low *TGFBR3* expression levels (black) are linked to poorer survival compared to patients with high *TGFBR3* expression (red) ($p<0.01$).

Table 11. Differences in expression of genes encoding proteins important in TGF-β regulated chemokines.

Affymetrix ID	Fold Change	Gene Symbol
Upregulated C-C motif chemokines		
206407_s_at	2.7	**CCL13**
216714_at	2.21	**CCL13**
207900_at	4.61	**CCL17**
209924_at	10.51	**CCL18**
32128_at	9.22	**CCL18**
216598_s_at	2.28	**CCL2**
205114_s_at	3.09	**CCL3**
204103_at	3.48	**CCL4**
1405_i_at	17.71	**CCL5**
204655_at	11.66	**CCL5**
1555759_a_at	5.33	**CCL5**
Upregulated C-C motif chemokine receptors		
205098_at	4.46	**CCR1**
205099_s_at	3.4	**CCR1**
206983_at	30.38	**CCR6**
206377_at	3.38	**CCR7**
Upregulated C-X-C motif chemokines		
204533_at	74.36	**CXCL10**
210163_at	37.95	**CXCL11**
211122_s_at	37.76	**CXCL11**
237038_at	7.05	**CXCL14**
223454_at	2.34	**CXCL16**
203915_at	63.08	**CXCL9**
Upregulated C-X-C motif chemokines receptors		
207681_at	11.9	**CXCR3**
211919_s_at	2.07	**CXCR4**
206974_at	5.86	**CXCR6**

Table 11. Differences in expression of genes encoding proteins important in TGF-β regulated chemokines.

Represents DNA microarray comparing human reduction mammoplasty periductal stroma and tumor stroma. RNA isolated from LCM material as described in Figure 40 was subjected to microarray analysis. Differences in expression of genes encoding proteins important in TGF-β signaling and chemokines.

Discussion

Loss of TGF-β signaling in stromal fibroblasts can initiate and promote carcinoma progression in adjacent epithelium. In our recent studies related to TGF-β signaling, it has become clear that stromal fibroblasts have the ability to suppress or initiate carcinomas in adjacent normal epithelium (Bhowmick*, et al*, 2004a; Bhowmick*, et al*, 2004b). Further, we have found that within an initiated tumor microenvironment, TGF-β signaling in stromal fibroblasts can have a profound influence upon tumor progression. The kidney capsule xenograft and genetic studies in mice have been able to provide useful information regarding stromal epithelial interactions that regulate adjacent carcinoma initiation and progression. In the mammary gland, it has now been shown that human mammary fibroblasts have the capacity to suppress tumorigenesis of adjacent epithelium (Kuperwasser*, et al*, 2004). Together the results, obtained through modified stromal TGF-β signaling in mice with those obtained using human fibroblast and epithelial cell recombination, suggest that stromal-epithelial interactions can have a significant impact on the regulation of adjacent carcinoma initiation and progression *in vivo*.

Considering that our focus was to gain a better insight into TGF-β pathway we chose to do laser capture microdissection (LCM) of tumor stroma followed by DNA microarray. The performed microarray analysis of tumor stroma, led us to a provocative finding that the expression of *TGFBR3* was markedly decreased in tumor stroma compared with control. This gene demonstrated the most consistent change among all the TGF-β pathway genes. To verify these results,

we have performed quantitative real-time PCR analysis on LCM samples for *TGFBR3*. These results have confirmed our microarray data by demonstrating a 44-fold decrease in *TGFBR3* in tumor stroma. The immunohistochemistry that have been performed demonstrates that there is a decrease of protein expression levels of TβRIII. After linking this data to clinical outcome in publicly available microarray data sets, we have determined that there is correlation between *TGFBR3* expression levels and patient outcome. Specifically, the loss of *TGFBR3* is linked to poor outcome.

To date the functional context of *TGFBR3* remains controversial in breast cancer, where studies report both tumor suppressive and tumor-promoting functions (Criswell*, et al*, 2008; Dong*, et al*, 2007). Currently there are no reports demonstrating the role of *TGFBR3* in the tumor microenvironment, despite the possibility that *TGFBR3* controversy in breast cancer might be influenced by tumor microenvironment. Microarray data generated through laser-capture microdissection of human breast cancers and control breast tissue followed by DNA microarray show that the most consistent change in TGF-β pathway protein expression is a marked reduction in expression of the *TGFBR3* in stromal cells. Since inactivating mutations in the gene encoding *TGFBR3* have not been reported, we suspect reduced expression through epigenetic mechanisms that could be reversible.

We expect our study will shed light on the role of *TGFBR3* in the tumor microenvironment and perhaps resolve the current controversy of *TGFBR3's* role in the tumor. Addressing the function of *TGFBR3* in the tumor microenvironment

could help us determine if the current data on *TGFBR3* in tumor is actually context dependent, meaning that the behavior of the tumor cell is modified/regulated by the extracellular *TGFBR3*.

Future direction

Despite the fact that *TGFBR3* is important for delivering TGF-β ligands to TβRII and initiation of TGF-β signaling, this molecule is still very little studied in an understudied component of the tumor microenvironment and deserves attention. *TGFBR3* has the potential to be new key player in the tumor microenvironment thus characterization of *TGFBR3*'s physiological function in tumor-stroma interaction, and its relationship to other key tumor-stroma molecular mediators, is an essential direction for providing an insight into tumor microenvironment and determining novel options for early diagnosis and anticancer therapy. In addition to our focus on *TGFBR3*, our patient breast cancer gene-expression profiling of tumor and adjacent tumor stroma can provide information, which could enhance the prediction of clinical outcome in comparison to current approaches performed in pathology. The patient microarray datasets will enable us to determine gene signatures which could then be translated and used for development of tests that could serve as a guide for more informed clinical decision-making. We are in need of new strategies that we can use either as a preventive measure or a treatment of metastatic disease. Stromal-epithelial interactions offer new targets for adjuvant therapy to prevent and suppress human breast cancer progression. Current strategies to treat human breast cancer are predominantly focused on targeting the carcinoma cell

population specifically, however there are a significant number of patients that will develop distant metastases even though standard therapies are applied. At present, the five-year survival rate for breast cancer is low when distant metastases are detected at the time of primary tumor diagnosis, and it is likely that conventional therapy in addition to targeting adjacent supporting cell populations would improve long-term survival within this patient population.

Completion of this project will augment our basic understanding of mechanisms of cancer progression and metastasis. Importance of stromal contribution to breast cancer initiation and progression and in understanding mechanisms for devising therapeutic strategies – will be necessary to target both the cancer cells and the microenvironment for effective treatment of metastatic disease.

CHAPTER VI

SUMMARY AND FUTURE DIRECTIONS

Treatment of patients with TNBC has been challenging due to the heterogeneity of the disease and the absence of well-defined molecular targets for efficient therapeutic intervention (Carey*, et al*, 2007; Pegram*, et al*, 1998; Wiggans*, et al*, 1979). As previously mentioned, TNBCs constitute 10%-20% of all breast cancers that frequently affect younger patients (Dent*, et al*, 2007) with tumors are generally larger in size, higher grade, with lymph node involvement at diagnosis thus biologically more aggressive (Cheang*, et al*, 2008; Dent*, et al*, 2007; Haffty*, et al*, 2006; Kreike*, et al*, 2007; Rakha*, et al*, 2007; Tan*, et al*, 2008; Viale*, et al*, 2009). In general, TNBC patients are associated with a higher recurrence rate after diagnosis, a shorter disease-free interval, rapid progression from distant recurrence and shorter overall survival regardless of stage at diagnosis (Abd El-Rehim*, et al*, 2005; Abd El-Rehim*, et al*, 2004; Carey*, et al*, 2006; Jones*, et al*, 2004; Lund*, et al*, 2009; Nguyen*, et al*, 2008; Nielsen*, et al*, 2004; van de Rijn*, et al*, 2002). This calls for further assessment of the treatment approaches currently used in clinical settings. There is a major need for deciphering the biology of TNBC, evaluating the driving pathways and determining new therapeutic options for TNBC patients.

Although there are common features that define TNBC (described in Chapter I) there is significant diversity within these tumors potentially creating

barriers to effective treatments. The genomic diversity of TNBC has been demonstrated by the Pietenpol laboratory where they confirmed the heterogeneity within TNBC by demonstrating distinct TNBC subtypes with unique molecular driver pathways. In addition, their *in vitro* cell line validation demonstrated that these subtypes responded differently to currently used therapies (Lehmann*, et al*, 2011). This means that current 'single disease' approach of treatment of primary TNBC tumors needs major improvement.

TNBC has worst overall survival compared to other breast cancers, mainly due to lack of targeted therapy but also driven by the biology of the disease. In addition, considering the emerging data that reveals the complexity and diversity of the TNBC (Shah*, et al*, 2012), it is evident that TNBC field requires further analysis of their important drivers and their mechanisms within the TNBC subtypes. Thus, my dissertation research presented herein has primarily focused on deciphering the role for TGF-β signaling in TNBC *in vivo* and *in vitro* (Jovanovic*, et al*, 2014a) as the TGF-β signaling was among top drivers, present in one-third of TNBC defined subtypes (Lehmann*, et al*, 2011). Considering the severity of TNBC disease as well as the previously established roles of TGF-β signaling in cancer initiation and progression through tumor cell autonomous and non-autonomous signaling, we hypothesized that TGF-β signaling acted as a tumor promoter in TNBC.

Chapter III presents the results that have led to an unanticipated discovery of the role of a gene member of TGF-β superfamily, *TGFBR3,* in a subset of TNBC (Figure 49).

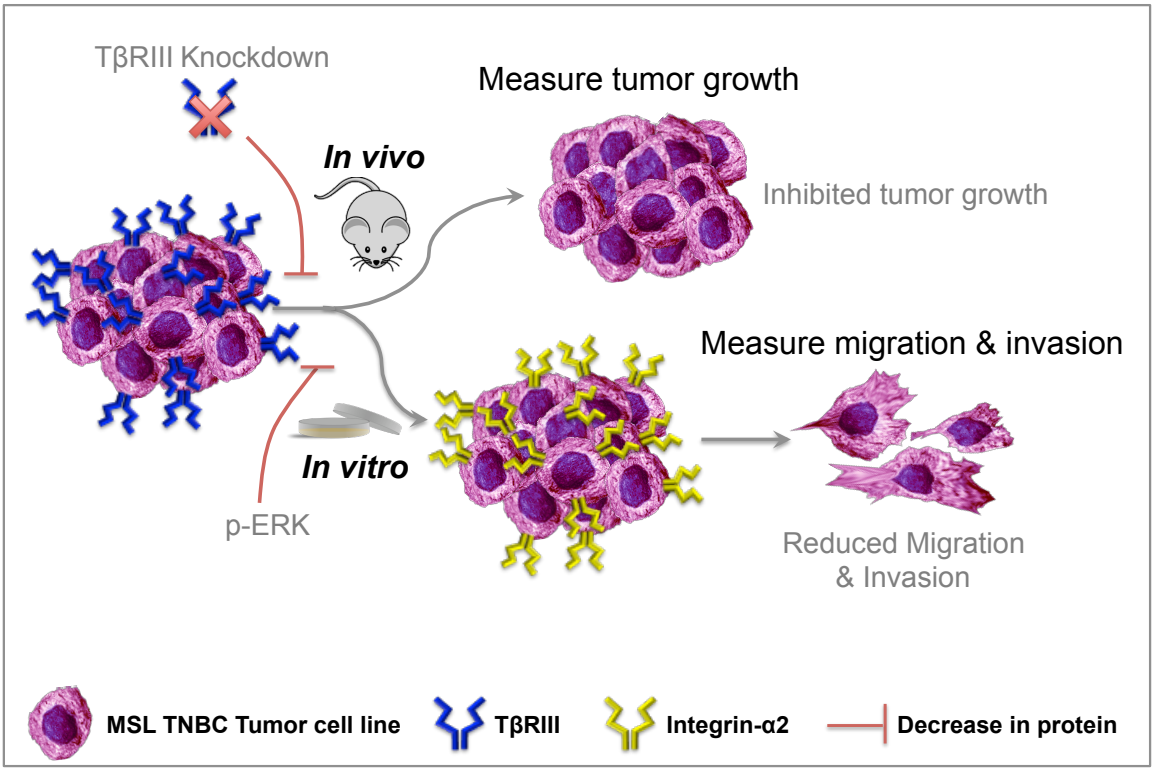

Figure 49. Chapter III model based on the acquired *in vitro* and *in vivo* results in MSL TNBC cells.

This discovery was surprising to us as within TGF-β field, the main focus of interest has been on TβRI and TβRII (due to their receptor-kinase activity); while research on TβRIII has lagged as has not been as extensively studied (due to its lack of intrinsic enzymatic activity). Furthermore, the limited publications on TβRIII have indicated a controversial role for TβRIII, demonstrating both tumor suppressive as well tumor promoting activities. This triggered our interest in determining whether known TGF-β context dependency applied to TβRIII and if defining this context (e.g. breast cancer type) would further elucidate role of TβRIII and potentially contribute to resolving the controversy.

The published results of Chapter III represent the first comprehensive report of the role of TβRIII in TNBC (Jovanovic*, et al*, 2014b). The results have led to the identification of robust expression of TβRIII within mesenchymal (M) and mesenchymal-stem like (MSL), the TNBC subtypes noted to have poorer response among the TNBC subtypes. Notably, the results demonstrate that the manipulation of TβRIII in representative MSL cell lines leads to decreased tumor growth *in vivo* and also decrease in motility and invasion *in vitro* (Figure 49), mechanisms that contribute to cancer progression. Further, upon knockdown of TβRIII in MSL, a global gene expression profile revealed integrin pathways to be among the top pathways altered. Interestingly, from the standpoint of TGF-β field, all the observed phenotypes resulting from knockdown of TβRIII appeared to be independent of TGF-β and this is additionally supported by data derived from using a TβRIII high expressing TNBC cell line with abrogated TGF-β signaling

(Figure 50, Figure 51). This indicated that TβRIII was responsible for the observed migration and invasion phenotypes and in case of this study it was interacting with integrin signaling via *ITGA2.* The ability of TβRIII to regulate invasion via Par6/Smurf1/RhoA pathway (ligand-dependent) has been previously shown in mouse *Tgfbr3* $^{-/-}$ epicaridial cells (Sánchez & Barnett, 2012). Interestingly, this study did not show any effect on migration. In addition, a separate study has demonstrated that in ovarian cancer cells TβRIII can regulate migration via Cdc42 while no effect on invasion was observed (Mythreye & Blobe, 2009). We are the first to report that TβRIII affected both migration and invasion via a single pathway, integrins, specifically through regulation of ITGA2 (Jovanovic*, et al*, 2014a). Together, these studies have made a significant step forward with regard to our understanding of the role of TβRIII within the TNBC. Putting our findings in context of the previous literature reviewed in the introduction chapter, our results show that TβRIII acts as a tumor promoter as it helps with promoting tumor growth, migration and invasion.

The TCGA based survival data from breast cancer patients (N=971 patients) indicate that increased expression levels of *TGFBR3* significantly correlates with poorer survival (Figure 52), indicating that TβRIII might be a valuable prognostic marker. Furthermore, considering the current need to identify and evaluate the potential therapeutic targets in TNBC, a future direction should include assessing targeting of TβRIII.

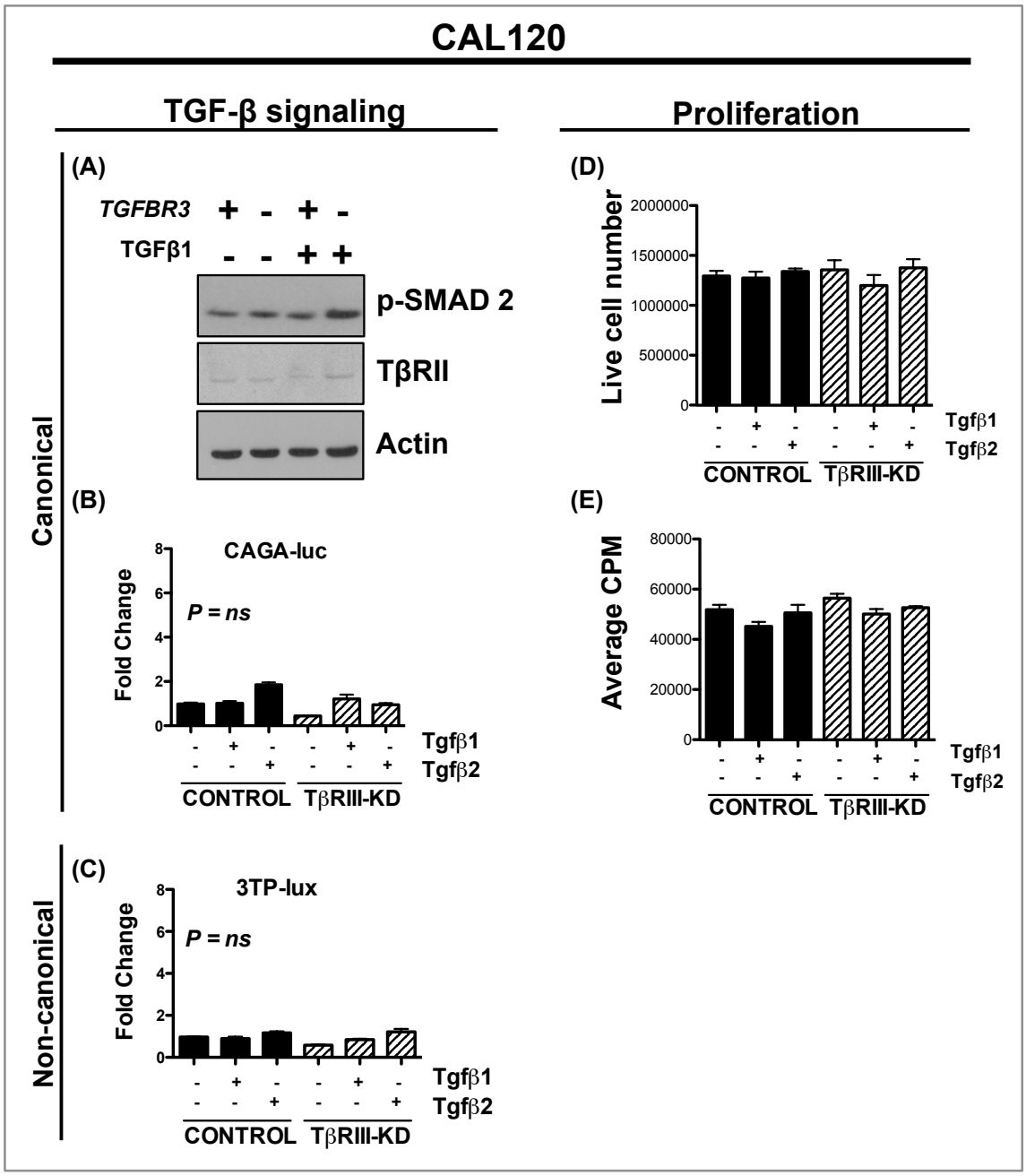

Figure 50. Abrogated TGF-β signaling in CAL120 TNBC cell line.

Figure 50. Abrogated TGF-β signaling in CAL120 TNBC cell line

A, Immunoblot analysis for phospho-SMAD2, TβRII and actin using protein harvested from CAL120 cells ± *TGFBR3* in presence or absence of TGF-β1 ligand. **B,** controls and TβRIII-KD CAL120 cells were co-transfected with CAGA-Luc and pRL-CMV renilla (used as internal control to correct for transfection efficiency). Eighteen hours post transfection cells were treated for 24hrs with 1ng/ml of TGF-β1 and TGF-β2. Cells were then collected and tested for promoter specific luciferase activity using a dual-luciferase reporter assay system was. Bar graph data represents mean of 4 replicates with SEM error bars (ns = not significant; for a two-tail Student *t*-test). **C,** controls and TβRIII-KD CAL120 cells were co-transfected with 3TP-lux and pRL-CMV renilla (used as internal control to correct for transfection efficiency). 18hrs post transfection cells were treated for 24hrs with 1ng/ml of TGF-β1 and TGF-β2. Cells were then collected and tested for promoter specific luciferase activity using a dual-luciferase reporter assay system was. Bar graph data represents mean of 4 replicates with SEM error bars (ns = not significant; for a two-tail Student *t*-test). **D,** Live cell count proliferation assay for CAL120 controls versus TβRIII-KD 72hrs post treatment with TGF-β1 and TGF-β2 ligands; graph bars represent the mean of 6 replicates with SEM error bars (ns = not significant; for a two-tail Student *t*-test). **E,** thymidine incorporation proliferation assay for CAL120 controls versus TβRIII-KD in presence or absence of TGF-β1 and TGF-β2 ligands; graph bars represent the mean of 6 replicates with SEM error bars (ns = not significant; for a two-tail Student *t*-test).

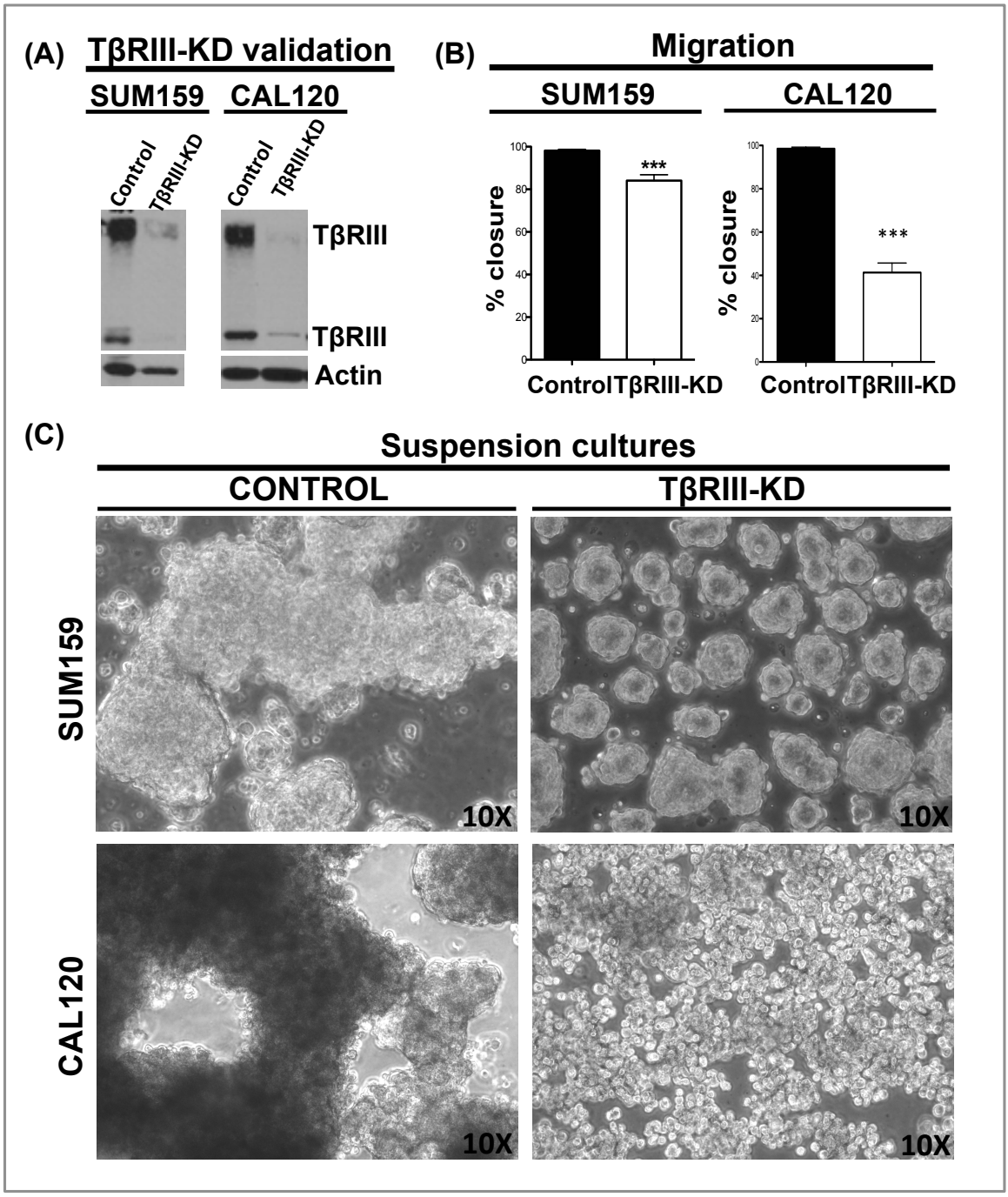

Figure 51. TβRIII functions independently of TGF-β signaling.

Figure 51. TβRIII functions independently of TGF-β signaling

A, immunoblot analysis of TβRIII protein expression in lysates harvested from SUM159 and CAL120 cells stably expressing control and TβRIII shRNA vector (TβRIII-KD). **B,** SUM159 and CAL120 cells were plated around magnetic stencils. After cells had adhered the magnetic stencils were removed and migration assay was monitored for 24hrs. Bar graphs represent percentages of closure for each cell line with TβRIII-KD in comparison to control; graph bars represent the mean of 3 replicates with SEM error bars (***P* = 0.001, ****P* < 0.0001 for a two-tail Student *t*-test). **C,** cell suspension assay where 12 well plates were layered with agarose gel to prevent cell adhesion. SUM159 and CAL120 cells were then plated on top of agarose gel. Representative 10x images of controls and TβRIII-KD were taken 48hr post cell plating.

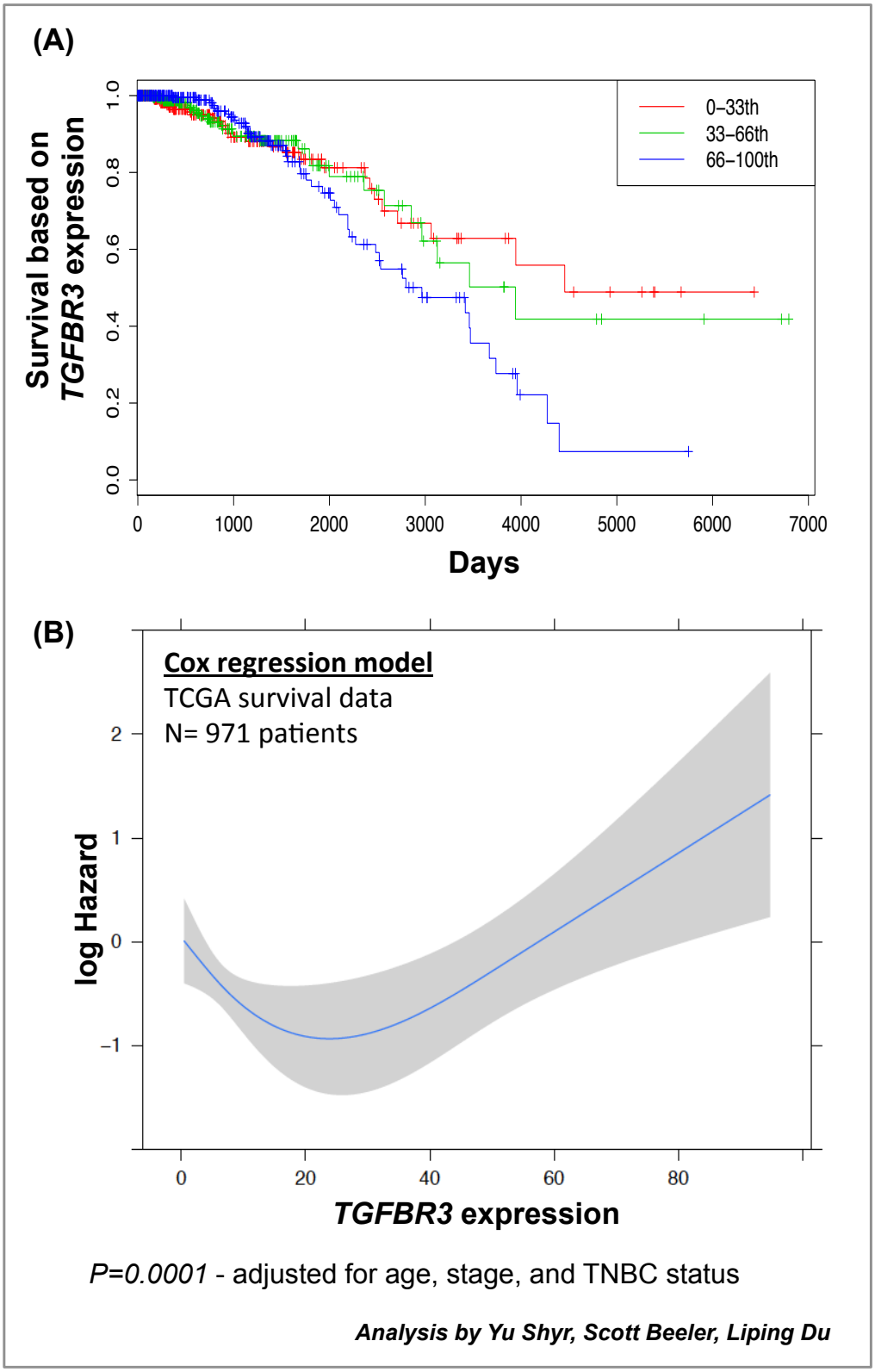

Figure 52. High expression of *TGFBR3* is associated with poorer survival in TCGA breast cancer cohort

Figure 52. **High expression of *TGFBR3* is associated with poorer survival in TCGA breast cancer cohort.**

A, Survival plot analysis for 971 Cancer Genome Atlas breast cancer patients with low (red line), medium (green line) and high *TGFBR3* expression levels (blue line) demonstrating trend of poorer survival in breast cancer patients with high *TGFBR3* expression (blue line). **B,** Cox regression model analysis for 971 Cancer Genome Atlas breast cancer patients adjusted for age, tumor stage and TNBC status. Log hazard increases with higher *TGFBR3* expression levels (****P* = 0.0001)

There is clear evidence and commonly held acceptance in favor of the addition of taxanes in the neoadjuvant setting for triple negative disease (Bear*, et al*, 2006) (Smith*, et al*, 2002) (Chakravarthy*, et al*, 2006). Interestingly, we now have preclinical evidence that doxorubicin and taxol treatment of MSL cells lacking TβRIII result in higher sensitivity, thus more cell death (Figure 53). Further studies would need to be performed in the future to follow up on this intriguing finding. However, the current data would indicate that combination therapy consisting of targeting TβRIII alongside with chemotherapy treatment might be beneficial for the MSL TNBC subset. This is an exciting idea as Chapter IV data (Figure 33) suggests that within the TNBC clinical trial, patients with mesenchymal-like genomic signatures fall into the non-responder categories. This reinforces the need for better-targeted therapy for this subtype, making TGF-β signaling axis more attractive candidate for targeted therapy.

Women with metastatic TNBC survive three to five years (~30%) and despite aggressive chemotherapy the majority die of their disease (Bostrom*, et al*, 2009; Shin*, et al*, 2008; Tsutsui*, et al*, 2002; van de Rijn*, et al*, 2002; Viale*, et al*, 2009). Thus understanding the metastatic potential of TNBC is essential. Although we do not have data for TβRIII effects on metastasis, based on the migration and invasion data we can speculate that TβRIII could promote metastasis. This would require additional experiments involving a prolonged duration of the *in vivo* xenograft experiments.

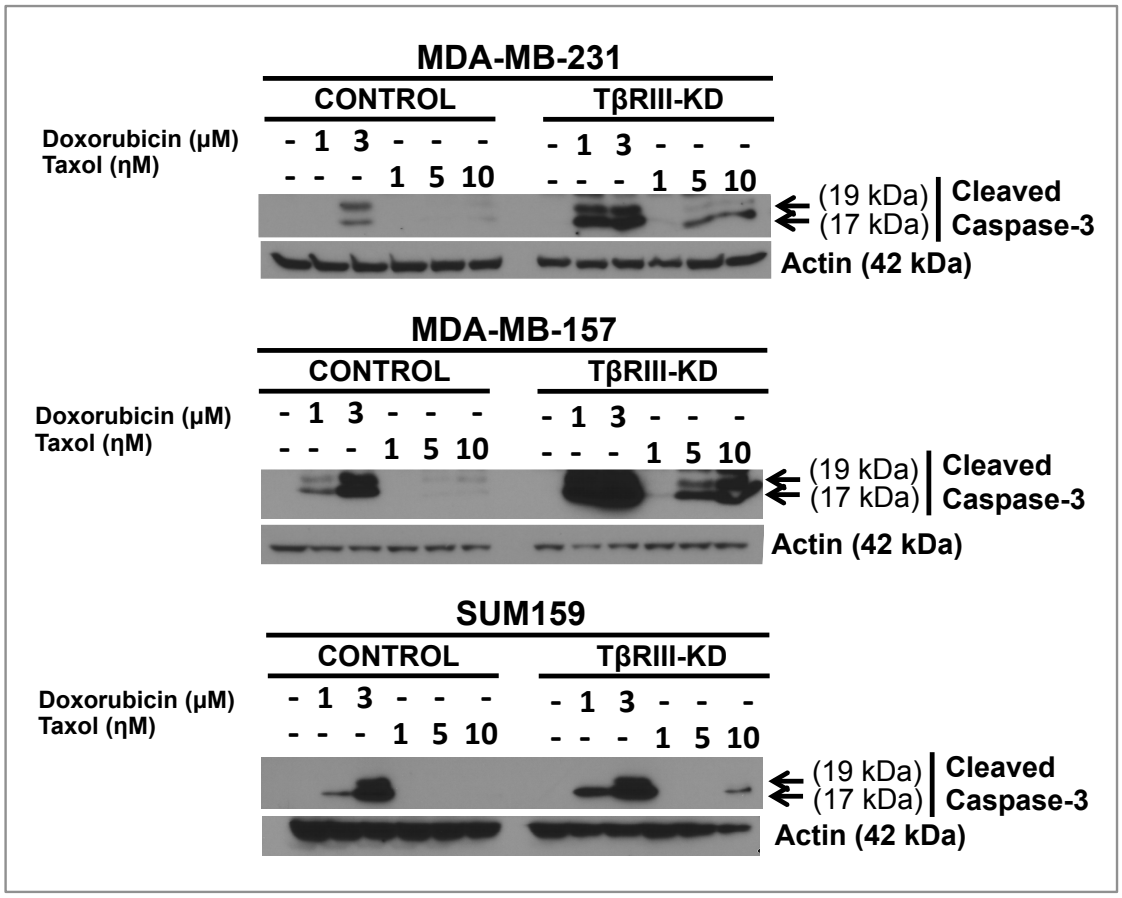

Figure 53. TβRIII-KD TNBC cells are more sensitive to chemotherapy treatments

Figure 53. TβRIII-KD TNBC cells are more sensitive to chemotherapy treatments

Controls and TβRIII-KDs MDA-MB-231, MDA-MB-157 and SUM159 MSL cell lines were treated at 70-80% confluency with individual chemotherapeutic drugs doxorubicin (1 and 3 μM) and paclitaxel (taxol, 1nM, 5nM and 10nM). Protein lysates were harvested at 48hr and immunoblot analysis performed for caspase-3, and actin. Results are representative of two independent experiments.

The majority of studies on breast development and cancer have focused on the epithelial cell component of the mammary gland. However, growing evidence shows that stromal components play an important role in modulating epithelial cell behavior (Bhowmick & Moses, 2005; Conklin & Keely, 2012). Recent studies indicate that the tumor microenvironment can modify a tumor cell's ability to recognize or respond to autocrine and paracrine signals. Thus, the surrounding microenvironment can have profound effects on tumor progression.

Currently, the study presented in Chapter V has not been completed, however interesting observations were made thus far among which we have observed that stromal gene expression has dramatically changed between controls and tumor-stroma indicating distinct gene expression based separation. However, at the present time, we do not have a full analysis of these changes. Thus future evaluations of genes and main pathways that are different between these two groups will be needed. At the moment we have only performed analyses for the TGF-β pathway.

Previously in our laboratory we have shown that abrogation of TGF-β signaling in stromal fibroblasts promotes tumorigenesis in adjacent epithelia (Bhowmick*, et al*, 2004a) increases production of chemokines, and thus promotes carcinoma growth and invasion (Cheng*, et al*, 2005; Cheng*, et al*, 2007). Little is known about the effect of stromal gene expression changes on the epithelial tumor progression in humans. Thus understanding the stromal gene expression changes could potentially help in finding new drug targets. Our goal

was to perform analysis of tumor stroma and determine if alteration of TGF-β signaling in fibroblasts contributes to progression of human breast cancer.

Our gene expression data, generated from tumor stromal cells collected by laser capture microdissection have provided some insight into TGF-β signaling. A loss of *TGFBR3* gene expression in peri-tumoral versus control stroma was the most consistent change among all the TGF-β pathway genes. Both qRT-PCR and immunohistochemistry validated our *TGFBR3* microarray findings, demonstrating a 44-fold decrease of *TGFBR3* expression in peri-tumoral stroma. Publicly available microarray datasets have further supported our observation of loss of *TGFBR3* in breast cancer stroma. Although this study has not been completed, interesting observations were made thus far and based on these preliminary findings, our future research goal is to determine the functional contribution of TβRIII in breast cancer stroma and evaluate its potential prognostic significance. To date TβRIII has been studied only in epithelial normal and cancer cells while currently nothing is known about the role of *TGFBR3* in the tumor microenvironment. Based on our preliminary data, our future direction we will be to determine the functional contribution of TβRIII to the breast tumor microenvironment. We will examine TβRIII signaling in the context of tumor-stroma (fibroblast) interactions and how TβRIII loss leads to tumor proliferation, motility, invasion and metastasis. We hypothesize that attenuation of TβRIII in human breast stroma leads to tumor progression through the alteration of paracrine signaling. Specifically, based on the data from Chapter III indicating that knockdown of TβRIII leads to increase in integrin-α2, it would be interesting

to evaluate integrin pathway within the stroma and determine if there is a similar relationship with TβRIII as what we see in the tumor. Investigating the function of TβRIII is vital to further our understanding of breast tumorigenesis. TβRIII is understudied and deserves attention considering that it might be a key player in the tumor microenvironment and a potential therapeutic target.

I anticipate that future direction for this part of thesis project will shed light on the role of TβRIII and the tumor microenvironment. Addressing the function of TβRIII in the tumor microenvironment could help us determine if the current data on TβRIII expression in tumors is actually context-dependent, meaning that in addition to the type of breast cancer we should consider that the behavior of the tumor cell is modified/regulated by stromal expression changes of TβRIII. This project will test the current paradigms not only in the field of TβRIII but also in the TGF-β and the TGF-β superfamily signaling pathways. Addressing the role of TβRIII is critical for further removing the barriers and moving forward the field of TGF-β in the tumor microenvironment. In summary, TβRIII has the potential to be a key player in the tumor microenvironment. Characterization of TβRIII's physiological function in tumor-stroma interactions, and its relationship to other key tumor-stromal molecular mediators, is an essential direction for providing an insight into the tumor microenvironment and determining novel options for diagnosis and cancer therapy. Understanding the contribution of stromal signaling to breast cancer initiation and progression will be necessary to target

both the cancer cells and the tumor microenvironment for effective treatment of this disease.

In addition to studying the role of TβRIII in tumor microenvironment a more comprehensive analysis will be performed on LCM tumor and its adjacent stroma. Considering that we currently have LCM data on both TNBC and non-TNBC patients it would be interesting to see whether tumor stroma separates according to its breast cancer type. The patient microarray gene expression data sets will enable us to determine gene signatures that may be translated in future studies and used for development of tests that could serve as a guide for more informed clinical decision-making. It is obvious that we are in need of new strategies that we can use either as a preventive measure or as a treatment of metastatic disease. Understanding the contribution of stromal signaling to breast cancer initiation and progression will be necessary to target both the cancer cells and the microenvironment for effective treatment of this disease.

The third part of this thesis was to determine if we can predict response to drug treatment based on genomic signatures of TNBC tumors. In this case we have utilized the recently completed a five year long TNBC clinical trial whose focus was to explore the pathologic complete response rate to cisplatin+paclitaxel ± RAD001 (mTOR inhibitor). The results of the trial were negative due to suboptimal dose of RAD001, however after exploring the genomic gene expression signatures, the major finding was the ability to predict clinical response. Furthermore, pathways that were significantly changed between responders and non-responders revolved around cell

cycle/proliferation and DNA damage response. Interesting, but not surprising, based on a previous study defining the diversity by TNBC subtype and differential *in vitro* drug response (Lehmann*, et al*, 2011), after making TNBC subtype calls we see that responders were more likely to align with basal-like subtypes while non-responders with mesenchymal-like and Luminal AR subtypes. This once again indicated to us the need for better alignment of treatment to TNBC. In addition to looking into genomics of TNBC epithelia, considering that we were also interested in role of tumor microenvironment, we performed genomic analysis on the matching tumor stroma. The result indicated that stroma was also able to segregate responders from non-responders thus predict response.

As this project is still ongoing, and considering that we do not have extensive numbers of TNBC patients with genomic data, it is still early to make solid conclusions. However, the genomic results thus far look very promising and will be further analyzed. Considering our finding presented in Chapter III revealing the importance of TGF-β signaling, specifically TβRIII, one of the follow up analysis should be further evaluation of this pathway/gene within the mesenchymal-like TNBC, which aligned with non-responders in our preliminary genomic analysis of the trial. Preliminary analysis of LCM tumors indicate that *TGFBR3* is increased in mesenchymal-like subtyped TNBCs from the trial (data not shown), however due to small number of mesenchymal-like patients evaluated statistical analysis are currently underpowered, thus proper conclusions cannot be made.

As this trial provides access to a cohort of 145 patients out of which 36% are patients with or without pathologic complete response, in the near future we will be performing RNA-seq analysis to evaluate inherent as well as acquired mutations within the residual disease tumor specimens. Furthermore, this clinical dataset will be beneficial for refining and validating gene signatures for TNBC subtyping. Follow up on discovered pathways would need to be performed via multistep validations (qRT-PCR, IHC, *in vitro* and *in vivo* drug tests on our TNBC subtyped cell lines). Overall, we would anticipate discovering novel subtype specific combination therapies for TNBC as well as gain better insight of pathway alterations that potentially lead to resistance, especially in the near-pCR patients. The overarching goal is to determine the more precise alignment of TNBC patients for future therapies.

In summary, this thesis is comprised of three parts dedicated to deciphering this highly heterogeneous disease, TNBC. The first approach was to further investigate the role of one of these newly defined TNBC's biological drivers – the TGF-β pathway. This pathway was demonstrated to be one of the upregulated drivers in mesenchymal (M) and mesenchymal-stem like (MSL) TNBC subtypes. Considering that TGF-β pathways can promote tumorigenesis and metastasis it was natural to pursue this pathway and evaluate its role in TNBC. The second approach in this thesis was to determine if we can predict response to drug treatment based on genomic signatures of TNBC tumors. In this case we have utilized the TNBC clinical trial whose focus was to explore the pathologic complete response rate for each individual treatment arm (cisplatin

± everolimus/mTOR inhibitor). Finally, using laser capture microdissection approach I was successful in not only collecting tumor epithelia but also its adjacent stroma. The goal was to look into the role of tumor microenvironment in TNBC in regard to the clinical response and decipher whether stroma aligns to the TNBC tumor subtypes and has unique driver pathways that might be contributing to the stroma state, thus feed into the aggressiveness of the tumor.

The cumulative results of this thesis provide insight into the TGF-β signaling axis within the TNBC MSL subtype implicating its prognostic and therapeutic utility in TNBC. It also indicates that within the clinical trial TNBC patients with MSL/M genomic signatures fall into the non-responder categories thus reinforcing the need for better-targeted therapy for this subtype, making TGF-β signaling axis more attractive candidate for targeted therapy. In addition to the ability of tumor epithelia genomic profile to predict response, we show that stroma can also predict the response of TNBC patients to chemotherapy. Combining these intriguing results helps identify new pieces for the TNBC puzzle, thus helping us make one step forward to better managing this disease.

REFERENCES

Abd El-Rehim, D. M., Ball, G., Pinder, S. E., Rakha, E., Paish, C., Robertson, J. F., Macmillan, D., Blamey, R. W. & Ellis, I. O. (2005). High-throughput protein expression analysis using tissue microarray technology of a large well-characterised series identifies biologically distinct classes of breast cancer confirming recent cDNA expression analyses. *Int J Cancer*, **116**, 340-350.

Abd El-Rehim, D. M., Pinder, S. E., Paish, C. E., Bell, J., Blamey, R. W., Robertson, J. F., Nicholson, R. I. & Ellis, I. O. (2004). Expression of luminal and basal cytokeratins in human breast carcinoma. *The Journal of pathology*, **203**, 661-671.

Adamo, B., Deal, A. M., Burrows, E., Geradts, J., Hamilton, E., Blackwell, K. L., Livasy, C., Fritchie, K., Prat, A., Harrell, J. C., Ewend, M. G., Carey, L. A., Miller, C. R. & Anders, C. K. (2011). Phosphatidylinositol 3-kinase pathway activation in breast cancer brain metastases. *Breast Cancer Res*, **13**, R125.

Akhurst, R. J. & Derynck, R. (2001). TGF-beta signaling in cancer--a double-edged sword. *Trends Cell Biol*, **11**, S44-51.

Alba, E., Calvo, L., Albanell, J., De la Haba, J. R., Arcusa Lanza, A., Chacon, J. I., Sanchez-Rovira, P., Plazaola, A., Lopez Garcia-Asenjo, J. A., Bermejo, B., Carrasco, E. & Lluch, A. (2012). Chemotherapy (CT) and hormonotherapy (HT) as neoadjuvant treatment in luminal breast cancer patients: results from the GEICAM/2006-03, a multicenter, randomized, phase-II study. *Ann Oncol*, **23**, 3069-3074.

Andre, F., Bachelot, T., Campone, M., Dalenc, F., Perez-Garcia, J. M., Hurvitz, S. A., Turner, N., Rugo, H., Smith, J. W., Deudon, S., Shi, M., Zhang, Y., Kay, A., Porta, D. G., Yovine, A. & Baselga, J. (2013). Targeting FGFR with dovitinib (TKI258): preclinical and clinical data in breast cancer. *Clin Cancer Res*, **19**, 3693-3702.

Andres, J. L., DeFalcis, D., Noda, M. & Massague, J. (1992). Binding of two growth factor families to separate domains of the proteoglycan betaglycan. *J Biol Chem*, **267**, 5927-5930.

Andres, J. L., Ronnstrand, L., Cheifetz, S. & Massague, J. (1991). Purification of the transforming growth factor-beta (TGF-beta) binding proteoglycan betaglycan. *J Biol Chem*, **266**, 23282-23287.

Andres, J. L., Stanley, K., Cheifetz, S. & Massague, J. (1989). Membrane-anchored and soluble forms of betaglycan, a polymorphic proteoglycan that binds transforming growth factor-beta. *J Cell Biol*, **109**, 3137-3145.

Ashby, W. J., Wikswo, J. P. & Zijlstra, A. (2012). Magnetically attachable stencils and the non-destructive analysis of the contribution made by the underlying matrix to cell migration. *Biomaterials*, **33**, 8189-8203.

Bader, A. G., Kang, S., Zhao, L. & Vogt, P. K. (2005). Oncogenic PI3K deregulates transcription and translation. *Nat Rev Cancer*, **5**, 921-929.

Barbieri, C. E., Perez, C. A., Johnson, K. N., Ely, K. A., Billheimer, D. & Pietenpol, J. A. (2005). IGFBP-3 is a direct target of transcriptional regulation by DeltaNp63alpha in squamous epithelium. *Cancer Res*, **65**, 2314-2320.

Barbieri, C. E. & Pietenpol, J. A. (2006). p63 and epithelial biology. *Exp Cell Res*, **312**, 695-706.

Barbieri, C. E., Tang, L. J., Brown, K. A. & Pietenpol, J. A. (2006). Loss of p63 leads to increased cell migration and up-regulation of genes involved in invasion and metastasis. *Cancer Res*, **66**, 7589-7597.

Baselga, J. (2011). Targeting the phosphoinositide-3 (PI3) kinase pathway in breast cancer. *Oncologist*, **16 Suppl 1**, 12-19.

Baselga, J., Gomez, P., Greil, R., Braga, S., Climent, M. A., Wardley, A. M., Kaufman, B., Stemmer, S. M., Pego, A., Chan, A., Goeminne, J. C., Graas, M. P., Kennedy, M. J., Ciruelos Gil, E. M., Schneeweiss, A., Zubel, A., Groos, J., Melezinkova, H. & Awada, A. (2013). Randomized phase II study of the anti-epidermal growth factor receptor monoclonal

antibody cetuximab with cisplatin versus cisplatin alone in patients with metastatic triple-negative breast cancer. *J Clin Oncol*, **31**, 2586-2592.

Baselga, J., Roché, H., Costa, F., Getúlio Martins Segalla, J., Pinczowski, H., Ma Ciruelos, E., Cabral Filho, S., Gómez, P., Van Eyll, B. & al, e. (2009). SOLTI-0701: A Multinational Double-Blind, Randomized Phase 2b Study Evaluating the Efficacy and Safety of Sorafenib Compared to Placebo When Administered in Combination with Capecitabine in Patients with Locally Advanced or Metastatic Breast Cancer (BC). *Cancer research*, **69**.

Bastien, R. R., Rodriguez-Lescure, A., Ebbert, M. T., Prat, A., Munarriz, B., Rowe, L., Miller, P., Ruiz-Borrego, M., Anderson, D., Lyons, B., Alvarez, I., Dowell, T., Wall, D., Segui, M. A., Barley, L., Boucher, K. M., Alba, E., Pappas, L., Davis, C. A., Aranda, I., Fauron, C., Stijleman, I. J., Palacios, J., Anton, A., Carrasco, E., Caballero, R., Ellis, M. J., Nielsen, T. O., Perou, C. M., Astill, M., Bernard, P. S. & Martin, M. (2012). PAM50 breast cancer subtyping by RT-qPCR and concordance with standard clinical molecular markers. *BMC Med Genomics*, **5**, 44.

Bauer, K. R., Brown, M., Cress, R. D., Parise, C. A. & Caggiano, V. (2007). Descriptive analysis of estrogen receptor (ER)-negative, progesterone receptor (PR)-negative, and HER2-negative invasive breast cancer, the so-called triple-negative phenotype: a population-based study from the California cancer Registry. *Cancer*, **109**, 1721-1728.

Bear, H. D., Anderson, S., Brown, A., Smith, R., Mamounas, E. P., Fisher, B., Margolese, R., Theoret, H., Soran, A., Wickerham, D. L. & Wolmark, N. (2003). The effect on tumor response of adding sequential preoperative docetaxel to preoperative doxorubicin and cyclophosphamide: preliminary results from National Surgical Adjuvant Breast and Bowel Project Protocol B-27. *J Clin Oncol*, **21**, 4165-4174.

Bear, H. D., Anderson, S., Smith, R. E., Geyer, C. E., Jr., Mamounas, E. P., Fisher, B., Brown, A. M., Robidoux, A., Margolese, R., Kahlenberg, M. S., Paik, S., Soran, A., Wickerham, D. L. & Wolmark, N. (2006).

Sequential preoperative or postoperative docetaxel added to preoperative doxorubicin plus cyclophosphamide for operable breast cancer:National Surgical Adjuvant Breast and Bowel Project Protocol B-27. *J Clin Oncol*, **24**, 2019-2027.

Bernabeu, C., Lopez-Novoa, J. M. & Quintanilla, M. (2009). The emerging role of TGF-beta superfamily coreceptors in cancer. *Biochim Biophys Acta*, **1792**, 954-973.

Bernsdorf, M., Ingvar, C., Jorgensen, L., Tuxen, M. K., Jakobsen, E. H., Saetersdal, A., Kimper-Karl, M. L., Kroman, N., Balslev, E. & Ejlertsen, B. (2011). Effect of adding gefitinib to neoadjuvant chemotherapy in estrogen receptor negative early breast cancer in a randomized phase II trial. *Breast Cancer Res Treat*, **126**, 463-470.

Bertucci, F., Finetti, P., Cervera, N., Esterni, B., Hermitte, F., Viens, P. & Birnbaum, D. (2008). How basal are triple-negative breast cancers? *Int J Cancer*, **123**, 236-240.

Bhowmick, N. & Moses, H. (2005). Tumor-stroma interactions. *Current opinion in genetics & development*, **15**, 97-101.

Bhowmick, N., Neilson, E. & Moses, H. (2004a). Stromal fibroblasts in cancer initiation and progression. *Nature*, **432**, 332-337.

Bhowmick, N. A., Chytil, A., Plieth, D., Gorska, A. E., Dumont, N., Shappell, S., Washington, M. K., Neilson, E. G. & Moses, H. L. (2004b). TGF-beta signaling in fibroblasts modulates the oncogenic potential of adjacent epithelia. *Science (New York, NY)*, **303**, 848-851.

Bierie, B., Chung, C. H., Parker, J. S., Stover, D. G., Cheng, N., Chytil, A., Aakre, M., Shyr, Y. & Moses, H. L. (2009). Abrogation of TGF-beta signaling enhances chemokine production and correlates with prognosis in human breast cancer. *J Clin Invest*, **119**, 1571-1582.

Bierie, B. & Moses, H. L. (2006a). TGF-beta and cancer. *Cytokine Growth Factor Rev*, **17**, 29-40.

Bierie, B. & Moses, H. L. (2006b). Tumour microenvironment: TGFbeta: the molecular Jekyll and Hyde of cancer. *Nat Rev Cancer*, **6**, 506-520.

Bierie, B., Stover, D. G., Abel, T. W., Chytil, A., Gorska, A. E., Aakre, M., Forrester, E., Yang, L., Wagner, K. U. & Moses, H. L. (2008). Transforming growth factor-beta regulates mammary carcinoma cell survival and interaction with the adjacent microenvironment. *Cancer Res*, **68**, 1809-1819.

Bissell, M. J., Radisky, D. C., Rizki, A., Weaver, V. M. & Petersen, O. W. (2002). The organizing principle: microenvironmental influences in the normal and malignant breast. *Differentiation*, **70**, 537-546.

Blobe, G. C., Liu, X., Fang, S. J., How, T. & Lodish, H. F. (2001a). A novel mechanism for regulating transforming growth factor beta (TGF-beta) signaling. Functional modulation of type III TGF-beta receptor expression through interaction with the PDZ domain protein, GIPC. *J Biol Chem*, **276**, 39608-39617.

Blobe, G. C., Schiemann, W. P., Pepin, M. C., Beauchemin, M., Moustakas, A., Lodish, H. F. & O'Connor-McCourt, M. D. (2001b). Functional roles for the cytoplasmic domain of the type III transforming growth factor beta receptor in regulating transforming growth factor beta signaling. *J Biol Chem*, **276**, 24627-24637.

Borresen-Dale, A. L. (2003). TP53 and breast cancer. *Hum Mutat*, **21**, 292-300.

Bostrom, P., Soderstrom, M., Palokangas, T., Vahlberg, T., Collan, Y., Carpen, O. & Hirsimaki, P. (2009). Analysis of cyclins A, B1, D1 and E in breast cancer in relation to tumour grade and other prognostic factors. *BMC Res Notes*, **2**, 140.

Boyd, N., Jensen, H., Cooke, G. & Han, H. (1992). Relationship between mammographic and histological risk factors for breast cancer. *JNCI Journal of the National Cancer Institute*, **84**, 1170.

Boyd, N., Rommens, J., Vogt, K., Lee, V., Hopper, J., Yaffe, M. & Paterson, A. (2005). Mammographic breast density as an intermediate phenotype for breast cancer. *Lancet Oncology*, **6**, 798-808.

Brown, K. A., Aakre, M. E., Gorska, A. E., Price, J. O., Eltom, S. E., Pietenpol, J. A. & Moses, H. L. (2004). Induction by transforming growth

factor-beta1 of epithelial to mesenchymal transition is a rare event in vitro. *Breast cancer research : BCR*, **6**, R215-231.

Brown, K. A., Pietenpol, J. A. & Moses, H. L. (2007). A tale of two proteins: differential roles and regulation of Smad2 and Smad3 in TGF-beta signaling. *Journal of cellular biochemistry*, **101**, 9-33.

Burstein, H. J., Elias, A. D., Rugo, H. S., Cobleigh, M. A., Wolff, A. C., Eisenberg, P. D., Lehman, M., Adams, B. J., Bello, C. L., DePrimo, S. E., Baum, C. M. & Miller, K. D. (2008). Phase II study of sunitinib malate, an oral multitargeted tyrosine kinase inhibitor, in patients with metastatic breast cancer previously treated with an anthracycline and a taxane. *J Clin Oncol*, **26**, 1810-1816.

Byrski, T., Gronwald, J., Huzarski, T., Grzybowska, E., Budryk, M., Stawicka, M., Mierzwa, T., Szwiec, M., Wisniowski, R., Siolek, M., Dent, R., Lubinski, J. & Narod, S. (2010). Pathologic complete response rates in young women with BRCA1-positive breast cancers after neoadjuvant chemotherapy. *J Clin Oncol*, **28**, 375-379.

Cameron, D., Brown, J., Dent, R., Jackisch, C., Mackey, J., Pivot, X., Steger, G. G., Suter, T. M., Toi, M., Parmar, M., Laeufle, R., Im, Y. H., Romieu, G., Harvey, V., Lipatov, O., Pienkowski, T., Cottu, P., Chan, A., Im, S. A., Hall, P. S., Bubuteishvili-Pacaud, L., Henschel, V., Deurloo, R. J., Pallaud, C. & Bell, R. (2013). Adjuvant bevacizumab-containing therapy in triple-negative breast cancer (BEATRICE): primary results of a randomised, phase 3 trial. *Lancet Oncol*, **14**, 933-942.

Carey, L., Winer, E., Viale, G., Cameron, D. & Gianni, L. (2010). Triple-negative breast cancer: disease entity or title of convenience? *Nat Rev Clin Oncol*, **7**, 683-692.

Carey, L. A., Dees, E. C., Sawyer, L., Gatti, L., Moore, D. T., Collichio, F., Ollila, D. W., Sartor, C. I., Graham, M. L. & Perou, C. M. (2007). The triple negative paradox: primary tumor chemosensitivity of breast cancer subtypes. *Clin Cancer Res*, **13**, 2329-2334.

Carey, L. A., Perou, C. M., Livasy, C. A., Dressler, L. G., Cowan, D., Conway, K., Karaca, G., Troester, M. A., Tse, C. K., Edmiston, S., Deming, S. L., Geradts, J., Cheang, M. C., Nielsen, T. O., Moorman, P. G., Earp, H. S. & Millikan, R. C. (2006). Race, breast cancer subtypes, and survival in the Carolina Breast Cancer Study. *JAMA*, **295**, 2492-2502.

Carey, L. A., Rugo, H. S., Marcom, P. K., Mayer, E. L., Esteva, F. J., Ma, C. X., Liu, M. C., Storniolo, A. M., Rimawi, M. F., Forero-Torres, A., Wolff, A. C., Hobday, T. J., Ivanova, A., Chiu, W. K., Ferraro, M., Burrows, E., Bernard, P. S., Hoadley, K. A., Perou, C. M. & Winer, E. P. (2012). TBCRC 001: randomized phase II study of cetuximab in combination with carboplatin in stage IV triple-negative breast cancer. *J Clin Oncol*, **30**, 2615-2623.

Chakravarthy, A. B., Kelley, M. C., McLaren, B., Truica, C. I., Billheimer, D., Mayer, I. A., Grau, A. M., Johnson, D. H., Simpson, J. F., Beauchamp, R. D., Jones, C. & Pietenpol, J. A. (2006). Neoadjuvant concurrent paclitaxel and radiation in stage II/III breast cancer. *Clin Cancer Res*, **12**, 1570-1576.

Cheang, M. C., Voduc, D., Bajdik, C., Leung, S., McKinney, S., Chia, S. K., Perou, C. M. & Nielsen, T. O. (2008). Basal-like breast cancer defined by five biomarkers has superior prognostic value than triple-negative phenotype. *Clin Cancer Res*, **14**, 1368-1376.

Cheifetz, S., Like, B. & Massague, J. (1986). Cellular distribution of type I and type II receptors for transforming growth factor-beta. *J Biol Chem*, **261**, 9972-9978.

Chen, Q., Lin, T. H., Der, C. J. & Juliano, R. L. (1996). Integrin-mediated activation of MEK and mitogen-activated protein kinase is independent of Ras. *The Journal of biological chemistry*, **271**, 18122-18127.

Chen, W., Kirkbride, K. C., How, T., Nelson, C. D., Mo, J., Frederick, J. P., Wang, X. F., Lefkowitz, R. J. & Blobe, G. C. (2003). Beta-arrestin 2 mediates endocytosis of type III TGF-beta receptor and down-regulation of its signaling. *Science*, **301**, 1394-1397.

Chen, X., Li, J., Gray, W. H., Lehmann, B. D., Bauer, J. A., Shyr, Y. & Pietenpol, J. A. (2012). TNBCtype: A Subtyping Tool for Triple-Negative Breast Cancer. *Cancer Inform*, **11**, 147-156.

Cheng, N., Bhowmick, N., Chytil, A., Gorksa, A., Brown, K., Muraoka, R., Arteaga, C., Neilson, E., Hayward, S. & Moses, H. (2005). Loss of TGF-β type II receptor in fibroblasts promotes mammary carcinoma growth and invasion through upregulation of TGF-α-, MSP-and HGF-mediated signaling networks. *Oncogene*, **24**, 5053-5068.

Cheng, N., Chytil, A., Shyr, Y., Joly, A. & Moses, H. L. (2007). Enhanced hepatocyte growth factor signaling by type II transforming growth factor-beta receptor knockout fibroblasts promotes mammary tumorigenesis. *Cancer research*, **67**, 4869-4877.

Choe, G., Horvath, S., Cloughesy, T. F., Crosby, K., Seligson, D., Palotie, A., Inge, L., Smith, B. L., Sawyers, C. L. & Mischel, P. S. (2003). Analysis of the phosphatidylinositol 3'-kinase signaling pathway in glioblastoma patients in vivo. *Cancer Res*, **63**, 2742-2746.

Chytil, A., Magnuson, M. A., Wright, C. V. & Moses, H. L. (2002). Conditional inactivation of the TGF-beta type II receptor using Cre:Lox. *Genesis*, **32**, 73-75.

Compton, L. A., Potash, D. A., Brown, C. B. & Barnett, J. V. (2007). Coronary vessel development is dependent on the type III transforming growth factor beta receptor. *Circulation research*, **101**, 784-791.

Conklin, M. W. & Keely, P. J. (2012). Why the stroma matters in breast cancer: insights into breast cancer patient outcomes through the examination of stromal biomarkers. *Cell Adh Migr*, **6**, 249-260.

Connolly, E. C., Freimuth, J. & Akhurst, R. J. (2012). Complexities of TGF-beta targeted cancer therapy. *Int J Biol Sci*, **8**, 964-978.

Copland, J. A., Luxon, B. A., Ajani, L., Maity, T., Campagnaro, E., Guo, H., LeGrand, S. N., Tamboli, P. & Wood, C. G. (2003). Genomic profiling identifies alterations in TGFbeta signaling through loss of TGFbeta

receptor expression in human renal cell carcinogenesis and progression. *Oncogene*, **22**, 8053-8062.

Courjal, F., Cuny, M., Simony-Lafontaine, J., Louason, G., Speiser, P., Zeillinger, R., Rodriguez, C. & Theillet, C. (1997). Mapping of DNA amplifications at 15 chromosomal localizations in 1875 breast tumors: definition of phenotypic groups. *Cancer Res*, **57**, 4360-4367.

Criswell, T., Dumont, N., Barnett, J. & Arteaga, C. (2008). Knockdown of the Transforming Growth Factor-{beta} Type III Receptor Impairs Motility and Invasion of Metastatic Cancer Cells. *Cancer research*, **68**, 7304.

Cui, W., Fowlis, D. J., Bryson, S., Duffie, E., Ireland, H., Balmain, A. & Akhurst, R. J. (1996). TGFbeta1 inhibits the formation of benign skin tumors, but enhances progression to invasive spindle carcinomas in transgenic mice. *Cell*, **86**, 531-542.

Davis, S. L., Eckhardt, S. G., Tentler, J. J. & Diamond, J. R. (2014). Triple-negative breast cancer: bridging the gap from cancer genomics to predictive biomarkers. *Ther Adv Med Oncol*, **6**, 88-100.

Dent, R., Trudeau, M., Pritchard, K. I., Hanna, W. M., Kahn, H. K., Sawka, C. A., Lickley, L. A., Rawlinson, E., Sun, P. & Narod, S. A. (2007). Triple-negative breast cancer: clinical features and patterns of recurrence. *Clin Cancer Res*, **13**, 4429-4434.

Deome, K. B., Faulkin, L. J., Jr., Bern, H. A. & Blair, P. B. (1959). Development of mammary tumors from hyperplastic alveolar nodules transplanted into gland-free mammary fat pads of female C3H mice. *Cancer Res*, **19**, 515-520.

Derynck, R., Lindquist, P. B., Lee, A., Wen, D., Tamm, J., Graycar, J. L., Rhee, L., Mason, A. J., Miller, D. A. & Coffey, R. J. (1988). A new type of transforming growth factor-beta, TGF-beta 3. *The EMBO journal*, **7**, 3737.

Derynck, R. & Zhang, Y. E. (2003). Smad-dependent and Smad-independent pathways in TGF-beta family signalling. *Nature*, **425**, 577-584.

Di Leo, A., Desmedt, C. & Bartlett, J. (2010). Final results of a meta-analysis testing HER2 and topoisomerase IIalpha genes as predictors of incremental benefit from anthracyclines in breast cancer. *J Clin Oncol*, **28**.

Djonov, V., Andres, A. C. & Ziemiecki, A. (2001). Vascular remodelling during the normal and malignant life cycle of the mammary gland. *Microscopy research and technique*, **52**, 182-189.

Dolle, J. M., Daling, J. R., White, E., Brinton, L. A., Doody, D. R., Porter, P. L. & Malone, K. E. (2009). Risk factors for triple-negative breast cancer in women under the age of 45 years. *Cancer Epidemiol Biomarkers Prev*, **18**, 1157-1166.

Dong, M., How, T., Kirkbride, K. C., Gordon, K. J., Lee, J. D., Hempel, N., Kelly, P., Moeller, B. J., Marks, J. R. & Blobe, G. C. (2007). The type III TGF-β receptor suppresses breast cancer progression. *The Journal of clinical investigation*, **117**, 206-217.

Edgar, R., Domrachev, M. & Lash, A. E. (2002). Gene Expression Omnibus: NCBI gene expression and hybridization array data repository. *Nucleic Acids Res*, **30**, 207-210.

Esparza-Lopez, J., Montiel, J. L., Vilchis-Landeros, M. M., Okadome, T., Miyazono, K. & Lopez-Casillas, F. (2001). Ligand binding and functional properties of betaglycan, a co-receptor of the transforming growth factor-beta superfamily. Specialized binding regions for transforming growth factor-beta and inhibin A. *J Biol Chem*, **276**, 14588-14596.

Farmer, H., McCabe, N., Lord, C. J., Tutt, A. N., Johnson, D. A., Richardson, T. B., Santarosa, M., Dillon, K. J., Hickson, I., Knights, C., Martin, N. M., Jackson, S. P., Smith, G. C. & Ashworth, A. (2005). Targeting the DNA repair defect in BRCA mutant cells as a therapeutic strategy. *Nature*, **434**, 917-921.

Feng, X. H. & Derynck, R. (2005). Specificity and versatility in tgf-beta signaling through Smads. *Annu Rev Cell Dev Biol*, **21**, 659-693.

Finak, G., Bertos, N., Pepin, F., Sadekova, S., Souleimanova, M., Zhao, H., Chen, H., Omeroglu, G., Meterissian, S., Omeroglu, A., Hallett, M. &

Park, M. (2008). Stromal gene expression predicts clinical outcome in breast cancer. *Nature medicine*, **14**, 518-527.

Finn, R. S., Gagnon, R., Di Leo, A., Press, M. F., Arbushites, M. & Koehler, M. (2009a). Prognostic and predictive value of HER2 extracellular domain in metastatic breast cancer treated with lapatinib and paclitaxel in a randomized phase III study. *J Clin Oncol*, **27**, 5552-5558.

Finn, R. S., Press, M. F., Dering, J., Arbushites, M., Koehler, M., Oliva, C., Williams, L. S. & Di Leo, A. (2009b). Estrogen receptor, progesterone receptor, human epidermal growth factor receptor 2 (HER2), and epidermal growth factor receptor expression and benefit from lapatinib in a randomized trial of paclitaxel with lapatinib or placebo as first-line treatment in HER2-negative or unknown metastatic breast cancer. *J Clin Oncol*, **27**, 3908-3915.

Fisher, B., Brown, A., Mamounas, E., Wieand, S., Robidoux, A., Margolese, R. G., Cruz, A. B., Jr., Fisher, E. R., Wickerham, D. L., Wolmark, N., DeCillis, A., Hoehn, J. L., Lees, A. W. & Dimitrov, N. V. (1997). Effect of preoperative chemotherapy on local-regional disease in women with operable breast cancer: findings from National Surgical Adjuvant Breast and Bowel Project B-18. *J Clin Oncol*, **15**, 2483-2493.

Fong, P. C., Boss, D. S., Yap, T. A., Tutt, A., Wu, P., Mergui-Roelvink, M., Mortimer, P., Swaisland, H., Lau, A., O'Connor, M. J., Ashworth, A., Carmichael, J., Kaye, S. B., Schellens, J. H. & de Bono, J. S. (2009). Inhibition of poly(ADP-ribose) polymerase in tumors from BRCA mutation carriers. *N Engl J Med*, **361**, 123-134.

Forrester, E., Chytil, A., Bierie, B., Aakre, M., Gorska, A. E., Sharif-Afshar, A.-R., Muller, W. J. & Moses, H. L. (2005). Effect of conditional knockout of the type II TGF-beta receptor gene in mammary epithelia on mammary gland development and polyomavirus middle T antigen induced tumor formation and metastasis. *Cancer research*, **65**, 2296-2302.

Foulkes, W. D., Stefansson, I. M., Chappuis, P. O., Begin, L. R., Goffin, J. R., Wong, N., Trudel, M. & Akslen, L. A. (2003). Germline BRCA1 mutations

and a basal epithelial phenotype in breast cancer. *J Natl Cancer Inst*, **95**, 1482-1485.

Gelmon, K. A., Tischkowitz, M., Mackay, H., Swenerton, K., Robidoux, A., Tonkin, K., Hirte, H., Huntsman, D., Clemons, M., Gilks, B., Yerushalmi, R., Macpherson, E., Carmichael, J. & Oza, A. (2011). Olaparib in patients with recurrent high-grade serous or poorly differentiated ovarian carcinoma or triple-negative breast cancer: a phase 2, multicentre, open-label, non-randomised study. *Lancet Oncol*, **12**, 852-861.

Gelsi-Boyer, V., Orsetti, B., Cervera, N., Finetti, P., Sircoulomb, F., Rouge, C., Lasorsa, L., Letessier, A., Ginestier, C., Monville, F., Esteyries, S., Adelaide, J., Esterni, B., Henry, C., Ethier, S. P., Bibeau, F., Mozziconacci, M. J., Charafe-Jauffret, E., Jacquemier, J., Bertucci, F., Birnbaum, D., Theillet, C. & Chaffanet, M. (2005). Comprehensive profiling of 8p11-12 amplification in breast cancer. *Mol Cancer Res*, **3**, 655-667.

Glading, A., Uberall, F., Keyse, S. M., Lauffenburger, D. A. & Wells, A. (2001). Membrane proximal ERK signaling is required for M-calpain activation downstream of epidermal growth factor receptor signaling. *The Journal of biological chemistry*, **276**, 23341-23348.

Gobbi, H., Arteaga, C. L., Jensen, R. A., Simpson, J. F., Dupont, W. D., Olson, S. J., Schuyler, P. A., Plummer, W. D. & Page, D. L. (2000). Loss of expression of transforming growth factor beta type II receptor correlates with high tumour grade in human breast in-situ and invasive carcinomas. *Histopathology*, **36**, 168-177.

Gobbi, H., Dupont, W. D., Simpson, J. F., Plummer, W. D., Jr., Schuyler, P. A., Olson, S. J., Arteaga, C. L. & Page, D. L. (1999). Transforming growth factor-beta and breast cancer risk in women with mammary epithelial hyperplasia. *J Natl Cancer Inst*, **91**, 2096-2101.

Goff, L., De Braud, F., Cohen, R. & al., e. (2012). Phase I study of PF-03446962, a fully human mAb against ALK 1, a TGFbeta receptor involved in tumor angiogenesis. *J Clin Oncol*, e13606.

Gomez, P., Roche, H., Costa, F. & al., e. (2010). Overall survival data from SOLTI-0701: a multinational, double-blind, placebo-controlled, randomized phase 2b studyevaluating the oral combination of sorafenib and capecitabine in patients with locally advanced or metastatic HER2-negative breast cancer. *Cancer Research*, **70**.

Gong, J. G., Costanzo, A., Yang, H. Q., Melino, G., Kaelin, W. G., Jr., Levrero, M. & Wang, J. Y. (1999). The tyrosine kinase c-Abl regulates p73 in apoptotic response to cisplatin-induced DNA damage. *Nature*, **399**, 806-809.

Gonzalez-Angulo, A. M., Timms, K. M., Liu, S., Chen, H., Litton, J. K., Potter, J., Lanchbury, J. S., Stemke-Hale, K., Hennessy, B. T., Arun, B. K., Hortobagyi, G. N., Do, K. A., Mills, G. B. & Meric-Bernstam, F. (2011). Incidence and outcome of BRCA mutations in unselected patients with triple receptor-negative breast cancer. *Clin Cancer Res*, **17**, 1082-1089.

Gordon, K. J., Dong, M., Chislock, E. M., Fields, T. A. & Blobe, G. C. (2008). Loss of type III transforming growth factor beta receptor expression increases motility and invasiveness associated with epithelial to mesenchymal transition during pancreatic cancer progression. *Carcinogenesis*, **29**, 252-262.

Gouon-Evans, V., Rothenberg, M. E. & Pollard, J. W. (2000). Postnatal mammary gland development requires macrophages and eosinophils. *Development (Cambridge, England)*, **127**, 2269-2282.

Gozgit, J. M., Wong, M. J., Moran, L., Wardwell, S., Mohemmad, Q. K., Narasimhan, N. I., Shakespeare, W. C., Wang, F., Clackson, T. & Rivera, V. M. (2012). Ponatinib (AP24534), a multitargeted pan-FGFR inhibitor with activity in multiple FGFR-amplified or mutated cancer models. *Mol Cancer Ther*, **11**, 690-699.

Graeser, M., McCarthy, A., Lord, C. J., Savage, K., Hills, M., Salter, J., Orr, N., Parton, M., Smith, I. E., Reis-Filho, J. S., Dowsett, M., Ashworth, A. & Turner, N. C. (2010). A marker of homologous recombination predicts pathologic complete response to neoadjuvant chemotherapy in primary breast cancer. *Clin Cancer Res*, **16**, 6159-6168.

Group, E. B. C. T. C. (2011). Relevance of breast cancer hormone receptors and other factors to the efficacy of adjuvant tamoxifen: patient-level meta-analysis of randomised trials. *Lancet*, **378**, 771-784.

Haffty, B. G., Yang, Q., Reiss, M., Kearney, T., Higgins, S. A., Weidhaas, J., Harris, L., Hait, W. & Toppmeyer, D. (2006). Locoregional relapse and distant metastasis in conservatively managed triple negative early-stage breast cancer. *Journal of Clinical Oncology*, **24**, 5652-5657.

Hau, P., Jachimczak, P., Schlingensiepen, R., Schulmeyer, F., Jauch, T., Steinbrecher, A., Brawanski, A., Proescholdt, M., Schlaier, J., Buchroithner, J., Pichler, J., Wurm, G., Mehdorn, M., Strege, R., Schuierer, G., Villarrubia, V., Fellner, F., Jansen, O., Straube, T., Nohria, V., Goldbrunner, M., Kunst, M., Schmaus, S., Stauder, G., Bogdahn, U. & Schlingensiepen, K. H. (2007). Inhibition of TGF-beta2 with AP 12009 in recurrent malignant gliomas: from preclinical to phase I/II studies. *Oligonucleotides*, **17**, 201-212.

Haugsten, E. M., Wiedlocha, A., Olsnes, S. & Wesche, J. (2010). Roles of fibroblast growth factor receptors in carcinogenesis. *Mol Cancer Res*, **8**, 1439-1452.

Hempel, N., How, T., Cooper, S. J., Green, T. R., Dong, M., Copland, J. A., Wood, C. G. & Blobe, G. C. (2008). Expression of the type III TGF-beta receptor is negatively regulated by TGF-beta. *Carcinogenesis*, **29**, 905-912.

Hempel, N., How, T., Dong, M., Murphy, S. K., Fields, T. A. & Blobe, G. C. (2007). Loss of betaglycan expression in ovarian cancer: role in motility and invasion. *Cancer Res*, **67**, 5231-5238.

Hennessy, B. T., Gonzalez-Angulo, A. M., Stemke-Hale, K., Gilcrease, M. Z., Krishnamurthy, S., Lee, J. S., Fridlyand, J., Sahin, A., Agarwal, R., Joy, C., Liu, W., Stivers, D., Baggerly, K., Carey, M., Lluch, A., Monteagudo, C., He, X., Weigman, V., Fan, C., Palazzo, J., Hortobagyi, G. N., Nolden, L. K., Wang, N. J., Valero, V., Gray, J. W., Perou, C. M. & Mills, G. B. (2009). Characterization of a naturally occurring breast cancer subset enriched in epithelial-to-mesenchymal transition and stem cell characteristics. *Cancer Res*, **69**, 4116-4124.

Huang, C., Jacobson, K. & Schaller, M. D. (2004). MAP kinases and cell migration. *J Cell Sci*, **117**, 4619-4628.

Hudis, C., Tauer, K., Hermann, R. & al, e. (2011). Sorafenib (SOR) plus chemotherapy (CRx) for patients (pts) with advanced (adv) breast cancer (BC) previously treated with bevacizumab (BEV). *J Clin Oncol*, **27**.

Huober, J., von Minckwitz, G., Denkert, C., Tesch, H., Weiss, E., Zahm, D. M., Belau, A., Khandan, F., Hauschild, M., Thomssen, C., Hogel, B., Darb-Esfahani, S., Mehta, K. & Loibl, S. (2010). Effect of neoadjuvant anthracycline-taxane-based chemotherapy in different biological breast cancer phenotypes: overall results from the GeparTrio study. *Breast Cancer Res Treat*, **124**, 133-140.

Inwald, E. C., Klinkhammer-Schalke, M., Hofstadter, F., Zeman, F., Koller, M., Gerstenhauer, M. & Ortmann, O. (2013). Ki-67 is a prognostic parameter in breast cancer patients: results of a large population-based cohort of a cancer registry. *Breast Cancer Res Treat*, **139**, 539-552.

Itoh, S. & ten Dijke, P. (2007). Negative regulation of TGF-beta receptor/Smad signal transduction. *Curr Opin Cell Biol*, **19**, 176-184.

Iyengar, P., Combs, T., Shah, S., Gouon-Evans, V., Pollard, J., Albanese, C., Flanagan, L., Tenniswood, M., Guha, C. & Lisanti, M. (2003). Adipocyte-secreted factors synergistically promote mammary tumorigenesis through induction of anti-apoptotic transcriptional programs and proto-oncogene stabilization. *Oncogene*, **22**, 6408-6423.

Jelinek, D. F., Tschumper, R. C., Stolovitzky, G. A., Iturria, S. J., Tu, Y., Lepre, J., Shah, N. & Kay, N. E. (2003). Identification of a global gene expression signature of B-chronic lymphocytic leukemia. *Mol Cancer Res*, **1**, 346-361.

Johnson, N., Li, Y. C., Walton, Z. E., Cheng, K. A., Li, D., Rodig, S. J., Moreau, L. A., Unitt, C., Bronson, R. T., Thomas, H. D., Newell, D. R., D'Andrea, A. D., Curtin, N. J., Wong, K. K. & Shapiro, G. I. (2011). Compromised CDK1 activity sensitizes BRCA-proficient cancers to PARP inhibition. *Nat Med*, **17**, 875-882.

Jones, C., Ford, E., Gillett, C., Ryder, K., Merrett, S., Reis-Filho, J. S., Fulford, L. G., Hanby, A. & Lakhani, S. R. (2004). Molecular cytogenetic identification of subgroups of grade III invasive ductal breast carcinomas with different clinical outcomes. *Clinical cancer research : an official journal of the American Association for Cancer Research*, **10**, 5988-5997.

Jovanovic B & HL., M. Expression data from TGFBR3 controls and TGFBR3 knockdown SUM159 3D cultures.

Jovanovic, B., Beeler, J., Pickup, M., Chytil, A., Gorska, A., Ashby, W., Lehmann, B., Zijlstra, A., Pietenpol, J. & Moses, H. (2014a). Tumor growth factor beta type III receptor is tumor promoter in triple negative breast cancer. *Breast Cancer Research*

Jovanovic, B., Beeler, J., Pickup, M., Chytil, A., Gorska, A. E., Ashby, W., Lehmann, B., Zijlstra, A., Pietenpol, J. A. & Moses, H. (2014b). Transforming growth factor beta receptor type III is a tumor promoter in mesenchymal-stem like triple negative breast cancer. *Breast Cancer Research*, **16**, R69.

Kalluri, R. & Zeisberg, M. (2006). Fibroblasts in cancer. *Nature reviews Cancer*, **6**, 392-401.

Karnoub, A. E., Dash, A. B., Vo, A. P., Sullivan, A., Brooks, M. W., Bell, G. W., Richardson, A. L., Polyak, K., Tubo, R. & Weinberg, R. A. (2007). Mesenchymal stem cells within tumour stroma promote breast cancer metastasis. *Nature*, **449**, 557-563.

Kaufmann, M., von Minckwitz, G., Smith, R., Valero, V., Gianni, L., Eiermann, W., Howell, A., Costa, S. D., Beuzeboc, P., Untch, M., Blohmer, J. U., Sinn, H. P., Sittek, R., Souchon, R., Tulusan, A. H., Volm, T. & Senn, H. J. (2003). International expert panel on the use of primary (preoperative) systemic treatment of operable breast cancer: review and recommendations. *J Clin Oncol*, **21**, 2600-2608.

Keeton, M. R., Curriden, S. A., van Zonneveld, A. J. & Loskutoff, D. J. (1991). Identification of regulatory sequences in the type 1 plasminogen activator inhibitor gene responsive to transforming growth factor beta. *J Biol Chem*, **266**, 23048-23052.

Kimbung, S., Biskup, E., Johansson, I., Aaltonen, K., Ottosson-Wadlund, A., Gruvberger-Saal, S., Cunliffe, H., Fadeel, B., Loman, N., Berglund, P. & Hedenfalk, I. (2012). Co-targeting of the PI3K pathway improves the response of BRCA1 deficient breast cancer cells to PARP1 inhibition. *Cancer Lett*, **319**, 232-241.

Kirkbride, K. C., Townsend, T. A., Bruinsma, M. W., Barnett, J. V. & Blobe, G. C. (2008). Bone morphogenetic proteins signal through the transforming growth factor-beta type III receptor. *J Biol Chem*, **283**, 7628-7637.

Knelson, E. H., Gaviglio, A. L., Tewari, A. K., Armstrong, M. B., Mythreye, K. & Blobe, G. C. (2013). Type III TGF-beta receptor promotes FGF2-mediated neuronal differentiation in neuroblastoma. *J Clin Invest*, **123**, 4786-4798.

Korse, C. M., Taal, B. G., Vincent, A., van Velthuysen, M. L., Baas, P., Buning-Kager, J. C., Linders, T. C. & Bonfrer, J. M. (2012). Choice of tumour markers in patients with neuroendocrine tumours is dependent on the histological grade. A marker study of Chromogranin A, Neuron specific enolase, Progastrin-releasing peptide and cytokeratin fragments. *Eur J Cancer*, **48**, 662-671.

Kreike, B., van Kouwenhove, M., Horlings, H., Weigelt, B., Peterse, H., Bartelink, H. & van de Vijver, M. J. (2007). Gene expression profiling

and histopathological characterization of triple-negative/basal-like breast carcinomas. *Breast cancer research : BCR*, **9**, R65.

Kruijf, E. M., Nes, J. G. H., Velde, C. J. H., Putter, H., Smit, V. T. H. B. M., Liefers, G. J., Kuppen, P. J. K., Tollenaar, R. A. E. M. & Mesker, W. E. (2010). Tumor–stroma ratio in the primary tumor is a prognostic factor in early breast cancer patients, especially in triple-negative carcinoma patients. *Breast cancer research and treatment*, 1-10.

Kuperwasser, C., Chavarria, T., Wu, M., Magrane, G., Gray, J. W., Carey, L., Richardson, A. & Weinberg, R. A. (2004). Reconstruction of functionally normal and malignant human breast tissues in mice. *Proceedings of the National Academy of Sciences of the United States of America*, **101**, 4966-4971.

Kusanagi, K., Inoue, H., Ishidou, Y., Mishima, H. K., Kawabata, M. & Miyazono, K. (2000). Characterization of a bone morphogenetic protein-responsive Smad-binding element. *Mol Biol Cell*, **11**, 555-565.

Kwan, K., Kyung, H., Tae RK, Yong SC, Tae HL & KP, H. (2014). Ki-67 as a Predictor of Response to Neoadjuvant Chemotherapy in Breast Cancer Patients. *J Breast Cancer*, **17**, 40-46.

Kwan, M. L., Kushi, L. H., Weltzien, E., Maring, B., Kutner, S. E., Fulton, R. S., Lee, M. M., Ambrosone, C. B. & Caan, B. J. (2009). Epidemiology of breast cancer subtypes in two prospective cohort studies of breast cancer survivors. *Breast Cancer Res*, **11**, R31.

Lampropoulos, P., Zizi-Sermpetzoglou, A., Rizos, S., Kostakis, A., Nikiteas, N. & Papavassiliou, A. G. (2012). TGF-beta signalling in colon carcinogenesis. *Cancer Lett*, **314**, 1-7.

Lee, J. D., Hempel, N., Lee, N. Y. & Blobe, G. C. (2010). The type III TGF- receptor suppresses breast cancer progression through GIPC-mediated inhibition of TGF- signaling. *Carcinogenesis*, **31**, 175-183.

Lehmann, B. D., Bauer, J. A., Chen, X., Sanders, M. E., Chakravarthy, A. B., Shyr, Y. & Pietenpol, J. A. (2011). Identification of human triple-negative

breast cancer subtypes and preclinical models for selection of targeted therapies. *J Clin Invest*, **121**, 2750-2767.

Lehmann, B. D. & Pietenpol, J. A. (2014). Identification and use of biomarkers in treatment strategies for triple-negative breast cancer subtypes. *J Pathol*, **232**, 142-150.

Leong, C. O., Vidnovic, N., DeYoung, M. P., Sgroi, D. & Ellisen, L. W. (2007). The p63/p73 network mediates chemosensitivity to cisplatin in a biologically defined subset of primary breast cancers. *J Clin Invest*, **117**, 1370-1380.

Liedtke, C., Mazouni, C., Hess, K. R., Andre, F., Tordai, A., Mejia, J. A., Symmans, W. F., Gonzalez-Angulo, A. M., Hennessy, B., Green, M., Cristofanilli, M., Hortobagyi, G. N. & Pusztai, L. (2008). Response to neoadjuvant therapy and long-term survival in patients with triple-negative breast cancer. *J Clin Oncol*, **26**, 1275-1281.

Lin, K. W., Nam, S. Y., Toh, W. H., Dulloo, I. & Sabapathy, K. (2004). Multiple stress signals induce p73beta accumulation. *Neoplasia*, **6**, 546-557.

Liu, J., Kuulasmaa, T., Kosma, V. M., Butzow, R., Vanttinen, T., Hyden-Granskog, C. & Voutilainen, R. (2003). Expression of betaglycan, an inhibin coreceptor, in normal human ovaries and ovarian sex cord-stromal tumors and its regulation in cultured human granulosa-luteal cells. *J Clin Endocrinol Metab*, **88**, 5002-5008.

Livak, K. J. & Schmittgen, T. D. (2001). Analysis of relative gene expression data using real-time quantitative PCR and the 2(-Delta Delta C(T)) Method. *Methods*, **25**, 402-408.

Lopez-Casillas, F., Cheifetz, S., Doody, J., Andres, J. L., Lane, W. S. & Massague, J. (1991). Structure and expression of the membrane proteoglycan betaglycan, a component of the TGF-beta receptor system. *Cell*, **67**, 785-795.

López-Casillas, F., Payne, H. M., Andres, J. L. & Massagué, J. (1994). Betaglycan can act as a dual modulator of TGF-beta access to signaling

receptors: mapping of ligand binding and GAG attachment sites. *The Journal of cell biology*, **124**, 557-568.

Lopez-Casillas, F., Wrana, J. L. & Massague, J. (1993). Betaglycan presents ligand to the TGF beta signaling receptor. *Cell*, **73**, 1435-1444.

Lopez-Knowles, E., O'Toole, S. A., McNeil, C. M., Millar, E. K., Qiu, M. R., Crea, P., Daly, R. J., Musgrove, E. A. & Sutherland, R. L. (2010). PI3K pathway activation in breast cancer is associated with the basal-like phenotype and cancer-specific mortality. *Int J Cancer*, **126**, 1121-1131.

Lord, C. J., Garrett, M. D. & Ashworth, A. (2006). Targeting the double-strand DNA break repair pathway as a therapeutic strategy. *Clin Cancer Res*, **12**, 4463-4468.

Lu, P., Weaver, V. M. & Werb, Z. (2012). The extracellular matrix: a dynamic niche in cancer progression. *J Cell Biol*, **196**, 395-406.

Lund, M. J., Trivers, K. F., Porter, P. L., Coates, R. J., Leyland-Jones, B., Brawley, O. W., Flagg, E. W., O'Regan, R. M., Gabram, S. G. A. & Eley, J. W. (2009). Race and triple negative threats to breast cancer survival: a population-based study in Atlanta, GA. *Breast cancer research and treatment*, **113**, 357-370.

Ma, X.-J., Dahiya, S., Richardson, E., Erlander, M. & Sgroi, D. C. (2009). Gene expression profiling of the tumor microenvironment during breast cancer progression. *Breast cancer research : BCR*, **11**, R7.

Mabuchi, S., Altomare, D. A., Cheung, M., Zhang, L., Poulikakos, P. I., Hensley, H. H., Schilder, R. J., Ozols, R. F. & Testa, J. R. (2007). RAD001 inhibits human ovarian cancer cell proliferation, enhances cisplatin-induced apoptosis, and prolongs survival in an ovarian cancer model. *Clin Cancer Res*, **13**, 4261-4270.

Marty, B., Maire, V., Gravier, E., Rigaill, G., Vincent-Salomon, A., Kappler, M., Lebigot, I., Djelti, F., Tourdes, A., Gestraud, P., Hupe, P., Barillot, E., Cruzalegui, F., Tucker, G. C., Stern, M. H., Thiery, J. P., Hickman, J. A. & Dubois, T. (2008). Frequent PTEN genomic alterations and

activated phosphatidylinositol 3-kinase pathway in basal-like breast cancer cells. *Breast Cancer Res*, **10**, R101.

Massague, J. (1985). Transforming growth factor-beta modulates the high-affinity receptors for epidermal growth factor and transforming growth factor-alpha. *J Cell Biol*, **100**, 1508-1514.

Massague, J. (2008). TGFbeta in Cancer. *Cell*, **134**, 215-230.

Massagué, J. (2012). TGFβ signalling in context. *Nature Reviews Molecular Cell Biology*, **13**, 616-630.

Massague, J. & Like, B. (1985). Cellular receptors for type beta transforming growth factor. Ligand binding and affinity labeling in human and rodent cell lines. *J Biol Chem*, **260**, 2636-2645.

Masuda, H., Baggerly, K. A., Wang, Y., Zhang, Y., Gonzalez-Angulo, A. M., Meric-Bernstam, F., Valero, V., Lehmann, B. D., Pietenpol, J. A., Hortobagyi, G. N., Symmans, W. F. & Ueno, N. T. (2013). Differential response to neoadjuvant chemotherapy among 7 triple-negative breast cancer molecular subtypes. *Clin Cancer Res*, **19**, 5533-5540.

Matos, I., Dufloth, R., Alvarenga, M., Zeferino, L. C. & Schmitt, F. (2005). p63, cytokeratin 5, and P-cadherin: three molecular markers to distinguish basal phenotype in breast carcinomas. *Virchows Arch*, **447**, 688-694.

Mayer, I. A., Abramson, V. G., Lehmann, B. D. & Pietenpol, J. A. (2014). New Clinical Strategies for Triple Negative Breast Cancer- Deciphering the heterogeneity. . *Clinical Cancer Research*.

McCabe, N., Turner, N. C., Lord, C. J., Kluzek, K., Bialkowska, A., Swift, S., Giavara, S., O'Connor, M. J., Tutt, A. N., Zdzienicka, M. Z., Smith, G. C. & Ashworth, A. (2006). Deficiency in the repair of DNA damage by homologous recombination and sensitivity to poly(ADP-ribose) polymerase inhibition. *Cancer Res*, **66**, 8109-8115.

Meulmeester, E. & Ten Dijke, P. (2011). The dynamic roles of TGF-beta in cancer. *J Pathol*, **223**, 205-218.

Miettinen, P. J., Ebner, R., Lopez, A. R. & Derynck, R. (1994). TGF-beta induced transdifferentiation of mammary epithelial cells to mesenchymal cells: involvement of type I receptors. *J Cell Biol*, **127**, 2021-2036.

Millikan, R. C., Newman, B., Tse, C.-K., Moorman, P. G., Conway, K., Dressler, L. G., Smith, L. V., Labbok, M. H., Geradts, J., Bensen, J. T., Jackson, S., Nyante, S., Livasy, C., Carey, L., Earp, H. S. & Perou, C. M. (2008). Epidemiology of basal-like breast cancer. *Breast cancer research and treatment*, **109**, 123-139.

Miyamoto, S., Teramoto, H., Gutkind, J. S. & Yamada, K. M. (1996). Integrins can collaborate with growth factors for phosphorylation of receptor tyrosine kinases and MAP kinase activation: roles of integrin aggregation and occupancy of receptors. *The Journal of cell biology*, **135**, 1633-1642.

Mondesire, W. H., Jian, W., Zhang, H., Ensor, J., Hung, M. C., Mills, G. B. & Meric-Bernstam, F. (2004). Targeting mammalian target of rapamycin synergistically enhances chemotherapy-induced cytotoxicity in breast cancer cells. *Clin Cancer Res*, **10**, 7031-7042.

Montagna, E., Maisonneuve, P., Rotmensz, N., Cancello, G., Iorfida, M., Balduzzi, A., Galimberti, V., Veronesi, P., Luini, A., Pruneri, G., Bottiglieri, L., Mastropasqua, M. G., Goldhirsch, A., Viale, G. & Colleoni, M. (2013). Heterogeneity of triple-negative breast cancer: histologic subtyping to inform the outcome. *Clinical breast cancer*, **13**, 31-39.

Morris, G. J., Naidu, S., Topham, A. K., Guiles, F., Xu, Y., McCue, P., Schwartz, G. F., Park, P. K., Rosenberg, A. L., Brill, K. & Mitchell, E. P. (2007). Differences in breast carcinoma characteristics in newly diagnosed African-American and Caucasian patients: a single-institution compilation compared with the National Cancer Institute's Surveillance, Epidemiology, and End Results database. *Cancer*, **110**, 876-884.

Moses, H. & Barcellos-Hoff, M. H. (2011). TGF-beta biology in mammary development and breast cancer. *Cold Spring Harb Perspect Biol*, **3**, a003277.

Mueller, M. M. & Fusenig, N. E. (2004). Friends or foes - bipolar effects of the tumour stroma in cancer. *Nature reviews Cancer*, **4**, 839-849.

Munger, J., Harpel, J., Gleizes, P., Mazzieri, R., Nunes, I. & Rifkin, D. (1997). Latent transforming growth factor-beta: structural features and mechanisms of activation. *Kidney Int.*, **51**, 1376-1382.

Muraoka, R. S., Dumont, N., Ritter, C. A., Dugger, T. C., Brantley, D. M., Chen, J., Easterly, E., Roebuck, L. R., Ryan, S., Gotwals, P. J., Koteliansky, V. & Arteaga, C. L. (2002). Blockade of TGF-beta inhibits mammary tumor cell viability, migration, and metastases. *J Clin Invest*, **109**, 1551-1559.

Mythreye, K. & Blobe, G. C. (2009). The type III TGF-beta receptor regulates epithelial and cancer cell migration through beta-arrestin2-mediated activation of Cdc42. *Proceedings of the National Academy of Sciences*, **106**, 8221-8226.

Mythreye, K., Knelson, E. H., Gatza, C. E., Gatza, M. L. & Blobe, G. C. (2013). TbetaRIII/beta-arrestin2 regulates integrin alpha5beta1 trafficking, function, and localization in epithelial cells. *Oncogene*, **32**, 1416-1427.

Nam, J. S., Terabe, M., Mamura, M., Kang, M. J., Chae, H., Stuelten, C., Kohn, E., Tang, B., Sabzevari, H., Anver, M. R., Lawrence, S., Danielpour, D., Lonning, S., Berzofsky, J. A. & Wakefield, L. M. (2008). An anti-transforming growth factor beta antibody suppresses metastasis via cooperative effects on multiple cell compartments. *Cancer Res*, **68**, 3835-3843.

Nguyen, P. L., Taghian, A. G., Katz, M. S., Niemierko, A., Abi Raad, R. F., Boon, W. L., Bellon, J. R., Wong, J. S., Smith, B. L. & Harris, J. R. (2008). Breast cancer subtype approximated by estrogen receptor, progesterone receptor, and HER-2 is associated with local and distant recurrence after breast-conserving therapy. *Journal of Clinical Oncology*, **26**, 2373-2378.

Nielsen, T. O., Hsu, F. D., Jensen, K., Cheang, M., Karaca, G., Hu, Z., Hernandez-Boussard, T., Livasy, C., Cowan, D., Dressler, L., Akslen,

L. A., Ragaz, J., Gown, A. M., Gilks, C. B., van de Rijn, M. & Perou, C. M. (2004). Immunohistochemical and clinical characterization of the basal-like subtype of invasive breast carcinoma. *Clinical cancer research : an official journal of the American Association for Cancer Research*, **10**, 5367-5374.

Nishimura, R., Osako, T., Okumura, Y., Hayashi, M. & Arima, N. (2010). Clinical significance of Ki-67 in neoadjuvant chemotherapy for primary breast cancer as a predictor for chemosensitivity and for prognosis. *Breast Cancer*, **17**, 269-275.

O'Shaughnessy, J., Osborne, C., Pippen, J. E., Yoffe, M., Patt, D., Rocha, C., Koo, I. C., Sherman, B. M. & Bradley, C. (2011a). Iniparib plus chemotherapy in metastatic triple-negative breast cancer. *N Engl J Med*, **364**, 205-214.

O'Shaughnessy, L. S., Schwartzberg, M. A., Danso, H. S., Rugo, K., Miller, D. A., Yardley, R. W., Carlson, R. S., Finn, E., Charpentier, M., Freese, S., Gupta, A., Blackwood-Chirchir & Winer, E. P. (2011b). A randomized phase III study of iniparib (BSI-201) in combination with gemcitabine/carboplatin (G/C) in metastatic triple-negative breast cancer (TNBC). *J Clin Oncol*, **29**.

O'Shaughnessy, J., Weckstein, D. J., Vukelja, S. J., McIntyre, K., Krekow, L., Holmes, F. A. & al., e. (2007). Randomized phase II study of weekly irinotecan/carboplatin with or without cetuximab in patients with metastatic breast cancer. *Breast Cancer Res Treat*, **106**.

Oettle, H., Seufferlein, T., Luger, T. & al., e. (2012). Final results of a phase I/II study in patients with pancreatic cancer, malignant melanoma, and colorectal carcinoma with trabedersen. *J Clin Oncol*, **30**.

Oft, M., Heider, K. H. & Beug, H. (1998). TGFbeta signaling is necessary for carcinoma cell invasiveness and metastasis. *Curr Biol*, **8**, 1243-1252.

Oft, M., Peli, J., Rudaz, C., Schwarz, H., Beug, H. & Reichmann, E. (1996). TGF-beta1 and Ha-Ras collaborate in modulating the phenotypic plasticity and invasiveness of epithelial tumor cells. *Genes Dev*, **10**, 2462-2477.

Ozdamar, B., Bose, R., Barrios-Rodiles, M., Wang, H. R., Zhang, Y. & Wrana, J. L. (2005). Regulation of the polarity protein Par6 by TGFbeta receptors controls epithelial cell plasticity. *Science*, **307**, 1603-1609.

Padua, D. & Massague, J. (2009). Roles of TGFbeta in metastasis. *Cell Res*, **19**, 89-102.

Paszek, M. J., Zahir, N., Johnson, K. R., Lakins, J. N., Rozenberg, G. I., Gefen, A., Reinhart-King, C. A., Margulies, S. S., Dembo, M., Boettiger, D., Hammer, D. A. & Weaver, V. M. (2005). Tensional homeostasis and the malignant phenotype. *Cancer cell*, **8**, 241-254.

Pegram, M. D., Lipton, A., Hayes, D. F., Weber, B. L., Baselga, J. M., Tripathy, D., Baly, D., Baughman, S. A., Twaddell, T., Glaspy, J. A. & Slamon, D. J. (1998). Phase II study of receptor-enhanced chemosensitivity using recombinant humanized anti-p185HER2/neu monoclonal antibody plus cisplatin in patients with HER2/neu-overexpressing metastatic breast cancer refractory to chemotherapy treatment. *J Clin Oncol*, **16**, 2659-2671.

Perou, C. M., Sorlie, T., Eisen, M. B., van de Rijn, M., Jeffrey, S. S., Rees, C. A., Pollack, J. R., Ross, D. T., Johnsen, H., Akslen, L. A., Fluge, O., Pergamenschikov, A., Williams, C., Zhu, S. X., Lonning, P. E., Borresen-Dale, A. L., Brown, P. O. & Botstein, D. (2000). Molecular portraits of human breast tumours. *Nature*, **406**, 747-752.

Piccart-Gebhart, M. J., Procter, M., Leyland-Jones, B., Goldhirsch, A., Untch, M., Smith, I., Gianni, L., Baselga, J., Bell, R., Jackisch, C., Cameron, D., Dowsett, M., Barrios, C. H., Steger, G., Huang, C. S., Andersson, M., Inbar, M., Lichinitser, M., Lang, I., Nitz, U., Iwata, H., Thomssen, C., Lohrisch, C., Suter, T. M., Ruschoff, J., Suto, T., Greatorex, V., Ward, C., Straehle, C., McFadden, E., Dolci, M. S. & Gelber, R. D. (2005). Trastuzumab after adjuvant chemotherapy in HER2-positive breast cancer. *N Engl J Med*, **353**, 1659-1672.

Pollard, J. W. (2004). Tumour-educated macrophages promote tumour progression and metastasis. *Nature reviews Cancer*, **4**, 71-78.

Polyak, K. & Metzger Filho, O. (2012). SnapShot: breast cancer. *Cancer cell*, **22**, 562-562 e561.

R Core Team (2013). R: A Language and Environment for Statistical Computing. Vienna, Austria.

Rakha, E. & Ellis, I. (2009). Triple-negative/basal-like breast cancer: review. *Pathology*, **41**, 40-47.

Rakha, E. A., El-Sayed, M. E., Green, A. R., Lee, A. H. S., Robertson, J. F. & Ellis, I. O. (2007). Prognostic markers in triple-negative breast cancer. *Cancer*, **109**, 25-32.

Ramirez, N. E., Zhang, Z., Madamanchi, A., Boyd, K. L., O'Rear, L. D., Nashabi, A., Li, Z., Dupont, W. D., Zijlstra, A. & Zutter, M. M. (2011). The alpha(2)beta(1) integrin is a metastasis suppressor in mouse models and human cancer. *J Clin Invest*, **121**, 226-237.

Reis-Filho, J. S. & Tutt, A. N. (2008). Triple negative tumours: a critical review. *Histopathology*, **52**, 108-118.

Renshaw, M. W., Price, L. S. & Schwartz, M. A. (1999). Focal adhesion kinase mediates the integrin signaling requirement for growth factor activation of MAP kinase. *The Journal of cell biology*, **147**, 611-618.

Roberts, A. B. & Wakefield, L. M. (2003). The two faces of transforming growth factor beta in carcinogenesis. *Proceedings of the National Academy of Sciences of the United States of America*, **100**, 8621-8623.

Rocca, A., Viale, G., Gelber, R. D., Bottiglieri, L., Gelber, S., Pruneri, G., Ghisini, R., Balduzzi, A., Pietri, E., D'Alessandro, C., Goldhirsch, A. & Colleoni, M. (2007). Pathologic complete remission rate after cisplatin-based primary chemotherapy in breast cancer: correlation with p63 expression. *Cancer Chemother Pharmacol*.

Rosenbluth, J. M., Mays, D. J., Pino, M. F., Tang, L. J. & Pietenpol, J. A. (2008). A gene signature-based approach identifies mTOR as a regulator of p73. *Mol Cell Biol*, **28**, 5951-5964.

Rouzier, R., Perou, C. M., Symmans, W. F., Ibrahim, N., Cristofanilli, M., Anderson, K., Hess, K. R., Stec, J., Ayers, M., Wagner, P., Morandi,

P., Fan, C., Rabiul, I., Ross, J. S., Hortobagyi, G. N. & Pusztai, L. (2005). Breast cancer molecular subtypes respond differently to preoperative chemotherapy. *Clin Cancer Res*, **11**, 5678-5685.

Rowland-Goldsmith, M. A., Maruyama, H., Matsuda, K., Idezawa, T., Ralli, M., Ralli, S. & Korc, M. (2002). Soluble type II transforming growth factor-beta receptor attenuates expression of metastasis-associated genes and suppresses pancreatic cancer cell metastasis. *Mol Cancer Ther*, **1**, 161-167.

Sánchez, N. S. & Barnett, J. V. (2012). TGFβ and BMP-2 regulate epicardial cell invasion via TGFβR3 activation of the Par6/Smurf1/RhoA pathway. *Cellular Signalling*, **24**, 539-548.

Schlingensiepen, K. H., Jaschinski, F., Lang, S. A., Moser, C., Geissler, E. K., Schlitt, H. J., Kielmanowicz, M. & Schneider, A. (2011). Transforming growth factor-beta 2 gene silencing with trabedersen (AP 12009) in pancreatic cancer. *Cancer Sci*, **102**, 1193-1200.

Schmierer, B. & Hill, C. S. (2007). TGFβ–SMAD signal transduction: molecular specificity and functional flexibility. *Nature Reviews Molecular Cell Biology*, **8**, 970-982.

Shah, S. P., Roth, A., Goya, R., Oloumi, A., Ha, G., Zhao, Y., Turashvili, G., Ding, J., Tse, K., Haffari, G., Bashashati, A., Prentice, L. M., Khattra, J., Burleigh, A., Yap, D., Bernard, V., McPherson, A., Shumansky, K., Crisan, A., Giuliany, R., Heravi-Moussavi, A., Rosner, J., Lai, D., Birol, I., Varhol, R., Tam, A., Dhalla, N., Zeng, T., Ma, K., Chan, S. K., Griffith, M., Moradian, A., Cheng, S. W., Morin, G. B., Watson, P., Gelmon, K., Chia, S., Chin, S. F., Curtis, C., Rueda, O. M., Pharoah, P. D., Damaraju, S., Mackey, J., Hoon, K., Harkins, T., Tadigotla, V., Sigaroudinia, M., Gascard, P., Tlsty, T., Costello, J. F., Meyer, I. M., Eaves, C. J., Wasserman, W. W., Jones, S., Huntsman, D., Hirst, M., Caldas, C., Marra, M. A. & Aparicio, S. (2012). The clonal and mutational evolution spectrum of primary triple-negative breast cancers. *Nature*, **486**, 395-399.

Shannon, J. M. & Hyatt, B. A. (2004). Epithelial-mesenchymal interactions in the developing lung. *Annual review of physiology*, **66**, 625-645.

Shao, Z. M., Nguyen, M. & Barsky, S. H. (2000). Human breast carcinoma desmoplasia is PDGF initiated. *Oncogene*, **19**, 4337-4345.

Sharma, P., Khan, Q., Kimler, B., Klemp, J., Connor, C., McGinness, M., Mammen, J., Tawfik, O., Fan, F. & Fabian, C. (2010). Results of a Phase II Study of Neoadjuvant Platinum/Taxane Based Chemotherapy and Erlotinib for Triple Negative Breast Cancer *Cancer Research*, **70**.

Shekhar, M. P., Werdell, J., Santner, S. J., Pauley, R. J. & Tait, L. (2001). Breast stroma plays a dominant regulatory role in breast epithelial growth and differentiation: implications for tumor development and progression. *Cancer research*, **61**, 1320-1326.

Shi, Y. & Massague, J. (2003). Mechanisms of TGF-beta signaling from cell membrane to the nucleus. *Cell*, **113**, 685-700.

Shiang, C. Y., Qi, Y., Wang, B., Lazar, V., Wang, J., Fraser Symmans, W., Hortobagyi, G. N., Andre, F. & Pusztai, L. (2010). Amplification of fibroblast growth factor receptor-1 in breast cancer and the effects of brivanib alaninate. *Breast Cancer Res Treat*, **123**, 747-755.

Shimanuki, T., Hara, T., Furuya, T., Imamura, T. & Miyazono, K. (2007). Modulation of the functional binding sites for TGF-beta on the type II receptor leads to suppression of TGF-beta signaling. *Oncogene*, **26**, 3311-3320.

Shin, B. K., Lee, Y., Lee, J. B., Kim, H. K., Lee, J. B., Cho, S. J. & Kim, A. (2008). Breast carcinomas expressing basal markers have poor clinical outcome regardless of estrogen receptor status. *Oncol Rep*, **19**, 617-625.

Shipley, G. D., Pittelkow, M. R., Wille, J. J., Jr., Scott, R. E. & Moses, H. L. (1986). Reversible inhibition of normal human prokeratinocyte proliferation by type beta transforming growth factor-growth inhibitor in serum-free medium. *Cancer Res*, **46**, 2068-2071.

Siegel, P. M., Shu, W., Cardiff, R. D., Muller, W. J. & Massague, J. (2003). Transforming growth factor beta signaling impairs Neu-induced mammary

tumorigenesis while promoting pulmonary metastasis. *Proc Natl Acad Sci U S A*, **100**, 8430-8435.

Silver, D. P., Richardson, A. L., Eklund, A. C., Wang, Z. C., Szallasi, Z., Li, Q., Juul, N., Leong, C. O., Calogrias, D., Buraimoh, A., Fatima, A., Gelman, R. S., Ryan, P. D., Tung, N. M., De Nicolo, A., Ganesan, S., Miron, A., Colin, C., Sgroi, D. C., Ellisen, L. W., Winer, E. P. & Garber, J. E. (2010). Efficacy of neoadjuvant Cisplatin in triple-negative breast cancer. *J Clin Oncol*, **28**, 1145-1153.

Smith, I. C., Heys, S. D., Hutcheon, A. W., Miller, I. D., Payne, S., Gilbert, F. J., Ah-See, A. K., Eremin, O., Walker, L. G., Sarkar, T. K., Eggleton, S. P. & Ogston, K. N. (2002). Neoadjuvant chemotherapy in breast cancer: significantly enhanced response with docetaxel. *J Clin Oncol*, **20**, 1456-1466.

Society, A. C. (2009). Breast Cancer Facts and Figures 2009-2010. 1-40.

Society, A. C. (2014). Cancer Facts and Figures 2014. *Atlanta: American Cancer Society*

Somlo, G., Frankel, P., Luu, T., Ma, C., Arun, B., Garcia, A., Cigler, T., Fleming, G., Harvey, H., Sparano, J., Nanda, R., Chew, H., Moynihan, T., Vahdat, L., Goetz, M., Hurria, A., Mortimer, J., Gandara, D., Chen, A. & Weitze, J. (2013). Efficacy of the combination of ABT-888 (veliparib) and carboplatin in patients with BRCA-associated breast cancer. *J Clin Oncol*, **31**.

Sorlie, T., Perou, C. M., Tibshirani, R., Aas, T., Geisler, S., Johnsen, H., Hastie, T., Eisen, M. B., van de Rijn, M., Jeffrey, S. S., Thorsen, T., Quist, H., Matese, J. C., Brown, P. O., Botstein, D., Lonning, P. E. & Borresen-Dale, A. L. (2001). Gene expression patterns of breast carcinomas distinguish tumor subclasses with clinical implications. *Proc Natl Acad Sci U S A*, **98**, 10869-10874.

Sorlie, T., Tibshirani, R., Parker, J., Hastie, T., Marron, J. S., Nobel, A., Deng, S., Johnsen, H., Pesich, R., Geisler, S., Demeter, J., Perou, C. M., Lonning, P. E., Brown, P. O., Borresen-Dale, A. L. & Botstein, D.

(2003). Repeated observation of breast tumor subtypes in independent gene expression data sets. *Proc Natl Acad Sci U S A*, **100**, 8418-8423.

Stenvers, K. L., Tursky, M. L., Harder, K. W., Kountouri, N., Amatayakul-Chantler, S., Grail, D., Small, C., Weinberg, R. A., Sizeland, A. M. & Zhu, H. J. (2003). Heart and liver defects and reduced transforming growth factor beta2 sensitivity in transforming growth factor beta type III receptor-deficient embryos. *Mol Cell Biol*, **23**, 4371-4385.

Stover, D. G., Bierie, B. & Moses, H. L. (2007). A delicate balance: TGF-beta and the tumor microenvironment. *Journal of cellular biochemistry*, **101**, 851-861.

Stuart-Harris, R., Caldas, C., Pinder, S. E. & Pharoah, P. (2008). Proliferation markers and survival in early breast cancer: a systematic review and meta-analysis of 85 studies in 32,825 patients. *Breast*, **17**, 323-334.

Tan, D. S. P., Marchió, C., Jones, R. L., Savage, K., Smith, I. E., Dowsett, M. & Reis-Filho, J. S. (2008). Triple negative breast cancer: molecular profiling and prognostic impact in adjuvant anthracycline-treated patients. *Breast cancer research and treatment*, **111**, 27-44.

Telli ML, Jensen, K., Kurian, A. & al., e. (2011). PrECOG 0105: Final efficacy results from a phase II study of gemcitabine (G) and carboplatin (C) plus iniparib (BSI-201) as neoadjuvant therapy for triple-negative (TN) and BRCA1/2 mutation-associated breast cancer. *J Clin Oncol*, **31**.

ten Dijke, P., Hansen, P., Iwata, K. K., Pieler, C. & Foulkes, J. G. (1988). Identification of another member of the transforming growth factor type beta gene family. *Proceedings of the National Academy of Sciences of the United States of America*, **85**, 4715-4719.

Tsutsui, S., Ohno, S., Murakami, S., Hachitanda, Y. & Oda, S. (2002). Prognostic value of epidermal growth factor receptor (EGFR) and its relationship to the estrogen receptor status in 1029 patients with breast cancer. *Breast Cancer Res Treat*, **71**, 67-75.

Tucker, R. F., Shipley, G. D., Moses, H. L. & Holley, R. W. (1984). Growth inhibitor from BSC-1 cells closely related to platelet type beta transforming growth factor. *Science*, **226**, 705-707.

Turley, R. S., Finger, E. C., Hempel, N., How, T., Fields, T. A. & Blobe, G. C. (2007). The type III transforming growth factor-beta receptor as a novel tumor suppressor gene in prostate cancer. *Cancer Res*, **67**, 1090-1098.

Turner, N., Lambros, M. B., Horlings, H. M., Pearson, A., Sharpe, R., Natrajan, R., Geyer, F. C., van Kouwenhove, M., Kreike, B., Mackay, A., Ashworth, A., van de Vijver, M. J. & Reis-Filho, J. S. (2010). Integrative molecular profiling of triple negative breast cancers identifies amplicon drivers and potential therapeutic targets. *Oncogene*, **29**, 2013-2023.

Turner, N., Tutt, A. & Ashworth, A. (2004). Hallmarks of 'BRCAness' in sporadic cancers. *Nature reviews Cancer*, **4**, 814-819.

Tutt, A. & Ashworth, A. (2008). Can genetic testing guide treatment in breast cancer? *Eur J Cancer*, **44**, 2774-2780.

Tutt, A., Robson, M., Garber, J. E., Domchek, S. M., Audeh, M. W., Weitzel, J. N., Friedlander, M., Arun, B., Loman, N., Schmutzler, R. K., Wardley, A., Mitchell, G., Earl, H., Wickens, M. & Carmichael, J. (2010). Oral poly(ADP-ribose) polymerase inhibitor olaparib in patients with BRCA1 or BRCA2 mutations and advanced breast cancer: a proof-of-concept trial. *Lancet*, **376**, 235-244.

Urruticoechea, A., Smith, I. E. & Dowsett, M. (2005). Proliferation marker Ki-67 in early breast cancer. *J Clin Oncol*, **23**, 7212-7220.

van 't Veer, L. J., Dai, H., van de Vijver, M. J., He, Y. D., Hart, A. A., Bernards, R. & Friend, S. H. (2003). Expression profiling predicts outcome in breast cancer. *Breast Cancer Res*, **5**, 57-58.

van 't Veer, L. J., Dai, H., van de Vijver, M. J., He, Y. D., Hart, A. A., Mao, M., Peterse, H. L., van der Kooy, K., Marton, M. J., Witteveen, A. T., Schreiber, G. J., Kerkhoven, R. M., Roberts, C., Linsley, P. S.,

Bernards, R. & Friend, S. H. (2002). Gene expression profiling predicts clinical outcome of breast cancer. *Nature*, **415**, 530-536.

van de Rijn, M., Perou, C. M., Tibshirani, R., Haas, P., Kallioniemi, O., Kononen, J., Torhorst, J., Sauter, G., Zuber, M., Köchli, O. R., Mross, F., Dieterich, H., Seitz, R., Ross, D., Botstein, D. & Brown, P. (2002). Expression of cytokeratins 17 and 5 identifies a group of breast carcinomas with poor clinical outcome. *The American journal of pathology*, **161**, 1991-1996.

van de Vijver, M. J., He, Y. D., van't Veer, L. J., Dai, H., Hart, A. A., Voskuil, D. W., Schreiber, G. J., Peterse, J. L., Roberts, C., Marton, M. J., Parrish, M., Atsma, D., Witteveen, A., Glas, A., Delahaye, L., van der Velde, T., Bartelink, H., Rodenhuis, S., Rutgers, E. T., Friend, S. H. & Bernards, R. (2002). A gene-expression signature as a predictor of survival in breast cancer. *N Engl J Med*, **347**, 1999-2009.

Viale, G., Rotmensz, N., Maisonneuve, P., Bottiglieri, L., Montagna, E., Luini, A., Veronesi, P., Intra, M., Torrisi, R., Cardillo, A., Campagnoli, E., Goldhirsch, A. & Colleoni, M. (2009). Invasive ductal carcinoma of the breast with the "triple-negative" phenotype: prognostic implications of EGFR immunoreactivity. *Breast cancer research and treatment*, **116**, 317-328.

Vivanco, I. & Sawyers, C. L. (2002). The phosphatidylinositol 3-Kinase AKT pathway in human cancer. *Nat Rev Cancer*, **2**, 489-501.

Voduc, D., Nielsen, T. O., Cheang, M. C. & Foulkes, W. D. (2008). The combination of high cyclin E and Skp2 expression in breast cancer is associated with a poor prognosis and the basal phenotype. *Hum Pathol*, **39**, 1431-1437.

Von Minckwitz, G., Schneeweiss, A., Salat, C. & al., e. (2013). A randomized phase II trial investigating the addition of carboplatin to neoadjuvant therapy for triple-negative and HER2-positive early breast cancer (GeparSixto). *J Clin Oncol*, **31**.

Walker, R. A. (2001). The complexities of breast cancer desmoplasia. *Breast Cancer Res*, **3**, 143-145.

Wang, M. Y., Lu, K. V., Zhu, S., Dia, E. Q., Vivanco, I., Shackleford, G. M., Cavenee, W. K., Mellinghoff, I. K., Cloughesy, T. F., Sawyers, C. L. & Mischel, P. S. (2006). Mammalian target of rapamycin inhibition promotes response to epidermal growth factor receptor kinase inhibitors in PTEN-deficient and PTEN-intact glioblastoma cells. *Cancer Res*, **66**, 7864-7869.

Wang, X. F. X., Lin, H. Y. H., Ng-Eaton, E. E., Downward, J. J., Lodish, H. F. H. & Weinberg, R. A. (1991). Expression cloning and characterization of the TGF-beta type III receptor. *Cell*, **67**, 797-805.

Weaver, V. & Werb, Z. (2007). G'rab'bing the microenvironment for invasion. *Dev Cell*, **13**, 462-463.

Weigelt, B., Horlings, H. M., Kreike, B., Hayes, M. M., Hauptmann, M., Wessels, L. F., de Jong, D., Van de Vijver, M. J., Van't Veer, L. J. & Peterse, J. L. (2008). Refinement of breast cancer classification by molecular characterization of histological special types. *J Pathol*, **216**, 141-150.

Westfall, M. D., Joyner, A. S., Barbieri, C. E., Livingstone, M. & Pietenpol, J. A. (2005). Ultraviolet radiation induces phosphorylation and ubiquitin-mediated degradation of DeltaNp63alpha. *Cell Cycle*, **4**, 710-716.

Westfall, M. D., Mays, D. J., Sniezek, J. C. & Pietenpol, J. A. (2003). The Delta Np63 alpha phosphoprotein binds the p21 and 14-3-3 sigma promoters in vivo and has transcriptional repressor activity that is reduced by Hay-Wells syndrome-derived mutations. *Mol Cell Biol*, **23**, 2264-2276.

Wickham, H. (2009). *ggplot2: elegant graphics for data analysis*: Springer New York.

Wiggans, R. G., Woolley, P. V., Smythe, T., Hoth, D., Macdonald, J. S., Green, L. & Schein, P. S. (1979). Phase-II trial of tamoxifen in advanced breat cancer. *Cancer Chemother Pharmacol*, **3**, 45-48.

Wiseman, B. & Werb, Z. (2002). Stromal effects on mammary gland development and breast cancer. *Science (New York, NY)*, **296**, 1046.

Woszczyk, D., Gola, J., Jurzak, M., Mazurek, U., Mykala-Ciesla, J. & Wilczok, T. (2004). Expression of TGF beta1 genes and their receptor types I, II, and III in low- and high-grade malignancy non-Hodgkin's lymphomas. *Med Sci Monit*, **10**, CR33-37.

Wrana, J. L., Attisano, L., Carcamo, J., Zentella, A., Doody, J., Laiho, M., Wang, X. F. & Massague, J. (1992). TGF beta signals through a heteromeric protein kinase receptor complex. *Cell*, **71**, 1003-1014.

Yang, A., Schweitzer, R., Sun, D., Kaghad, M., Walker, N., Bronson, R. T., Tabin, C., Sharpe, A., Caput, D., Crum, C. & McKeon, F. (1999). p63 is essential for regenerative proliferation in limb, craniofacial and epithelial development. *Nature*, **398**, 714-718.

Yang, Y. A., Dukhanina, O., Tang, B., Mamura, M., Letterio, J. J., MacGregor, J., Patel, S. C., Khozin, S., Liu, Z. Y., Green, J., Anver, M. R., Merlino, G. & Wakefield, L. M. (2002). Lifetime exposure to a soluble TGF-beta antagonist protects mice against metastasis without adverse side effects. *J Clin Invest*, **109**, 1607-1615.

You, H. J., Seo, J.-M., Moon, J.-Y., Han, S.-S., Ko, Y.-G. & Kim, J.-H. (2007). Leukotriene synthesis in response to A23187 is inhibited by methyl- beta-cyclodextrin in RBL-2H3 cells. *Mol Cells*, **23**, 57-63.

Zutter, M. M., Mazoujian, G. & Santoro, S. A. (1990). Decreased expression of integrin adhesive protein receptors in adenocarcinoma of the breast. *Am J Pathol*, **137**, 863-870.